

Lincoln University Digital Thesis

Copyright Statement

The digital copy of this thesis is protected by the Copyright Act 1994 (New Zealand).

This thesis may be consulted by you, provided you comply with the provisions of the Act and the following conditions of use:

- you will use the copy only for the purposes of research or private study
- you will recognise the author's right to be identified as the author of the thesis and due acknowledgement will be made to the author where appropriate
- you will obtain the author's permission before publishing any material from the thesis.

Interactions between isolates of the fungus
Beauveria bassiana* and *Zea mays

A thesis
submitted in partial fulfilment
of the requirements for the Degree of
Doctor of Philosophy

at
Lincoln University
by
Aimee C. McKinnon

Lincoln University
2017

Abstract of a thesis submitted in partial fulfilment of the
requirements for the Degree of Doctor of Philosophy.

Interactions between isolates of the fungus
Beauveria bassiana* and *Zea mays

by

Aimee C. McKinnon

Entomopathogenic fungi from the genus *Beauveria* play an important role in controlling insect populations and have been utilised widely for the biological control of insect pests. Only relatively recently has research focused more on the ecology of these fungi. Various studies have reported that *Beauveria bassiana* have the ability to become endophytic and may colonise a broad range of plant hosts, while still maintaining pathogenicity to insects. However, the nature of these interactions within plant tissues and the mechanism for colonisation still require elucidation. The aim of this project was to address some of the fundamental questions relating to endophytic colonisation and host interaction *in planta*. Three putative endophytic isolates of *Beauveria* were subsequently investigated for interactions with a single *Zea mays* (maize) cultivar Pioneer 34H31. The overall hypothesis was that isolates of *B. bassiana* differ in their ability to colonise a single maize cultivar, as evidenced by differential effects to the plant microbiome (in the rhizosphere roots/soil), as well as plant growth and immune response following inoculation. In order to test this hypothesis, endophytic isolates had to be first obtained. Consequently, a nested PCR protocol was developed based on the translation elongation factor 1-alpha (*ef1α*) gene that was designed to find and amplify isolates *in planta* from the genus *Beauveria*. The nested protocol was also designed to enable species differentiation by sequence analysis and quantification of fungal biomass *in planta*. A prior review of the literature pertaining to *Beauveria* endophyte detection methodology for PCR indicated the need to optimise plant surface sterilisation for reliable detection of *Beauveria* in plant tissues. However, elimination of *Beauveria* inocula and/or DNA from the plant surfaces proved difficult. The focus of the project therefore shifted more to the plant host response to all plant-associated *Beauveria*. This was achieved by (1) testing the plant growth response to three different *B. bassiana* putative endophytic isolates (BG11, FRh2 and J18) versus the growth-promoting *Trichoderma atroviride*

isolate LU132, all of which were introduced artificially through a wound made to the emerging maize seedlings to avoid the confounding effects of surface inoculation, (2) by assessing the impact of the three *B. bassiana* isolates applied topically to roots of maize on the rhizosphere soil community structure and function and (3) by investigating differences in gene expression in maize roots in the response to the topical application of two different *B. bassiana* isolates (BG11 and J18), relative to a no-inoculum control using an RNA microarray transcriptome analysis. Results of the growth experiment showed predominantly neutral or negative effects to plant growth in terms of biomass, although plants exhibited root architecture changes as a result of one *B. bassiana* isolate (FRh2), and a higher chlorophyll content for another isolate (J18) when measured with a SPAD-502 chlorophyll meter, providing initial evidence for phenotypic differences between the selected study isolates. However, variation between the three *B. bassiana* isolates was less evident in the ecological study of the rhizosphere of maize. Neither the microbial community structure nor function was significantly affected by the presence of the isolates. However, retention of the inocula in the rhizosphere over 30 days after inoculation (DAI) was positively affected by a simulated herbivory treatment made to the maize foliage at 23 DAI, as was the general microbial community composition. The transcriptome analysis indicated putative differential gene expression in maize roots as a result of colonisation by the two *B. bassiana* isolates, suggesting that they may differ in their ability to colonise and/or effect the plant host immune response. Isolate J18-treated plants upregulated genes encoding for antioxidant glutathione S-transferases (GSTs) relative to BG11-treated plants, presumably to counteract excesses of reactive oxygen species (ROS). In contrast, BG11-treated plants upregulated a larger suite of genes involved in plant defence including ethylene responsive transcription factors, auxin responsive and dehydration responsive genes. Overall, this research suggests that the relationship between *Beauveria* and the plant host is modulated by the plant host, but may sometimes also be isolate-dependent.

Keywords: Biological control, insect pathogen, biopesticide, microbiome, microbial diversity, rhizosphere, endophyte, transcriptomics, DGGE, MicroResp™.

Acknowledgements

Firstly, I would like to express my thanks and appreciation to my supervisory team, Travis Glare, Hayley Ridgway, Artemio Mendoza Mendoza and Andrew Holyoake. Your combined expertise, kind supervision, genuine encouragement and support whenever needed has enabled me to conduct (and continue) this work. My thanks also to Maria Eugenia Moran-Diez, Michael Rostas and Jennifer Bufford for all your expert advice, help and for kindly making yourselves available to me. You are all champions!

I would like to also thank the Tertiary Education Commission (TEC, NZ) and the Bio-Protection Research Centre (BPRC) for funding this PhD project, and to Pioneer for supplying the maize seed. To the team at New Zealand Genomics Limited (NZGL) in Auckland, who helped and advised me with the microarray experiment and data analysis, in particular, Liam Williams, Vicky Fan and Luke Boyle; I offer my sincere appreciation for all your time and labour.

Special thanks is due those people in particular who assisted me during experimental trials, namely, Nyssa Glare, Marsha Ormskirk, Michael (Kooki) Kuchar, Maria Eugenia, Jessica Yardley and Leila Dadian. For those who helped out with 'the investigation' process prior to this project, Celine Blond, Michael Rostas, Maya Raad and Jenny Brookes. You made a difficult time less difficult for me. Thanks to Stu Larson for the ever helpful assistance and for putting up with my useless storage systems. To Jess Yardley and Abigail Durrant, thank you for kindly proof-reading the chapters.

I would also like to extend my thanks to all the staff and students at the Bio-Protection Research Centre who have offered their help and support, and for making this whole experience way more fun. In particular, my office mates' Damian Bienkowski, Natalia Cripps-Guazzone, Priscila Freitas and Kooki for your friendship and support, great advice and for the many laughs. You are all awesome people and I have been blessed to share this time with you. My thanks are due also to Sam Brown, for all his expertise with R and various other things! To all the AGLS folks, who have helped me out, Sandy Hammond, Celine Blond, Wisnu Wicaksono and Candice Hume, thank you all for your time.

I wish to express my sincere gratitude to my family for their help in making my studies possible, for all the prayers and for believing in me. Your continual encouragement throughout this time has been amazing and it's taken longer than I ever anticipated! I really thank God for you.

And to Francesco Martoni, for noticing me, for providing me with decent Italian coffee, hugs and kindness. Your passion and enthusiasm for science, your work ethic and your belief in me has inspired me to cross this finish line. Grazie! Ti voglio bene.

Table of Contents

Abstract	ii
Acknowledgements	iv
Table of Contents	v
List of Tables	viii
List of Figures	x
 Chapter 1 General introduction.....	 1
1.1 Plant protection and biological control	1
1.2 Endophytes for plant protection	2
1.3 Entomopathogenic fungi-plant interactions.....	4
1.3.1 <i>Beauveria bassiana</i>	5
1.3.2 The rhizosphere.....	8
1.4 The plant host.....	12
1.4.1 The plant immune response.....	13
1.5 Techniques for analysing the plant microbiome	19
1.5.1 Putative endophyte detection.....	19
1.5.2 Microbial diversity analysis	19
1.5.3 Transcriptomic analysis by microarray.....	20
1.6 Research rationale and aims.....	20
 Chapter 2 Developing methods for molecular detection of endophytic <i>Beauveria</i>	 22
2.1 Introduction	22
2.2 General Methods.....	24
2.2.1 Taxonomic identification of fungal species	24
2.2.2 Conidial suspensions for inoculation.....	25
2.2.3 DNA isolation from plant material	26
2.2.4 Amplification of plant genomic DNA.....	26
2.3 Development of multi-species PCR for detection of <i>Beauveria</i> spp. <i>in planta</i>	27
2.3.1 Primer design.....	27
2.3.2 Optimisation of PCR.....	29
2.4 Surface sterilisation methodology for PCR detection of <i>Beauveria bassiana</i>	33
2.4.1 Maize PMA™ treatment assay.....	33
2.4.2 Onion surface sterilisation assay.....	35
2.4.3 Microscopic visualisation of colonised maize tissue	36
2.5 Results.....	37
2.5.1 Optimisation of PCR.....	37
2.5.2 Surface sterilisation for PCR detection.....	43
2.5.3 Microscopic visualisation of colonised maize tissue	45
2.6 Discussion	46
 Chapter 3 Plant growth response to artificial inoculation with <i>Beauveria bassiana</i>.....	 49
3.1 Introduction	49
3.2 Methods.....	51
3.2.1 Maize growth conditions.....	51
3.2.2 Fungal cultures	52

3.2.3	Inoculation.....	52
3.2.4	Plant growth experiment A: Assessing the invasive inoculation technique and determining growth response measures.....	54
3.2.5	Plant growth experiment B and root architecture study	57
3.3	Results.....	58
3.3.1	Plant growth experiment A	58
3.3.2	Plant growth experiment B	61
3.3.3	Root architecture analysis	64
3.4	Discussion	67
Chapter 4 Ecological study of <i>Beauveria bassiana</i> isolates in the rhizosphere of <i>Zea mays</i>		73
4.1	Introduction	73
4.2	Methods.....	74
4.2.1	Inocula preparation	74
4.2.2	Maize growth conditions and inoculation.....	75
4.2.3	Experimental design	75
4.2.4	DNA preparation and PCR/qPCR detection.....	76
4.2.5	Quantification of <i>Beauveria bassiana</i> in the rhizosphere by CFU counts	77
4.2.6	Assessment of <i>Beauveria bassiana</i> in the roots and rhizosphere of <i>Zea mays</i> by PCR detection	78
4.2.7	Assessment of the microbial community composition using DGGE	79
4.2.8	Assessment of the microbial community function using MicroResp™	83
4.3	Results.....	84
4.3.1	<i>Beauveria</i> in the rhizosphere soil (CFU quantity analysis)	84
4.3.2	PCR detection of <i>Beauveria bassiana</i> in the rhizosphere and roots of maize	85
4.3.3	Assessment of the microbial community composition using DGGE	92
4.3.4	Assessment of the microbial community function using MicroResp™	96
4.4	Discussion	97
4.4.1	Quantification and detection of <i>Beauveria bassiana</i> in the rhizosphere.....	97
4.4.2	The influence of inocula on the soil microbial community structure and function.....	100
4.4.3	Conclusion	102
Chapter 5 Transcriptomic analysis of <i>Zea mays</i> in response to root colonisation by two <i>Beauveria bassiana</i> isolates		103
5.1	Introduction	103
5.2	Methods.....	104
5.2.1	Plant growth and inoculation	104
5.2.2	Experimental design	105
5.2.3	RNA isolation from roots and quality assessment	106
5.2.4	Microarray processing and hybridisation.....	106
5.2.5	Microarray data analysis	107
5.3	Results.....	109
5.3.1	Assessment of the microarray samples for differential gene expression	109
5.3.2	Differential gene expression and gene ontology	110
5.3.3	Gene functional classification.....	116
5.4	Discussion	118
5.4.1	Biological functions of enriched differentially expressed genes.....	118
5.4.2	Conclusions.....	124
Chapter 6 General discussion		125

Appendix A Phylogenetic identification of genera and/or species	130
Appendix B Pioneer maize hybrid cultivars	134
Appendix C Soil nutrient analysis	135
Appendix D RNA quality control assessment	136
Appendix E Differentially expressed gene (DEG) lists for <i>Beauveria bassiana</i> isolate BG11- and J18- versus control comparisons.....	138
References	146

List of Tables

Table 2.1.	Table of fungal isolates used in this study.	25
Table 2.2.	Novel primer pairs designed for a 2-step nested PCR protocol. Designed from the translation elongation factor alpha-1 (<i>ef1α</i>) gene to target multiple <i>Beauveria</i> species <i>in planta</i> . Primer melting temperature (TM), the target amplicon size in base-pair (bp), and the type of experiment are described.	29
Table 2.3.	Reagent concentrations for master-mix used in real time PCR. Based on the protocol optimised for <i>Beauveria</i> translation elongation factor 1-alpha (<i>ef1α</i>) target with primers EF4F and EF4R	31
Table 2.4.	Concentration of inocula. Conidial suspension concentrations were calculated relative to inoculum volume (80 µL) and applied to onion epidermis	33
Table 2.5.	Treatments used during the PMA assay with inoculated <i>Zea mays</i> (maize) roots. Surface sterilisation, designated SS in the treatment description, was accomplished with either of two different surface sterilisation protocols A and B.....	34
Table 2.6.	Surface sterilisation protocol(s). Outlined are agent solutions and concentrations, where applicable, used in the onion epidermis surface sterilisation optimisation assay.	36
Table 2.7.	Quantifying fungal DNA with nested PCR. Estimated are the number of amplicons available per dilution sample provided from PCR on translation elongation factor 1-alpha (<i>ef1α</i>) target EF3-5, for use in quantitative PCR (as nested step 2) with <i>ef1α</i> target EF4-4.	40
Table 2.9.	Percentage of positive <i>Beauveria bassiana</i> . Represented by <i>ef1α</i> bands (treatments' 1-4) or viable colonies (treatment 5 only) detected from <i>Zea mays</i> (maize) roots following surface sterilisation (SS) using protocol's A or B, for each treatment used during the maize PMA™ assay (6 experiments).....	43
Table 3.1.	Growth parameters tested in <i>Zea mays</i> (maize) growth experiment A. Table shows group means for the treatments used with LSD (5%) values and letters under each mean (rows shaded grey), to indicate differences between treatments derived from the Fisher's Unprotected LSD multiple comparisons procedure. Overall probability (Pr; F statistic, ANOVA) values are also provided for the treatment factor (isolate) for each parameter tested.	59
Table 3.2.	Growth parameters tested in <i>Zea mays</i> (maize) growth experiment B. Table shows group means for the treatments used with LSD (5%) values to indicate differences (where applicable) between treatments derived from the Fisher's Unprotected LSD multiple comparisons procedure. Overall probability (Pr; F statistic, ANOVA) values are also provided for the treatment factor (isolate) for each parameter tested.....	62
Table 3.3.	Plant root growth parameters tested using WINRHIZO. Table shows group means for the treatments used in the <i>Zea mays</i> (maize) root architecture analysis, with LSD (5%) values and letters under each mean (rows shaded grey) to indicate differences between treatments from a general ANOVA. Overall probability (Pr; F statistic, ANOVA) values are also provided for the treatment factor (isolate) for each parameter tested. Parameters tested include total length, projected root area (ProjArea), surface area (SurfArea), root diameter (Diam) and root volume, number of tips, forks and crossings.	65
Table 4.1.	Primer target sets and PCR conditions for denaturant gradient gel electrophoresis (DGGE) microbial community analysis	81
Table 4.2.	Quantification of <i>Beauveria</i> in rhizosphere soil versus bulk soil. Comparison of mean CFU g ⁻¹ dry soil (reported in log ₁₀) of <i>Beauveria</i> recovered at three sample times (days after inoculation, DAI) for rhizosphere (rhiz) and bulk soil, and ratio (rhiz:bulk) data. Means are reported with corresponding 5% LSD values in order to contrast isolate treatments.	85

Table 4.3.	Amplification of <i>Beauveria</i> isolates and non-target control. Tukey contrast pairwise comparisons with probability values show no differences between <i>Beauveria bassiana</i> isolate treatment mean cycle threshold (CT) values, except compared to the no-inoculum control (as expected). Based on amplifications on <i>Zea mays</i> (maize) root DNA, compared across three sample times: 6, 15, 30 days after inoculation (DAI). ...90	90
Table 4.4.	Number of missing data values representing absent cycle threshold values in qPCR experiments. Data represents <i>Beauveria</i> genus <i>ef1α</i> nested primer set (EF3-5; EF4-4) detected from root tissue of <i>Zea mays</i> (maize) at 6 and 30 days after inoculation (DAI).92	92
Table 4.5.	Statistical support of all ordination models. Analysis table of non-metric multiple dimension scaling (nMDS) ordination stress tests on microbial community composition data from denaturing gradient gel electrophoresis (DGGE).....93	93
Table 5.1.	Experimental design layout for inoculated <i>Zea mays</i> (maize) plants used in the maize cRNA microarray experiment.106	106
Table 5.2.	Comparison of the response of <i>Zea mays</i> (maize) roots to fungal colonisation at 3 days after inoculation (DAI). Comparisons made using microarray probe intensity value isolate-treatment means (reported in real space), to represent differential gene expression ($P \leq 0.05$). Plants were treated with either <i>Beauveria bassiana</i> isolate BG11 or J18. The gene list comprises annotated transcripts of maize only (uncharacterised genes omitted). Data is presented for genes downregulated in BG11-treated plants relative to J18 and ordered by indicated gene function. Group means for the control plants (non-inoculated group) are highlighted in grey. In the BG11 and J18 treatment mean columns (4 and 5), either orange or green is used to indicate direction of gene expression relative to the control group: orange infers downregulation and green infers upregulation.111	111
Table 5.3.	Comparison of the response of <i>Zea mays</i> (maize) roots to fungal colonisation at 3 days after inoculation (DAI). Comparisons made using microarray probe intensity value isolate treatment means (reported in real space), to represent significantly different gene expression (where $P \leq 0.05$). Plants were treated with either <i>Beauveria bassiana</i> isolate BG11 or J18. The gene list comprises annotated transcripts of maize only (uncharacterised genes omitted). Data is presented for genes upregulated in BG11-treated plants relative to J18 and ordered by indicated gene function. Group means for the control plants (non-inoculated group) are highlighted in grey. In the BG11 and J18 treatment mean columns (4 and 5), either orange or green is used to indicate direction of gene expression relative to the control group: orange infers downregulation and green infers upregulation.113	113
Table 5.4.	Differential gene expression in gene families. Table shows functional gene clusters with corresponding enrichment scores produced from Gene Set Enrichment Analysis (GSEA) in the database for annotation, visualisation and identification (DAVID) based on the putatively downregulated (coded in orange) differentially expressed gene list compiled from annotated transcripts produced from <i>Zea mays</i> (maize) in response to two different <i>Beauveria bassiana</i> isolate inocula (BG11 versus J18).....116	116
Table 5.5.	Differential gene expression in gene families. Table shows functional gene clusters with corresponding enrichment scores produced from the gene set enrichment analysis (GSEA) in the database for annotation, visualisation and identification (DAVID) based on the upregulated (coded in green) differentially expressed gene list compiled from annotated transcripts produced from <i>Zea mays</i> (maize) in response to two different <i>Beauveria bassiana</i> isolate inocula (BG11 versus J18).....117	117

List of Figures

Figure 1.1.	The rhizosphere regions illustrated. Figure sourced from: http://www.nature.com/scitable/knowledge/library/	10
Figure 1.2.	The hypersensitive response. A leaf showing characteristic symptoms of localised cell death. Photo sourced from: https://source.wustl.edu/2012/06/key-part-of-plants-rapid-response-system-revealed/	14
Figure 1.3.	Reactive oxygen species (ROS) as secondary messengers. Diagram illustrates the various hormone signalling cascades activated by ROS in response to biotic and abiotic stress. Diagram modified from Sharma et al. (2012).....	15
Figure 2.1.	Design of primers for selective PCR. Figure shows a multiple sequence alignment of 11 fungal translation elongation factor 1-alpha (<i>ef1α</i> or EF-1α) sequences. The alignment was used to design nested primer pairs EF3F and EF5R (set 1), and EF4F and EF4R (internal amplicon in set 1); primer set position is indicated by green annotation in the alignment image. Primers were designed from within a 989 bp fragment generated from EF 983F and EF 2218R. Red arrows indicate the position of these primers on the 'ef1α primer map', extracted from Binder and Hibbett (2003). 28	28
Figure 2.2.	Electrophoresis gel images comparing amplification of multiple fungal species DNA. Plot (a) shows amplification of the translation elongation factor 1-alpha (<i>ef1α</i>) gene using universal PCR primers, and, plot (b) shows amplification of the <i>ef1α</i> 406 bp amplicon by novel primers EF3F and EF5R (30 cycles) with a 1 kb DNA ladder (Hyperladder II, Biorline, USA).	38
Figure 2.3.	Real time qPCR cycle threshold means. Plot shows amplification of multiple fungal species and plant host DNA (onion and maize), versus <i>Beauveria bassiana</i> isolates (BG11, FRh2, J18) (Y axis) over mean cycle threshold (CT) values (X axis) with standard deviation error bars (where possible), using EF4F and EF4R as nested step 2 PCR target amplification on EF3F and EF5R generated product.....	39
Figure 2.4.	Testing of nested PCR amplification efficiency. Plot shows a standard curve representing mean cycle threshold (CT), with standard deviation error bars, plotted over log ₁₀ DNA concentration (ng/μL) from <i>Beauveria</i> . The regression equation intercept and slope of the curve, with amplification efficiency (%E) from qPCR target translation elongation factor 1-alpha (<i>ef1α</i>) EF3F and EF5R is also included.	40
Figure 2.5.	Comparison of qPCR standard curves. Plots contrast the analysis of EF4F and EF4R target on a PCR template versus direct amplification of gDNA. Plot (a) shows amplification of diluted template produced in a prior PCR of a 10-fold dilution series of <i>Beauveria bassiana</i> gDNA (isolate J18) spiked in <i>Zea mays</i> (maize) gDNA and plot (c) shows the corresponding standard curve with regression equation and amplification efficiency (%E). Plot (b) shows direct amplification of a 10-fold dilution series of <i>Beauveria bassiana</i> gDNA (isolate J18) in H ₂ O and plot (d) shows the corresponding standard curve produced with the regression equation and amplification efficiency (%E).	41
Figure 2.6.	Amplification of mixed DNA. Plot shows a standard curve representing mean cycle threshold (CT), plotted over log ₁₀ dilution factor obtained from DNA of inoculated onion epidermis. Included is the regression equation intercept and slope of the curve, from qPCR target translation elongation factor 1-alpha (<i>ef1α</i>) EF4F and EF4R.	42
Figure 2.7.	Percentage of total positive <i>Beauveria bassiana</i> . Represented by <i>ef1α</i> bands (treatments' 1-4) and viable colonies (treatment 5) detected following surface sterilisation (SS) protocol's A or B, for each treatment used during the <i>Zea mays</i> (maize) PMA™ assay.	44
Figure 2.8.	Images of putative <i>Beauveria bassiana</i> colonies growing from surface sterilised (SS) plant tissue. Tissue treated following 3 hours of incubation of inoculum (from experimental treatment 5). Image (a) shows early stage growth from cut ends of root	

	(3 days after SS) and (b) shows sporulating culture from later stage growth (12 days after SS).....	45
Figure 2.9.	Confocal images of <i>Beauveria bassiana</i> colonising the maize root surface after surface sterilisation. Tissue was surface sterilised following 3 days of incubation after inoculation. Fungal material was stained to fluoresce green using WGA-Alexa fluor 488 conjugate and plant material red with propidium iodide dye. Image (a) shows <i>B. bassiana</i> isolate BG11 colonising to the first three layers of the parenchyma cells. Images' (b) and (c) shows how intricately the fungal mycelia (BG11) interacts with the root surface.....	46
Figure 3.1.	A photograph of an inoculated <i>Zea mays</i> (maize) seedling. Seedling shown 5 days after sowing, growing on 1% agar. The arrow indicates the location the razor incision made to the base of the emerging shoot with fungal hyphae inserted.....	53
Figure 3.2.	The growth and development stages of <i>Zea mays</i> (maize). Vegetative growth ranges between vegetative emergence (VE) to V(n), where n = number of leaves, through to vegetative tasseling (VT); followed by reproductive stages (R1 – R6). Figure sourced from Pioneer (Du Pont): https://www.pioneer.com/home/site/us/agronomy/library/staging-corn-growth/ ..	54
Figure 3.3.	Sampling of <i>Zea mays</i> (maize) plants at 30 days after inoculation (for treated plants) for the plant growth experiment A. Photograph (a) shows the single photon avalanche diode (SPAD) ratio measurement for chlorophyll content and photograph (b) shows the measurement of the internode distance (mm). Photo credit: David Hollander.	55
Figure 3.4.	Sampling of <i>Zea mays</i> (maize) plants at 30 days after inoculation (for treated plants) for the plant growth experiment A. Photograph (a) shows the measurement of the above ground plant length photograph (b) shows the root-mass length being measured. Photo credit: David Hollander.	56
Figure 3.5.	High resolution scanned image (400 dpi) of maize roots. Harvested at 30 days after inoculation and then prepared for root parameter analysis in WinRHIZO.	58
Figure 3.6.	Treatment means for growth parameters measured in the <i>Zea mays</i> (maize) plant growth experiment A. Treatment differences were determined by a least significant difference (LSD) test (5%); half LSD bars are featured for visual reference. Plot (a) illustrates chlorophyll content (SPAD ratio) differences between the treatment groups. Plot (b) shows the differences in overall biomass (plant dry weight, g) for each treatment group.....	60
Figure 3.7.	Treatment means for growth parameters measured in the <i>Zea mays</i> (maize) plant growth experiment A. Treatment differences were determined by a least significant difference (LSD) test (5%); half LSD bars are featured for visual reference. Plot (a) illustrates differences between the groups for the ratio of root biomass over shoot biomass. Plot (b) shows the differences in the ratio between root length and shoot length.	61
Figure 3.8.	Treatment means for growth parameters measured in the <i>Zea mays</i> (maize) plant growth experiment B. Treatment differences were determined by a least significant difference (LSD) test (5%); half LSD bars are featured for visual reference. Plot (a) illustrates chlorophyll content (SPAD ratio) differences between the treatment groups. Plot (b) shows treatment biomass (g), which were not statistically different ($P > 0.05$).	63
Figure 3.9.	Treatment means for growth parameters measured in the <i>Zea mays</i> (maize) plant growth experiment B. Treatment differences were determined by a least significant difference (LSD) test (5%); half LSD bars are featured for visual reference. Plot (a) illustrates group means for the ratio of root biomass over shoot biomass. Plot (b) shows the means for the ratio between root length and shoot length.	64
Figure 3.10.	Root structure analysis for <i>Zea mays</i> (maize) performed in WinRHIZO 4.1: (A) shows a scanned image of an experimental root sample under analysis, and the two plots show the mean root length (cm) estimated for each experimental treatment. Plot (b)	

	shows mean root length for fine roots ($0 \leq 0.5$), contrasted with thicker roots ($3.0 \leq 3.5$) in plot (c). Statistical differences are indicated by letters next to half LSD bars (5% significance level) for each treatment.	66
Figure 3.11.	Root structure analysis for <i>Zea mays</i> (maize) performed in WinRHIZO 4.1. Plot (a) shows mean projected area (cm ²) for fine roots ($0.5 < P.A. \leq 1.0$), contrasted with thicker roots ($3.5 \leq 4.0$) in the plot (b). Statistical differences are indicated by letters (where applicable) next to the half LSD bars (5% significance level) for each isolate treatment and controls.....	67
Figure 3.12.	Root structure analysis for <i>Zea mays</i> (maize) performed in WinRHIZO 4.1. Plot (a) shows root volume (cm ³) for fine roots ($0.5 \leq 1.0$), contrasted with thicker roots ($3.5 \leq 4.0$) in plot (b). Statistical differences are indicated by letters next to the half LSD bars (5% significance level) for each isolate treatment and controls.	67
Figure 4.1.	Photograph of <i>Beauveria bassiana</i> , cultured on potato dextrose agar (PDA).	77
Figure 4.2.	Electrophoresis gel image of <i>ef1α</i> product. The bands (176 bp) were amplified using EF4F and EF4R primers in the second step of a nested PCR from the rhizosphere soil of <i>Zea mays</i> (maize) plants (30 cycles), for 6 and 15 days after inoculation (DAI) with <i>Beauveria bassiana</i> isolates BG11, FRh2 and J18. In wells' 1-3 are the no-template controls (NTC) (from both the 1 st and 2 nd PCRs), followed by a <i>B. bassiana</i> positive control and then the experimental samples (not all data is shown).....	85
Figure 4.3.	Percentage of <i>ef1α Beauveria bassiana</i> positive in the rhizosphere soil of <i>Zea mays</i> (maize). Calculated from positive PCR detection over three sampling events, 6, 15 and 30 days after inoculation (DAI). Positive samples were summed for each isolate treatment and control, and then calculated as percent present (Y axis) over samples.	86
Figure 4.4.	<i>Beauveria</i> in the rhizosphere soil of damaged <i>Zea mays</i> (maize) plants. Comparison of the herbivory (H) versus non-herbivory (N) control treatment means, presented as percentage of <i>ef1α Beauveria bassiana</i> detected by PCR in samples from the rhizosphere soil of <i>Zea mays</i> (maize) at 30 days after inoculation (DAI), for different isolate treatments versus a no-inoculum control.	86
Figure 4.5.	Electrophoresis gel image of <i>ef1α</i> product. The bands (176 bp) were amplified using EF4F and EF4R primers in the second step of a nested PCR from the rhizosphere of <i>Zea mays</i> (maize) plants at 30 days after inoculation (DAI) with <i>Beauveria bassiana</i> isolates BG11, FRh2 and J18. In wells' 1-3 are the no-template controls (NTC) (from the 1 st and 2 nd PCRs), followed by a <i>B. bassiana</i> positive control and then the experimental samples.....	87
Figure 4.6.	Percentage of <i>ef1α Beauveria bassiana</i> detected by PCR in or on the root tissue of <i>Zea mays</i> (maize). Presence of the isolates were recorded over three sampling events, 6, 15 and 30 days after inoculation (DAI). The number of positive samples were summed for each isolate treatment and control, and then calculated as percent present over samples (Y axis).	87
Figure 4.7.	DNA concentration (ng/μL) yield. Yield was plotted over a range (experiment minimum and maximum) of <i>Zea mays</i> (maize) root tissue weights (g) using the MO BIO Power Plant Pro DNA isolation kit.	88
Figure 4.8.	The relationship between DNA sample tissue weight and PCR amplification. Plot shows cycle threshold means for <i>ef1α</i> target (primers EF4F and EF4R) from all qPCR replicates (over three nested qPCR experiments and all sample times) of all samples treated with <i>Beauveria bassiana</i> (the no-inocula control samples are excluded here), plotted over root tissue weight in grams (g) and fitted with a linear regression line (adjusted $R^2 = 0.34$).....	89
Figure 4.9.	Amplification variation between thermal cycling experiments. Cycle threshold means (CT) compared over three real-time qPCR experiments for <i>ef1α</i> (primers EF4F and EF4R) amplifying the same DNA template (diluted 1/1000 μL H ₂ O); generated from primary PCR (amplicon from primers EF3F and EF5R) of pure <i>Beauveria bassiana</i> (0.32 ng/μL), prepared prior in a 10-fold dilution series, to test consistency between	

	PCR experiments and replicates. A 5% least significant difference (LSD) bar representing all treatments is displayed.	89
Figure 4.10.	Amplification of <i>Beauveria</i> isolates and non-target control at different harvest times. Cycle threshold means (CT) from qPCR amplification of the <i>ef1α</i> <i>Beauveria</i> gene in or on the root tissue of <i>Zea mays</i> (maize) over three sampling events, 6, 15 and 30 days after inoculation (DAI). A 5% least significant difference (LSD) bar representing all treatments is displayed.	91
Figure 4.11.	Depiction of the generalised linear model (GLM) to test isolate differences. Figure shows the coefficient plot of model estimates with standard error bars, based on cycle threshold (CT) values from qPCR amplification of the <i>ef1α</i> <i>Beauveria</i> gene in or on the root tissue of <i>Zea mays</i> (maize). The isolate treatment reference in the model is the control group, sample time reference is 6 days after inoculation (DAI), and the block reference is block 1.	91
Figure 4.12.	Denaturing gradient gel electrophoresis images. Gels show the general fungi set generated from PCR using the nested primer pairs AU2 & AU4 and FF-390 & FR1-GC, representing all fungi in the <i>Zea mays</i> (maize) rhizosphere soil DNA from 30 days after inoculation (DAI) samples (3 replicates per treatment). The first lane of each gel (2 gels are shown with 12 lanes per gel) indicates the reference sample (BG11 sample 7) from which bands were calibrated in Phoretix™.	92
Figure 4.13.	Grouping of community data visualised for <i>Beauveria</i> isolate versus for the herbivory treatment. Depicted by non-metric multiple dimension scaling (nMDS) plots representing dissimilarities between PCR amplicon profiles from denaturing gradient gel electrophoresis (DGGE) experiments on samples from 30 days after inoculation (DAI) of <i>Zea mays</i> (maize) rhizosphere soil DNA, with isolate and herbivory treatments indicated (plots legends), for alphaproteobacteria (a, b) and betaproteobacteria (c, d) groups.	94
Figure 4.14.	Grouping of community data visualised for <i>Beauveria</i> isolate versus for the herbivory treatment. Depicted by non-metric multiple dimension scaling (nMDS) plots representing dissimilarities between PCR amplicon profiles from denaturing gradient gel electrophoresis (DGGE) experiments on samples from 30 days after inoculation (DAI) of <i>Zea mays</i> (maize) rhizosphere soil DNA, with isolate and herbivory treatments indicated (plots legends), for arbuscular mycorrhizal fungi (a, b) and total fungi (c, d) groups.	95
Figure 4.15.	Grouping of functional community data visualised for <i>Beauveria</i> isolate versus for the herbivory treatment. Non-metric multiple dimension scaling (nMDS) plots representing marginal dissimilarities in two dimensions, between respiration profiles of the microbial communities from 30 days after inoculation (DAI) of <i>Zea mays</i> (maize) rhizosphere soil, obtained from MicroResp™ colorimetric readings. Plots are distinguished by either isolate (a) or herbivory (b) treatments as grouping factors. ..	96
Figure 5.1.	Multidimensional scaling (MDS) plot of maize microarrays replicates. MDS ordination plot based on Euclidean distance of the log2 fold change (FC) values generated from microarray intensities to represent gene expression profiles from roots of <i>Z. mays</i> (maize) in response to colonisation/inoculation of two different <i>B. bassiana</i> isolates (BG11, J18) versus a no-inoculum control (green). Samples are coloured coded to microarray replicate.	109
Figure 5.2.	Multidimensional scaling (MDS) plot of maize microarrays by treatment. MDS ordination plot based on Euclidean distance of the log2 fold change (FC) values generated from microarray intensities, to represent gene expression profiles from the roots of <i>Z. mays</i> (maize) in response to colonisation/inoculation of two different <i>B. bassiana</i> isolates (BG11, J18) versus a no-inoculum control (green). Samples are coloured by inoculum treatment or control.	110

Chapter 1

General introduction

1.1 Plant protection and biological control

Plant crops grown for human and livestock consumption are continually challenged by environmental stresses such as drought, high-salt and extreme temperatures, in addition to pathogen and pest attacks, all of which have adverse effects on plant growth and crop yields (Oerke 2006). Globally, crops such as maize, *Zea mays* L. (Cyperales: Poaceae), have shown increased productivity over the past century, but the combined global crop losses due to weeds, pests and diseases may be up to 40% of net plant productivity, of which ~20% are the result of insect herbivory (Mitchell et al. 2016).

Reducing damage from herbivory can result in significant economic savings as well as improving sustainability of food and forage production. Though there are various chemical pesticides used to control pests, the concern for public health, the environment and the impact on non-target organisms presents an ongoing challenge for primary production (Maroni et al. 2006). Additionally, the development of pest resistance to pesticides is occurring more frequently as a result of the increased exposure to these chemicals (Harvey-Samuel et al. 2015). Biological control agents can be used as alternatives to chemical pesticides in 'biopesticide' formulations that can be host specific, are frequently found resident in the natural environment and generally pose no threat to human health (Cook 1993; Eilenberg et al. 2001; Kepler et al. 2017). Furthermore, biological control can be an effective means to control pests and is therefore an important alternative, or at least a supplement, to chemical pesticide use especially in integrated pest management (IPM) programmes (Chandler et al. 2011).

Certain fungi and bacteria can be used as biological control (biocontrol) agents to control insect pests and pathogens of plants (Porrás-Alfaro and Bayman 2011; Whipps 2001). As a subject, the potential for biocontrol has generated a substantial amount of research in the past few decades and from a range of disciplinary backgrounds. Generally, biocontrol agents have been used to control: (1) invertebrate pests with parasitoids, predators or pathogens, (2) weeds by using herbivores and pathogens and (3) plant pathogens with antagonistic microbial control agents (Deacon and Berry 1993; Kepler et al. 2017; Ownley et al. 2004; Scheepmaker and Butt 2010; Shores et al. 2010). Frequently, living agents are applied as biopesticides to the intended environment in relatively significant volumes. This approach is known as 'inundation biological control', which is defined by Eilenberg et al. (2001) as 'The use of living organisms to control pests when control is achieved exclusively by the released organisms themselves'. Such inundation biocontrol agents are often lethal

microbial pathogens and/or their products. For example, *Bacillus thuringiensis* (Bt) is a bacterial biocontrol agent that produces certain insecticidal toxins (Cry toxins) that are lethal to most insects when ingested (Hofte and Whiteley 1989). However, the concept of biopesticides for inundative application as an alternative to synthetic pesticides has resulted in biocontrol agents being selected for pest control on the basis of pathogenicity and efficacy, with little focus on ecological suitability or function (Waage 1997).

Plants are not merely individual organisms, but hosts to complex communities of microbes and invertebrates. Every plant has a unique and diverse composition of microorganisms colonised on its outer and internal tissues, all of which collectively constitute the microbiome. The health of the host plant may both depend and be affected by the composition of the microbial flora in the microbiome (Porras-Alfaro and Bayman 2011), as the interactions may be negative, positive or anything in between.

1.2 Endophytes for plant protection

Among the microorganisms that interact with plants within the microbiome, are the endophytes which live and grow within the plant's tissues (Bacon and White 2016). The term "endophyte" was first coined by De Bary (1866) and constitutes an organism, usually a bacterium or fungus, which lives within plant tissues yet without causing symptoms of disease (Wilson 1995). Plant roots as well as foliage, flowers, seeds and stems can be colonised by endophytes, although the endophytic organism may not remain within the host for the full duration of a lifecycle (Schulz and Boyle 2005). The term 'endophyte' is broad, and includes multiple functional groups such as latent pathogens, latent saprotrophs, mycorrhizal and rhizobia colonisers, in addition to mutualistic and commensalistic symbionts (Porras-Alfaro and Bayman 2011). For this reason, the definition of an endophyte is more indicative of the organism's location rather than function. Generally, symbiotic interactions are more frequently defined by the fitness benefits provided to each organism involved in the association (Rodriguez et al. 2008). In a plant-fungal symbiosis, the benefits to host plants can be either positive (mutualism), neutral (commensalism and neutralism) or negative (parasitism, competition and amensalism) (Singh et al. 2011). Nevertheless, extensive research conducted over decades on microbial endophytes (Clay 1989; Petrini 1986) and rhizobacteria (Kloepper et al. 2004) has revealed the complex yet important role that the plant microbiome plays in supporting plant growth and fitness (Bacon and White 2016). Endophytic microbes have been reported to confer benefits to the host in three different ways: 1) by alleviating abiotic stress of the host plant; 2) by defending host plants from biotic stressors; and 3) by supporting the host nutritionally, usually by enhancing nitrogen, phosphorus, iron or vitamin acquisition (White Jr et al. 2014). While the potential to harness the functional aspect of non-pathogenic endophytes and epiphytes for plant protection is

generally recognised, the outcome of manipulating microbiome populations via the introduction of certain organisms still requires elucidation, in terms of how the function may be altered and/or what mechanisms are involved (Bacon and White 2016). The diversity of endophyte species within a host plant can be extensive (Arnold and Lutzoni 2007) and the functional role of each member of the microbiome is often unclear, but there is potential to obtain novel plant growth promoting and/or defending endophytic microbes for plant protection.

The degree of intimacy between plants and microorganisms can vary substantially. Microorganisms that require plant tissues to complete their life cycle are classified as “obligate.” On the other end of the spectrum are the “opportunistic” endophytes that live predominantly outside plant tissues and on occasion may enter the plant endosphere (Hardoim et al. 2008). Between these two classes are an intermediate group, which comprises the vast majority of endophytic microorganisms, and these are classed as the “facultative” endophytes. Whether facultative endophytes take advantage of the plant as a vector for dissemination (i.e. as a parasite) or are actively selected by the host is still a subject of debate (Hardoim et al. 2015; Kale and Tyler 2011; Saikkonen et al. 2010b; Tyler and Triplett 2008). Facultative endophytes must consume some nutrients provided by plants and therefore theoretically reduce the ecological fitness of the host plant. Yet there may still be a lack of observable disease symptoms, and this lack of symptoms is a point often used as an argument that facultative endophytes must be mutualists in plants, even when the nature of the interaction is unclear (Hardoim et al. 2015).

Once a symbiosis is established, the endophyte may be restricted in terms of distribution and metabolic activity within plant tissues; remain localised in tissues in a nearly dormant phase or proliferate systemically throughout multiple tissues of the host (Rodriguez et al. 2009). Endophytes are typically observed in intercellular spaces (Christensen et al. 2008); although bacterial endophytes, in particular, may become intracellular and enter into host cells via the cytoplasm or become confined within periplasmic spaces, i.e. between the cell wall and the cell plasma membrane (Thomas and Sekhar 2014). Epiphytes are organisms that may collectively play an important role in plant microbiomes, and are defined as non-pathogenic fungi, bacteria, or algae that remain restricted to plant surfaces (above or below-ground), without penetrating to internal tissues (Zambell and White 2015).

Carroll (1988) defined two groups of endophytic fungi: constitutive mutualists (Class I endophytes) and inducible mutualists (Class II endophytes). The Class I Clavicipitaceous endophytes, which are represented by the genus *Epichloë* (also formerly *Neotyphodium* for anamorphic species) (Leuchtman et al. 2014), are systemic, vertically transmitted from seed, and infect grasses exclusively (*Festuca* and *Lolium* spp.). The Class II endophytes are more taxonomically diverse, infect

a broad range of hosts, are typically characterised by non-systemic infection of the host and are horizontally transmitted (Rodriguez et al. 2008). Today, the Class I *Epichloë* spp. endophytes are widely exploited for biological plant protection in agricultural pest management and a considerable amount of research has been conducted on this group in particular (Cheplick and Clay 1988; Clay 1989; Eaton et al. 2010; Felitti et al. 2006; Kauppinen et al. 2016; Khan et al. 2010; Qawasmeh et al. 2015; Saikkonen et al. 2010a; Tanaka et al. 2005; Young et al. 2006). Although these fungi are generally thought to be beneficial to the host and may provide protection from herbivory, they can also be parasitic during the reproductive phase of their lifecycle in which they castrate the host plant to produce stromata, structures which form in the place of the seed head of the grass plant (Clay and Jones 1984; Wilson 1995). From this example alone it is evident that the endophyte-host interaction is complex, and it is consequently important to understand the complete life-history strategy of an endophytic organism, along with the ecological implications of artificial introduction. The potential application of Class II endophytes for the biocontrol of pests is still relatively unexplored. An increasingly studied group of putative endophytes belongs to the fungal entomopathogens, fungi known to cause infections in insects (Vega et al. 2012).

1.3 Entomopathogenic fungi-plant interactions

Two genera from the order Hypocreales, are fungal entomopathogens that are most frequently studied for their endophytic biocontrol potential. These are *Metarhizium* Sorokin (Clavicipitaceae) and *Beauveria* Vuillemin (Cordycipitaceae) (Sung et al. 2007; Vidal and Jaber 2015). In the *Metarhizium* genus, there is considerable phylogenetic divergence. Certain species, such as *M. acridum*, are known to have limited insect-host ranges compared to other species such as *M. robertsii* that have broad insect-host ranges (Humber 2008). The application of *Metarhizium* and *Beauveria* spp. as biocontrol agents to directly control insect pests in agroecosystems was already well established by the 20th century (Madelin 2012), and since then many commercial formulations have been designed and approved for crop protection (Faria and Wraight 2007). Following the original literature from Vakili (1990) and Bing and Lewis (Bing and Lewis 1991; Bing and Lewis 1992a; Bing and Lewis 1992b; Bing and Lewis 1993), who first reported the endophytic establishment of *B. bassiana* (Bals.) Vuill. in the leaves of *Zea mays*, the idea of using *Beauveria* and later *Metarhizium* as endophytic agents for plant protection has since generated much interest and research (Behie et al. 2015; McKinnon et al. 2017; Sasan and Bidochka 2012; Vega et al. 2008; Vidal and Jaber 2015). However, there has been a relatively limited number of studies investigating the biological processes involved in plant host colonisation and persistence (Landa et al. 2013; Quesada-Moraga et al. 2014; Sasan and Bidochka 2012; Wagner and Lewis 2000). Furthermore, endophytism has not yet been proven for all species (Barelli et al. 2016). Although literature indicates a frequent association with multiple plant species, with reports of isolation of *B. bassiana*, in particular, from both above and

below ground plant organs (see McKinnon et al. (2017) for a review), the genotypic basis for endophytism and the biological mechanism involved in proliferation within a plant host have not been elucidated. Among species of *Metarhizium*, *M. robertsii* and *M. brunneum* are the species that have been shown capable of growing internally within plants. Specifically, *M. robertsii* has been reported to colonise roots of switchgrass (Sasan and Bidochka 2012), wheat, haricot bean, soybean (Behie et al. 2015) and *Arabidopsis thaliana* (Liao et al. 2017), and *M. brunneum* from broad bean leaves (Jaber and Enkerli 2017). Among species of *Beauveria*, only one report (Jaber and Enkerli 2017) has recorded any species (*B. brongniartii*) other than *B. bassiana* as endophytic. In that study, isolates of *B. brongniartii*, *B. bassiana* and a single isolate of *M. brunneum* were inoculated and recovered from broad bean leaves at 7 and 14 days after inoculation by culturing surface sterilised leaf fragments on selective media.

In order to infect insects, entomopathogenic fungi must adhere to the insect host's cuticle (Wang and St Leger 2007; Zhang et al. 2011). Adherence to plant cuticle is therefore presumably an important mechanism to predicate plant colonisation for endophytic establishment by these fungi (Barelli et al. 2016). Wang and St Leger (2007) demonstrated that the gene *Mad2* in *M. robertsii* encodes a plant adhesin that is necessary for attachment to plant roots. For example, the *Mad2* gene was found to be significantly upregulated when *Metarhizium* was grown in the presence of root exudates and a transgenic knockout (for *Mad2*) of the fungus was not able to adhere to onion epidermis. A suggested orthologue of *Mad2* was reported within the genome of *B. bassiana* (but with 47% identity), suggesting a gene similar to *Mad2* may enable *Beauveria*-plant adhesion (Xiao et al. 2012). Additionally, certain hydrophobin proteins have been demonstrated to be important elements involved in plant and insect cuticle attachment for *B. bassiana* (Zhang et al. 2011). Proteases are considered important during cuticular penetration for insect infection but may also be involved in plant colonisation. Proteases found in *Metarhizium* (Pr1 subtilisin-like) and *B. bassiana* are homologues of the fungal protease, At1, from the grass endophyte *Acremonium typhinum* (Reddy et al. 1996). However, At1 is also homologous to proteases involved in general fungal plant pathogenicity but nonetheless may facilitate symbiotic development also through the degradation of the plant cell wall and apoplastic proteins that enable colonisation (Reddy et al. 1996).

1.3.1 *Beauveria bassiana*

Identity of *Beauveria* spp.

Agostino Bassi (1773–1856) was the first to demonstrate that the muscardine disease of silkworms was caused by the pathogenic fungal agent *Beauveria bassiana* (then named *Botrytis bassiana*). Indeed, this was the first demonstration of the germ theory of disease (Goettel et al. 2010). In 1837, *B. bassiana* was found to infect other insect species, enabling the prospect of using insect pathogenic

(entomopathogenic) fungi to control insect pests (Audoin 1837). Since then, species of *Beauveria* have been reported to have relatively broad insect-host ranges, to occur world-wide and have been found in a many habitats, although principally from soil and phyllosphere (Bissett and Widden 1988; Glare et al. 2008; Meyling et al. 2009; Rehner et al. 2006). Insect hosts of *Beauveria* species are found in multiple insect orders such as Coleoptera, Hymenoptera, Heteroptera, Homoptera, Lepidoptera, Diptera, Orthoptera, Siphonaptera, Isoptera, Mantodea, Thysanoptera, Neuroptera, and Blattodea. Members of the *Beauveria* genus have characteristic branched, penicillate or trichodermoid conidiophores with dense clusters of sympodial and globose or flask-shaped conidiogenous cells that have apical denticulate (or zig-zag) rachis (Zimmermann 2007). Conidia are hyaline, globose to broadly ellipsoidal and are formed in spherical clusters. The conidial clusters are thus thought to look like snow balls or cotton balls (Rehner et al. 2011). The most recent taxonomic analysis of the *Beauveria* genus was conducted using molecular identification methods to conduct a multilocus phylogenetic analysis that comprised 12 well supported terminal lineages for *Beauveria*, with clades for *B. amorpha*, *B. bassiana*, *B. brongniartii*, *B. caledonica*, *B. malawiensis*, *B. vermiconia*, *B. asiatica*, *B. australis*, *B. kipukae*, *B. pseudobassiana*, *B. sungii* and *B. varroae* (Rehner et al. 2011). A recent study from China described an additional species, *Beauveria araneola*, that is reported to be phylogenetically distinct within the genus and was isolated from a spider (Chen et al. 2017).

The infection process for *Beauveria* spp. on insect hosts has been well characterised (Vega et al. 2012). It involves the mass production of asexual conidia on cadavers of insect hosts that may germinate on contact with a susceptible host to form a tube that can directly penetrate the insect cuticle. The fungus then multiplies in the haemocoel of the insect, eventually causing death. The fungus then emerges through the cadaver and in suitable conditions, sporulates. An abundance of conidia may consequently become available in the environment to infect susceptible insect hosts.

***Beauveria* as a plant coloniser**

Following the report that *B. bassiana* was able to grow endophytically within the green tissues of maize without causing disease (Bing and Lewis 1991), the same endophytic isolates were shown to effectively control European corn borer, *Ostrinia nubilalis* (Lepidoptera: Crambidae), under laboratory conditions (Bing and Lewis 1992b). Eventually, Wagner and Lewis (2000) and Gomez-Vidal et al. (2006) attempted to visualise the endophytic colonisation of *B. bassiana* in *Z. mays* using light and transmission- or scanning- electron microscopy (TEM and SEM). Although their images demonstrated fungal colonisation of inoculated plant tissue, other resident fungal endophytes may have been present and were neither identified nor differentiated from the inoculum. More recently, *B. bassiana* isolate EABb-04/01-Tip transformed with a green fluorescent protein (GFP) was visualised in association with opium poppy leaf, leaf-vein and stem, using confocal microscopy (Landa et al. 2013). Hyphal growth was observed primarily on or near epidermal cells and by 10-15 days after

inoculation (DAI) the quantity of fluorescent conidia/hyphae had significantly declined. Behie et al. (2015) also evaluated *Beauveria* and *Metarhizium* inoculated root samples of haricot bean using confocal microscopic techniques. However, they did not present any images of internal colonisation by the fungus in the bean roots but rather provided images of the fungi cultivated from crushed plant tissue imprints. Both studies (Behie et al. 2015; Landa et al. 2013) suggest that endophytic occurrence may be rare or opportunistic in nature, even after inundative application.

The study of endophytes is generally acknowledged to be method-dependent and thus problematic (Hyde and Soyong 2008). Whilst the biocontrol potential of endophytic *Beauveria* spp. is currently highly topical, there are still fundamental questions to be addressed concerning the functional role of endophytic isolates. The majority of studies pertaining to *Beauveria*-plant associations involve cultivation of the fungi from surface sterilised plant tissue fragments (McKinnon et al. 2017; Vidal and Jaber 2015). Predominantly, these studies isolate the fungi following inoculation of the plants with specific *Beauveria* isolate, although there are a number of studies that have also isolated *B. bassiana* from plant tissue during a survey of naturally occurring endophytes (Campos et al. 2010; Ganley and Newcombe 2006; Gonzalez and Tello 2011; Reay et al. 2010; Vega et al. 2008). Several studies have also used molecular methods (Castillo Lopez et al. 2014a; El-Deeb et al. 2012; Jia et al. 2013; Landa et al. 2013; Quesada-Moraga et al. 2006; Quesada-Moraga et al. 2014; Reddy et al. 2009) and microscopy (Gomez-Vidal et al. 2006; Quesada-Moraga et al. 2006; Wagner and Lewis 2000) to detect the fungi *in planta*.

Isolation methods used in natural endophyte surveys have frequently been employed in artificially inoculated systems, yet a distinction should be made. Natural endophyte surveys presume no prior association of any target fungus in particular. For this reason, it may not necessary to absolutely exclude the epiphytic community with stringent methodology, which may be present in limited quantity in contrast with inoculated tissues (Porrás-Alfaro and Bayman 2011; Schulz and Boyle 2005). In contrast, it is common practice to apply the artificial inoculum in high quantity to plant surfaces, with the presumption that inundative application will maximize the opportunity for endophytic colonisation. It is logical to consider therefore, that the exclusion of propagules remaining on external surfaces after inoculation is highly important in order to confirm endophytic effects to plants and herbivores, and that the isolation and detection methods used be appropriate for this scenario. Only with the use of stringent methodology, can the genuine biocontrol potential of endophytic *Beauveria*, in addition to other 'endophytic' insect pathogenic fungi, be properly elucidated (Hyde and Soyong 2008; Schulz and Boyle 2005).

A recent study by Behie and Bidochka (2014) showed that both *Metarhizium* and *Beauveria* are able to translocate insect-derived nitrogen to plants in close proximity to the cadaver via the rhizosphere.

Since up to 31% of plant nitrogen in an ecosystem can be lost to insects as a result of herbivory, this study illustrates a potential strategy whereby plants can reacquire nitrogen otherwise lost through insect consumption, by supporting an association with an endophytic insect pathogenic fungus (Behie et al. 2012). While studies like this suggest the potential to provide benefit to plants through endophytic and rhizosphere associations, possible interactions within the plant microbiome, following inundative inoculation (Eilenberg et al. 2001), have scarcely been investigated (Larsen et al. 2015).

There is a broad range of microorganisms including bacteria and fungi that may mediate or inhibit biocontrol activities in the rhizosphere and within the natural endophyte community of a plant host (Hardoim et al. 2015). Biocontrol can also involve multiple modes of action, including: parasitism, antagonism, competition for nutrients and space and/or induction of plant defences (Whipps 2001). Possible non-target effects of biocontrol agents to other resident microorganisms in the microbiome and their functions have been largely ignored within inoculated systems (Brimner and Boland 2003), yet such interactions in the microbiome may impact successful integration of potentially beneficial microorganisms, such as *Beauveria*, in agroecosystems. A few studies have demonstrated that interactions among taxonomically related microbial endophytes can alter entire populations inside the host plant (Andreote et al. 2009; Elasri et al. 2001). Furthermore, bacterial and fungal endophytic communities are typically investigated independently, but potential interactions between these groups warrant investigation and may reveal a fascinating new field in endophyte research (Frey-Klett et al. 2011).

While the vast majority of endophytes are typed as commensals with unknown functions in plants, only a small group of endophytes have been shown to have either positive (mutualistic) or negative (antagonistic) effects on plants (Hallmann et al. 1997). These properties are often tested under strict environmental conditions in plant-endophyte interaction studies (Hardoim et al. 2015). For example, studies of plant-endophyte interactions that use *Beauveria* are commonly based on controlled, optimised conditions for growth of the host-plants and not on variable, field-realistic conditions. Effects observed from endophytes and/or rhizosphere colonising insect pathogenic fungi in healthy plants may change drastically when the same host plants are subjected to less favourable or even stressful conditions (Gonzalez et al. 2016; Hardoim et al. 2015).

1.3.2 The rhizosphere

The plant rhizosphere describes the area that includes a few millimetres of soil surrounding the plant root, where many important and multipartite biological processes occur (Bruck 2010). Complex interactions between roots, root exudates, microorganisms and invertebrates take place in the rhizosphere. Hiltner (1904) first defined the “rhizosphere effect” after observing that

microorganisms were more abundant and active in close proximity to plant roots. He observed that bacterial populations increased by 10-1000 fold in the area immediately surrounding the roots compared to the greater 'bulk' soil outside of the root zone (Lugtenberg et al. 2002). This increase in microbial population has since been attributed to the influence of root exudates, which can either stimulate or inhibit the microbiome, in terms of the community structure and function (St. Leger 2008). Microbial interactions that occur in the rhizosphere typically include those associated with detritus and/or those that rely on living plant roots (Barea et al. 2002). The rhizosphere is divided into three regions. These are (1) the rhizoplane (the root surface), (2) the endorhizosphere (internal root system) and (3) the ectorhizosphere (the soil layer that adheres to the root surface) (Figure 1.1). The roots themselves are also an important component of the rhizosphere, and include the root endophytic microorganisms (Lareen et al. 2016; Larsen et al. 2015). Root exudates include low-molecular weight compounds such as organic acids, sugars, amino acids, phenolics and other secondary metabolites, as well as high-molecular weight compounds, such as proteins and polysaccharides (Badri and Vivanco 2009). The quantity and composition of plant exudates released into the soil is dependent upon the plant species, its stage of growth and nutrient status. Exudates produced from a single root may provide anywhere between 0.03 mg and 15 mg per gram of soil within the submillimetre soil zone (Burgmann et al. 2005). The rhizoplane also includes a layer of mucigel, a gelatinous coating which encapsulates the root surface providing both nutrients and a refuge to a suite of bacterial and fungal species (Lugtenberg et al. 2002). The plant may therefore regulate the microbial community by promoting and acquiring those organisms that can assist the plant by solubilising inorganic nutrients, which in turn, render the soil-nutrient reservoir bioavailable to the host (Lee et al. 2012).

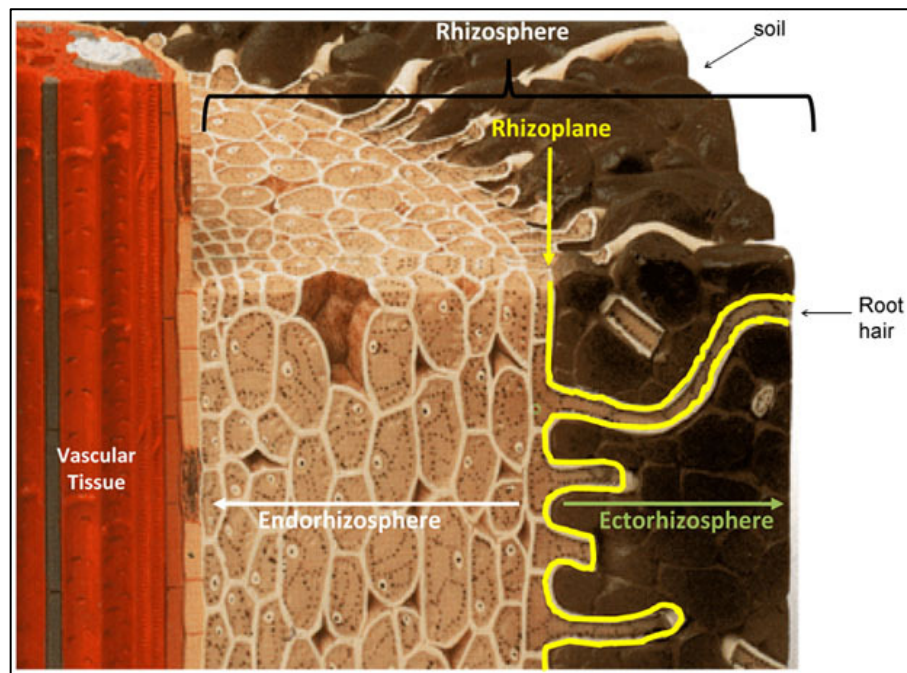


Figure 1.1. The rhizosphere regions illustrated. Figure sourced from: <http://www.nature.com/scitable/knowledge/library/>.

Carbon flows from the plant to the rhizosphere as simple organic compounds providing the necessary nutrition to support the microbiological processes that are crucial for soil ecosystem functioning (Jones et al. 2009). In particular, photosynthates flow rapidly from the plant to the soil that supports the rhizosphere microbiome, which then provides food for microbial grazers and their predators in a cascade effect (Fitter et al. 2005). Bacteria and fungi are the dominant members of the microbiome that affect plant and soil C, N and P dynamics (Philippot et al. 2013). However, bacterial and fungal grazers (protozoa, nematodes, mites and collembolans) and predators of grazers (predator mites and nematodes) are also considered important regulators of biogeochemical processes (Bonkowski 2004; Coleman 2008). Beneficial microorganisms (plant growth promoters) and pests (pathogens and soil-dwelling insects) are common residents of the rhizosphere (Morgan et al. 2005; Raaijmakers et al. 2009; Whipps 2001), all of which may influence C, N and P biogeochemical processes in the soil. Functional aspects pertaining to beneficial members of the rhizosphere microbiome, with respect to plant nutrition and health, include organic matter decomposition, P solubilisation and transport, N fixation and the biocontrol of root pests (Larsen et al. 2015; Philippot et al. 2013).

The rhizosphere microbiome can also host certain biocontrol agents that are able to antagonise soil-borne plant pathogens (Baker 1991; Whipps 1997). The ability to colonise and grow within the rhizosphere is termed rhizosphere competence. More specifically, rhizosphere competent organisms are able to exploit the free carbon from root exudates and sloughed root cap-cells for growth and sustenance (Bruck 2010). There are many fungal species that are rhizosphere competent. Hu and St

Leger (2002) inadvertently discovered that an isolate of *Metarhizium anisopliae* persisted in the rhizosphere during field trials intended to track transgenic fungal clones over time. Rhizosphere competence was observed to be most pronounced in the top three cm of the soil profile. The cause for this effect was attributed to either the plant root density at that particular depth and/or the conidial inoculation application method (i.e. soil drench at the surface). Furthermore, the dispersal and distribution of the inoculated fungi correlated directly with the arrangement of the roots within the soil profile, providing evidence for rhizosphere colonisation (Hu and St Leger 2002). Following this discovery, Bruck (2005) and shortly after St. Leger (2008) demonstrated that *M. anisopliae* can persist for longer in the rhizosphere compared to in bulk soil. Bruck (2005) observed that the number of colony forming units (CFUs) for *M. anisopliae* actually increased over time in the rhizosphere, which suggests that *M. anisopliae* can utilise available carbon provided in the rhizosphere for growth, rather than just persist longer there as a result of improved soil structure, compared to the bulk soil. Three additional species of *Metarhizium*, *M. robertsii*, *M. brunneum* and *M. guizhouense*, were tested for plant-specific rhizosphere associations (Wyrebek et al. 2011). The results suggested a non-random association of these *Metarhizium* spp. with certain plants, for example, *M. robertsii* was the only species isolated from grass roots, *M. guizhouense* associated exclusively with trees (particularly the sugar maple, *Acer saccharum*) and *M. brunneum* was isolated from the rhizosphere of shrubs and trees. The three species were only found to co-occur in the rhizosphere of wildflowers. Wyrebek et al. (2011) concluded that the distribution of *Metarhizium* species may therefore be dependent on plant species distribution.

The mucigel coating on the rhizoplane provides a hydrophobic surface for fungi to adhere to. The surface of conidia from species of *Metarhizium* and *Beauveria* have a specialised rodlet layer; a spore coat structure formed from hydrophobin proteins (Zhang et al. 2011). As a result, species of *Beauveria* and *Metarhizium* are highly hydrophobic and can adhere to many hydrophobic surfaces including insect and plant cuticle (Kirkland and Keyhani 2011). Pava-Ripoll et al. (2011) evaluated multiple isolates of *M. anisopliae* and *B. bassiana* for their ability to germinate in the presence of root exudates from haricot bean and found that the germination rate of *M. anisopliae* was comparable with the rhizosphere competent ascomycete fungus *Trichoderma harzianum* (Hypocreales; Hypocreaceae) (Harman 2006). The germination rates of *Beauveria* isolates were significantly lower in this study compared to *T. harzianum* and *M. anisopliae*, but germination still occurred effectively. Genes that were upregulated in response to the root exudates included the aforementioned subtilisin Pr1A, and in *M. anisopliae*, the *Mad2* adhesion gene was also upregulated (Pava-Ripoll et al. 2011).

Isolates of *Beauveria* have frequently been isolated from the roots of certain plants (Fisher et al. 2011). Although less studied compared to *Metarhizium*, it is probable that the rhizosphere is an

important interface for mediating plant-*Beauveria* interactions. A recent study by Zitlalpopoca-Hernandez et al. (2017) suggested that *Beauveria* can interact with and protect important arbuscular mycorrhiza fungal (AMF) associations in the rhizosphere from herbivorous insects, thereby promoting plant growth indirectly by defending beneficial plant-AMF associations. Specifically, Zitlalpopoca-Hernandez et al. (2017) showed that dual inoculation with *B. bassiana* and indigenous AMF of maize plants mitigated the negative effects from root herbivory by larvae of *Phyllophaga vetula* (Coleoptera: Melolonthidae). The mechanism underlying this was thought to be resulting from improved uptake of soil nutrients such as N and P. Root herbivory by larvae of *P. vetula* was also observed to decrease shoot growth and N content in the maize foliage. Interestingly, mortality of *P. vetula* following exposure to the *B. bassiana* inoculum was found to be low in their study (5%). The AMF treatment also tended to reduce the population density of *B. bassiana*, suggesting that competition for plant derived nutrients occurred between the fungi. Another study by Gualandi et al. (2014) observed an increase in AMF root colonisation in *Echinacea purpurea* plants following inoculation with *B. bassiana* but the possible mechanisms for this increase were not studied. However, AMF have previously been observed to compete for nutrients with other root associated fungi such as *T. harzianum* and *Clonostachys rosea* (Green et al. 1999; Ravnskov et al. 2006) and a decline in population density resulting from the lack of competitive ability of *B. bassiana* in the soil has been previously reported by Zimmermann (2007). Such complex multitrophic interactions in the rhizosphere may be important to consider when selecting biocontrol agents intended for the management of root herbivores (Zitlalpopoca-Hernandez et al. 2017).

1.4 The plant host

Plants can adjust their phenotype to maximise interactions with beneficial organisms while minimising detrimental associations (Dicke 2016). Unlike animals, plants lack mobile defender cells and a somatic adaptive immune system. Instead, they rely on localised innate immunity of individual cells, in addition to certain systemic signals that emanate from infection sites (Jones and Dangl 2006). Horizontally transmitted plant-fungal associations involve (1) fungal penetration into plant tissues (Ernst et al. 2003), (2) intercellular colonisation of plant organs by the invading fungus (Gao and Mendgen 2006) and (3) expression of a biotrophic lifestyle in the fungus, where the invader grows only on living host tissue (Pieterse and Dicke 2007; Rodriguez et al. 2009). Endophytes, like pathogens, must be able to overcome or manipulate the plant's surveillance system but in order to establish a compatible interaction (Singh et al. 2011). Once the plant detects the presence of an invader, defence pathways are elicited resulting in the expulsion, suppression, or death of the colonising fungus (Dangl and Jones 2001). Fungal endophytes and root colonisers are either able to communicate with the plant to indicate that they are not pathogens or they are restricted and tolerated by the plant within intercellular spaces that do not disrupt plant functions (Rodriguez et al.

2009). For example, during early stage interaction, a plant-derived membrane has been observed to surround and separate the hyphae of the endophytic coloniser *Piriformospora indica* from the plant cytoplasm (Jacobs et al. 2011; Lahrmann et al. 2013; Lahrmann and Zuccaro 2012). The structural partitioning of this interaction is similar to that of transcellular and arbuscular hyphae of AMF, which are also encapsulated by a peri-fungal membrane in the plant (Banhara et al. 2015; Bonfante and Genre 2010). Prior to colonisation the AMF species, *Glomus intraradices*, has been shown to release a diffusible factor that prepares or 'primes' the plant root for penetration (Conrath et al. 2002). This communication molecule, named the myc (mycorrhizal) factor, was identified as a lipochitooligosaccharide (LCO), and resembles the Nod factors found in rhizobia (Maillet et al. 2011). Myc factors prepare the root for fungal colonisation in two ways, by inducing specific transcriptional changes, which trigger the SYM (symbiotic) signalling pathway, and by inducing morphological changes that stimulate an increase in plant root surface area for hyphal contact, such as increased root-hair growth (Kosuta et al. 2003; Oldroyd et al. 2009). Colonisation of switchgrass roots by *M. robertsii* was shown to cause extensive root hair development, so it may be possible that the entomopathogenic fungi also release a myc-like factor prior to root penetration (Barelli et al. 2016; Sasan and Bidochka 2012), however, this has not yet been determined.

1.4.1 The plant immune response

There is significant overlap in the array of mechanisms involved in the plant response to invasion by either an endophyte or pathogen (Hardoim et al. 2015). In order to determine the type of endophyte a microorganism is (i.e. obligate, facultative, or opportunistic) and the benefits it may confer to the host, it is important to first understand the processes that plants mobilise to counteract specific types of invasion.

Plant response to pathogens

To activate resistance to disease, plants require the ability to recognise pathogens and initiate defence mechanisms to limit and overcome infection (Jones and Dangl 2006). Resistance in the host often manifests as a hypersensitive response (Figure 1.2), which leads to localised cell death at the infection site. Other defence-related responses include structural alterations of plant tissues and the production of various defence molecules, such as the antimicrobial proteins phytoalexins and pathogenesis-related (PR) proteins (Chisholm et al. 2006; Dangl and Jones 2001). Structural responses in the plant include the closure of stomata and the strengthening of cell walls (Frederickson Matika and Loake 2014). A characteristic feature that indicates the activation of all these responses is the engagement of a nitrosative burst with the corresponding activation and generation of reactive oxygen species (ROS) (Grant and Loake 2000; Yun et al. 2011).



Figure 1.2. The hypersensitive response. A leaf showing characteristic symptoms of localised cell death. Photo sourced from: <https://source.wustl.edu/2012/06/key-part-of-plants-rapid-response-system-revealed/>

In low quantities, ROS can function as signalling molecules to induce the mitogen-activated protein kinase (MAPK) cascade, which is known to induce a defensive immune response (Frederickson Matika and Loake 2014). Additionally, ROS molecules can act as secondary messengers in a number of hormone signalling cascades aside from MAPK, which may result in subsequent plant immune responses such as stomatal closure, programmed cell death, gravitropism, and acquisition of tolerances to various biotic and abiotic stresses (Sharma et al. 2012) (Figure 1.3).

During pathogenic invasion, the plant immune system is first activated by recognition of certain microbial elements such as chitin, glycoproteins, flagellin and lipopolysaccharides. These transmembrane receptors are termed pathogen- or microbial-associated molecular pattern (PAMPs, MAMPs) receptors, depending upon the type of microorganism that is invading. MAMP/PAMP-triggered immunity (MTI), also known as basal resistance, is the result. To counteract this response, successful pathogens release a suite of effector proteins to target and prepare potential host cells, resulting in effector-triggered susceptibility. Plants have consequently developed an array of resistance (R) proteins that can each recognise specific pathogen effectors, to produce effector-triggered immunity (ETI) (Jones and Dangl 2006). These primary and secondary immune responses are governed by phytohormones regulated in undamaged/uninfected cells.

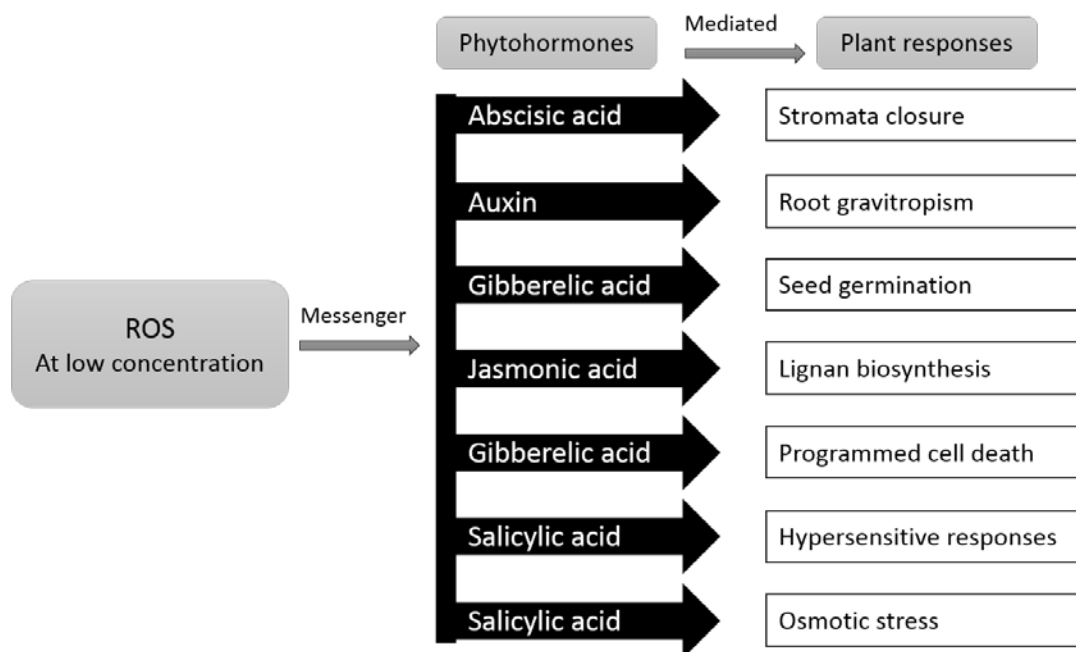


Figure 1.3. Reactive oxygen species (ROS) as secondary messengers. Diagram illustrates the various hormone signalling cascades activated by ROS in response to biotic and abiotic stress. Diagram modified from Sharma et al. (2012).

The aforementioned hypersensitive response (HR), a form of programmed cell death, is a part of the ETI response. Salicylic acid (SA) is an endogenous signal molecule that plays a key role in signalling for such resistance (Matzinger 2002; Van der Biezen and Jones 1998). Accumulation of SA precedes and accompanies the HR response, to subsequently activate a molecular signal transduction pathway via the induction of specific PR proteins, leading to systemic acquired resistance (SAR). Subsequently, SAR primes resistance throughout the entire plant against a broad range of pathogens. (Dempsey and Klessig 2012; Frederickson Matika and Loake 2014). However, SAR can be triggered by exposing the plant to virulent, avirulent, and nonpathogenic microbes (Fu and Dong 2013).

Plants respond to pathogens that kill host tissue during colonisation (necrotrophs) by inducing SAR, which effectively immunises the host against any subsequent infection. In addition to salicylic acid, signal transduction pathways are induced by other phytohormones such as jasmonates and ethylene, which activate various defence-related genes (Glazebrook 2005; Zipfel and Felix 2005). The activation of these pathways leads to induced systemic resistance (ISR); an alternative basal resistance response in plants traditionally associated with biotrophic organisms such as plant growth-promoting rhizobacteria (PGPR) and some fungal endophytes (Choudhary et al. 2007; Straub et al. 2013). However, crosstalk is sometimes thought to occur between the defence pathways that are mediated by salicylates, jasmonates and ethylene (Gutterson and Reuber 2004). The coordination of these hormone pathways presumably enables the plant to more finely modulate the defence response to a specific pathogen (Xu et al. 2011). In the past, analyses of plant signalling pathways and their interactions have focused on only a few genes at a time (Gomez-Gomez and Boller 2002). As a result,

the extent of overlap occurring in gene activation from different signalling molecules during a pathogenic invasion has perhaps been underestimated. Gene expression profiles of plants can now be compared using cDNA microarray and transcriptomic analyses, which have greatly improved our overall understanding of the molecular activity involved in the plant defence response (Henry et al. 2013; Jones and Dangl 2006).

An additional type of immune response operates in plants, the adaptive immune response, which occurs predominantly within the cell using polymorphic NB-LRR protein products encoded by most resistance genes (Jones and Dangl 2006; Marone et al. 2013). They are characterised by their nucleotide binding (NB) and leucine rich repeat (LRR) domains. These NB-LRR proteins are somewhat related to animal CATERPILLER/NOD/NLR proteins⁷ and STAND ATPases⁸ (Marone et al. 2013). For example, pathogen effectors are recognised by NB-LRR proteins, and trigger similar immune responses across a diversity of organisms from different kingdoms. In plants, NB-LRR-mediated disease resistance is effective against pathogens that are obligate biotrophs, or hemi-biotrophic pathogens but not against necrotrophs (Glazebrook 2005).

Plant response to endophytic colonisation

Endophytic colonisation is thought to induce systemic resistance in plants (ISR), often leading to a higher tolerance to pathogens (Hardoim et al. 2015; Robert-Seilantiz et al. 2011). There is increasing evidence that initial colonisation of plants by so-called beneficial microorganisms activates an immune response in plants similar to that against pathogenic invasion, however, successful endophytes manage to evade host defences and subsequently can establish under certain conditions (Saikkonen et al. 2010a; Schulz et al. 1999; Zamioudis and Pieterse 2012).

For example, root colonisation by *Trichoderma hamatum* has been shown to activate a wide range of plant responses that ultimately enhance the defensive capacity of the host (Alfano et al. 2007; Bailey et al. 2006; Moran-Diez et al. 2012). Indeed, the effects of *Trichoderma* on plant immunity are not just restricted to the root but often may extend to influence aboveground plant tissues as well. Consequently, plants infected with endophytic *Trichoderma* isolates frequently show higher resistance to a broad-spectrum of plant pathogens (Martinez-Medina et al. 2010; Mathys 2012). This systemic type of resistance is likely attributed to the modulation of the plant defence network following early *Trichoderma*-induced signalling, to elicit those cascades that promote a more efficient activation of defence responses (Martínez-Medina et al. 2013).

Endophytic bacterial strains of *Pseudomonas* and *Bacillus* have more frequently been reported to stimulate ISR (Kloepper and Ryu 2006) compared to fungal endophytes. The factors contributing to ISR induction in association with endophytic bacteria include antibiotics, N-acylhomoserine lactones, salicylic acid, jasmonic acid, siderophores, volatiles, flagella and lipopolysaccharides (Bordiec et al.

2011; Hardoim et al. 2015). Interestingly, disease resistance has also been shown to correspond with changes in the resident endophytic community composition (Pavlo et al. 2011). Apart from the above examples from *Trichoderma*, fungal endophytes are generally less frequently associated with the protection of plant hosts via ISR (Bae et al. 2011).

Generally, fungal endophytes are better known for their ability to actively antagonise plant pathogens and herbivores (Ownley et al. 2004). Compounds such as alkaloids, steroids, terpenoids, peptides, polyketones, flavonoids, quinols, phenols, and chlorinated compounds may be produced *in planta* by endophytes (Gunatilaka 2006). Some of these compounds in particular are important for the protection and deterrence of insect herbivores (Hardoim et al. 2015; Siegel et al. 1990). The majority of the literature pertaining to *Beauveria* as an endophyte indicates that ingestion of inoculated plant material has either a negative or neutral effect on insect herbivores (McKinnon et al. 2017). Negative effects have been particularly evident on aphid reproduction rather than actual mortality by mycosis (Castillo Lopez et al. 2014b; Gurulingappa et al. 2011) and on insect feeding (as measured by herbivore weight) (Powell et al. 2009; Prabhavathi et al. 2013; Quesada-Moraga et al. 2009; Zhang and Vidal 2012; Zitlalpopoca-Hernandez et al. 2017). Currently, the mechanism underlying negative effects to insect herbivores is unclear. A few studies have reported that *B. bassiana*-infected plant tissue caused mycosis in herbivores (Vidal and Jaber 2015). In these studies though, it was not clearly demonstrated that the infection was caused by the endophytic form of the fungus since residual plant surface inocula was frequently not considered (McKinnon et al. 2017). Furthermore, it is not yet understood what mechanism is involved that can result in any lethal/sub-lethal effects to the insect herbivore following consumption of endophyte-infected plant material.

Endophytic establishment is sometimes observed to enhance plant growth, despite the fact that the endophyte obtains valuable nutrients provided by, and at the expense of, the plant host (Singh et al. 2011). The production of phytohormones by endophytes is thought to be the major mechanism leading to plant growth promotion, which is usually evident by marked morphological and architectural changes in the host (Khan et al. 2012a; Khan et al. 2012b; Senthilraja et al. 2013; Straub et al. 2013). The ability to produce or regulate auxins such as indole-3-acetic acid (IAA), and gibberellins, are traits commonly associated with beneficial root-endophytes (Felten et al. 2009; Khan et al. 2012a; Yang et al. 2012). Production of these compounds are, therefore, considered important factors enabling plant colonisation by endophytes. Increased root branching and root-hair growth has been observed as a response to colonisation by certain rhizosphere-associated fungi (Sasan and Bidochka 2012). For example, *Trichoderma*-inoculated maize roots were shown to grow deeper, thicker roots, with increased surface area (Harman et al. 2004b). A recent study by Liao et al. (2017) demonstrated that *Metarhizium* produced IAA during plant colonisation of *Arabidopsis thaliana*, which both enhanced root growth and virulence to associated insects. Endophytic

colonisation by *P. indica* has also been shown to stimulate root growth in several plant species (Varma et al. 1999) and Sasan and Bidochka (2012) also observed increased root hair development in switchgrass as a result of the presence of *Metarhizium* in the rhizosphere.

Plant response to stress

Another benefit that endophytes may confer to plants is through an increased tolerance to abiotic stresses, such as drought, high-salt and low-temperature, all of which otherwise have highly adverse effects on plant growth and crop yields (Xu et al. 2011). Generally, abiotic stress results in altered plant morphology and physiology, which are caused by certain changes to metabolic processes and reduced cell division. In order to survive these stresses, plants have evolved a complex signalling network that facilitates the production of signals in response to environmental stimuli, and are subsequently able to adapt their phenotype to their changing surroundings. This adaptive strategy is modulated by the expression of certain responsive genes (Sharma et al. 2012; Xu et al. 2011).

Transcription factors are regulatory proteins that mediate primary and secondary metabolism, growth and development. They are involved in many processes that enable the plant to respond appropriately to specific environmental stimuli, such as pathogen attack, salt and osmotic stress, wounding, dehydration, hypoxia and temperature stress (refer to Figure 1.3). Additionally, they play an important role in the production of stress-related hormones such as ethylene, jasmonic acid and abscisic acid (Licausi et al. 2013). Ethylene and jasmonic acid signalling pathways have the potential to both be regulated by the same family of transcription factors, namely, the ethylene responsive factor (ERF) gene family (Gutterson and Reuber 2004). For example, the overexpression of certain ERFs in transgenic plants has been shown to modulate both ET and JA pathways simultaneously, resulting in an increased resistance to multiple fungal and bacterial invaders (McGrath et al. 2005; Xu et al. 2011).

Endophytic colonisation by *P. indica* was shown to enhance salt tolerance in barley (Baltruschat et al. 2008) and drought tolerance in Chinese cabbage (Sun et al. 2010). In both studies, increases in antioxidant enzymes were observed, and were asserted to be involved in the mechanism underlying enhanced stress tolerance in these plants. Fungal colonisation of cacao seedlings by *Trichoderma* inhibited the plant response to drought stress (Bae et al. 2009) while promoting growth, and the bacterial endophyte *Burkholderia phytofirmans* increased drought tolerance levels in both maize and wheat plants (Naveed et al. 2014a; Naveed et al. 2014b).

1.5 Techniques for analysing the plant microbiome

1.5.1 Putative endophyte detection

Microscopy enables the visual detection of endophyte colonisation of plant tissue. Techniques include light microscopy, transmission and scanning electron microscopy, as well as confocal laser and fluorescent microscopy, the latter two of which allow visual tracking of target microorganisms *in situ* (Schulz and Boyle 2005). However, the identification of putative endophytes using microscopy can be tedious due to the difficulty of differentiating plant organs and because of the rarity of endophytic establishment. Furthermore, unless a labelled/transformant endophytic isolate is used (e.g. with a green fluorescent protein marker), resident endophytes and/or pathogens may confound the identity of the subject of study.

Colonisation of plant tissues by putative endophytes is most frequently assessed by culture-dependent and independent methods. Culture dependent methods involve direct isolation of fungal material from plant tissue to growth media, and culture independent methods the molecular detection of endophytic DNA from plant material by polymerase chain reaction (PCR). Aside from microscopy, most methods require surface sterilisation of plant tissue to eliminate surface inocula or epiphytes in addition to their DNA, prior to detection to determine endophytism (McKinnon et al. 2017).

1.5.2 Microbial diversity analysis

Studies of microbial diversity also typically involve culture-dependent and independent methods, in addition to biochemical methods. For instance, in order to distinguish between different types of microorganisms, microbiologists traditionally studied metabolic properties such as carbon, nitrogen and energy source utilisation as well as physiological tolerances and conditions required for growth (Roald et al. 1989).

A number of molecular-based approaches have been developed to study microbial diversity. For example, techniques include DNA–cDNA and mRNA–cRNA hybridisation (i.e. microarray), DNA cloning, DNA sequencing and other PCR-based methods such as denaturant gradient gel electrophoresis (DGGE), temperature gradient gel electrophoresis (TGGE), as well as ribosomal intergenic spacer analysis (RISA), automated ribosomal intergenic spacer analysis (ARISA), and restriction fragment length polymorphism (RFLP) (Fakruddin 2013). In DGGE or TGGE, DNA fragments of the same length that have base-pair sequence variation can be separated. To achieve this, DNA is amplified using PCR with universal primers that target part of the 16S or 18S rRNA sequences (bacteria or fungi). The separation occurs due to differences in mobility of partially melted DNA molecules passing through acrylamide gels that consist of a linear gradient of DNA denaturants (urea

and formamide). The sequence variation within the DNA amplicons causes the difference in melting behaviour when subjected to the denaturant (Muhling et al. 2008). More recently, next generation sequencing (NGS) technologies has enabled more complex and higher through-put of DNA to be sequenced from multiple taxa and from environmental DNA samples, as well as from whole genomes of organisms. Such technologies produce large data sets that are more complex and thus challenging to analyse.

1.5.3 Transcriptomic analysis by microarray

Microarray technology uses hundreds to millions of DNA probes arranged on a solid surface array to simultaneously target multiple RNA or (cDNA) molecules in a sample. Samples to be tested are fluorescently labelled and applied to the DNA microarray so that the nucleic acids hybridise with their complementary probes. The fluorescent signal is retained by the RNA or DNA probes on the array that can be then scanned using a laser spectrofluorometric device; providing digital fluorescent intensity values for each probe. These signal intensities represents DNA target abundance which infers transcript expression level, assuming the array has high homology to the RNA or DNA represented in the target sample (Clarke and Zhu 2006). Consequently, plant RNA samples can be interrogated and compared for differences in expression levels of specific and known gene or whole gene pathways, such as those involved in activity against pathogens or endophytes (Schenk et al. 2000; Zuccaro et al. 2011). The advantage of employing microarray, in contrast with next generation sequencing, is that the analysis process is well established and currently less data intensive. For instance, the microarray targets only the transcripts of the organism of interest. This is an advantage when the RNA sample is mixed with an organism that has little to no annotation published. Additionally, there are free online platforms available to investigate differentially expressed gene sets to enable efficient interpretation of the biological pathways involved.

1.6 Research rationale and aims

Increasing evidence indicates that *B. bassiana* is frequently associated with plants. To date, studies have primarily focused on and reported the potential for activity against insects and plant pathogens as a result of endophytic colonisation by these entomopathogens. However, the functional role of the fungi *in planta* and/or the plant response to colonisation by *B. bassiana*, in addition to the mechanisms underlying these responses, still require elucidation, particularly for important crop-plant species. Furthermore, little is known or has been reported on whether there is phenotypic variation among isolates of *B. bassiana* for endophytic capability. Should such variation exist, it may be important to inform the selection process of endophytic isolates intended for biocontrol purposes.

The present study aimed to elucidate the interactions of *Beauveria* with the maize (*Zea mays*) Pioneer cultivar '34H31' at the ecological, physiological and molecular level. The overall hypothesis for this project can thus be summarised as follows: *B. bassiana* isolates differ in their ability to colonise a single maize cultivar, which is evident by differential effects to the plant microbiome (in the rhizosphere), as well as plant growth and immune response following inoculation.

Questions tested included whether introduction of *Beauveria* to the roots and rhizosphere of maize impacted the soil microbial community, whether *B. bassiana* colonisation of maize affected plant growth and/or elicited plant defence mechanisms, such as those commonly associated with beneficial endophytes, and whether the inoculation of different isolates resulted in different, measureable, responses. Moreover, the presence of *B. bassiana* in roots and soil was measured over time to determine whether changes in the plant host microbiome and/or plant defensive response following foliage damage could affect the persistence of the fungus below-ground, in order to demonstrate a reciprocal interaction between the plant and *Beauveria*.

Accordingly, Chapters 2-5 had the following research aims:

- To develop a PCR protocol to specifically amplify isolates from the genus *Beauveria* that can also enable species differentiation by sequence analysis.
- To optimise plant surface sterilisation methodology for detection of *Beauveria* in maize tissues.
- To test the plant growth response to three different *B. bassiana* isolates, introduced artificially as putative endophytes.
- To test the impact of three different *B. bassiana* isolates applied to roots of maize on the rhizosphere soil community structure and function.
- To investigate differences in gene expression in maize roots in the response to two different *B. bassiana* isolates, relative to a no-inoculum control.

Chapter 2

Developing methods for molecular detection of endophytic *Beauveria*

2.1 Introduction

There is a continuum from epiphyte to endophyte with horizontally transmitted fungi (Schulz and Boyle 2005). Consequently, when isolating endophytes from plant tissue, it is often difficult to ascertain where (at the time of isolation) the fungus predominantly resides, outside or in the plant (Hyde and Soyong 2008). Most frequently, endophytes of *Beauveria bassiana* have been isolated to media following surface sterilisation of plant tissue. While the surface sterilisation procedure used does vary, the common practice involves submersion in ethanol (EtOH) and sodium hypochlorite (NaOCl), in either order (McKinnon et al. 2017). In order to isolate fungi from internal tissues, viable surface epiphytes must be thoroughly removed or avoided. For each plant host and tissue type, the chosen procedure should be optimised to ensure sterility (Schulz and Boyle 2005).

Molecular detection methods such as polymerase chain reaction (PCR) also rely on efficacious surface sterilisation, in addition to removal of epiphytic deoxyribonucleic acid (DNA), as DNA from nonviable propagules (conidia and hyphae) can still be amplified after surface disinfection (Nocker et al. 2007). Indeed, removal of plant surface microbes and their DNA has previously been demonstrated as important when using a PCR-based approach to investigate endophytes (Burgdorf et al. 2014). This is because standard surface sterilisation techniques employed in culture-dependent studies frequently do not guarantee the complete elimination of surface organisms (Manter et al. 2010), so neither can they logically guarantee the removal of the DNA belonging to these same organisms. Furthermore, plant surfaces are often tested for sterility by culturing the post-treated surface (by imprint or from a rinse of water) onto nutrient agar medium (Schulz et al. 1998; Sessitsch et al. 2002), yet Guo (2010) for example indicated that some surface sterilisation methods may not adequately denature epiphytic DNA in molecular diversity studies of endophytes. Consequently, DNA contamination cannot be ascertained by these standard sterility control methods.

Nevertheless, with the right measures taken, PCR-based detection can be a rapid and highly sensitive method for targeting specific endophytes such as *Beauveria*. The primers and protocol must be designed and optimised to ensure adequate specificity and sensitivity. Ideally, the PCR should be optimised such that DNA from plant host, or the host microbiome (e.g. from other fungi) is not amplified. Sensitivity is also a concern where the quantity of the endophyte DNA is diluted by the plant host DNA pool, to the point where the endophyte DNA falls below the level of detection

(Tellenbach et al. 2010). To deal with potential surface DNA contamination remaining after surface sterilisation, propidium monoazide (PMATM, Biotium) may be used. PMA is a photoreactive dye that is able to intercalate the DNA in ruptured (nonviable) cells rendering it unavailable for PCR amplification (Nocker et al. 2006). PMA can therefore be used effectively to treat plant material prior to tissue grinding and DNA isolation, for endophyte detection (Wicaksono et al. 2016).

In addition to detecting the presence of endophytes it may be possible with PCR to quantify their biomass *in vivo*. Kinetic PCR (kPCR) enables quantification of target DNA within a sample DNA pool, and has the advantage that sensitivity is independent of the target copy number (Freeman et al. 1999; Schmittgen 2001). The distinguishing feature of kPCR compared to other quantitative PCR methods is that target copy number is determined from the fractional cycle at which a threshold amount of amplicon DNA is attained (threshold cycle, CT), and this is set at a point where the target amplicon just becomes detectable, yet still within the exponential phase of amplification (Higuchi et al. 1993; Morrison et al. 1998). This approach minimises interfering factors associated with latter stages of amplification and provides the potential for precise quantitative calculations (Rutledge and Cote 2003). Absolute quantification is typically achieved using a standard curve, constructed by amplifying known amounts of target DNA in simultaneous reactions performed under identical conditions to that of the sample.

In recent literature, methods for the molecular detection of endophytic *B. bassiana* from plant tissues have been reported (Landa et al. 2013; Quesada-Moraga et al. 2014). These methods have adopted the use of two primer sets from the internal transcribed spacer (ITS) region of ribosomal DNA (rDNA), for a two-step nested protocol. However, these primers were designed to amplify a specific isolate of *B. bassiana*, isolate EABb 04/01-Tip and not to amplify ITS1-5.8S-ITS2 sequences of opium poppy *Papaver somniferum* or other fungi different from *B. bassiana* (Landa et al. 2013).

For the purpose of this project, a novel nested PCR protocol with primers designed to detect species from the *Beauveria* genus, while excluding non-target fungi and plant host DNA was developed. Furthermore, a series of experiments are reported in this chapter that were designed to optimise and demonstrate the efficacy of surface sterilisation for a novel PCR based endophyte detection protocol that used PMA dye on inoculated and surface sterilised *Zea mays* (maize) roots and onion epidermis to deal with surface DNA. At the outset of this project, an endophytic isolate of *Beauveria* suitable for the intended plant host, maize, was yet to be obtained. The following PCR protocol was therefore designed to allow rapid and sensitive screening of plant material in order to test multiple species of *Beauveria*, introduced artificially by inoculation, for the confirmation of endophytism.

Concurrent experiments conducted by Post-Doctoral Fellow Maria Eugenia Moran-Diez, utilised the methodology developed herein to assess both the colonisation ability of selected *B. bassiana* isolates

in association with maize and the efficacy of surface sterilisation. This was accomplished by using confocal laser scanning microscopy (CLSM) to visualise colonised maize-root tissues before and after surface sterilisation. Because her results compliment and inform this present study, some images (used with permission) will be presented later in this chapter (see Section 2.3).

2.2 General Methods

2.2.1 Taxonomic identification of fungal species

For the purpose of PCR primer design, and for experimental screening of plant material to test for *Beauveria* spp. colonisation, 35 fungal isolates of multiple species were acquired and cultivated (International Collection of Microorganisms from Plants (ICMP), Landcare Research, Lincoln University and Bio-Protection Research Centre Culture Collection, Christchurch, NZ) (Table 2.1). Genomic DNA was extracted from pure culture of each isolate obtained. Fungi were cultured on sterile cellophane, placed over 10% Sabouraud dextrose agar (SDA, Difco, USA), and incubated for 6 days at 25°C, prior to DNA extraction. Cellophane was aseptically scraped using a surgical blade to obtain pure hyphal tissue. DNA was isolated using the REExtract-N-Amp™ Plant PCR Kit (Sigma-Aldrich), according to the manufacturer's instructions.

To amplify the target fungal ITS region for species identification, the REExtract-N-Amp™ Plant PCR Kit (Sigma-Aldrich) master-mix was prepared according to the technical manual, with each 20 µL volume reaction consisting of: 10 µL of the kit Hot Start PCR mix, 0.8 µM of each primer (ITS5_F: GGAAGTAAAAGTCGTAACAAGG and ITS4_R: TCCTCCGCTTATTGATATGC White et al. (1990)), and 4 µL of gDNA suspended in the kit elution buffer. Amplifications were carried out in a Veriti 96 well Thermal Cycler (Applied Biosystems) with the following cycling conditions: step (1) 95°C for 5 minutes, step (2) 30 cycles consisting of: 95°C for 30 seconds, 60°C for 30 seconds, 72°C for 1 minute; step (3) 72°C for 7 minutes. The quality and size of the PCR products were assessed by agarose gel electrophoresis, using a 1% gel in 1× TAE (40 mM Tris-OH, 20 mM Acetic Acid, pH 7.8, 1 mM ethylenediaminetetraacetic acid (EDTA)). The REExtract-N-Amp™ Plant PCR Kit contained an inert loading dye in the mix, so 5 µL of each PCR product was loaded in the agarose gel containing a DNA gel stain (0.5 x RedSafe™), together alongside 7 µL of a 1 kb DNA ladder (Hyperladder II, Bioline, USA) and including the negative-template control (NTC) water. PCR products were separated by electrophoresis in 1× TAE buffer at 100 V for 30 minutes and then visualised following exposure to UV light using the Versadoc Imaging Systems Model 3000 (Bio-Rad, USA).

PCR products were sequenced in one direction (5'-3') to confirm species identity (Sanger sequencing, Lincoln University Sequencing Unit, New Zealand). Species identity was then confirmed by alignment of these nucleotide sequences of the ITS region in MEGA version 5 (Tamura et al. 2011) along with

those obtained in the GenBank database using the Basic Local Alignment Search Tool (BLAST; Altschul et al. (1990)). Additionally, the amplicon sequences were trimmed to 384 nucleotide base-pairs (bp) in length following the alignment and compared using the Maximum-Likelihood method by (Tamura and Nei 1993) (see Appendix A).

Table 2.1. Table of fungal isolates used in this study.

Isolate	Species	Host (insect/plant) ¹	District	Isolated by
BG11	<i>Beauveria bassiana</i>	<i>Taraxacum officinale</i> dandelion root	Christchurch	A. Clouston
E1063	<i>B. bassiana</i>	<i>Vespula germanica</i> (Hymenoptera: Vespidae)	Nelson	N. Cummings
E1069	<i>B. bassiana</i>	<i>V. germanica</i>	Nelson	N. Cummings
FBHU	<i>B. bassiana</i>		Selwyn	A. McKinnon
FDB	<i>B. pseudobassiana</i>	Coleoptera: Coccinellidae	Selwyn	D. Bienkowski
FRh2	<i>B. bassiana</i>	<i>Hylastes/Hyalurgis</i>	Riverheads	S. Reay
E1079	<i>B. caledonica</i>	<i>Dermaptera</i>	Nelson	N. Cummings
F532	<i>B. caledonica</i>			
FRh1	<i>B. caledonica</i>	<i>Hylastes/Hyalurgis</i>	Riverheads	S. Reay
NC142	<i>B. caledonica</i>	<i>Prionoplu reticularis</i> (Coleoptera: Cerambycidae)	Westland	N. Cummings
NC44	<i>B. caledonica</i>	n.d.	Taupo	N. Cummings
NC49	<i>B. caledonica</i>	Coleoptera	Taupo	N. Cummings
Bweta	<i>B. malawiensis</i>	<i>Hemideina crassidens</i>	Westland	N. Cummings
E1059	<i>B. malawiensis</i>	<i>Vespula vulgaris</i> (Hymenoptera: Vespidae)	Westland	N. Cummings
E1060	<i>B. malawiensis</i>	<i>V. vulgaris</i>	Westland	N. Cummings
NC215	<i>B. malawiensis</i>	<i>V. vulgaris</i>	Westland	N. Cummings
NC220	<i>B. malawiensis</i>	Orthoptera: Tettigoniidae	Westland	N. Cummings
NC222	<i>B. malawiensis</i>	<i>Vespula</i> sp.	Westland	N. Cummings
E1067	<i>B. pseudobassiana</i>	<i>Vespula</i> sp.	Nelson	N. Cummings
E1080	<i>B. pseudobassiana</i>	Coleoptera: Scarabaeidae	Nelson	N. Cummings
E1083	<i>B. pseudobassiana</i>	n.d.	Nelson	N. Cummings
E1139	<i>B. pseudobassiana</i>	<i>P. marginale</i>	Nelson	N. Cummings
E1175	<i>B. pseudobassiana</i>	<i>V. vulgaris</i>	Nelson	N. Cummings
NC209	<i>B. pseudobassiana</i>	<i>A. zealandica</i>	Westland	N. Cummings
NC120801.1	<i>B. pseudobassiana</i>	n.d.	Westland	N. Cummings
NC120826.1	<i>B. pseudobassiana</i>	n.d.	Westland	N. Cummings
NC120514.2	<i>B. pseudobassiana</i>	n.d.	Westland	N. Cummings
J1	<i>Alternaria alternata</i>	<i>Pinus radiata</i> needle	Canterbury	J. Brookes
J8	<i>Fusarium oxysporum</i>	<i>Pinus radiata</i> needle	Canterbury	J. Brookes
J10	<i>Aspergillus nidulans</i>	<i>Pinus radiata</i> needle	Canterbury	J. Brookes
J18²	<i>B. bassiana</i>	<i>Zea mays</i> L. leaf	Canterbury	J. Brookes
LU132	<i>Trichoderma atroviride</i>			
C14	<i>Metarhizium anisopliae</i>	n.d.	Canterbury	M.C. Lefort
ICMP 11019	<i>Lecanicillium lecanii</i>	<i>Cecidophyopsis ribis</i> Westwood (mite)	Timaru	W Thomas
ICMP 14476	<i>Verticillium dahliae</i>	<i>Vitis vinifera</i> L. (Rhamnales: Vitaceae)	Marlborough	M. Braithwaite

¹ Note: n.d. = not determined, absent information indicates soil or other source for isolation.

² Note: Although isolate J18 (in bold) is included in the table, this isolate was acquired after the plant screening commenced.

2.2.2 Conidial suspensions for inoculation

Inocula were prepared as conidial suspensions for direct application to roots of maize seedlings.

Suspensions were produced from cultures grown on potato dextrose agar (PDA; Difco, BD, USA) after three weeks at 20°C. Five mL of sterile 0.05% (v/v) Tween 80 was added to each plate (with five plates per isolate), scraped gently with a hockey stick to blend conidia and then poured through two

layers of Miracloth™ (Merck Millipore) to obtain 25 mL of conidial suspension per isolate. The concentration of conidia per mL was calculated based on counts made from 10 µL of a 10⁻² dilution placed on a Neubauer hemocytometer counting chamber. Conidial concentrations were then adjusted in 0.05% Tween 80 based on the hemocytometer calculation to achieve 10⁷ or 5 x 10⁷ conidia mL⁻¹, respectively, with the volume depending upon the experiment.

To check the viability of conidia for each isolate, 100 µL of a 10⁻⁵ dilution from each suspension was spread onto PDA, with three replicates per suspension and incubated for 10 days at 20°C. After 10 days, the number of colony forming units (CFUs) were counted. The average number of viable conidia per isolate was multiplied by 10 to get CFU/mL, and then the CFU/mL values were multiplied again by 10⁵ to estimate the quantity of viable conidia per mL of original suspension. By this method, the percentage of viable conidia for each isolate suspension was above 94%.

2.2.3 DNA isolation from plant material

Maize

Maize (*Zea mays*) were grown from seed of cultivar Pioneer 34H31. Seeds were first surface sterilised by soaking them in a 2.5% sodium hypochlorite (NaOCl) and 0.02% Tween 80 solution for seven minutes, followed by two washes in sdH₂O, with one minute per wash. Surface sterilisation efficacy was assessed by rolling a subset of 10 surface sterilised seeds onto 10% potato dextrose agar (PDA), and then these 'imprinted' control plates were incubated for 14 days at 25°C to check for growing cultures (Schulz et al. 1998). Genomic DNA was obtained from 6 day old seedlings, from root material and following inoculation, using the MO BIO PowerPlant® Pro DNA Isolation Kit, according to the kit protocol but with the following modification: tissue lysis was conducted with the FastPrep-24™ (MP Biomedicals) at 5 m/s for 40 seconds.

Onion epidermis

Single epidermal layers were aseptically peeled from brown onions (*Allium* sp.) and cut with a sterile blade into 1 cm² pieces. These pieces were rinsed for 20 seconds in 70% ethanol, followed by 1 minute in sdH₂O, and then placed in pairs on 1% bacteriological agar (Difco, BD, USA) immediately prior to inoculation. All epidermal pieces were inoculated prior to DNA isolation with 40 µL each of a 5 x 10⁷ CFU mL⁻¹ conidial suspension prepared from sporulating cultures *B. bassiana* isolate BG11. For each genomic DNA extraction, two epidermis pieces were used per sample, following treatment, and DNA was obtained using the MO BIO PowerPlant® Pro DNA Isolation Kit, as described for maize.

2.2.4 Amplification of plant genomic DNA

For amplification of genomic DNA (gDNA) obtained from plant tissues (maize, onion), the reagent concentrations for the PCR master mix, for 25 µL volume reactions, consisted of: 1.5 U/reaction Fast

Start Taq DNA polymerase (Roche Diagnostics GmbH, Mannheim, Germany), 1 X buffer, 2 mM MgCl₂, 0.2 mM deoxynucleotide triphosphate (dNTP) (Roche Diagnostics GmbH), 0.2 X bovine serum albumin (BSA, Sigma-Aldrich), 0.4 mM of each primer and 2 µL of eluted DNA. Universal forward and reverse primers were used to amplify plant chloroplast gDNA, psbA3_f (5'-GTTATGCATGAACGTAATGCTC-3') (Sang et al. 1997) and trnHf_05 (5'-CGCGCATGGTGGATTACAATCC-3') (Tate and Simpson 2003). Cycling conditions for PCR amplifications were as follows: step (1) 95°C for 5 minutes, step (2) 35 cycles consisting of: 95°C for 30 s, 63°C for 30 s, 72°C for 1 minute; step (3). 72°C for 7 minutes. Negative-template controls were included in all amplifications. PCR products were visualised on 1 % TAE-agarose gel as previously described, to check band size and purity, and secondary products were sequenced in one direction (5'-3') to confirm species identity (Sanger sequencing, Lincoln University Sequencing Unit, New Zealand).

2.3 Development of multi-species PCR for detection of *Beauveria* spp. in planta.

2.3.1 Primer design

Using the Basic Local Alignment Search Tool (BLAST) (Altschul et al. 1990) against the nucleotide database of the National Center for Biotechnology Information (NCBI), seven partial sequences of the translation elongation factor 1-alpha gene (*ef1α*) were obtained from various fungal genera (Figure 2.1), including *Beauveria*, by using a *B. bassiana ef1α* sequence (GenBank accession: AY531924.1, Rehner and Buckley 2005) as a reference query. Four additional *ef1α* sequences were acquired by using this reference sequence as a query against genome sequences of *B. bassiana* (isolates K4 and E17-P), *B. caledonica* (FRh1), and *B. malawiensis* (Bweta, Figure 2.1) (unpublished, BPRC, Lincoln University) in a Stand Alone BLAST search (Zhang et al. 2000). Nucleotide alignment (ClustalW alignment Higgins and Sharp (1988)), trimming and phylogenetic analysis were performed in Genious Pro ver. 5.6.5. (Biomatters^{LTD}), and subsequently the aligned *ef1α* sequences were analysed with the software package Spider (SPecies Identity and Evolution in R) (Brown et al. 2012). The ClustalW alignment of the 11 overlapping *ef1α* sequences resulted in a 989 bp-long nucleotide multiple sequence alignment (MSA). Using Spider, the *ef1α* sequence files for the *Beauveria* species represented in the MSA were designated collectively as a single species vector, in order to compare the genus '*Beauveria*' against the other fungal genera represented. This enabled Spider to find possible sites of genetic variation that were unique to the '*Beauveria*' vector in the MSA of the *ef1α* fragment, compared to an outgroup (i.e. *Trichoderma reesei*, *Verticillium dahliae*, *Metarhizium anisopliae* and *Aspergillus nidulans*, Figure 2.1).

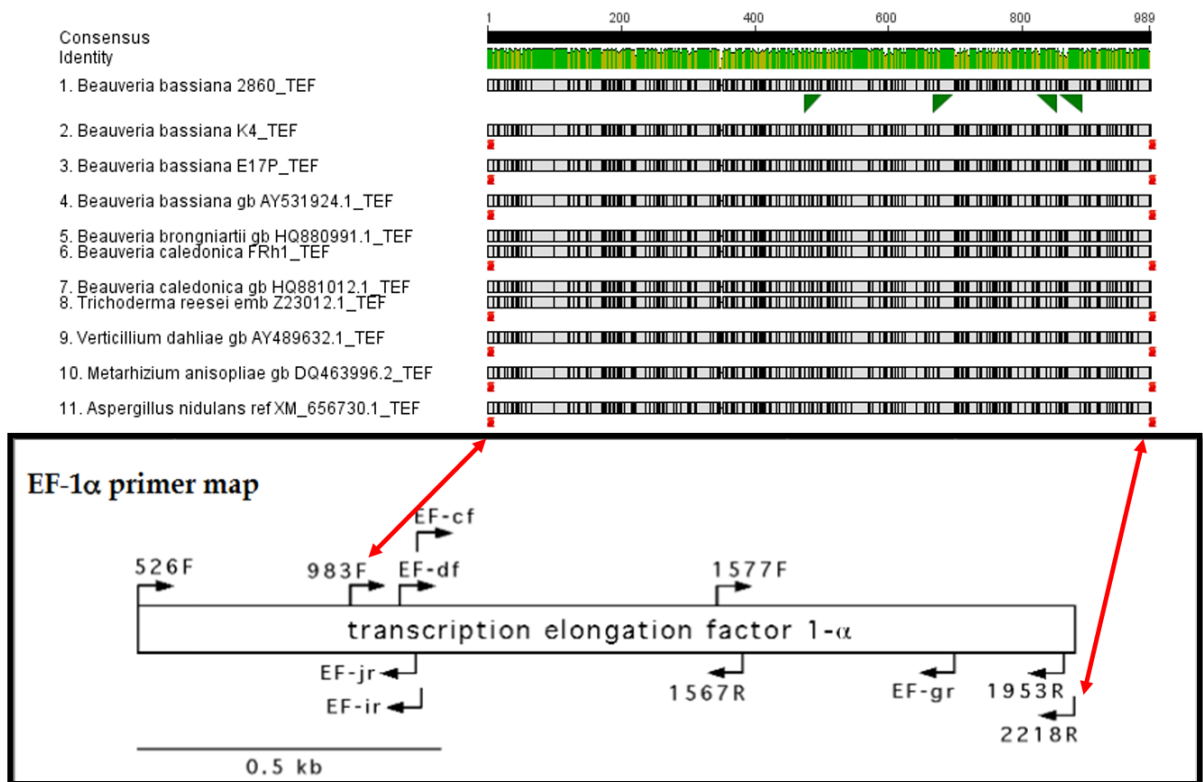


Figure 2.1. Design of primers for selective PCR. Figure shows a multiple sequence alignment of 11 fungal translation elongation factor 1-alpha (*ef1α* or EF-1α) sequences. The alignment was used to design nested primer pairs EF3F and EF5R (set 1), and EF4F and EF4R (internal amplicon in set 1); primer set position is indicated by green annotation in the alignment image. Primers were designed from within a 989 bp fragment generated from EF 983F and EF 2218R. Red arrows indicate the position of these primers on the '*ef1α* primer map', extracted from Binder and Hibbett (2003).

Using the informative sites identified by SpiderR, two pairs of primers were designed manually by visualisation in Geneious Pro for nested PCR/qPCR (Figure 2.1, Table 2.2).

The first primer pair EF3F and EF5R (designated 'EF3-5' collectively) were designed to amplify the three *Beauveria* species. An *in silico* test of primer specificity was conducted by using the EF3-5 primer sequences as queries in BLASTN 2.2.27 (Altschul et al. 1997) against the non-redundant GenBank database, set with parameters for the identification of short, near matches. A second pair, EF4F and EF4R (designated 'EF4-4' collectively) were designed to be general based on the MSA but nested within the EF3-5 amplicon and thus suitable for a two-step nested PCR protocol. This second pair were also designed to be suitable for real time qPCR. For example, the target amplicon for EF4-4 was designed to be shorter (< 200 bp) in order to maximise amplification efficiency. Additionally, the primer sets were designed such that single nucleotide polymorphisms (SNPs) within the target amplicons generated by both primer sets enabled species differentiation for *Beauveria* and for non-target genera via sequencing analysis. The Primer Express software (Applied Biosystems, Roche,

Branchburg, NJ) was used as an additional *in silico* test to assess the secondary structure, dimerisation, and melting temperature of the primer sets (Table 2.2). All primers used in this study were synthesised by Integrated DNA Technologies (IDT™, San Diego, CA, USA).

Table 2.2. Novel primer pairs designed for a 2-step nested PCR protocol. Designed from the translation elongation factor alpha-1 (*ef1α*) gene to target multiple *Beauveria* species *in planta*. Primer melting temperature (TM), the target amplicon size in base-pair (bp), and the type of experiment are described.

Primer ID	Sequence (5'→3')	TM	Amplicon (bp)	PCR type
EF3F	ACGGTGCCCGTCGGT	60	406	<i>Beauveria</i> multi-species nested pair 1
EF5R	ACTTGATGAACTTGGGGTTGTTC	55		
EF4F	GTCGCTGGTGACTCCAAGAA	59	176	<i>Beauveria</i> nested pair 2 ¹ , and/or qPCR
EF4R	GTACGGCGGTCGATCTTCTC	60		

1. Primers' EF4F and EF4R are not specific for *Beauveria*, unless used in a two-step nested experiment.

2.3.2 Optimisation of PCR

Fungal DNA isolation and amplification

High quality genomic DNA of isolates BG11, C14, E1063, FRh2, J1, J8, J10, J18, LU132, ICMP 11019 and ICMP 14476 (Table 2.1) was extracted for the purpose of PCR optimisation from pure hyphae (see section 2.2.1) using the MO BIO PowerPlant® Pro DNA Isolation Kit, according to the kit instructions but with the following modification: tissue lysis was conducted with the FastPrep-24™ (MP Biomedicals) at 5 m/s for 30 seconds. DNA from these isolates represented the genera selected by SpiderR in the MSA constructed for primer design, and thus their genomic DNA was used in preliminary PCR optimisation experiments to verify prior *in silico* tests. Amplification of the *ef1α* gene from the isolates' DNA samples was first conducted using a touchdown PCR protocol described by Rehner and Buckley (2005). Touchdown PCR reagent concentrations were the same as previously described in section 2.2.1, except with universal *ef1α* forward and reverse primers EF 983_F (GCYCCYGGHCAYCGTGAYTTYAT) and EF 2218R (ATGACACCRCRACRGCRGTYTG) (Rehner and Buckley 2005). Cycling conditions for touchdown PCR amplifications were as follows: step (1) 94°C for 2 minutes, step (2) 9 cycles consisting of: 94°C for 30 seconds, 66°C-56°C each for 30 seconds, decreased by 1°C per cycle, 72°C for 1.30 minutes; step (3) 36 cycles consisting of: 94°C for 30 s, 56°C for 30 s, 72°C for 1 minutes; step (4) 72°C for 7 minutes. Negative-template controls were included in all amplifications. PCR products were visualised on 1 % TAE-agarose gel as previously described, to check band size and purity, and secondary products were sequenced in one direction to confirm species identity (Lincoln University Sequencing Unit, New Zealand) by BLASTn, as previously described in section 2.2.1.

Initial PCR components and conditions for assessing amplification specificity and sensitivity using novel nested primers

For comparison with the universal primers, amplification of the *ef1α* gene was also performed using the novel primers EF3F and EF5R. PCR reagent concentrations used in the first step of the *ef1α* nested protocol, were prepared in a 25 µl volume reactions consisting of: 1.5U/reaction Fast Start Taq DNA polymerase (Roche Diagnostics GmbH), 1 X buffer, 2 mM MgCl₂, 0.2 mM deoxynucleotide triphosphate (dNTP) (Roche Diagnostics GmbH), 0.2 X bovine serum albumin (BSA, Sigma-Aldrich), 0.4 mM of each primer (EF3F and EF 5R, Table 2.2) and 2 µL of eluted DNA. The cycling conditions were as follows: Step (1) 95°C for 5 minutes, step (2) 30 cycles consisting of: 95°C for 30 seconds, 65°C for 30 seconds, 72°C for 1 minute; step (3). 72°C for 7 minutes.

Specificity experiments

The PCR protocol for the EF3-5 and EF4-4 primer sets was initially optimised to target species of the *Beauveria* genus represented in this study by testing the genomic DNA obtained from multiple fungal species, listed in Table 2.1. The parameter optimised was annealing temperature, following a temperature gradient of 55°C - 70°C in 1 degree steps in a Veriti 96 well Thermal Cycler (Applied Biosystems). Each optimisation experiment was replicated three times for each set of primers.

The specificity of the nested PCR protocol was tested by real-time amplification of a subset of fungal species, namely: *Alternaria alternata*, *Aspergillus nidulans*, *Fusarium oxysporum*, *Lecanicillium lecanii*, *Trichoderma atroviride* and *Verticillium dahliae* (Table 2.1), against DNA from *B. bassiana* isolates BG11, FRh2 and J18, using the EF4-4 primer sets on EF3-5 primer-generated DNA template. Real-time PCR amplifications were conducted in an Applied Biosystems StepOnePlus™ Real Time PCR System (Applied Biosystems®), using the PCR reagent concentrations (Table 2.3) and thermal cycling conditions recommended for use with SYBR® Green 1 fluorescent dye in the Applied Biosystems StepOnePlus™ machine, as per the 'Universal SYBR Green Quantitative PCR Protocol' described in the technical documents by Sigma-Aldrich (Merck). The real time cycling conditions used are summarised as follows:

- Step (1) 94°C for 2 minutes, step (2) 40 cycles consisting of: 94°C for 15 seconds, 60°C for 1 minute; followed with an optional melting curve (3), step and hold: 95°C for 15 seconds, 60°C for 1 minute and 95°C for 15 seconds.

Positive and negative template controls (NTC, ddH₂O and master-mix) were included in each PCR run, including the NTC from the step 1 reaction in the nested PCR. Each sample reaction in the qPCR had three technical replicates. PCR product from the first step of the nested protocol were first visualised on 1% TAE-agarose gel as previously described, to check amplification and purity. The product was then diluted 1:1000, by taking 1 µL PCR product and mixing it by vortex into 999 µL H₂O. Real time

PCR, as the second step of the nested PCR protocol, enabled the optimisation of the cycle number required in order to target the *Beauveria* spp. represented, to minimise late stage non-target amplification.

Table 2.3. Reagent concentrations for master-mix used in real time PCR. Based on the protocol optimised for *Beauveria* translation elongation factor 1-alpha (*ef1α*) target with primers EF4F and EF4R

Reagent component	Concentration per 16 µL
DNA template	10 ng ⁵
Buffer ¹	1 X
MgCl ₂ ¹	4 mM
Deoxynucleotide triphosphate (dNTP) ¹	0.6 mM
Primer (each) ²	0.5 µM
ROX passive reference dye ³	0.625 µM
SYBR Green 1 ⁴	1:30000 dilution
FastStart Taq DNA polymerase ¹	1.5 U/µl

1. Roche Diagnostics GmbH, Mannheim, Germany
2. Primer stock concentration = 10 µM
3. Invitrogen™, USA
4. Bio-Rad Laboratories Inc, Hercules, CA, USA
5. DNA concentration on average, however, target DNA cannot be first quantified *in planta*.

Secondary reaction EF4-4 PCR products were visualised for on 1.8 % TAE-agarose gel, to check band size and purity, and then sequenced (5' – 3') to confirm species identity (Sanger sequencing, Lincoln University Sequencing Unit, New Zealand). All Real-time PCR amplifications were conducted in an Applied Biosystems StepOnePlus™ Real Time PCR System (Applied Biosystems®).

Sensitivity experiments

Kinetic PCR and the application of standard curves

In this study, kPCR was used to investigate the sensitivity of amplification, using the nested PCR protocol with primers EF4-4, to amplify amplicon template generated from known amounts of *B. bassiana* DNA in the EF3-5 pre-amplification round, in order to construct a series of standard curves. To accomplish this, the number of amplicon copies produced from the PCR pre-amplification step (EF3-5) was estimated using the following PCR amplification equation (Rutledge and Cote 2003):

$$N_C = N_0 \times (E + 1)^C$$

Where N_C is number of amplicon molecules, N_0 is the initial number of target molecules, E is the amplification efficiency (expressed as a percentage) and C is number of thermal cycles. The amplification efficiency (%E) is derived using the following formula (Rutledge and Cote 2003):

$$E(\%) = \left(\frac{10^{-1}}{\text{slope}} - 1 \right) \times 100$$

Given that the slope estimate is derived from a qPCR standard curve, the amplification efficiency for a standard PCR reaction with primers EF3-5 was first estimated from a qPCR experiment conducted on a serial dilution of pure *B. bassiana* DNA spiked into sdH₂O. This enabled the construction of another standard curve, that represented the lower limits of target detection, by calculating the estimated number of *ef1α* copies per genome available for amplification per picogram (pg) of DNA, according to formulae supplied by Applied Biosystems (2003), and based on the genome size of *B. bassiana* isolate ARSEF 2860 of 33.7 Mbp (Xiao et al. 2012). In *B. bassiana sensu lato*, *ef1α* is single copy per genome, thus the number of amplicons produced from *ef1α* in a PCR is able to be calculated based on the number of genome copies represented in a given sample, if the PCR efficiency is also known.

Estimating translation elongation factor 1-alpha (ef1α) copy number by qPCR standard curve analysis with primers EF3F and EF5R

To determine PCR amplification efficiency with primers EF3F and EF5R, a gDNA dilution series consisting of *B. bassiana* isolate BG11 template in ddH₂O, was prepared with the following concentrations: 100 ng (10⁻¹), 10 ng (10⁻²), 1 ng (10⁻³), 0.1 ng (10⁻⁴) and 0.01 ng (10⁻⁵) of template gDNA, respectively. The PCR reagents were the same as those listed in Table 2.3, and the cycling conditions were as follows: Step (1) 95°C for 2 minutes, step (2) 40 cycles consisting of: 95°C for 30 seconds, 60°C for 45 seconds, and 72°C for 45 seconds.

Assessing EF4F and EF4R quantitative PCR amplification efficiencies from comparative standard curve analyses on gDNA versus PCR generated target template

The sensitivity of the nested PCR protocol was initially demonstrated by comparing two qPCR standard curves, constructed from: (1) EF4-4 target amplification of *B. bassiana* gDNA directly, versus (2) EF4-4 target amplification of diluted PCR template (1:1000), which was generated by primers' EF3-5 via amplification of the same gDNA stock, in a standard PCR reaction. A 10-fold dilution series were prepared using gDNA stock of *B. bassiana* isolate J18 [3.2 ng/μL], spiked into a maize DNA and ddH₂O diluent [1.6 ng/μL]. The conditions used in the following real time PCR experiments for the EF4-4 target were adjusted as follows: Step (1) 95°C for 2 minutes, step (2) 40 cycles consisting of: 95°C for 30 seconds, 62°C for 45 seconds, 72°C for 45 seconds.

Assessing nested PCR amplification efficiency from standard curve analysis of an inoculum dilution series

To further assess the sensitivity and specificity of the nested PCR, the amplification efficiency of real-time qPCR using DNA obtained from inoculated plant tissue was assessed. To achieve this, onion epidermis pieces were inoculated prior to DNA extraction with a 10-fold dilution series of a conidial

suspension. Briefly, the stock conidial suspension was made from pure culture of *B. bassiana* isolate BG11 (refer to section 2.2.2), prepared in 5 mL 0.05% Tween 80 at a concentration of 5×10^7 conidia per mL. The serial dilution was then prepared, by adding 1 mL of the stock suspension into 9 mL 0.05% Tween 80, for a 10^{-1} suspension and this was repeated in series from 10^{-1} until a 10^{-5} dilution was achieved. A single onion epidermis piece was prepared for each inoculation/DNA sample, according to the method described in section 2.2.3 for onion epidermis. However, each onion epidermis piece was inoculated with 80 μ L per each dilution suspension. The total quantity of conidia per each dilution and inoculation was estimated in Table 2.4. The inoculated onion epidermis pieces were incubated for three hours at 20°C prior to DNA extraction (see section 2.2.3.2 for DNA isolation from onion epidermis). DNA concentrations were not quantified as the CT values were compared relative to estimated inoculum concentration, and compared to prior standard curves described previously for EF4-4 target amplification of PCR template, which was generated by primers' EF3-5 after 30 cycles.

Table 2.4. Concentration of inocula. Conidial suspension concentrations were calculated relative to inoculum volume (80 μ L) and applied to onion epidermis

Suspension dilution	Conidia mL ⁻¹	Conidia per cm ² epidermis
1.00E+00	5.00E+07	4.00E+06
1.00E-01	5.00E+06	4.00E+05
1.00E-02	5.00E+05	4.00E+04
1.00E-03	5.00E+04	4.00E+03
1.00E-04	5.00E+03	4.00E+02

2.4 Surface sterilisation methodology for PCR detection of *Beauveria bassiana*

2.4.1 Maize PMATM treatment assay

The following assay was conducted in order to test and compare the efficacy of two different surface sterilisation protocols, using maize roots. The effectiveness of propidium monoazide (PMATM) dye for dealing with potential surface DNA contamination after surface sterilisation was also investigated. The experiments were repeated three times for each surface sterilisation protocol used, with six replicates per treatment per experiment, arranged in a complete randomised block design (treatments for all experiments are indicated below in Table 2.5). Individual roots of 180 five-day old maize seedlings were inoculated each with 20 μ L of a 5×10^7 conidia per mL suspension, prepared

from pure culture of E1063 (Table 2.1; section 2.2.2) which was applied directly to the middle section of the root by pipette, while avoiding contact with the agar to achieve a total of 10^6 conidia per inoculum volume on the rhizoplane. The seedlings were grown on 40 mL of 1% agar (10 g of agar in 1 L H₂O; autoclaved prior to pouring), prepared in 500 mL volume sterile plastic containers with screwable lids (LabServ, NZ). Growth conditions and seed preparation was conducted according to the method described in section 2.2.3 for maize. The inoculated section of root was indicated by making a cut with a sterile blade to the agar media surrounding it. The inoculated seedlings were then incubated at 20°C for 3 hours, and then inoculated roots aseptically cut from the plant in 1.5 cm long fragments (including the area where the inoculum was applied) for subsequent treatment (Table 2.5). Inoculated samples were either surface sterilised (SS) or not, and/or treated with PMA™ or not. Samples from treatments' 1-4 were all processed for DNA isolation following their respective treatment, according to the method described in section 2.2.3. Samples from treatment 5 were placed on *Beauveria* semi-selective media (BSM; consisting of quarter strength PDA, 350 mg/L streptomycin sulphate, 50 mg/L tetracycline hydrochloride and 125 mg of cyclohexamide; Sigma-Aldrich) (Brownbridge et al. 2012) and then incubated at 25°C for 20 days to check for the presence or absence of *Beauveria* spp. colonies. Detection of *B. bassiana* DNA was achieved using the novel primer sets, with the same reagents and conditions in a two-step nested protocol as described in "Initial PCR components and conditions for assessing amplification specificity and sensitivity using novel nested primers" (section 2.3.2), except with a standard PCR reaction for the second step with primers EF4-4.

Table 2.5. Treatments used during the PMA assay with inoculated *Zea mays* (maize) roots. Surface sterilisation, designated SS in the treatment description, was accomplished with either of two different surface sterilisation protocols A and B.

Treatment code	
1	Inoculum, SS, PMA
2	Inoculum, PMA ¹
3	Inoculum ¹
4	Inoculum, SS
5	Inoculum, SS, cultured on PDA

1. Treatment 2 and 3 were considered as additional inoculum positive/PMA controls.

Surface sterilisation protocol A

Treatments 1, 4 and 5 (Table 2.5) were surface sterilised based on a sodium hypochlorite (NaOCl) bleach procedure adapted from Schulz et al. (1993), which was as follows: 10 seconds 0.05% Tween

80, 5 minutes 2.5% NaOCl, sdH₂O rinse, 1 minute 70% EtOH, 2 times sdH₂O washes, performed on inoculated and cut root samples. This protocol was designated protocol A. For each experiment (exp. 1-3), 100 µL of the final wash water was incubated on potato dextrose agar (PDA; Difco, USA) at 25°C for 14 days, to test the sterility of the water. Root samples from treatment 5 were additionally rolled onto PDA after surface sterilisation, prior to culturing those samples on fresh BSM media.

Surface sterilisation protocol B

Surface sterilisation (protocol B) was performed on treatments 1, 4 and 5 (Table 2.5) according to the method described by (Arnold and Lutzoni 2007), which was: 10 seconds 96% EtOH, 2 minutes 0.525% NaOCl, 2 minutes 70% EtOH and 2 x sdH₂O washes. Controls for sterility in experiments (exp 4-6) were used as described for protocol A experiments' 1-3.

Propidium monoazide treatment

The following protocol for the treatment of surface sterilised plant tissue for endophyte detection with propidium monoazide (PMATM) dye, was first adopted by Wicaksono et al. (2016), based on the manufacturer's instructions (Biotium, PMATM dye Product Information sheet). Surface sterilised samples were individually placed in 0.6 mL centrifuge tubes, and to each of these, 500 µL of ddH₂O was added, followed by 1.25 µL of a 20 mM PMATM stock solution, for a concentration of 50 µM per sample. Tubes were then vortexed briefly, to ensure full submersion of the samples in the solution and then transferred immediately to an enclosed box in order to incubate in the dark for 5 minutes. To limit light exposure during the reaction phase (dark incubation), no more than 10 samples were processed for the PMATM treatment at a time. The tubes were subsequently transferred to a foil-lined tray resting on ice, on a shaking table (low rpm) and exposed to a halogen light lamp for 5 minutes. The lamp was set 20 cm directly from the samples at a 45° angle and the samples were manually turned at least once during the 5 minute light exposure. The samples were stored in the tubes at 4°C. Prior to the isolation of DNA, the solution was extracted using a pipetman. To test the activity of the PMATM treatment, four 500 µL aliquots of a conidial suspension were heat treated to 85°C for 10 minutes. Two of the four heat treated samples were then processed with PMATM, along with each batch of experimental samples. These four heat-treated suspensions were included as DNA positive samples for comparison in subsequent PCR experiments to confirm that target amplification of DNA was completely hindered by the PMATM dye.

2.4.2 Onion surface sterilisation assay

To elucidate the efficacy of surface sterilisation for PCR detection, a study was conducted using *B. bassiana* isolate BG11 as inoculum on onion epidermis. It was hypothesised that using onion epidermis could minimise potential absorption of the inoculum by the plant tissue, thus viable propagules or DNA detected from *Beauveria* after surface sterilisation were attached to the

epidermal surface (and not endophytic or absorbed, as may occur with live plant roots). Epidermal pieces were inoculated in pairs with 40 μ L each of suspension (see section 2.2.3 for onion epidermis), to obtain two epidermal pieces per experimental replicate for a combined estimated inoculum load of 4×10^6 conidia (in 80 μ L suspension) per sample. The inoculated pieces were incubated for either 24 hours or 96 hours and then surface sterilised using a protocol with differing NaOCl concentrations, as summarised in Table 2.6.

Table 2.6. Surface sterilisation protocol(s). Outlined are agent solutions and concentrations, where applicable, used in the onion epidermis surface sterilisation optimisation assay.

Component	Tween 80	%EtOH	sdH ₂ O rinse	%NaOCl	sdH ₂ O rinse
Concentration	0.05	85	NA	2.00	NA
				3.25	
				5.00	
Duration	30 s	1 min	30 s	5 min	2 min ¹

1. The final rinse step was repeated, with 1 min per rinse.

The experiment consisted of four replicates per treatment, for incubation period and NaOCl concentration, in a two factorial design. Genomic DNA was obtained following the respective treatment, as previously described in section 2.2.3 for onion epidermis. Detection of *B. bassiana* DNA was achieved using the novel *ef1 α* primer sets, in a two-step nested protocol with two standard PCRs, as described in previously in section 2.4.1.

2.4.3 Microscopic visualisation of colonised maize tissue

WGA-Alexa fluor / Propidium Iodide staining procedure

The following methods were employed by Post-Doctoral Fellow Maria Eugenia Moran-Diez in order to visualise maize root tissue before and after surface sterilisation (see Table 2.6; protocol used 5% active NaOCl). All maize root tissue was inoculated 3 days prior using conidial suspensions of *B. bassiana* isolates' BG11, FRh2 or J18 (prepared as previously described). Root samples that were not surface sterilised were washed in 0.01% Tween 80 for 15 seconds followed by three washes in sterile water. Five day-old maize seedlings (cultivar Pioneer 34H31) were used in this experiment, these were grown under sterile conditions from surface sterilised seed.

To prepare root tissues for confocal laser scanning microscopy (CLSM), roots were treated with propidium iodide (Sigma-Aldrich, Merck, USA) and WGA-Alexa Fluor 488 conjugate (Molecular

Probes, Eugene, OR, USA) according to the procedure described by Ramonell et al. (2005), to stain chitin in the fungal infection structures. Briefly, roots were aseptically cut and soaked in 80% EtOH for 12 hours at room temperature. Following this period, roots were treated with 10% KOH and incubated for a further 16 hours. Roots were then transferred into 1× phosphate-buffered saline (PBS; pH 7.4) containing 0.1% Triton X-100 and stained with WGA-Alexa Fluor 488 at 10 µg/mL for four hours at 4°C. The roots were then washed in 1× PBS (pH 7.4) buffer for three hours and in then soaked in fresh buffer overnight at 4°C. Propidium iodide (PI) in 1× PBS (pH 7.4) (20 µg/ml) was then used as a counterstain for the plant tissues, followed by a final wash with 1× PBS buffer, for three hours.

Confocal microscopy

Confocal microscopy was performed using a Fluoview FV10i instrument (Olympus). Fluorescence was excited with an argon laser at 488 nm and detected at wavelengths of 500–520 nm (WGA-Alexa Fluor 488 conjugate) or 600–620 nm (PI). Images were processed and arranged using the Fluoview viewer software (Olympus).

2.5 Results

2.5.1 Optimisation of PCR

Specificity assessment

The *in silico* test of primer specificity using EF3F and EF5R primer sequences as a sequence query against the GenBank database revealed that the primer set matched multiple *Beauveria* species sequences (e.g. ~10), however, the number of *Beauveria* species was not quantified because of the large number of sequences not identified to species level in the GenBank database, neither were the primers exclusively specific for the *Beauveria* genus. Related entomopathogenic fungal taxa *L. lecanii* and *Isaria farinosa* also matched the primer sequences on the *ef1α* gene.

The fungal species *A. alternata*, *A. nidulans*, *L. lecanii*, *T. atroviride*, *V. dahliae* and *B. bassiana* isolates' BG11, FRh2 and J18, were amplified using *ef1α* universal primers EF 983_F and EF 2218R and produced an approximately 1000 bp fragment (Figure 2.2). *Fusarium oxysporum* ('*F. oxy*') produced non-specific amplification with this primer set (Figure 2.2, plot a). Amplification was only successful in terms of visible bands for the three *B. bassiana* isolates and the *L. lecanii* (*L. lecan*), using the EF3-5 primers, after 30 thermal cycles (Figure 2.2, plot b).

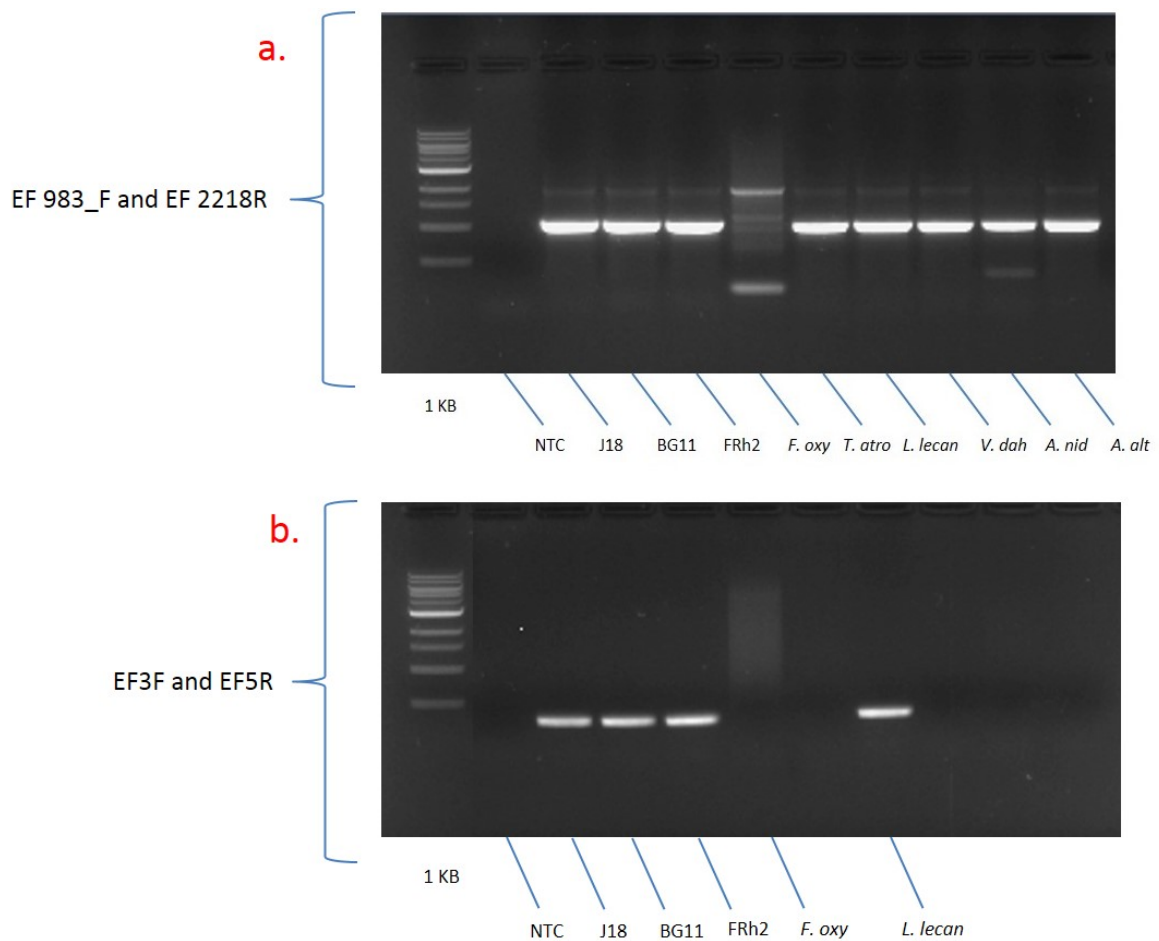


Figure 2.2. Electrophoresis gel images comparing amplification of multiple fungal species DNA. Plot (a) shows amplification of the translation elongation factor 1-alpha (*ef1α*) gene using universal PCR primers, and, plot (b) shows amplification of the *ef1α* 406 bp amplicon by novel primers EF3F and EF5R (30 cycles) with a 1 kb DNA ladder (Hyperladder II, Bioline, USA).

Real-time amplification of the PCR product generated by primers EF3-5 using the internal EF4-4 primers demonstrated that the nested protocol was specific for the three *B. bassiana* isolates and the *L. lecanii* (Figure 2.3). Using the nested protocol, amplification of the non-target DNA samples occurred after 20 cycles, whereas, the target DNA (i.e. *Beauveria*) was detected before 5 cycles. Based on the cycle threshold values observed in this assay, the number of cycles for the first step of the nested PCR protocol was reduced to either 20 or 25. The number of cycles for the second step of the nested protocol was reduced to 30.

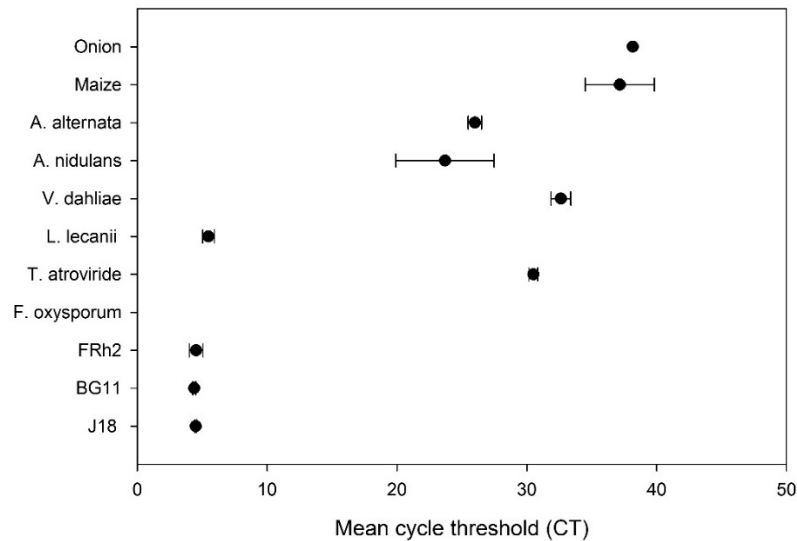


Figure 2.3. Real time qPCR cycle threshold means. Plot shows amplification of multiple fungal species and plant host DNA (onion and maize), versus *Beauveria bassiana* isolates (BG11, FRh2, J18) (Y axis) over mean cycle threshold (CT) values (X axis) with standard deviation error bars (where possible), using EF4F and EF4R as nested step 2 PCR target amplification on EF3F and EF5R generated product.

Sensitivity assessment

Estimating translation elongation factor 1-alpha (ef1 α) copy number by qPCR standard curve analysis with primers EF3F and EF5R

The estimated amplification efficiency from the first step of the nested PCR (target EF3-5) was 59% (Figure 2.4). The lower concentration (0.01 ng; 10^{-5}) was omitted from the standard curve analysis since the 10^{-4} CT mean exceeded 30 cycles, and 30 cycles was the number used in the PCR amplification equation in order to estimate amplicon quantity produced, in subsequent experiments, from EF3-5 standard PCR amplification. Omitting 10^{-5} dilution increased the overall PCR amplification efficiency from 54% to 59%.

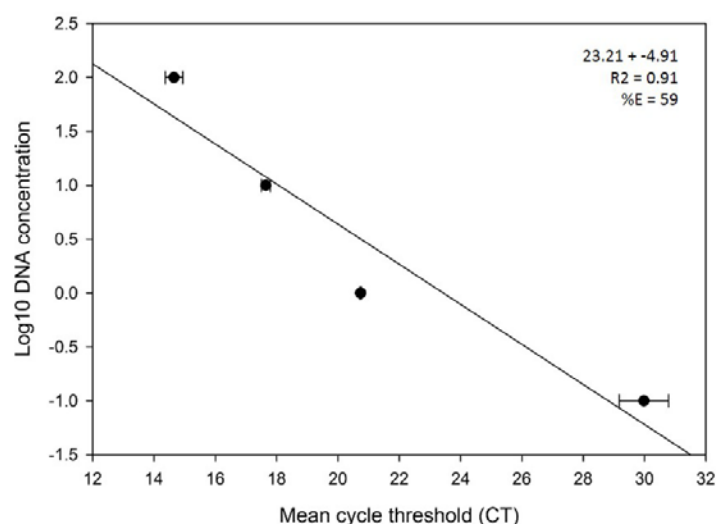


Figure 2.4. Testing of nested PCR amplification efficiency. Plot shows a standard curve representing mean cycle threshold (CT), with standard deviation error bars, plotted over log10 DNA concentration (ng/μL) from *Beauveria*. The regression equation intercept and slope of the curve, with amplification efficiency (%E) from qPCR target translation elongation factor 1-alpha (*ef1α*) EF3F and EF5R is also included.

Based on a PCR amplification efficiency of 59% and 30 thermal cycles, the likely number of *Ef1α* amplicons generated from the EF3-5 target was estimated in Table 2.7 (column 4).

Table 2.7. Quantifying fungal DNA with nested PCR. Estimated are the number of amplicons available per dilution sample provided from PCR on translation elongation factor 1-alpha (*ef1α*) target EF3-5, for use in quantitative PCR (as nested step 2) with *ef1α* target EF4-4.

Dilution ¹	DNA concentration pg per 2 μl	Number of available <i>ef1α</i> copies ²	Number of amplicons (N0) generated ³	Number of amplicons per 1 μL ⁴
Stock	640	17328	26424657	52849
0.1	64	1733	2642466	5285
0.01	6.4	173	264247	528
0.001	0.64	17	26425	52
0.0001	0.064	1	2185	5

1. 10 fold dilution prepared by 2:18 μL, of J18 stock DNA (3.2 ng/μL) into maize DNA:ddH₂O as a diluent [1.6 ng/μL]

2. DNA concentration pg/genome mass pg

3. PCR amplification equation, with an amplification efficiency of 59%; with EF3-5 target and 30 cycles

4. Amplicon number available after dilution of product for step 2 PCR (1/500 μL ddH₂O)

Assessing EF4F and EF4R quantitative PCR amplification efficiencies from comparative standard curve analyses on gDNA versus PCR generated target template

The nested PCR protocol was more sensitive than a single real-time PCR. The standard curve constructed from the nested PCR protocol, for EF4-4 target amplification on PCR product (EF3-5) template had an amplification fluorescent threshold (FT) at cycle 5.002 on the Y intercept, compared to EF4-4 target amplification of gDNA directly, which had an FT of 17.381 (Figure 2.5). In both standard curves, the PCR amplification efficiency (%E) was over-estimated with 114% for the nested protocol and 123% for the single qPCR. Omitting the final dilution (10^{-4}), improved the efficiencies to 100% for the nested PCR and 110% for single qPCR using EF4-4 primers.

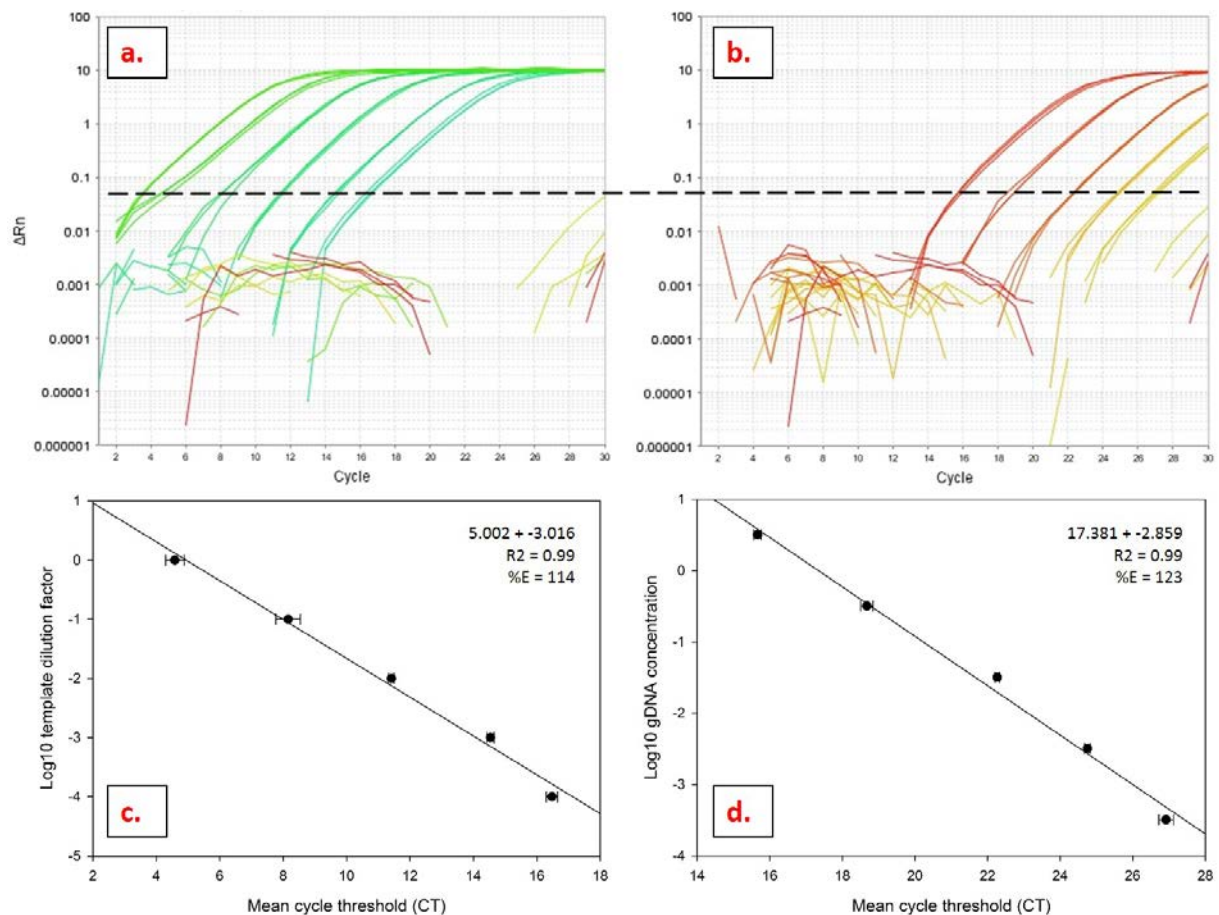


Figure 2.5. Comparison of qPCR standard curves. Plots contrast the analysis of EF4F and EF4R target on a PCR template versus direct amplification of gDNA. Plot (a) shows amplification of diluted template produced in a prior PCR of a 10-fold dilution series of *Beauveria bassiana* gDNA (isolate J18) spiked in *Zea mays* (maize) gDNA and plot (c) shows the corresponding standard curve with regression equation and amplification efficiency (%E). Plot (b) shows direct amplification of a 10-fold dilution series of *Beauveria bassiana* gDNA (isolate J18) in H₂O and plot (d) shows the corresponding standard curve produced with the regression equation and amplification efficiency (%E).

Assessing nested PCR amplification efficiency from standard curve analysis of an 'inoculum and host' dilution series

Beauveria bassiana target DNA obtained from inoculated onion epidermis samples was high, based on the 10^{-1} to 10^{-3} dilution mean CT observed (Figure 2.6). This was seen by the low intercept (4.76) and over-estimated amplification efficiency of 207%, likely resulting from high numbers of template amplicon copies available for qPCR for these dilution samples, generated prior from the EF3-5 PCR.

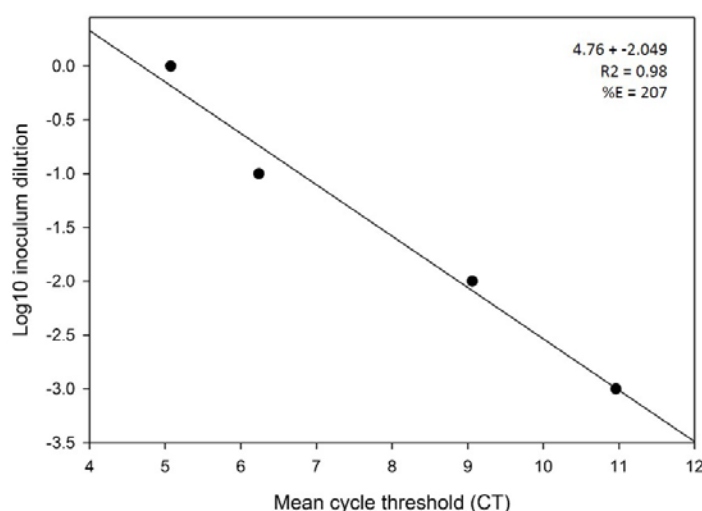


Figure 2.6. Amplification of mixed DNA. Plot shows a standard curve representing mean cycle threshold (CT), plotted over log10 dilution factor obtained from DNA of inoculated onion epidermis. Included is the regression equation intercept and slope of the curve, from qPCR target translation elongation factor 1-alpha (*ef1α*) EF4F and EF4R.

Nested PCR protocol summary

Following the results of the specificity and sensitivity experiments, the two step nested protocol was optimised, generally, to the following conditions:

For standard PCR with primers EF3F and EF5R (nested step 1)

- Step (1) 95°C for 5 minutes, step (2) 25 cycles consisting of: 95°C for 30 seconds, 65°C for 30 seconds, 72°C for 1 minute; step (3) 72°C for 7 minutes.

Standard PCR with primers EF4F and EF4R (nested step 2)

- Step (1) 95°C for 5 minutes, step (2) 30 cycles consisting of: 95°C for 30 seconds, 65°C for 30 seconds, 72°C for 1 minute; step (3) 72°C for 7 minutes.

Real-time PCR with primers EF4F and EF4R (nested step 2)

- Step (1) 95°C for 2 minutes, step (2) 35 cycles consisting of: 95°C for 15 seconds, 64°C for 30 seconds, and 72°C for 45 seconds; followed with an optional melting curve (3), step and hold: 95°C for 15 seconds, 60°C for 1 minute and 95°C for 15 seconds.

2.5.2 Surface sterilisation for PCR detection

Maize PMATM treatment assay

Beauveria bassiana isolate E1063 was more frequently amplified using the EF3-5 and EF4-4 nested PCR protocol in samples that were surface sterilised using protocol B (Arnold and Lutzoni 2007), compared to protocol A (Schulz et al. 1993). *Ef1α* was also more frequently detected in the PMATM treated samples that were not previously surface sterilised (treatment 2), compared to root samples that were not treated at all (i.e. inoculum only positive controls; treatment 3) (Table 2.9; Figure 2.7).

Table 2.8. Percentage of positive *Beauveria bassiana*. Represented by *ef1α* bands (treatments' 1-4) or viable colonies (treatment 5 only) detected from *Zea mays* (maize) roots following surface sterilisation (SS) using protocol's A or B, for each treatment used during the maize PMATM assay (6 experiments).

Treatment	Percent positive (A)			Percent positive (B)			Averages	
	Exp 1	Exp 2	Exp 3	Exp 4	Exp 5	Exp 6	A	B
(1) inoc, SS, PMA	0	17	0	33	33	50	6	39
(2) inoc, PMA (+)	33	100	100	83	100	100	78	94
(3) inoc (+)	0	100	50	50	100	83	50	78
(4) inoc, SS	33	0	0	50	0	0	11	17
(5) inoc, SS, cultured	83	67	100	100	100	100	83	100

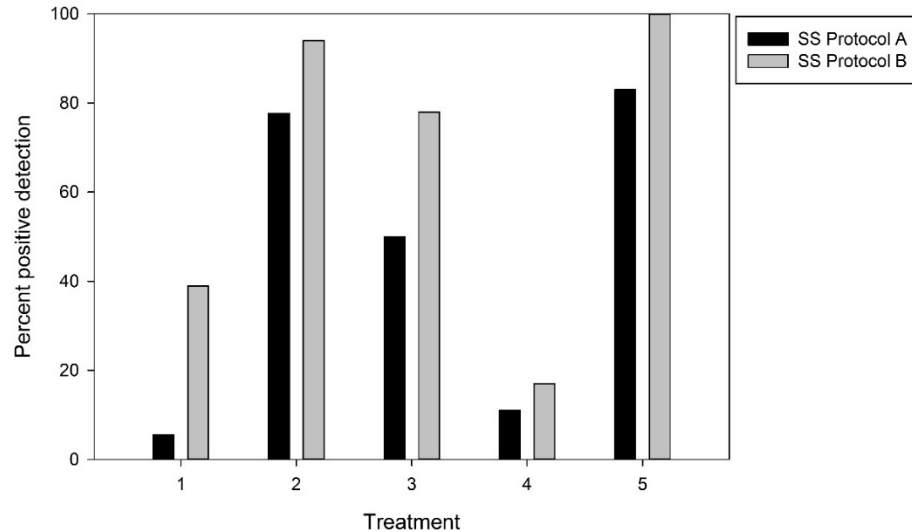


Figure 2.7. Percentage of total positive *Beauveria bassiana*. Represented by *ef1α* bands (treatments' 1-4) and viable colonies (treatment 5) detected following surface sterilisation (SS) protocol's A or B, for each treatment used during the *Zea mays* (maize) PMA™ assay.

Overall, protocol B (0.525% NaOCl) resulted in more *Beauveria* positives on average, particularly for treatments' 1 and 4, compared to the protocol A (2.5% NaOCl). Additionally, protocol B had a greater frequency of observed putative *B. bassiana* fungal colonies growing from cultured root samples for treatment 5 (Table 2.9) compared to the protocol A. However, for both protocols, the recovery of viable fungal colonies from surface sterilised cultured root samples (treatment 5) was high at 83% and 100% of samples on average (Table 2.9, see 'Averages' column) (Figure 2.7, 2.8). In contrast, *ef1α* was not effectively amplified as expected in the PCR experimental positives, particularly for treatment 3 in experiment 1 (SS protocol A). For the heat treated conidial suspensions, amplification was 100% successful in suspensions not treated with PMA, and suspensions treated with PMA demonstrated the efficacy of the dye because they showed no detected amplification of any DNA (data not illustrated).



Figure 2.8. Images of putative *Beauveria bassiana* colonies growing from surface sterilised (SS) plant tissue. Tissue treated following 3 hours of incubation of inoculum (from experimental treatment 5). Image (a) shows early stage growth from cut ends of root (3 days after SS) and (b) shows sporulating culture from later stage growth (12 days after SS).

Onion epidermis surface sterilisation assay

Using onion epidermis, surface sterilisation efficacy was assessed for the elimination of surface epiphytes introduced by inoculation. From this assay, the *ef1 α* target (EF3-5; EF4-4) was only detected in a single sample, which was treated with 3.25% NaOCl in the surface sterilisation protocol after a 96 hour incubation period. Additional inoculated epidermal pieces (96 hour treatment) that were incubated on the BSM selective media following surface sterilisation with 3.25% active NaOCl showed no fungal growth, demonstrating that the inoculum detected in this assay by PCR was not likely viable.

2.5.3 Microscopic visualisation of colonised maize tissue

Using confocal imaging colonisation of the maize root surface by the three *B. bassiana* isolates was observed, however, no specific infection structures were found to validate endophytic establishment. A substantial network of hyphal growth was seen to cover root epidermal layers for all isolates (Moran-Diez, pers. communication) but this fungal growth was generally found to be restricted to the superficial parenchymal layers irrespective of when (in terms of days after inoculation) colonisation was observed using microscopy. In Figure 2.9 (a, b and c), *B. bassiana* isolate BG11 can be seen with hyphae in-tact after surface sterilisation was performed.

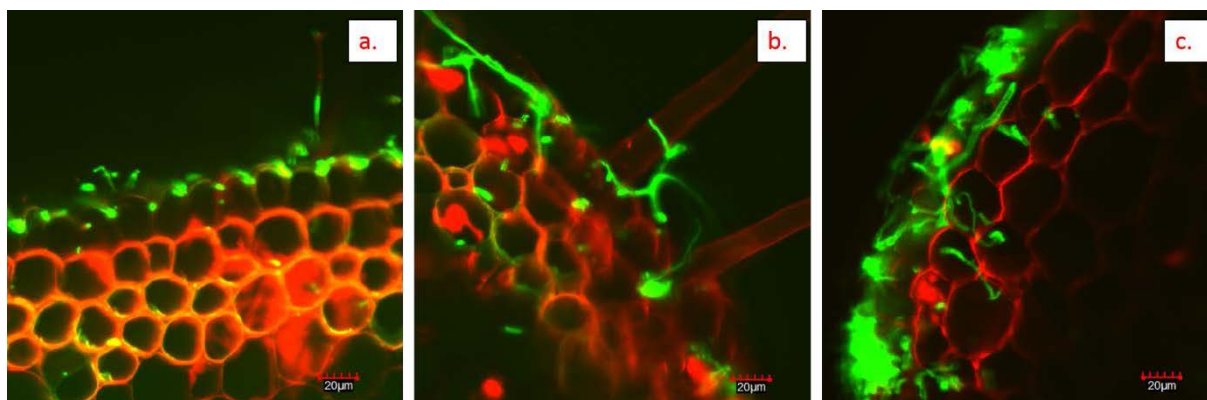


Figure 2.9. Confocal images of *Beauveria bassiana* colonising the maize root surface after surface sterilisation. Tissue was surface sterilised following 3 days of incubation after inoculation. Fungal material was stained to fluoresce green using WGA-Alexa fluor 488 conjugate and plant material red with propidium iodide dye. Image (a) shows *B. bassiana* isolate BG11 colonising to the first three layers of the parenchyma cells. Images (b) and (c) show how intricately the fungal mycelia (BG11) interacts with the root surface.

2.6 Discussion

In this chapter, a sensitive and selective PCR based detection method was developed for the detection of multiple *Beauveria* species from maize and onion DNA. The nested protocol was optimised by using a high annealing temperature (65°C) and a low number of cycles (25 thermal cycles), to effectively remove non-target amplification, while still remaining sensitive enough to amplify less than 0.32 pg/µL, or between 1-17 *ef1α* copies. Consequently, the primers were deemed sufficiently exclusive for the purposes of this project. Weak amplification of maize gDNA by primers EF4-4, meant that primers EF4-4 were not suitable to use directly on plant gDNA to target *Beauveria* (i.e. not as a nested protocol). When the nested PCR was standardised, it was possible to estimate target DNA quantity by comparing sample CT values within a predetermined range, since the standard curve proved reproducible between PCR experiments.

The elimination of inoculum on plant surfaces was problematic for PCR. Maize roots were inoculated with a conidial suspension immediately prior (< 10 min) to surface sterilisation and DNA extraction. Given that *B. bassiana* requires a minimum of 12 hours incubation at room temperature for spore germination to occur (Vega et al. 2012) endophytic growth was unlikely to have occurred prior to the sterilisation process. However, the maize roots retained some inoculum possibly via absorption of the liquid suspension into vascular tissues, thus confounding the results. For this reason, the onion epidermis assay was developed, as a novel procedure for verifying the elimination of surface inoculum for PCR detection. Onion epidermis can be manually peeled to a single cell layer, providing a plant surface which enables 'epiphytic' adhesion of the inoculum while excluding the possibility of

endophytic colonisation or absorption of the inoculum. Furthermore, onion epidermis may be ideal for microscopic visualisation of the inoculum before and after surface sterilisation, directly on the epidermal surface. In future studies, the number of conidia remaining after sterilisation could be estimated using microscopy, and subsequent PCR experiments could determine a detection threshold for conidia per cm². Thus, the novel onion epidermis surface sterilisation assay may be a useful control experiment, in future studies, to ascertain surface sterilisation method efficacy and enable the identification of false endophyte-positive discovery rates.

In the experiments with maize, target DNA (i.e. *Beauveria*) was more often detected in PMA treated samples. This may be a result of PMA enhancing the PCR sensitivity, perhaps by an interaction with the reagents or by reducing the total DNA pool available for amplification (Nocker et al. 2006), as the DNA from damaged plant host tissues was likely also inactivated following surface sterilisation. The inclusion of a PMA binding step for endophyte detection, therefore, requires stringent surface sterilisation to ensure all surface inoculum are sufficiently damaged, as DNA from non-viable intact conidia/cells on the surface still result in amplification. Studies that have focused on *in planta* quantification of entomopathogenic fungi are relatively limited. Landa et al. (2013) developed a PCR/qPCR protocol to monitor *B. bassiana* in opium poppy tissues. Their method also used a two-step nested-PCR approach to target the ITS region and were able to detect as little as 10 femtogram (fg) of *B. bassiana* DNA from the plant leaves. The plant leaves were assessed for endophytic colonisation by *B. bassiana* at only a maximum of 5 days after inoculation and the potential for residual surface DNA of inocula remaining after surface sterilisation was not considered. Considering also that the microscopic analysis by CLSM provided evidence herein that the selected *B. bassiana* hyphae remained structurally in-tact following surface sterilisation with 5% NaOCl, it is likely that many published surface sterilisation protocols are inappropriate for PCR detection.

Hegedus and Khachatourians (1996b) developed *Beauveria*-specific PCR primers (P1 and P3) and protocol to identify multiple species of *Beauveria* within infected grasshoppers, based on a *B. bassiana* DNA probe 'pBb2' designed from mitochondrial DNA (Hegedus and Khachatourians 1993). An assessment of the sensitivity of their PCR detection system, indicated that amplification was achieved consistently down to 10 pg (10000 fg) of pure fungal gDNA, which was a great improvement at the time compared to direct DNA probing methods (Hegedus and Khachatourians 1996a). Castrillo et al. (2003) reported a strain-specific PCR protocol that used three sequence-characterised amplified region (SCAR) markers designed from a single *B. bassiana* isolate. However, one of the three primer sets was later used to amplify a different *B. bassiana* isolate, indicating that these primers may be useful for other isolates of *B. bassiana* (Biswas et al. 2012). The *ef1α* primers and protocol developed for this present study demonstrated a relatively high level of sensitivity,

despite targeting a single-copy gene (detecting to < 320 per μL fg DNA), and were able to amplify multiple *Beauveria* species while excluding maize and onion DNA, as well as tomato and *Arabidopsis* when employed in other studies (McKinnon et al. unpublished data). Similar levels of sensitivity using real-time qPCR have previously been demonstrated from barley roots inoculated with the fungal endophytes *Fusarium equiseti* and *Pochonia chlamydosporia* (Macia-Vicente et al. 2009), suggesting that the *ef1 α* PCR protocol developed herein is suitable for further use in following experiments for the detection of *Beauveria* from plant DNA.

Conclusion

Based on the experiments in this chapter, surface sterilisation was considered not sufficiently reliable to exclude surface inoculum for endophyte detection using PCR. However, analogous to mycorrhizal colonisation, the colonisation of *B. bassiana* on root surfaces may be important in eliciting a plant-host response, as is the internal (endophytic) colonisation (Sikes 2010). Therefore, it was decided for the following experiments, not to exclude the plant surface microbiome and thus subsequent chapters focus more on the plant response to colonisation, rather than colonisation frequency to measure endophytic ability in the selected study isolates.

Chapter 3

Plant growth response to artificial inoculation with *Beauveria bassiana*

3.1 Introduction

Corn or maize (*Zea mays*) is an important crop world-wide, as a resource for human food, as a forage crop for animal feed and for starch-based ethanol production (Alexandrov et al. 2009). In 2016, the estimated value indicated for maize grown in the USA for grain crops alone was above US \$51 billion, according to the United States Department for Agriculture (USDA) Crop Values Summary (2017). Maize growth is adversely affected by multiple stresses, such as drought, high salinity and low temperatures (Seki et al. 2003), as well as pathogens and insect herbivory (Erb et al. 2009).

Certain fungi are known to promote plant growth and productivity in a variety of crops (Whipps 2001). *Trichoderma* spp. in particular, constitute a major group of culturable plant growth promoting fungi in soils that can significantly enhance plant biomass and yield (Zhang et al. 2013). For example, the application of *Trichoderma harzianum* to the rhizosphere of maize resulted in substantial root growth in response to the fungal colonisation, and this enhancement was thought to compensate for the stress-induced growth reduction, by combating oxidative stress (Bjorkman et al. 1998). However, many plant growth promoting agents are inhibited in field conditions despite their growth-promotion effects *in vitro*. This has been attributed to their inability to colonise root systems effectively (Ramirez and Kloepper 2010; Zhang et al. 2013). Even for obligate symbiotic endophytes, such as for species from the genus *Epichloë*, natural infection of the host plant (grasses) is thought to occur relatively infrequently. Latch and Christensen (1985) investigated methods for infecting host grasses artificially with *Epichloë* grass endophytes and found that infection rates were higher when the fungus was introduced through a wound made to the seedling. To date, this remains a standard method for inoculating naïve grasses for *Epichloë* spp. endophyte establishment (Kauppinen et al. 2016). Although invasive techniques for artificial inoculation elicit plant defence responses, wounded seedlings occasionally do not survive the procedure (Howe and Jander 2008; Latch and Christensen 1985). Nevertheless, where a symbiosis successfully forms, plant growth and fitness are typically enhanced, often as a result of improved nutrient acquisition and abiotic stress tolerance in the host (Li et al. 2007; Shores and Harman 2008; Zhang et al. 2013). For the plant host, the colonisation process is thought to be homologous to the introduction of a pathogen, however, the endophyte has the ability to evade subsequent host defences in order to persist biotrophically within the host tissues (Singh et al. 2011), where it derives most if not all nutrients but without causing harm (Carroll

1986). Invasive inoculation methods, such as injection of liquid inocula, have also been reported for the establishment of *Beauveria bassiana* in a variety of important plants such as maize (Cherry et al. 1999), tomato (El-Deeb et al. 2012) and date palm (Gomez-Vidal et al. 2009).

Entomopathogenic fungi including *B. bassiana*, *Lecanicillium lecanii*, *Metarhizium anisopliae* and *Isaria* spp. can antagonise plant pathogens and also promote plant growth when applied for endophytic establishment (Ownley et al. 2008a; Ownley et al. 2004; Vega et al. 2009). For instance, the application of *B. bassiana* as an endophyte to tomato and cotton by seed treatment increased crop stand counts and plant heights when co-inoculated with fungal damping-off disease (*Rhizoctonia solani*) (Griffin et al. 2005; Ownley et al. 2008a; Ownley et al. 2004). This positive effect was attributed to the antagonistic activity of *B. bassiana* to *R. solani* by either direct competition or by induced systemic resistance in the plants (Ownley et al. 2008b). A study that used *M. anisopliae* conidia applications to seedlings for control of wireworms increased stand count of corn in addition to the yield (Kabaluk and Ericsson 2007). However, the mechanism underlying the increase in yield was thought to correlate with the reduction in wireworm herbivory resulting from the presence of the fungi. Castillo-Lopez and Sword (2015) conducted a study on cotton plants inoculated by conidial seed treatments of either *B. bassiana* or *Purpureocillium lilacinum*. They reported plant growth promotion effects by measuring dry biomass (above and below-ground) for both species. They applied two different conidial concentrations for each fungus and found no significant difference in the effect resulting from inoculum load.

In this chapter, the growth of maize (*Zea mays*) was measured in order to investigate the response of the plant to artificial inoculation with isolates of *B. bassiana*. Three experiments were conducted: Plant growth experiments' A and B were duplicate experiments to test various plant-growth parameters in the presence of the *B. bassiana* inocula. However, in plant growth experiment B, these isolates were further compared with a plant growth-promoting isolate of *Trichoderma atroviride* (LU132) (Cripps-Guazzone 2014), with the idea that the *T. atroviride* isolate would serve as a positive 'endophyte' experimental control. A third experiment was then conducted using the same *B. bassiana* isolates and *T. atroviride* isolate LU132. The objective of this third experiment was to assess possible root architecture changes as a result of the inocula. In all these experiments, the inoculation method used was adapted from the invasive 'micro-slit' technique used for artificial inoculation of *Epichloë* endophytes in grass (Latch and Christensen 1985). The advantage of employing this technique, was that surface colonisation by the inoculum was avoided. The difference of using hyphal material compared to injecting with liquid suspension was that the fungi was introduced in a vegetative mode (rather than infective), to simulate a biotrophic endophyte. Herein, however, we do not assume that the *B. bassiana* isolates were able to persist as endophytes following introduction, as all plant material was destructively sampled to measure growth. Any effects to plant growth

observed were thus attributed to the result of the initial inoculation, although this may infer endophytic establishment when compared to the control treatments.

3.2 Methods

3.2.1 Maize growth conditions

Maize cultivar Pioneer 34H31 was selected for this study because it is moderately resistant to certain common diseases (Common rust, *Fusarium* ear rot), under optimum field conditions (refer to Appendix B). However, this cultivar was also successfully infected previously with the endophytic isolate *Trichoderma virens* Gv29.8 (Lawry 2016) and preliminary experiments indicated it is compatible with *B. bassiana* (Chapter 2). In the following experiment, the maize plants were challenged deliberately with poor soil nutrient availability and minimal water input (described in methodology below), to increase susceptibility to fungal colonisation and thus enhance the potential to observe possible beneficial effects resulting from endophytic establishment (Hiruma et al. 2016). The rationale for doing this, was that protective endophytes are often only proven to be beneficial when the host-plant is subjected to a particular stress such as nutrient deficiency, desiccation or pest and pathogen invasion.

Plant growth experiments A and B

For plant growth experiment A, a total of 150 seed of *Z. mays* cultivar Pioneer 34H31 were surface sterilised (7 minutes in a 2.5% NaOCl and 0.02% Tween 80 solution, followed by 2 x washes in sdH₂O; Chapter 2) and placed in pairs on 1% agar (10 g of agar in 1 L H₂O; autoclaved prior to pouring) in deep Petri dishes (25 x 100 mm), for incubation at 25°C for seven days in the dark. On day five, the seedlings were removed aseptically from plates and inoculated (see section 3.2.3 below). Following inoculation, the plants were immediately returned to fresh 1% agar plates (1 plate per seedling) for further incubation at 25°C for two days. After a total of seven days of growth, 120 of the seedlings were planted individually in 2.5 L pots containing non-sterile pasture silt blended with river sand (4:1 silt:river sand, Appendix C).

For plant growth experiment B, a total of 200 seed of *Z. mays* cultivar Pioneer 34H31 were processed as described for experiment A, to provide 120 seedlings for the experiment plus an additional 15 seedlings for each isolate treatment used (section 3.2.2) to compensate for any plant death following inoculation. The 120 seedlings used in experiment B were those that recovered well from the inoculation procedure (i.e. no browning of shoots or roots, indicative of necrosis, was observed).

After planting, the pots were arranged for both experiments in randomised blocks, as described in section 3.2.4 and 3.2.5, and maintained in a plant growth chamber for 30 days according to the

following conditions: 16 hours light at 25°C, 8 hours dark at 20°C with a constant 68% (+/- 2%) relative humidity. The plants were maintained with a low water input regime to facilitate a water deficit and grown in relatively low soil nutrient levels (Appendix C). Daily watering was done manually using a hose on the misting setting to provide approximately 4 mm water per pot per day within the first 13 days of growth, and then watering was increased to twice daily, 5 mm each time, as the plant shoots exceeded 200 mm.

Plant root architecture study

For the plant root structure study, a total of 70 seeds of *Z. mays* cultivar Pioneer 34H31 were processed as described in section 3.2.1 for plant growth experiment A, to provide an additional 10 seedlings for each isolate treatment used (section 3.2.2), to compensate for any seedlings lost following the inoculation. Seeds were sown individually in pots as described previously in section 3.2.1. The pots were arranged in randomised blocks, as described further in section 3.2.5 and maintained in a shade-house at the Lincoln University Nursery (Lincoln, New Zealand) for 30 days between October and November (spring) of 2015. The average minimum temperature recorded in the shade house for that period was 15°C and average maximum was 24°C. Relative humidity was not monitored, and the plants were maintained in the same soil source (Appendix C) used for the previous experiments. Daily watering was done manually using a hose on the misting setting to provide approximately 10 mm of water per pot per day.

3.2.2 Fungal cultures

In plant growth experiment A, three *B. bassiana* isolates, BG11, FRh2 and J18 were used (Chapter 2, Table 2.1). These isolates were selected based on their diverse origin with BG11 isolated from the stem of a dandelion plant (genus *Taraxacum*: Asteraceae), FRh2 from a pine bark beetle (*Hylastes ater*) cadaver that was recovered from a living pine tree, and J18 from maize leaf (Table 2.1). Previous work by Raad (2016) also suggested endophytic ability in isolates BG11 and FRh2 following inoculation to *Arabidopsis thaliana*.

The plant growth experiment B and root architecture study included the same *B. bassiana* isolates, however, a single isolate of *Trichoderma atroviride* (LU132) was used as a positive experimental control, since this isolate is a rhizosphere coloniser and endophyte of maize (Cripps-Guazzone 2014), and *Trichoderma* spp. are known to promote plant growth (Brotman 2013; Zhang et al. 2013).

3.2.3 Inoculation

Fungal inoculum was obtained from pure hyphae of non-sporulating culture from each isolate. For the *B. bassiana* isolates, fungi were cultured on PDA (39 g L⁻¹ in water) and harvested following 9 days

incubation at 25°C in the dark. *Trichoderma atroviride* required less growth time for the acquisition of non-sporulating hyphae, and was cultured on PDA for 5 days at 25°C in the dark (Steyaert 2007).

Maize seedlings were inoculated under sterile conditions using a modified technique originally described by Latch and Christensen (1985) for infecting grass seedlings with *Epichloë* endophytes. A sterile surgical razor blade was used to make a 3-5 mm incision through the outer 1-2 leaf sheaths forming on the emerging shoot, at the junction of the mesocotyl (first internode) and coleoptile node of the *Z. mays* seedling. Using a sterile needle, approximately 1 mm³ mass of fungal hyphae was inserted into the wound, and then the wound was gently closed and pressed over the hyphae for 30 s using sterile flat-edged tweezers (Figure 3.1). As an experimental control, the same procedure for inoculation was applied to a group of seedlings in the experiment but with no fungi included, this treatment was designated as the 'wounded control' (control-w).

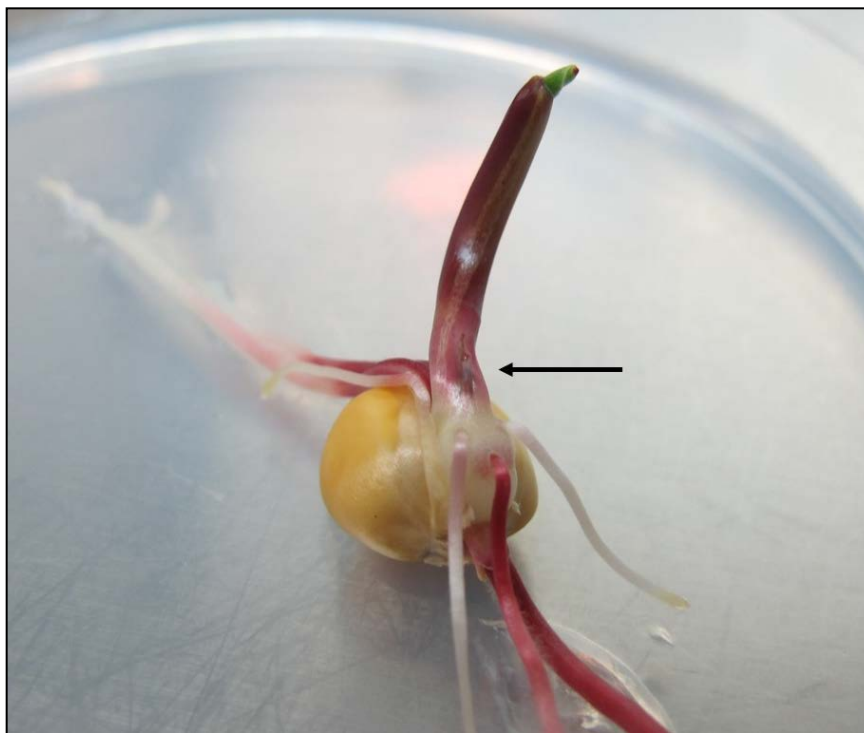


Figure 3.1. A photograph of an inoculated *Zea mays* (maize) seedling. Seedling shown 5 days after sowing, growing on 1% agar. The arrow indicates the location the razor incision made to the base of the emerging shoot with fungal hyphae inserted.

3.2.4 Plant growth experiment A: Assessing the invasive inoculation technique and determining growth response measures.

Experimental design

The experiment was arranged in a randomised complete block design (RCBD) by isolate treatment, with 24 replicates per treatment, each represented in 24 blocks. The five treatments included the three *B. bassiana* isolates J18, FRh2, BG11 and two plant controls (control-nil = no inoculum; control-w = wounded but no inoculum, as previously described). All surviving plants were sampled destructively at 30 days after inoculation (DAI). By 30 DAI, maize plants were still in a vegetative (active) growth phase prior to tasseling and seed production (V6; Figure 3.2).

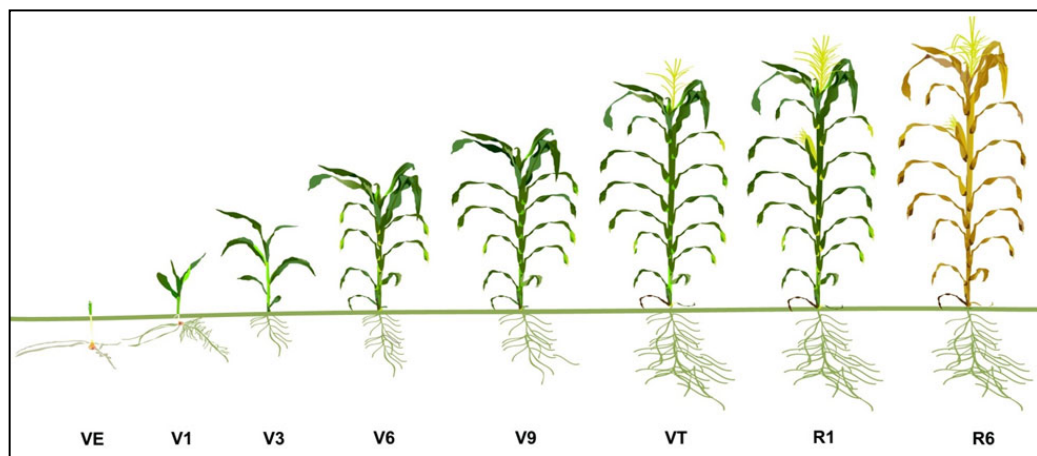


Figure 3.2. The growth and development stages of *Zea mays* (maize). Vegetative growth ranges between vegetative emergence (VE) to V(n), where n = number of leaves, through to vegetative tasseling (VT); followed by reproductive stages (R1 – R6). Figure sourced from Pioneer (Du Pont): <https://www.pioneer.com/home/site/us/agronomy/library/staging-corn-growth/>.

Growth parameters and sampling

At the 30 DAI harvest, the following growth parameters were measured:

- chlorophyll content
- internode lengths (mm)
- number of leaves
- shoot length (mm)
- shoot fresh weight (g)
- root length (mm)
- root fresh weight (g)

Prior to sampling, chlorophyll content was measured by a non-destructive method using a SPAD-502 chlorophyll meter (Konica-Minolta) (Figure 3.3a). Single photon avalanche diode (SPAD), is an

instrument that is sensitive enough to detect a single photon. The SPAD-502 meter provides a ratio of light transmitted at 920 nm, which is not absorbed by chlorophyll, to that at 650 nm, which is absorbed. This ratio is used as a proxy measure to indicate chlorophyll content in the leaf. Generally, SPAD ratios below 40 have been shown to correlate with a chlorophyll deficiency and thus reduced photosynthesis (Argenta et al. 2004; Castro et al. 2011; Torres Netto et al. 2002). On each plant, the third and fourth leaves were systematically assessed with the SPAD meter, with three readings per leaf. Measurements were taken from the flat of the leaf blade to avoid the leaf vein, starting from the mid-section and moving towards the tip. Resulting readings were approximately 10 cm apart. SPAD ratio values were averaged by the instrument automatically after three readings, consequently, each plant had two ratios which were averaged for analysis. Following the SPAD measurement, the number of leaves was counted.

Plant shoots were then cut at the base with scissors, at the soil line. The internode length (mm) was measured on the stem between the leaf petioles to just below the whorl, starting from the soil line at the base of the stem (Figure 3.3b).



Figure 3.3. Sampling of *Zea mays* (maize) plants at 30 days after inoculation (for treated plants) for the plant growth experiment A. Photograph (a) shows the single photon avalanche diode (SPAD) ratio measurement for chlorophyll content and photograph (b) shows the measurement of the internode distance (mm). Photo credit: David Hollander.

The whole shoot, from base to the tip of the whorl was measured (mm) (Figure 3.4a) and then weighed to the gram (g). The shoots was then placed in paper bags and oven dried at 65°C for 48 hours. Dried shoots were weighed again (g) and the dry weights recorded. The root mass was carefully extracted, intact, from the soil by manually loosening the soil around the roots within the pot. The roots were then shaken lightly by hand to remove any loose soil. The root mass length was then measured (in mm), starting from the soil line to the longest observed root tip (Figure 3.4b).

Roots were soaked and washed gently by hand in tap water to remove remaining soil aggregates, then dried by pressing between paper towels and stored in paper bags. The bags were oven dried as previously described for the shoots and the dry weights subsequently recorded.



Figure 3.4. Sampling of *Zea mays* (maize) plants at 30 days after inoculation (for treated plants) for the plant growth experiment A. Photograph (a) shows the measurement of the above ground plant length photograph (b) shows the root-mass length being measured. Photo credit: David Hollander.

Data analysis

Plant growth variables

In addition to root and shoot biomass (dry weights), root and shoot lengths, SPAD and the number of leaves, certain growth variables were calculated for analysis. These included total biomass, which is the sum of shoot and root biomass, root biomass to shoot biomass ratio (RB:SB), total length (sum of shoot and root length), root length to shoot length ratio (RL:SL), water content (WC), calculated from the difference between total fresh weight and total dry weight for each plant and the summed total for internodal length.

Statistical analyses were performed in Genstat 16 (VSN International Ltd.) using General Analysis of Variance (ANOVA) tests to determine the effect of the inoculum treatment on plant growth, relative to the controls. The treatment means (isolate and controls) were contrasted for each variable in a Fisher's Unprotected Least Significance Difference (LSD) multiple comparisons test (also known as an unrestricted LSD test) (Saville 1990) using a 5% significance threshold. Means plots were

subsequently produced for statistically significant variables according to treatment using SigmaPlot version 12.0 (Systat Software, Inc.). Additionally, the percentage of plants that survived after inoculation was calculated and plotted for each treatment.

3.2.5 Plant growth experiment B and root architecture study

Experimental design and data analysis

The plant growth experiment B was arranged in a RCBD by isolate treatment, with 20 replicates per treatment, represented each in 20 blocks. Six treatments were used including the three *B. bassiana* isolates J18, FRh2, BG11 and two plant controls (control-nil; control-w), but with the addition of *T. atroviride* isolate LU132. All surviving plants were sampled destructively at 30 days after inoculation (DAI). Sampling and growth parameters measured and calculated for this experiment were the same as described previously for the plant growth experiment A (section 3.2.4; growth parameters and sampling).

The experimental design for the root architecture study was also a RCBD by isolate treatment, with the same six treatments as for the plant growth experiment B but represented in five blocks, for five replicates and a total of 30 plants. The root mass was harvested and washed as described in section 3.2.4, but stored in sealable plastic bags for immediate analysis (root parameter analysis with WinRHIZO).

Root parameter analysis with WinRHIZO

The commercial software package WinRHIZO 4.1 (Regent Instruments Inc., Quebec, Canada, 2000) was used to analyse and measure root architecture parameters. The program uses a skeletonisation algorithm to map and index root parameters via image analysis. The root samples were first digitised by creating grey-scale images (400 dpi), with a transmitted light unit (TLU), EPSON EXPRESSION 10000XL 3.49 instrument. The WinRHIZO software then uses a non-statistical method to compute morphological measurements based on the information extracted from the image files. The parameters measured were total length (cm), projected area (cm²), surface area (cm²), average diameter (mm), root volume (cm³) and the number of root tips, forks and crossings. The software also indexes certain parameters, such as length, projected area, surface area and volume, by root diameter class (mm), ranging from ≤ 0.5 mm and > 4.5 mm. To prepare the root samples for scanning (Figure 3.5), roots were laid out in a transparent, water filled tray (8 mm water depth).



Figure 3.5. High resolution scanned image (400 dpi) of maize roots. Harvested at 30 days after inoculation and then prepared for root parameter analysis in WinRHIZO.

Statistical analysis of root parameters

Multivariate statistical analysis was initially performed using R (v. 1.0.143, RStudio, Inc.), to test for overall differences between the treatments in the data collectively. To achieve this, the data was first normalised and converted to a distance matrix using the Euclidean distance coefficient in the ‘vegdist’ function from Vegan (v 2.3-5). The resemblance matrix was then analysed for variation among the treatments using adonis (Vegan), which is analogous to a permutational multivariate ANOVA (Anderson 2001). In adonis, significance testing is conducted using F-tests based on sequential sums of squares from permutations of the raw data (on the distance matrix), rather than from permutations of residuals. Univariate analysis was also conducted for the individual root parameters in Genstat 16 using ANOVA and Fishers Unprotected LSD tests, as described previously in section 3.2.4; data analysis.

3.3 Results

3.3.1 Plant growth experiment A

The proportion of *B. bassiana* treated plants that survived after inoculation in experiment A was 16/24 for isolate BG11, 16/24 for FRh2 and 13/24 for J18, respectively. All plants in the two control groups (control-nil and control-w) survived. The data obtained in experiment A was therefore analysed using only 13 replicates at random from each treatment group (13 being the lowest common denominator), as a result of the high death rate of plants in the inoculated treatments, and the block structure was omitted to enable analysis using an ANOVA test. The number of leaves per plant ranged between five and seven, with minimal variance and was thus not analysed statistically.

For the individual growth measurements summarised in Table 3.1, isolate J18 treated plants showed less growth on average compared to the other isolate treatments and controls, however, this was only statistically significant ($P \leq 0.05$) from the LSD test in shoot biomass and shoot length between J18 and the wounded control (control-w) and between J18, FRh2 and control-w. Mean root biomass and root length was not statistically different between any of the isolates or controls. Overall, a consistent trend was observed for isolate J18 treated plants, which were smaller, although not statistically significant, compared to all other treatments (Table 3.1).

Table 3.1. Growth parameters tested in *Zea mays* (maize) growth experiment A. Table shows group means for the treatments used with LSD (5%) values and letters under each mean (rows shaded grey), to indicate differences between treatments derived from the Fisher's Unprotected LSD multiple comparisons procedure. Overall probability (Pr; F statistic, ANOVA) values are also provided for the treatment factor (isolate) for each parameter tested.

	<i>Group means</i>					LSD	F Pr
	Control-nil	Control-w	BG11	FRh2	J18		
Shoot biomass (g)	0.6893	0.7963	0.6145	0.6922	0.5134	0.23	0.182
	ab	b	ab	ab	a		
Root biomass (g)	1.969	1.74	1.787	1.655	1.166	0.83	0.383
Shoot length (mm)	409.8	409.4	314.4	400.9	308.6	99.90	0.081
	b	b	ab	ab	a		
Root length (mm)	404.9	465.9	443.6	456.3	441.2	76.90	0.571
Internode sum (mm)	90.37	103.17	85.5	83.42	81.67	17.98	0.130
	ab	b	ab	a	a		

The indicated chlorophyll content (SPAD) in isolate J18 treated plants was significantly higher compared to the other treatments ($P \leq 0.05$) except compared to the control-w treatment (Figure 3.6a). The SPAD ratio means for all plants fell below 40, suggesting that the plants may be slightly deficient in chlorophyll or showing a reduction in photosynthesis (Argenta et al. 2004; Castro et al. 2011; Torres Netto et al. 2002). Overall, there was a significant difference between the treatments in the ANOVA model for the SPAD ratios ($P = 0.02$) but not for combined biomass (i.e. shoot and root dry weights summed) ($P = 0.316$). However, combined biomass means for each treatment reinforced the trend observed previously in shoot biomass, for example, J18 treated plants showed reduced biomass compared to all other treatments, although this was only statistically significant between J18 and the control-nil group (Figure 3.6b).

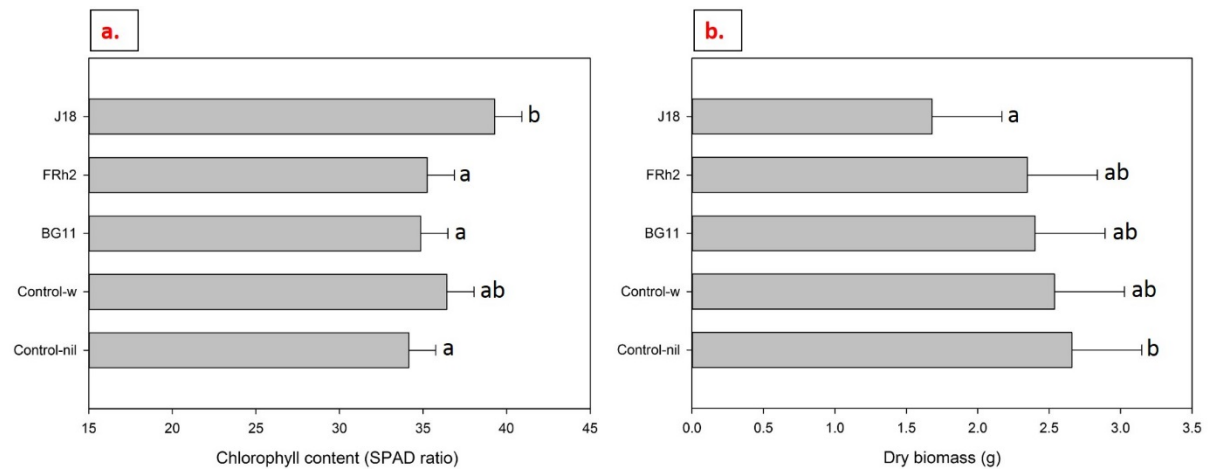


Figure 3.6. Treatment means for growth parameters measured in the *Zea mays* (maize) plant growth experiment A. Treatment differences were determined by a least significant difference (LSD) test (5%); half LSD bars are featured for visual reference. Plot (a) illustrates chlorophyll content (SPAD ratio) differences between the treatment groups. Plot (b) shows the differences in overall biomass (plant dry weight, g) for each treatment group.

When the plant biomass was analysed as a ratio, specifically as the ratio of root biomass to shoot biomass, a significant difference was observed between isolate BG11 treated plants compared to the other two *B. bassiana* and the wounded control treatments ($P \leq 0.05$), although, there was no overall significance between treatments ($P = 0.06$) in the ANOVA model. The root biomass was consistently heavier than the shoot biomass for all plants (i.e. ratio values all exceeded 1, where 1 = no difference between root and shoot biomass). This difference was particularly pronounced for the BG11 treatment (Figure 3.7a), which had a significantly larger root to shoot biomass ratio compared to all treatments ($P \leq 0.05$) with the exception of the control-nil group. This pronounced difference between root and shoot growth in BG11 treated plants was reflected again in the mean ratio of root to shoot length (Figure 3.7b), in spite of higher observed variability within the groups (5% LSD = 2.47; $P = 0.04$). Furthermore, only the ratio for J18 treated plants was not statistically different to BG11.

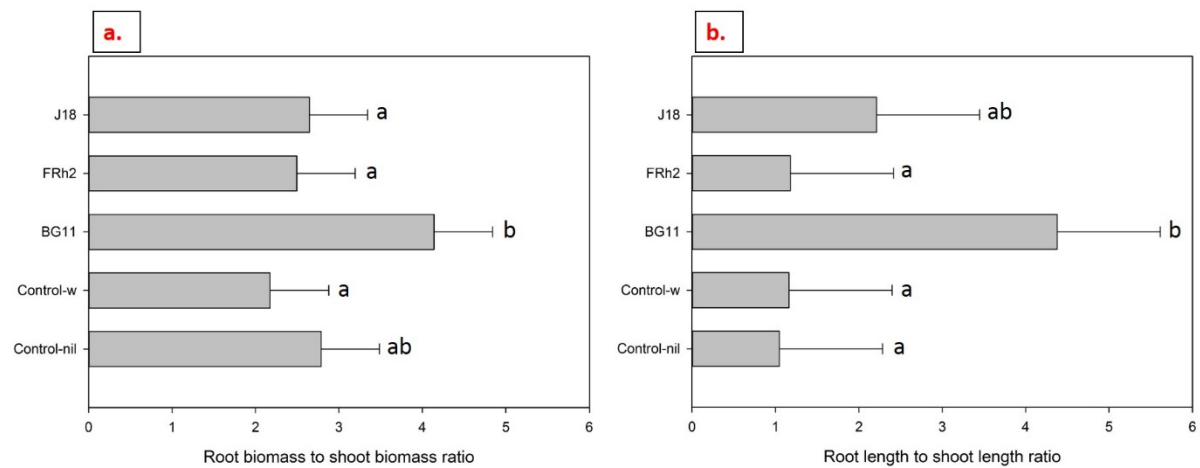


Figure 3.7. Treatment means for growth parameters measured in the *Zea mays* (maize) plant growth experiment A. Treatment differences were determined by a least significant difference (LSD) test (5%); half LSD bars are featured for visual reference. Plot (a) illustrates differences between the groups for the ratio of root biomass over shoot biomass. Plot (b) shows the differences in the ratio between root length and shoot length.

3.3.2 Plant growth experiment B

All plants survived inoculation and the subsequent data generated was represented in analyses.

There were no statistical differences overall between treatments, both from the ANOVA model and from the multiple comparisons of means using the Fisher's Unprotected LSD (5%) test on the individual growth parameters (Table 3.2). The number of leaves counted per plant was, once again, between five and seven and was therefore not analysed statistically.

Table 3.2. Growth parameters tested in *Zea mays* (maize) growth experiment B. Table shows group means for the treatments used with LSD (5%) values to indicate differences (where applicable) between treatments derived from the Fisher's Unprotected LSD multiple comparisons procedure. Overall probability (Pr; F statistic, ANOVA) values are also provided for the treatment factor (isolate) for each parameter tested.

	<i>Group means</i>						LSD	F Pr
	Con-nil	Con-w	LU132	BG11	FRh2	J18		
Shoot biomass (g)	1.105	1.16	1.284	1.209	1.129	1.218	0.1821	0.405
Root biomass (g)	1.505	1.446	1.629	1.589	1.531	1.731	0.2977	0.482
Shoot length (mm)	538	568.6	571.3	561.7	564.4	568.7	35.59	0.459
Root length (mm)	338.3	345.9	357	339.9	353.7	335.1	28.13	0.571
Internode sum (mm)	125	125.1	126.6	127.3	124.6	122.4	11.13	0.967

There was a significant difference between the treatments in the ANOVA for the SPAD ratios (chlorophyll content) ($P = 0.02$), where isolate J18 treated plants had again the highest SPAD ratio (Figure 3.8a). Multiple comparisons of the means determined statistical differences between J18 and both the control groups (control-nil, control-w) ($P \leq 0.05$) but not when compared to the three other inoculum treatments: *B. bassiana* isolates FRh2 and BG11, and the *T. atroviride* isolate LU132. The latter three isolate treatments were also significantly different to the control-nil group ($P \leq 0.05$), which had the lowest SPAD ratio mean (Figure 3.8a). In contrast with plant growth experiment A, there were no statistical differences observed for the treatment in the ANOVA of the combined biomass (the sum of root and shoot dry biomass) ($P = 0.49$), neither were differences found between treatments in the multiple comparisons test ($P > 0.05$). The general trend observed for combined biomass, however, suggested that LU132 and J18 had a marginal positive effect on plant growth although this was not statistically different to the 5% level.

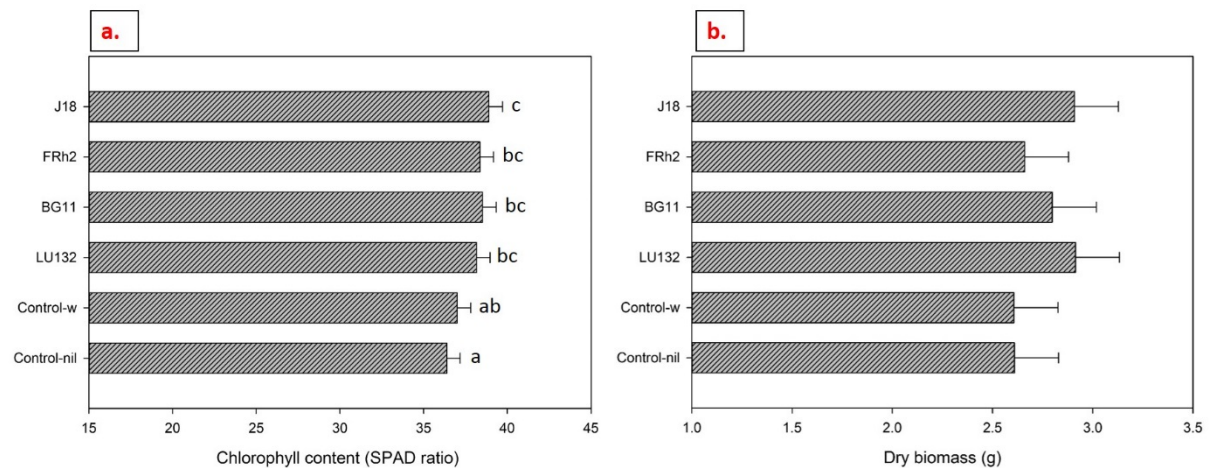


Figure 3.8. Treatment means for growth parameters measured in the *Zea mays* (maize) plant growth experiment B. Treatment differences were determined by a least significant difference (LSD) test (5%); half LSD bars are featured for visual reference. Plot (a) illustrates chlorophyll content (SPAD ratio) differences between the treatment groups. Plot (b) shows treatment biomass (g), which were not statistically different ($P > 0.05$).

The analysis of the ratio of root biomass to shoot biomass also showed no overall significance between treatments ($P = 0.54$) in the ANOVA model. Neither were any individual differences observed between treatments in the Fishers Unprotected LSD test ($P > 0.05$). Once again, root biomass was consistently heavier than the shoot biomass for all plants (i.e. ratio values all exceeded 1), as in plant growth experiment A but were all below a ratio of 2 (Figure 3.9a). No statistically significant difference was observed for the treatment as an explanatory factor in the analysis of the mean ratio of root to shoot length ($P = 0.58$) and there were no differences observed in the LSD multiple comparisons test (Figure 3.7b).

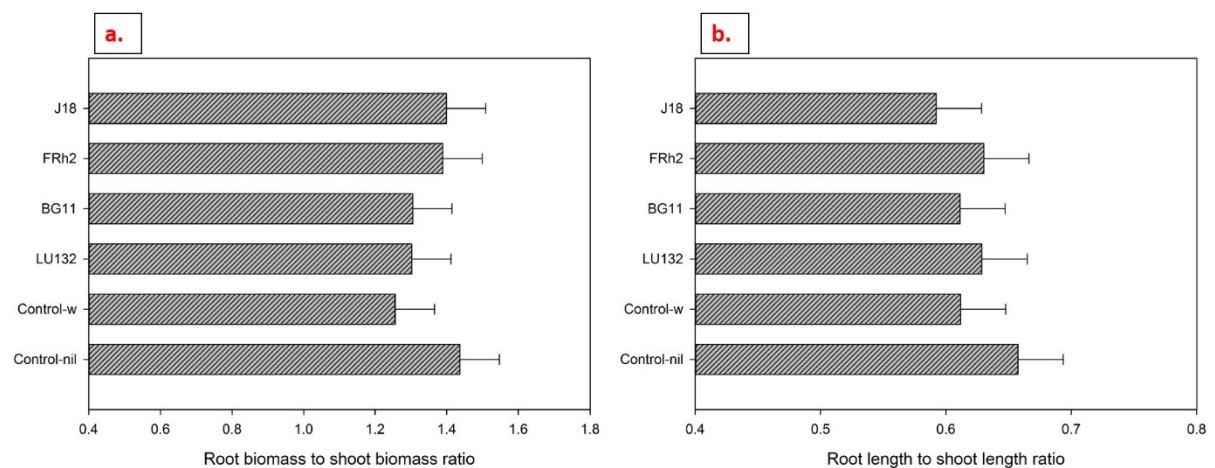


Figure 3.9. Treatment means for growth parameters measured in the *Zea mays* (maize) plant growth experiment B. Treatment differences were determined by a least significant difference (LSD) test (5%); half LSD bars are featured for visual reference. Plot (a) illustrates group means for the ratio of root biomass over shoot biomass. Plot (b) shows the means for the ratio between root length and shoot length.

3.3.3 Root architecture analysis

For the root architecture study, all plants survived and were represented in the WinRHIZO analysis. The multivariate analysis conducted using adonis (R) showed no significant difference between treatments overall ($P = 0.709$). However, univariate analyses of root parameters in general ANOVA tests showed significant treatment effects for root length (all root diameter sizes included) ($P = 0.001$) and for the number of root crossings ($P = 0.007$), which is a parameter representative of root mass density (Table 3.3). Furthermore, significant differences were observed between the three *B. bassiana* isolates for root length (cm) ($P \leq 0.05$) in the multiple comparisons of the means (Fishers Unprotected LSD test), where the mean length for isolate BG11 treated plants was significantly shorter than the J18 and FRh2. Indeed, both isolates' FRh2 and J18 were comparable to LU132 and the control-w group (Table 3.3). For the number of crossings, the 5% LSD test revealed significant differences between isolate BG11 and FRh2, but not between FRh2 and J18, suggesting that root density was generally lower for BG11. Significant differences were also observed between individual treatments when contrasted with 5% LSD tests for projected root area (ProjArea), root surface area (SurfArea), the number of tips and forks (Table 3.3), however, most of the statistical differences observed were between BG11 and LU132 treated plants.

Table 3.3. Plant root growth parameters tested using WINRHIZO. Table shows group means for the treatments used in the *Zea mays* (maize) root architecture analysis, with LSD (5%) values and letters under each mean (rows shaded grey) to indicate differences between treatments from a general ANOVA. Overall probability (Pr; F statistic, ANOVA) values are also provided for the treatment factor (isolate) for each parameter tested. Parameters tested include total length, projected root area (ProjArea), surface area (SurfArea), root diameter (Diam) and root volume, number of tips, forks and crossings.

	<i>Group means</i>						LSD	F Pr
	Control-nil	Control-w	LU132	BG11	FRh2	J18		
Length (cm)	3049	3336	3385	2676	3441	3105	332	0.001
	b	bcd	cd	a	d	bc		
ProjArea (cm ²)	221.8	224.3	257.3	188.8	226.7	231.3	54	0.257
	ab	ab	b	a	ab	ab		
SurfArea (cm ²)	696.8	704.7	808.4	593	712.1	726.5	171	0.257
	ab	ab	b	a	ab	ab		
Diam (mm)	0.7274	0.6778	0.7666	0.6976	0.6581	0.7416	0.14	0.616
Volume (cm ³)	13.19	12.23	15.49	10.66	12.02	13.61	5.56	0.582
Tips	9177	7926	10072	7311	7328	7413	258	0.169
	ab	ab	b	a	a	a		
Forks	42310	45978	49306	37412	45397	44956	7657	0.075
	ab	b	b	a	b	ab		
Crossings	6231	7237	7254	5645	7552	6728	1007	0.007
	ab	bc	c	a	c	bc		

Root parameters compared by diameter class

Treatment differences in root structure parameters were further illustrated when the roots were partitioned by size (diameter, mm). For example, in Figure 3.10 root length was compared between treatments first in fine roots (size class $0 \leq 0.5$ cm; Figure 3.10b) and then in thicker roots ($3.0 \leq 3.5$ cm; Figure 3.10c). For the finer roots, the three *B. bassiana* isolate treatments were statistically different to each other ($P \leq 0.05$) but for thicker roots, the statistical difference was primarily accounted for by *T. atroviride* isolate LU132 versus all other treatments, with the exception of isolate J18, which was comparable.

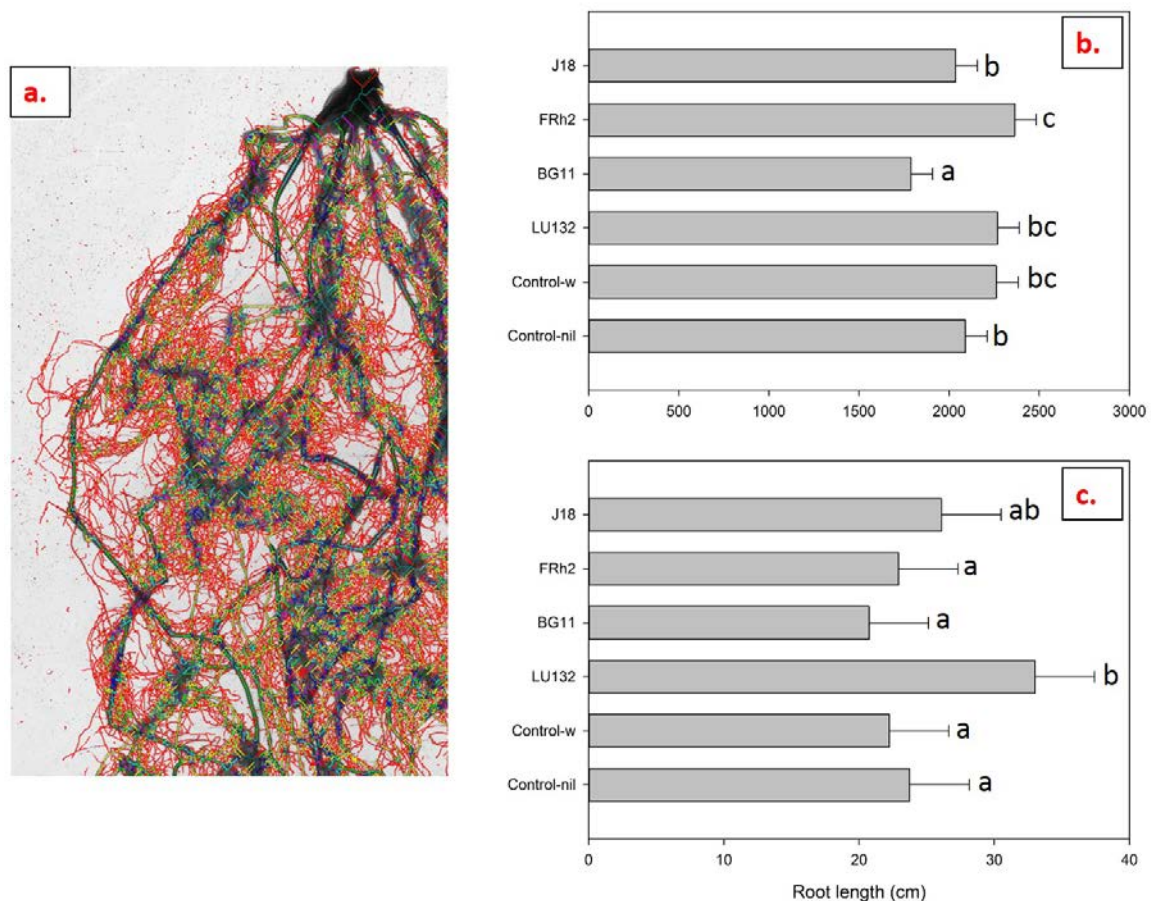


Figure 3.10. Root structure analysis for *Zea mays* (maize) performed in WinRHIZO 4.1: (A) shows a scanned image of an experimental root sample under analysis, and the two plots show the mean root length (cm) estimated for each experimental treatment. Plot (b) shows mean root length for fine roots ($0 \leq 0.5$), contrasted with thicker roots ($3.0 \leq 3.5$) in plot (c). Statistical differences are indicated by letters next to half LSD bars (5% significance level) for each treatment.

For the projected area (cm^2) and root volume (cm^3) parameters, the analysis of the fine root diameter class produced a similar trend for the isolate treatments, in both instances BG11 was significantly smaller compared to the other treatments (apart from the control-nil in the projected area analysis) (Figure 3.11a and Figure 3.12a). In contrast, the trend for the thicker roots was different between these two parameters (Figure 3.11b and Figure 3.12b), although there were no statistically significant differences found between treatments in the projected area comparison (Figure 3.11b). For root volume, the observed treatment differences in thicker roots reflected the same trend seen in finer roots.

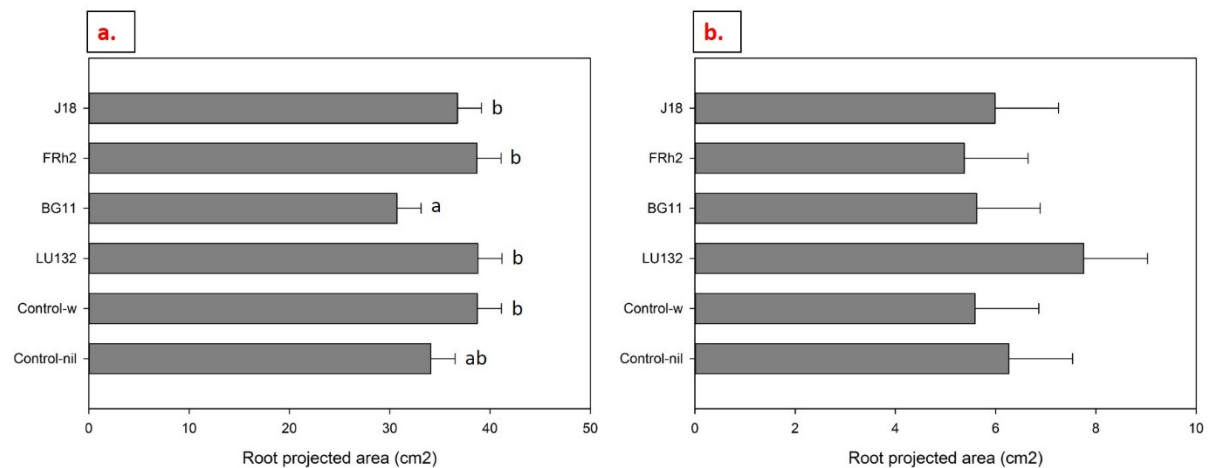


Figure 3.11. Root structure analysis for *Zea mays* (maize) performed in WinRHIZO 4.1. Plot (a) shows mean projected area (cm²) for fine roots (0.5 < P.A. ≤ 1.0), contrasted with thicker roots (3.5 ≤ 4.0) in the plot (b). Statistical differences are indicated by letters (where applicable) next to the half LSD bars (5% significance level) for each isolate treatment and controls.

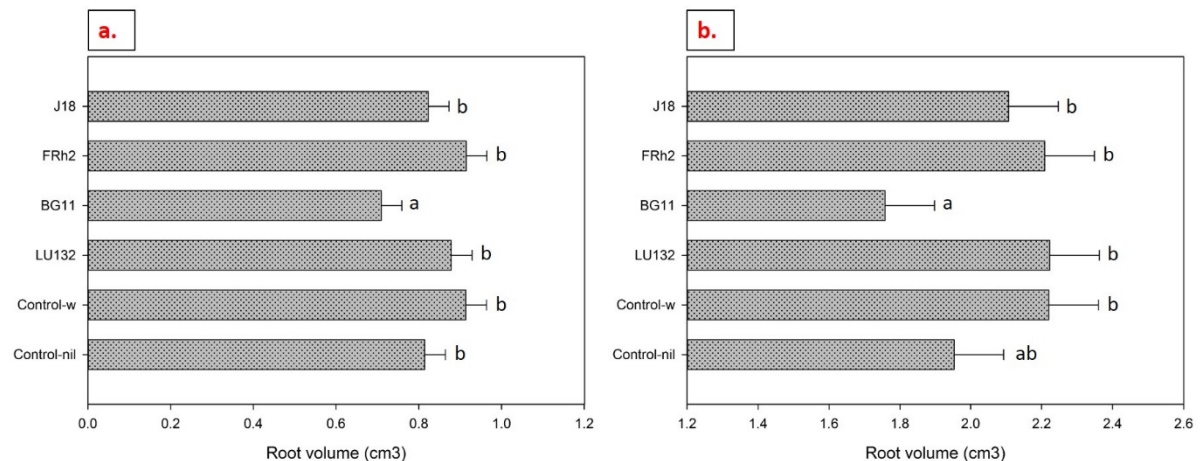


Figure 3.12. Root structure analysis for *Zea mays* (maize) performed in WinRHIZO 4.1. Plot (a) shows root volume (cm³) for fine roots (0.5 ≤ 1.0), contrasted with thicker roots (3.5 ≤ 4.0) in plot (b). Statistical differences are indicated by letters next to the half LSD bars (5% significance level) for each isolate treatment and controls.

3.4 Discussion

In this chapter, the growth of maize was measured in order to investigate the response of the plant to artificial inoculation with isolates of *B. bassiana*. The results showed net negative plant growth in the plant growth experiment A from the fungal endophyte inoculation based on plant dry biomass, shoot and internode lengths. However, in experiment B no significant effects were observed, negative or positive, for the same parameters. The literature indicates that genotype-specific interactions may occur between plants and endophytes to either enhance, reduce, or have no effect on plant fitness (Rodriguez et al. 2009; Saikkonen et al. 2010b). Prior studies have generally shown

plant growth promotion following a conidial application of entomopathogenic endophytes, on root and shoot growth (Griffin et al. 2005; Gurulingappa et al. 2010; Kabaluk and Ericsson 2007; Liao et al. 2017; Castillo-Lopez and Sword 2015; Ownley et al. 2008a; Ownley et al. 2004). However of these studies, only two suggested the potential for plant growth enhancement mediated directly by endophytes and in the absence of pathogen or insect attack (Liao et al. 2017; Castillo-Lopez and Sword 2015). Predominantly, these studies have shown the enhancement of plant growth when endophytic entomopathogens were applied for the biocontrol of soil pathogens or insect herbivores and thus positive plant growth was attributed to the reduction of damage resulting in increased yield, due to the absence of stress.

A study by Gurulingappa et al. (2010) observed enhanced plant growth of wheat as a result of a topical foliage spray application with *B. bassiana*, whereas in the same study, the entomopathogenic fungi *Lecanicillium lecanii* and *Aspergillus parasiticus* had no effect on the growth of wheat. In contrast, *L. lecanii* was observed to significantly reduce only the above-ground biomass of cotton plants, while *A. parasiticus* significantly reduced the combined biomass for cotton. Although the mechanisms that mediate either positive or negative effects were not examined, this study supported the notion that genotype-specific interactions occur between plants and entomopathogenic endophytes.

To date, there are no other studies that have introduced hyphae of *Beauveria* into a wound and then measured the growth response in plants. However, by this method, *Epichloë* endophytes are able to proliferate in grasses and enhance growth, as long as the grass seedlings survive the process (Latch and Christensen 1985). In contrast, introduction of the *B. bassiana* isolates by this inoculation method was occasionally detrimental to plant growth, suggesting that under certain circumstances these isolates may be more parasitic than beneficial in terms of plant growth.

In the root architecture experiment, most of the differences observed were between *B. bassiana* isolate BG11 and *T. atroviride* isolate LU132. Overall, BG11-treated plants showed negative growth effects relative to the *Trichoderma* treatment, and occasionally also compared to the controls. Again, this suggests that this *B. bassiana* isolate may have been more parasitic than mutualistic to the plants. However, endophytic fungi have the ability to express different functional roles *in planta* in response to the host genotype or because of varying environmental factors (Francis and Read 1995; Singh et al. 2011) and moreover, depending on the physiological state of the plant, certain endophytic fungi may be either mutualistic or parasitic. Therefore, many plant-fungal interactions are considered to be simultaneously balanced and antagonistic, where the plant host is essentially tolerating the presence of the coloniser (Schulz and Boyle 2005). As an example of this balanced antagonism, when the fungus *Colletotrichum magna* was introduced into different tomato cultivars,

the fungus was observed to express either a mutualistic, commensal or parasitic lifestyle (Redman et al. 2001). Given that commercially grown tomato (*Solanum lycopersicum*) is known to have minimal genetic variation between cultivars but have the ability to express high levels of phenotypic plasticity (Miller and Tanksley 1990; Tanksley 2004), the different interactions resulting from the association suggest that subtle differences between the host genomes have profound effects on the outcome of the symbiotic interaction (Rodriguez and Redman 2008; Singh et al. 2011). It is possible therefore that the same *B. bassiana* isolates used in this study may provide growth benefits to plants if introduced by a different method, for example as a conidial suspension to the rhizoplane, though this was not tested in this study. The introduction of the *T. atroviride* isolate LU132 to maize by this invasive inoculation method resulted in a general plant growth promotion effect. This effect was anticipated, since this particular isolate has previously shown growth promotion effects to maize, even in dry and nutrient-poor conditions (Cripps-Guazzone 2014). Interestingly, studies by Lee et al. (2016) and Nieto-Jacobo et al. (2017) demonstrated that growth promotion is not a universal trait for all *Trichoderma* species and isolates. Both studies tested multiple isolates for growth effects in *Arabidopsis* and observed promotion, no effect at all, and detrimental effects on the plants. Indeed, Nieto-Jacobo et al. (2017) attributed the variability in plant growth enhancing potential between isolates (i.e. of *T. atroviride*) to be more a result of environmental parameters than because of the plant-host genotype. These studies, along with the present study, indicate the importance of screening potential biocontrol isolates under certain conditions for differential effects to plants.

In the present study, isolate FRh2-treated plants had a higher quantity of fine diameter roots (measured by length), whereas LU132 treated plants dominated the thicker root-class estimate. This study highlighted the potential for important although subtle physiological changes that may occur in plant roots as a direct result of fungal endophyte inoculation (Barelli et al. 2016; Malinowski et al. 1999). A study by (Sasan and Bidochka 2012) showed that plants colonised by *Metarhizium* had a significantly greater number of lateral roots and root hair formations in comparison with untreated plants. They used confocal microscopy to investigate colonisation of root surfaces using *M. robertsii* on a grass species, switchgrass (*Panicum virgatum*), and a legume, haricot bean (*Phaseolus vulgaris*). The proliferation of lateral roots and the stimulation of fine root-hair development is generally considered an integral part of early-stage interaction in non-phytopathogenic, root colonising and rhizosphere fungi (Felten et al. 2009; Harrison 2005). Another study conducted with *Metarhizium* spp. reported increased leaf collar formation and foliage biomass in maize plants as a result of seed treatments using various isolates (Liao et al. 2014). The production of auxins by endophytic fungi and the induction of jasmonic acid defence pathways in the plant are thought to be mechanisms that contribute to the stimulation of fine-root and root hair growth (Liao et al. 2017; Nieto-Jacobo et al. 2017). In summary, there was more often no effect to plant growth observed in terms of biomass

following artificial inoculation with isolates of *Beauveria* and *Trichoderma* used in this study. However, plant architecture (fine roots, thick roots, density) and biochemistry (chlorophyll) was sometimes differentially affected as a result of the application of different isolates.

The difference observed between the two growth experiments (A and B), i.e. the negative and neutral effects observed to plant growth, may be attributed to the inoculation concentration and/or methodology discrepancies. The method was tedious and difficult to standardise, as it was impossible to accurately measure the quantity of hyphae that was ultimately applied to the wound. For instance, in the first experiment, a slightly larger quantity of hyphae was likely used for inoculation. This may have inundated the plants and lead to adverse effects subsequently observed. In the second growth experiment (B), more plants were inoculated than required and as a result, the inoculum was perhaps applied more sparingly and no seedlings were lost. It is possible therefore that a higher inoculum dose may have resulted in greater plant losses in addition to the negative growth effects observed in experiment A. Morphological differences in the growth of the fungal isolates used including hyphal density, activity and metabolite production may have also varied among the isolates within and between experiments, contributing to the variability observed, although such parameters were not measured. Nevertheless, it is interesting to note that very different effects to plants can be observed depending upon the degree of systemic exposure to the fungi. Although difficult to standardise, with some optimisation this method of inoculation may be an effective way to introduce and test for beneficial endophytes.

From previous literature, *B. bassiana* has been inoculated into plants by injecting liquid conidial suspensions (Cherry et al. 1999; El-Deeb et al. 2012), however, growth effects and disease resistance was only assessed in the study by El-Deeb et al. (2012). In particular, the effect of endophytic colonisation on tomato foliage fresh weight was investigated and a growth promotion effect was observed. However, it was unclear whether they used an experimental control for the inoculation method, such as a wounded-control (e.g. plants injected with water) as this was not stated in their methods. Wounding of plants induces massive accumulation of reactive oxygen species (ROS) at the wound-site, enabling immunity and may inhibit fungal colonisation but also indirectly enhance growth or yield (L'Haridon et al. 2011). For example, wounded leaves of *Arabidopsis thaliana* have been shown to produce ROS within minutes following wounding, and become resistant to pathogenic attack by the fungus *Botrytis cinerea* (Beneloujaephajri et al. 2013). This rapid response of the plants is known as wound-induced resistance (WIR) and this reaction can be purposefully induced by wounding plants in order to 'prime' them for disease resistance (Chassot et al. 2008; Koo and Howe 2009).

In this study, positive differences were only observed between *Trichoderma* (LU132) and the wounded control for the thicker root-length parameter, and in the chlorophyll content (SPAD) ratios, where *B. bassiana* isolate J18-treated plants had significantly higher indicated chlorophyll content compared to the wounded control. Considering that the priming effect likely occurred in the maize seedlings in this study, any significant differences that occurred between the wounded control (control-w) and the inoculated treatments are of particular interest, as it was more likely a direct result of the fungi. In contrast with the results in this study, Greenfield et al. (2016) observed a reduction in indicated chlorophyll content using SPAD measurements in cassava plants following inoculation with certain commercial isolates of *B. bassiana* and *Metarhizium*, and this tended to correspond with plant growth promotion effects. The plants were inoculated by soil drench (i.e. conidial suspension) in this instance and the soil was sterilised prior to planting. The negative ratios for chlorophyll were thought to be attributed to an increase of nutrient/resource allocation to stem and roots resulting in lower chlorophyll requirements (Greenfield et al. 2016).

In the growth experiments (A and B) conducted in this present study, indicated chlorophyll content also did not correlate with plant biomass but the mechanism underlying the effect to chlorophyll is unknown and requires elucidation. Biochemical analyses to determine the true concentration of these pigments were not conducted in the present study, nor by Greenfield et al. (2016). Wellburn (1994) originally recommended that calibration curves should be made for the species/cultivar of study that correlate with portable chlorophyll meter (SPAD-502) values in order to accurately estimate leaf chlorophyll content. However, Uddling et al. (2007) found that a single calibration curve could be used for multiple wheat cultivars grown over multiple seasons, and Dwyer et al. (1991) found that six maize hybrids had similar relationship curves. Recent studies by Xiong et al. (2015) and (Parry et al. 2014) showed that SPAD ratios fluctuate under different environmental conditions (i.e. in field conditions) but otherwise they found that different crops (including maize) shared a common relationship between SPAD and chlorophyll content per leaf area, when measurement conditions were standardised. For papaya plants, SPAD ratios of ≤ 30 , indicated leaf senescence (Castro et al. 2011; Torres Netto et al. 2002) and in maize, SPAD values over 45 tended to indicate sufficient nitrogen levels for optimum grain yield (Argenta et al. 2004; Parry et al. 2014; Piekielek et al. 1995). In the present study, plants were grown under a standardised light regime and in nutrient-poor soils for the duration of experiments' A and B. Thus SPAD values of below 40 likely correlated with less than optimum chlorophyll content (i.e. for grain yield) but were perhaps within a healthy range at least for vegetative growth (Argenta et al. 2004).

A few studies, conducted primarily on endophytic bacteria-plant interactions, have investigated the mechanisms underlying plant growth promotion, and these have shown that the effects may result from fixation of soil nutrients or from the production and/or regulation of growth hormones in plants

by the microbe (e.g. auxins, gibberellins, cytokinins and ethylene) (Glick et al. 1998; Harman et al. 2004a; Castillo-Lopez and Sword 2015; Yang et al. 2012). However, *M. robertsii* was recently shown to promote lateral root growth and root hair development of *Arabidopsis* seedlings via production of an auxin, indole-3-acetic acid (IAA) (Liao et al. 2017). Comparative genomic studies may enable the mechanism of host infection and functional role of endophytes to be elucidated, to improve understanding of plant growth promotion and biocontrol. Microarray, next generation sequencing, metagenomics, and metatranscriptomics are just some of the techniques available to investigate the plant-endophyte relationship (Kaul et al. 2016). In addition to exploring the plant host response to colonisation, the effect of inoculation and colonisation of *B. bassiana* on the plant microbiome, both within the plant and in the rhizosphere, may be important to consider because such factors may also influence plant health and growth. In the following chapters, the ecological impacts of inoculation and the plant host response to *Beauveria* will be assessed in order to address these questions.

Chapter 4

Ecological study of *Beauveria bassiana* isolates in the rhizosphere of *Zea mays*

4.1 Introduction

Isolates of *Beauveria bassiana* exhibit considerable variation in pathogenicity towards insects. Typically, the criteria for selection of isolates for biocontrol purposes are based on observed insect mortality rates in bioassays, in addition to the ease of inducing conidiation in culture. With the primary focus on pathogenicity, suitability for a specific ecological niche and ability of a *B. bassiana* isolate to function well in the intended environment of application have often not been considered (Waage 1997). With evidence mounting of *B. bassiana* having an opportunistic endophytic strategy to its lifecycle (Vidal and Jaber 2015), it is worthwhile to consider the degree of isolate variation in the ability of the fungus to colonise plant tissue (Kia et al. 2017). Additionally, it may be important to understand whether certain isolates preferentially occupy the rhizosphere of plants, rather than only the internal tissues (St. Leger 2008). However, within the rhizosphere zone, microbial associations may occur at various locations along a longitudinal gradient. For example, the rhizosphere is thought to include internal aspects of the plant root-cortex and endodermis (endorrhizosphere), as well as the rhizoplane of the root and the soil directly attached to it (ectorrhizosphere) (McNear Jr 2013).

Generally, the below-ground functions of the plant microbiome are thought to be predominantly nutritional, with various and ubiquitous mycorrhizal and rhizobial associations that enhance the access of the host plant to organic and inorganic soil nutrient reserves (Bacon and White 2016). Entomopathogenic fungi from the genus *Metarhizium* are considered common rhizosphere colonisers in many ecosystems. Found frequently in soil, these fungi are pathogenic to various insect species, which are a rich source of nitrogen in the environment (Behie et al. 2012). Behie et al. (2012) demonstrated that the root colonising capability and insect pathogenicity of *Metarhizium* can be coupled to translocate nitrogen, via the fungal mycelial network, from the insect cadaver to the plant host. Species of *Beauveria* are also frequently isolated from soil. Indeed it has been common practice to acquire new *Beauveria* sp. isolates from soil by using insects as baits (Zimmermann 1986). Barelli et al. (2016) hypothesised that the potential for insect pathogenic *B. bassiana* to colonise plant tissues suggests that active transfer of nitrogen from insects to plants may also occur in isolates of this species, yet this has not been tested.

In exchange for nitrogen, endophytic and rhizosphere competent species of *Metarhizium* and *Beauveria* may acquire plant-derived carbon, such as raffinose (Fang and St Leger 2010) or perhaps

sucrose, as has been demonstrated for endophytic isolates of *Trichoderma virens* (Vargas et al. 2009). Although there is at least one preliminary study that investigated possible mechanisms for plant-derived carbohydrate utilisation by *Metarhizium* (Fang and St Leger 2010), as of yet, there are no published studies addressing the same for *Beauveria*. However, the soil microbial community may interact with inocula to affect carbon utilisation through competition, and consequently also affect plant colonisation or persistence after initial establishment (Lugtenberg et al. 2002). On the other hand, inundative inoculation of endophytic *Beauveria* isolates could also impact the microbial community, altering the composition or function by displacement, which in turn may have important repercussions for the health of the plant host (Lareen et al. 2016). Furthermore, when plants are subjected to stress, such as that resulting from insect herbivory, they elicit a suite of defensive compounds in response (Howe and Jander 2008). In the rhizosphere, changes in root exudates resulting from the plant defence response can impact the microbial community diversity, density and activity, ultimately shaping the functional microbiome (Pangesti et al. 2013). Recent studies provide evidence that plants have a sophisticated defence system, whereby they actively recruit non-pathogenic root-associated microbes following attack by insects or pathogens (Lakshmanan et al. 2012; Lee et al. 2012; Rudrappa et al. 2008).

The primary aim of the following experiments was to investigate the interaction of *B. bassiana* in the rhizosphere of maize (*Zea mays*), in order to test for any differences between isolates of *B. bassiana* as a plant coloniser. The potential impact of differences among the *Beauveria* inocula on the resident microbial community, in terms of composition and function, were also assessed. The second objective was to assess potential changes in the microbiome of the rhizosphere, including the persistence of the *B. bassiana* inocula, by inducing plant host stress through intensive wounding of the foliage. The purpose of inducing this stress was to test for any reciprocal interaction between the plant-host, the microbiome and fungi inocula. For example, should above-ground damage to the plant affect below ground microbial community composition or the inocula persistence, then this suggests that the plant may interact with the microbiome via exudates or physiological alterations.

In this study, the plant root surface was inoculated by root-dip prior to planting in soil, in order to establish rhizoplane colonisation (as observed in the histological study in Chapter 2) and increase the likelihood of an interaction with the resident rhizosphere microbial community.

4.2 Methods

4.2.1 Inocula preparation

Inocula of *B. bassiana* isolates BG11, J18 and FRh2 were prepared as conidial suspensions for direct application to roots of maize. Suspensions were prepared according to the protocol described in

Chapter 2 (section 2.2.2) from cultures grown on potato dextrose agar (PDA; Difco, NY) for 3 weeks at 20°C in the dark. Based on the estimated quantity of conidia per mL harvested, 180 mL volume suspensions were prepared for each isolate in sdH₂O and 0.05% Tween 80 [50:50] at a concentration of 10⁷ conidia per mL and used immediately for inoculation (section 4.2.2). The viability of the conidia were later estimated (see Chapter 2; section 2.2.2), to check for any significant variation between the inocula in terms of viable concentration (data not shown).

4.2.2 Maize growth conditions and inoculation

Approximately 200 seed from maize cultivar Pioneer 34H31 were surface sterilised (7 minutes in a 2.5% NaOCl and 0.02% Tween 80 solution, followed by 2 x washes in sdH₂O; Chapter 2) and placed in pairs on 1% agar (10 g of agar in 1 L H₂O; autoclaved prior to pouring) in deep Petri dishes (25 x 100 mm), and incubated at 25°C for 8 days in the dark. On day 5, the seedlings were removed aseptically from plates and inoculated by dipping and soaking the roots from below the seed for 1 minute in each of the respective isolate treatment solutions (180 mL suspension in 500 mL containers). Control plates were treated with sdH₂O and 0.05% Tween 80 solution for 1 minute. All plants were then returned to fresh 1% agar plates (1 per each seedling) for incubation, for a further 3 days at 25°C. Subsequently, 96 of the seedlings were planted individually in 2.5 L pots containing non-sterile silt blended with river sand (4:1 silt:river sand, Appendix C). The seedlings planted were selected based on the primary root length (18-25 mm) to maintain as much homogeneity as possible in plant size and growth stage. The pots were arranged in randomised blocks in a plant growth chamber and maintained for 30 days according to the following conditions: 16 hours light at 25°C, 8 hours dark at 20°C with a constant 68% (+/- 2%) relative humidity. Daily watering was done manually using a hose on the misting setting to provide approximately 6 mm water per pot per day within the first 13 days of growth, and then watering was increased to twice daily, 6 mm each time, as the plant shoots exceeded 200 mm.

4.2.3 Experimental design

The experiment was arranged in a split-plot design consisting of six blocks. Within each block, four time treatments were represented in randomised order. Randomisation of samples was achieved using the Excel (Office 2010, Microsoft) random number function to generate random numbers in a separate column, and then the sample order was assigned using the sort function according to the numbers generated. The time treatments constituted the main-plots which were arranged further in a randomised complete block design (RCBD) by isolate treatment (sub-plots). The main-plot time treatments were 6 days after inoculation (DAI), 15 DAI, 30 DAI and 30 DAI with a simulated herbivory treatment; designated 30+H. The isolate sub-plot treatments were the BG11, FRh2, J18 treated and control plants which consisted of six replicates per main-plot time treatment.

At 23 DAI, one week prior to the 30 DAI sampling, the 30+H plants were treated by removing approximately 33% of the leaves per plant with scissors to simulate herbivory/wound stress. Of the leaves that were cut, approximately $\frac{3}{4}$ of the leaf was removed.

At each indicated time-treatment, plants were destructively sampled to obtain root material, rhizosphere and bulk soil for various analyses.

Soil and plant tissue sampling

At each sample time (6, 15, 30 DAI), the total rhizosphere soil was collected from each plant. Plants were carefully extracted from their pots and gently shaken to remove excess and/or loose soil. The roots were then gently brushed with a sterile paintbrush to remove the rhizosphere soil onto sterilised trays. From the collected soil three subsamples were taken and these were, a 5 mL volume sample for a soil dilution series (CFU quantification), a 2 mL volume sample for DNA extraction and a 100 g sample at 30 DAI only for MicroResp™. The MicroResp protocol, similar to Biolog™, enables the assessment of the community-level physiological profiles via the measurement of carbon substrate utilisation (from CO₂ levels) in the soil (Campbell et al. 2003). The remaining pot soil was used to measure soil moisture content (SMC). Five separate root fragments (5 cm in length) were taken from each plant from 10 cm below the soil line. The root fragments were washed gently in 0.05% Tween 80 and trimmed further to 1 cm pieces with a sterile blade. All soil and plant material was weighed prior to DNA isolation and the weights were later adjusted/recorded according to DNA kit protocol. Soil for DNA extraction and MicroResp™ was stored at -20°C and all root material was stored at 4°C until required for processing.

4.2.4 DNA preparation and PCR/qPCR detection

DNA from rhizosphere soil was extracted using the MO BIO PowerSoil® DNA Isolation Kit according to the protocol provided. DNA from root samples was isolated using the MO BIO PowerPlant® Pro DNA Isolation Kit according to the kit instructions but with the following modification: tissue lysis was conducted with the FastPrep-24™ (MP Biomedicals) at 5 m/s for 40 seconds. Qubit™ high sensitivity double-stranded DNA assays were performed to assess DNA concentration relative to tissue sample weights (g) prior to analysis. Soil DNA yields typically ranged from 2-5 ng/μl and root DNA yields from 18-22 ng/μL. PCR on soil DNA was conducted as previously described (Chapter 2; section 2.5.1 'nested PCR protocol summary') for the *ef1α* nested primers (EF3-5, EF4-4), however, cycle lengths were optimised to 30 cycles (step one, EF3-5) and 23 cycles (step two, EF4-4) to minimise potential non-target amplification. PCRs on root DNA samples were also optimised for the number of cycles, with 30 cycles on both steps for 6 DAI samples and 35 cycles on step 2 for the remaining samples (15 DAI, 30 DAI). Real time qPCR was conducted on template generated from root DNA samples only and

according to the optimised protocol previously described (Chapter 2; section 2.5.1 'nested PCR protocol summary'). Standard curves were produced from qPCR experimental data on two different *B. bassiana* DNA dilution series. These were done by first amplifying, in a standard PCR (step one, EF3-5, 20 cycles), pure *B. bassiana* gDNA from isolate BG11 spiked in either water or diluted gDNA of *Z. mays* in a 1:10 dilution series (10 µL DNA into 90 µL sdH₂O, or, *Z. mays* gDNA and sdH₂O). Step two of the PCRs in these experiments were conducted on 1/1000 dilutions of the PCR product with the EF4-4 primers to ascertain PCR detection cycle thresholds for the comparison of isolate treatments in/on the plant root samples.

4.2.5 Quantification of *Beauveria bassiana* in the rhizosphere by CFU counts

To each 5 mL volume of soil taken for CFU quantification from the rhizosphere, 45 mL of 0.05% Tween 80 was added in sterile 50 mL tubes and then shaken using a Stuart™ Flask shaker (SF1; Sigma-Aldrich) for 5 minutes at 500 osc/minutes. The samples were diluted further in a 10-fold series in 0.05% Tween 80 to 10⁻³, and 100 µl each of the 10⁻² and 10⁻³ dilutions were plated on *Beauveria* Semi-selective Media (BSM: quarter strength PDA, containing 350 mg/L streptomycin sulphate, 50 mg/L tetracycline hydrochloride and 125 mg of cyclohexamide (Sigma)) (Brownbridge et al. 2012); with two plates per dilution. The dilution plates were incubated in the dark at 20°C for 14 days. The number of CFUs per gram of dry soil was calculated from the number of *B. bassiana* colonies observed by visual assessment of sporulating cultures. The morphology of *Beauveria* sp. on quarter strength PDA is distinctive when conidia are present and are easily identified by eye or under stereo microscope. For example, Figure 4.1 shows a typical colony of *B. bassiana*, which appears floccose and velvety to powdery. In the instance where there was insufficient conidia for the identification of *Beauveria* colonies by eye, fungal hyphal samples were identified under compound microscope in order to visualise the distinctive zig-zag rachis with septate hyphae (Glare and Inwood 1998).



Figure 4.1. Photograph of *Beauveria bassiana*, cultured on potato dextrose agar (PDA).

The number of *Beauveria* sp. colonies counted was then multiplied by the respective dilution factor, averaged over the $10^{-2}/10^{-3}$ plates and then adjusted by the SMC to achieve the CFU g⁻¹ dry soil (McKinnon 2011).

Analysis of CFU data

Statistical analysis for CFU data was performed in Genstat (Version 16.1.10916). The herbivory data was omitted for this analysis, in order to balance the design for the model. The CFU g⁻¹ dry soil data (y variate) was logarithmically transformed ($\log_{10}(x+1)$) for all analyses. Initially, the comparison of isolates for differences between rhizosphere and bulk soil CFU quantities over time was assessed separately using two-way ANOVAs (for isolate treatment and days after inoculation 'DAI'), with subsequent pairwise comparisons of the isolate means using Fisher's unprotected LSD (5%) tests. The difference between the rhizosphere (R) and bulk (B) soil CFU quantities was also analysed as a \log_{10} ratio (R:B), and a Fisher's unprotected LSD test was again performed to compare individual treatments (Control, BG11, FRh2, J18).

4.2.6 Assessment of *Beauveria bassiana* in the roots and rhizosphere of *Zea mays* by PCR detection

Root and soil DNA was amplified with the *ef1α* nested primer sets according to the protocol(s) described previously (Chapter 2; section 2.5.1 'nested PCR protocol summary'). From the experiment, four of the six biological replicates were processed in total for PCR. Positive (isolate BG11 gDNA) and negative (sdH₂O, secondary sdH₂O) controls were included in each PCR/qPCR experiment. PCR product from the *ef1α* primers' EF4-4, from the second step of the standard nested PCR experiments were visualised on a 1% TAE (Chapter 2; section 2.2.1). PCR product was then directly sequenced (Lincoln University Sequencing Unit, New Zealand) and sequence quality was assessed in Chromas Pro (v 1.7.6; Technelysium Pty Ltd). The resulting sequences typically ranged from 105-125 bp, once trimmed of ambiguous sequence. These were checked for identity using BLASTn (Altschul et al. 1990) and aligned against *ef1α* sequences sourced from the experimental isolates (BG11, FRh2, J18) in addition to other *Beauveria* spp. *ef1α* sequences (see Appendix A for phylogeny inferred from *ef1α* EF4-4 amplicons generated from nested PCR on root DNA). Data was recorded as present or absent (binary 1/0) for root and soil DNA samples once confirmed as positive for *B. bassiana* using BLASTn or negative where there were either no bands or non-target amplification. Cycle threshold values and standard calibration curves were also generated for comparative real time qPCR analysis.

Data analysis of PCR binary data

The presence or absence of *B. bassiana* was compared independently in roots and in soil for the three isolates (BG11, FRh2, J18) and the control treatment over time (6, 15, 30 DAI), by calculating

the percentage present in samples. Statistical analysis could not be successfully conducted on binary data due to the small number of experimental replicates.

Data analysis of real-time qPCR data

Initially, DNA concentration obtained from a subset of extracted root tissue samples (Qubit™ assay) were plotted against the weight (in grams) of those same root tissue samples. The root weights selected represented the spectrum of minimum to maximum tissue weights for all samples in the experiment. The mean CT values for all inoculated samples (controls were omitted) were then plotted over the root tissue weights for those samples, with subsequent regression analysis. The mean CT values generated through amplification of the template obtained from primary PCR of the *B. bassiana* DNA dilution series (i.e. the standard curve data) were assessed in three ways: (1) They were assessed independently for each of three experiments in scatter plots, including standard deviations of the mean CTs, (2) they were plotted over the estimated starting concentration of the genomic DNA (pg/μL) and (3) they were compared statistically by contrasting the means for the three separate PCR experiments using a two way ANOVA in Genstat, with a Fisher's unprotected LSD (5%) test to determine PCR replication efficiency and reproducibility among experiments.

Data analysis of cycle threshold (CT) values

The three isolates (BG11, FRh2, J18) and the control treatment were compared for the 30 DAI time point only, using a generalised linear model (GLM; or logistic regression model) R (v. 3.2.3, package stats 3.2.2), with isolate treatment and herbivory as predictors in the model, using a Poisson-Normal error distribution. The model was visually assessed for fit using the packages/functions `coefplot` (v. 1.2.4) and `ggplot2` (v. 2.1.0). The control treatment was used as a reference level in the model, to contrast all other treatments ('1Ctrl'). Treatment means were compared further using Tukey pairwise contrasts in a general linear hypothesis (GLH) multiple comparisons procedure (package `multcomp` 1.4-5). Samples with missing CT values were omitted from GLM analysis, therefore, at each sample time (DAI) the total number of data points per treatment group varied.

4.2.7 Assessment of the microbial community composition using DGGE

PCR

Rhizosphere DNA from 30 DAI soil samples were amplified by multiple primers sets (Table 4.1) in separate PCR experiments to assess whether the inoculum treatments and/or the herbivory treatment had any effect on the soil microbial community composition. Using the protocol(s) optimised for denaturant gradient gel electrophoresis (DGGE), four target groups were successfully amplified in three replicates of each soil treatment: alphaproteobacteria, betaproteobacteria, general fungi and arbuscular mycorrhizal fungi (AMF).

The reagent concentrations per 25 μ L reaction consisted of 1 x buffer with 1.5 mM MgCl_2 , 200 μ M dNTPs, 5 pmol primer (for each forward and reverse primer), 1 U Taq DNA polymerase and 1 μ L of DNA template. Secondary PCR experiments used 1 μ L PCR product from the primary experiment for template but were diluted 1:10 in sdH_2O . The PCR experiments for DGGE product preparation were conducted in a Kyrtec SuperCycler SC300 thermal cycler using reagents from the FastStart DNA amplification kit (Roche).

Table 4.1. Primer target sets and PCR conditions for denaturant gradient gel electrophoresis (DGGE) microbial community analysis

Target group	Primer set	Reference	PCR	Conditions
Alphaproteobacteria	F203A & L1401 341GC & 518R	da Silva et al. (2003); Gomes et al. (2001); Muhling et al. (2008)	1	96°C 4 min, 30 x (94°C 1 min, 64°C 2 min, 74°C 1 min), 74°C 10 min.
			2	96 °C 4 min, 30 x (96 °C 1 min, 56 °C 30 sec, 74 °C 1 min), 74 °C 10 min.
Betaproteobacteria	β359F & β682R 518FGC & β682R	Muhling et al. (2008)	1	96°C 4 min, 30 x (94°C 1 min, 63°C 1 min, 74°C 1 min), 74°C 10 min.
			2	96°C 4 min, 30 x (96°C 1 min, 60°C 1 min, 74°C 1 min), 74°C 10 min.
Fungi	AU2 & AU4 FF-390 & FR1-GC	Muyzer et al. (1993) Vainio and Hantula (2000)	1	95°C 3 min, 35 x (94°C 1 min, 50°C 1 min, 72°C 1 min), 72°C 7 min.
			2	95°C 2 min, 8 x (95°C 30 sec, 55-48°C ¹ 30 sec, 72°C 1 min), 27 x (95°C 30 sec, 47°C 30 sec, 72°C 1 min) 72°C 7.5 min.
Arbuscular mycorrhizal fungi	AML1 & AML2 Glo-1 & NS 31-GC	Lee et al. (2008) Simon et al. (1992)	1	95°C 3 min, 35 x (94°C 1 min, 50°C 1 min, 72°C 1 min), 72°C 7 min.
			2	95°C 3 min, 35 x (94°C 45 sec, 52°C 45 sec, 72°C 1 min), 72°C 7 min.

1. Touchdown PCR, 1 °C per cycle.

DGGE

For each target group, PCR product was run on an 8% polyacrylamide gel (37.5:1 acrylamide: bis-acrylamide, BioRad) in 0.5 x TAE buffer. Varying gradients of denaturant were added to each gel for each group, and these were prepared from combinations of two gel mixes: a 0% denaturant gel (20 mL of 8% acrylamide, 1 mL of 50x TAE, 1 mL glycerol in 100 mL Millipore water) and a 100% denaturant gel (20 mL of 8% acrylamide, 42 g urea, 40 mL formamide, 1 mL of 50x TAE, 1 mL glycerol in 100 mL Millipore water). The gradients for each group were 40% of the 0% denaturant with 60% of the 100% denaturant gel for the alphaproteobacteria, 40-55% for Betaproteobacteria, 25-55% for the general fungi and 30-45% for AMF. In a 1:1 ratio, 10 µL PCR product per sample was mixed with 10 µL PCR loading dye (0.25% bromophenol blue) for loading into gel wells. All gels were run at 58°C in a Cipher DGGE electrophoresis system (CBS Scientific). For the proteobacteria gels, the DGGE was operated at 60 V for 18 hours and for fungi/AMF, the DGGE were run at 90 V for 17 hours.

Upon completion of the run, each gel was fixed in 250 mL 1x Cairn's fixation solution (ethanol, acetic acid and H₂O; in 4: 0.25: 0.75 parts) for 3 minutes with gentle shaking. Following fixation, gels were stained in 250 mL of silver stain solution (1x Cairn's fixation solution with 0.5 g silver nitrate per gel) for 10 minutes. The gels were then rinsed and washed for 2 minutes with Millipore water to remove excess stain prior to being bathed in a developer solution (500 mL H₂O, 15 g sodium hydroxide, 0.5 mL formaldehyde) for 35 minutes. Following development, the gels were washed for 5 minutes in Cairn's 1x fixation solution, rinsed in Millipore water and then soaked in Cairn's preservation solution (250 mL 96% EtOH, 100 mL glycerol, 650 mL H₂O) for 7 minutes. Gels were wrapped carefully in cellophane and oven-dried overnight at 65°C. Once dried, gels were scanned (Canon copier/scanner, image Runner ADV C2020) to obtain PDF images for analysis within the Phoretix™ software (TotalLab, New Castle, UK). Lanes were manually calibrated in Phoretix™ and bands detected per sample to represent species presence/absence for each target group.

Data analysis for DGGE

The DGGE presence/absence data was converted to distance matrices based on Jaccard's coefficient for measuring similarity. This was accomplished in R using the 'vegdist' function from the Vegan Package (v 2.3-5). Non-metric multiple dimension scaling (nMDS) was conducted from the distance matrices using the metaMDS function in Vegan with a maximum of 100 random starts and 3 dimensions for improved convergence. NMDS uses rank orders for 'species' rather than absolute numbers, based on the distance matrix. Stress plots were used to assess the nMDS analysis output and 2 dimensional nMDS plots were then produced with the ggplot2 package (same as described previously) to represent the data. Stress parameters assist in assessing how well the data is represented in the nMDS. Typically, stress values of > 0.05 provide an excellent representation in

reduced dimensions (e.g. 2 or 3), > 0.1 is great, > 0.2 is acceptable and a value > 0.3 provides a poor representation (Clarke 2014). Plots were arranged with either the isolate treatment or herbivory treatment (versus non-herbivory) indicated to visualise any potential effects.

4.2.8 Assessment of the microbial community function using MicroResp™

The MicroResp™ experimental set-up was as described by (Campbell et al. 2003), consisting of two opposing 96-well microtiter plates; one a deep-well plate with 1.2 mL volume wells (Raylab, New Zealand) to hold soil samples with added carbon sources and the other to detect accumulated carbon dioxide (CO₂) from the respiration of the live soil microbial community (ThermoFisher, New Zealand). CO₂ absorption was detected via a gel that contained a pH indicator dye, which results in a colour change (i.e. ranging from pink to yellow at 570 nm). The indicator dye contained cresol red (12.5ppm, wt/wt), potassium chloride (150 mM), and sodium bicarbonate (2.5 mM), and was set in 150 µL of Noble agar (1%) for each well of the detection plate. Prior to conducting the assay, the soil samples required adjustment of the gravimetric soil water content (GWC) to 40% of the water-holding capacity, so that with the addition of the carbon source solution, the final GWC of the soil was 60% of its water-holding capacity. This was calculated according to the following formula (Wakelin et al. 2013):

$$\% \text{ moisture} = \frac{(\text{g field moist soil}) - (\text{g dry soil})}{(\text{g field moist soil})} \times 100$$

A mixed sample obtained from the rhizosphere of multiple experimental plants was used to enable calculation of the soil GWC, by weighing the sample before and after drying it in the oven at 120°C overnight. To prepare the soil for the MicroResp™ assay, 100 g of soil was collected from the upper rhizosphere (5 -200 mm depth) of all the 30 DAI *Z. mays* plants and stored in sealed plastic bags at 4°C. The soil was processed through a 2 mm sieve to eliminate large aggregates, stones and roots. Approximately 0.45 g of fresh soil was added per well, per plate, and then each plate was sealed in a zip-lock plastic bag for incubation at 20°C for 7 days. Prior to adding the different carbon substrates, the plate containing the indicator gel was read with an absorbance microplate reader at 570 nm (spectrophotometer). The carbon substrates were then added to the 1.2 mL wells containing the rhizosphere samples at a concentration of 20 mg g⁻¹ dry soil (calculated using the GWC obtained for each sample) per substrate. The substrates used in this experiment were: L-arabinose, D-fructose, D-galactose, α-D-glucose, D-Xylose, maltose, sucrose, raffinose, citric acid, glycoloc, tartaric, glycerol 50%, D-(+)-glucosamine hydrochloride, urea, triton x-100, L-proline, glycine, L-alanine, arginine, L-serine, cysteine and tryrosine. Two water only substrate controls were included in the experiment. The carbon substrates used were considered representative of what may be present generally in plant root exudates. The two plates were then sealed with a silicone rubber gasket with

interconnecting holes and incubated for 4 hours at 20°C. Following incubation, the plates were separated and the plate containing the indicator gel was read immediately at 570 nm.

Data analysis for MicroResp™

MicroResp™ data was analysed within the software Primer-7 (Clarke and Gorley, 2015. PRIMER v7: User Manual/Tutorial. PRIMER-E, Plymouth, 296 pp.) and also in R (v. 3.2.3) for further analyses (described below). In Primer-7, all data was first normalised and a resemblance matrix produced using the Euclidean distance coefficient. The isolate treatment and herbivory were designated as factors, for a two-factor crossed analysis of similarities (ANOSIM) with 999 set permutations. ANOSIM is a nonparametric permutation procedure to compare between-groups and within-groups dissimilarities on multivariate data (Clarke and Green 1988). This procedure calculates an R statistic, wherein $R = 0$, the grouping of treatments is considered random (i.e. there is no interpretable grouping) and $R = 1$, if all replicates within groups are more similar to each other than any replicates between the groups (Klimek et al. 2016). The overall or 'global' R value was consequently used to express differences as dissimilarity between isolate (BG11, FRh2, J18) and control treatments, and the herbivory (H) and non-herbivory (N) groups. For the analysis in R (v. 3.2.3), the data was also normalised and converted to Euclidean distance resemblances using the Vegan package (v 2.3-5). Non metric MDS (nMDS) plots were then produced for isolate and herbivory factorial visualisation using Vegan.

4.3 Results

4.3.1 *Beauveria* in the rhizosphere soil (CFU quantity analysis)

Beauveria spp. cultures were observed from the rhizosphere soil of all inoculated plants (Table 4.2). Significantly more *Beauveria* CFUs were recovered from the rhizosphere of plants inoculated with each of the three isolates when compared to the control ($P \leq 0.01$). However, a low level of background and/or cross contamination of *Beauveria* spp. was detected from control plant soils, particularly at the 30 DAI sample time (Table 4.2). For all the fungal isolate treated soils, the quantity of *Beauveria* CFUs declined significantly in the rhizosphere soil from 15 to 30 DAI ($P < 0.001$).

In the bulk soil samples, no *Beauveria* spp. were detected at 6 DAI, however, *Beauveria* cultures were observed from 15 – 30 DAI, including in the control bulk soils. Significantly more CFU's were detected in the J18 bulk soil samples compared to the other two isolate treatments (BG11 and FRh2) at 15 and 30 DAI, respectively ($P \leq 0.05$; Table 4.2).

There were no statistically significant differences in the CFU quantities between the plants wounded to simulate herbivory (H) compared to those not subjected to wounding (N), when the 30 DAI samples were assessed independently using ANOVA, in rhizosphere ($P = 0.93$) or bulk ($P = 0.62$) soils.

Table 4.2. Quantification of *Beauveria* in rhizosphere soil versus bulk soil. Comparison of mean CFU g⁻¹ dry soil (reported in log₁₀) of *Beauveria* recovered at three sample times (days after inoculation, DAI) for rhizosphere (rhiz) and bulk soil, and ratio (rhiz:bulk) data. Means are reported with corresponding 5% LSD values in order to contrast isolate treatments.

	log10 rhiz CFU g ⁻¹ soil			log10 bulk CFU g ⁻¹ soil			log10 ratio rhiz:bulk		
	Time (DAI)			Time (DAI)			Time (DAI)		
Treatment	6	15	30	6	15	30	6	15	30
Control	1.52	0	1.87	0	1.31	1.14	1.5	-1.3	0.74
BG11	5.44	5.23	1.54	0	0.66	0.64	5.4	4.6	0.90
FRh2	4.46	4.97	1.11	0	0.66	0.64	4.5	4.3	0.46
J18	4.88	5.52	0.78	0	2.87	1.71	4.9	2.7	-0.94
LSD (5%)	1.04	1.04	1.04	0.90	0.90	0.90	2.51	2.51	2.51

4.3.2 PCR detection of *Beauveria bassiana* in the rhizosphere and roots of maize

Detection in soil

Over time, a decline in the frequency of detection of *Beauveria ef1α* by PCR was observed, indicating that there were temporal differences in the inoculum levels in the rhizosphere soil. Samples confirmed positive in the rhizosphere soil by PCR and gel electrophoresis (Figure 4.2) and from BLASTn results on nucleic acid sequence data (not shown) for *B. bassiana*, were summed and then calculated as percent present in samples for each isolate treatment and control, over the three sampling times: 6, 15 And 30 DAI (Figure 4.3). Detection of *B. bassiana* was more frequent across all treatments in 6 DAI and 15 DAI soil DNA compared to 30 DAI soil DNA. In control soil, *Beauveria* was detected in at 30 DAI, but not in 6 and 15 DAI rhizosphere soils.

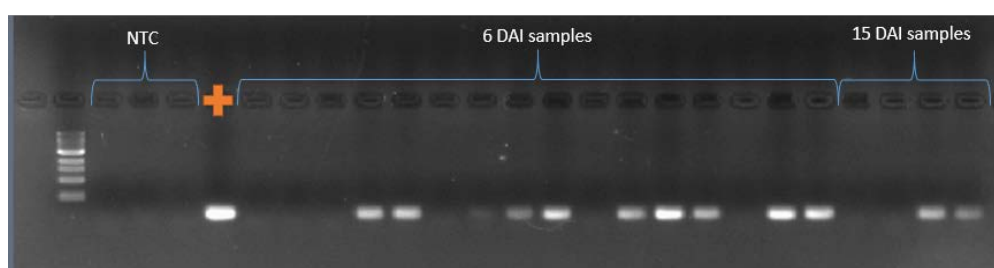


Figure 4.2. Electrophoresis gel image of *ef1α* product. The bands (176 bp) were amplified using EF4F and EF4R primers in the second step of a nested PCR from the rhizosphere soil of *Zea mays* (maize) plants (30 cycles), for 6 and 15 days after inoculation (DAI) with *Beauveria bassiana* isolates BG11, FRh2 and J18. In wells' 1-3 are the no-template controls (NTC) (from both the 1st and 2nd PCRs), followed by a *B. bassiana* positive control and then the experimental samples (not all data is shown).

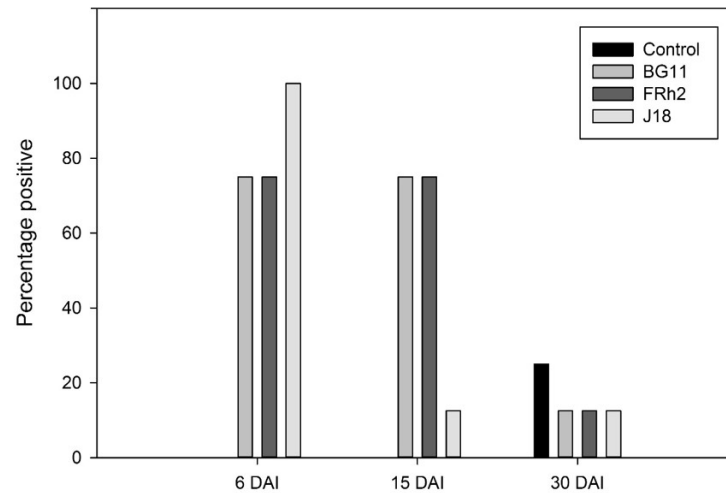


Figure 4.3. Percentage of *ef1α Beauveria bassiana* positive in the rhizosphere soil of *Zea mays* (maize). Calculated from positive PCR detection over three sampling events, 6, 15 and 30 days after inoculation (DAI). Positive samples were summed for each isolate treatment and control, and then calculated as percent present (Y axis) over samples.

Though it was not possible to test for statistical significance, there was an observed trend in the quantity of *B. bassiana* detected in the rhizosphere soil by PCR at 30 DAI only, for the plants subjected to wounding (herbivory simulation) compared to those not wounded (Figure 4.4). Only the no-inoculum control soils contained levels of *Beauveria* that were detectable with nested PCR within the non-herbivory (N) treatment.

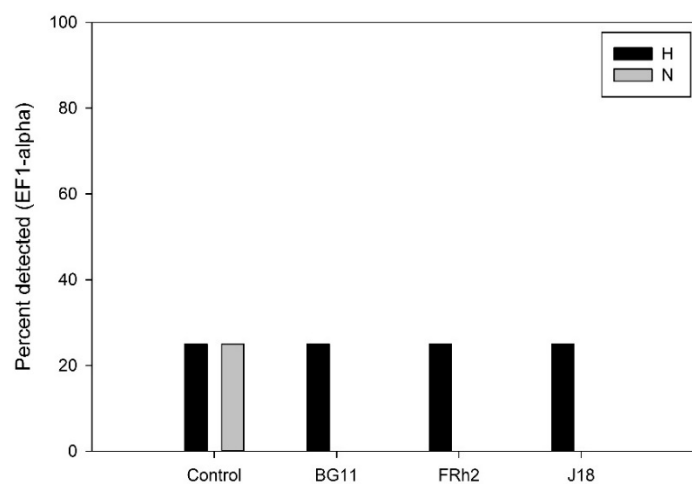


Figure 4.4. *Beauveria* in the rhizosphere soil of damaged *Zea mays* (maize) plants. Comparison of the herbivory (H) versus non-herbivory (N) control treatment means, presented as percentage of *ef1α Beauveria bassiana* detected by PCR in samples from the rhizosphere soil of *Zea mays* (maize) at 30 days after inoculation (DAI), for different isolate treatments versus a no-inoculum control.

Detection in roots

The detection frequency of *B. bassiana* found on/in roots by PCR was higher than that observed in the rhizosphere soil samples. Samples confirmed positive in the roots by PCR and gel electrophoresis (Figure 4.5) and from BLAST on nucleic acid sequence data (not shown) for *B. bassiana*, were also summed and calculated as percent present in samples for each isolate treatment and control, over the three sampling times: 6, 15 And 30 DAI (Figure 4.6). In 6 and 15 DAI samples, *B. bassiana* was confirmed present in 100% of inoculated root samples. By 30 DAI, only BG11 was 100% present, whereas the isolates FRh2 and J18 were detected less frequently.

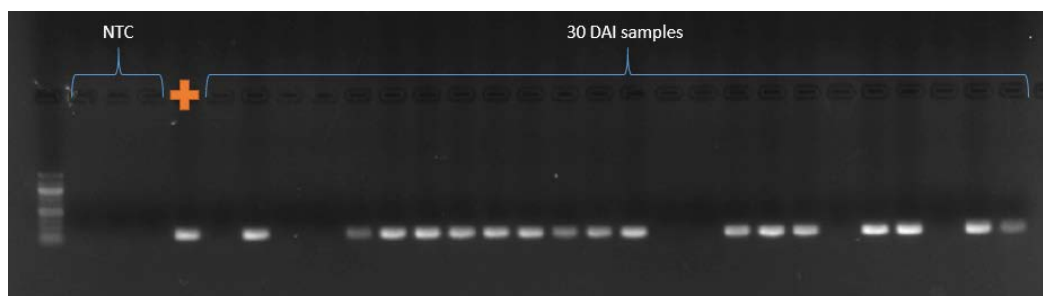


Figure 4.5. Electrophoresis gel image of *ef1α* product. The bands (176 bp) were amplified using EF4F and EF4R primers in the second step of a nested PCR from the rhizosphere of *Zea mays* (maize) plants at 30 days after inoculation (DAI) with *Beauveria bassiana* isolates BG11, FRh2 and J18. In wells' 1-3 are the no-template controls (NTC) (from the 1st and 2nd PCRs), followed by a *B. bassiana* positive control and then the experimental samples.

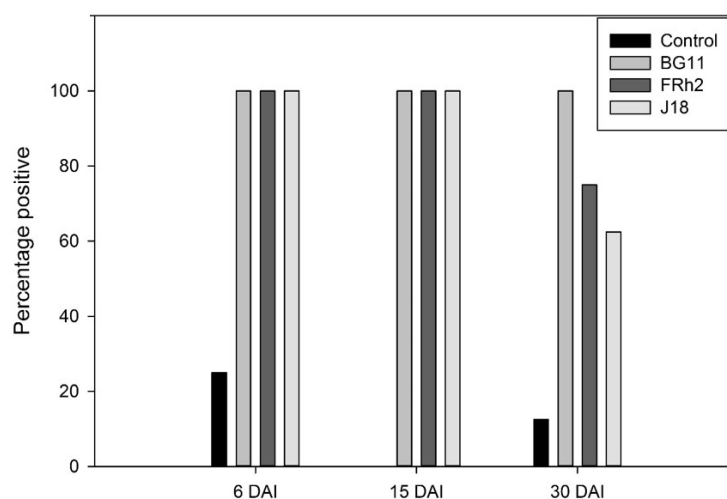


Figure 4.6. Percentage of *ef1α* *Beauveria bassiana* detected by PCR in or on the root tissue of *Zea mays* (maize). Presence of the isolates were recorded over three sampling events, 6, 15 and 30 days after inoculation (DAI). The number of positive samples were summed for each isolate treatment and control, and then calculated as percent present over samples (Y axis).

Real time qPCR data for detection in roots

In addition to direct PCR detection of *Beauveria* from root DNA, real time qPCR was performed on the same DNA to determine cycle threshold differences and thus potential fungal biomass fluctuations between the experimental harvest times and isolates.

In order to determine whether the qPCR data was comparable, the total genomic DNA concentration range that was produced relative to the maize root material weight (g) obtained at harvest, was assessed. The plot in Figure 4.7 indicated that smaller (e.g. 0.01 - 0.2 g) tissue samples may have resulted in higher DNA yield (Figure 4.7).

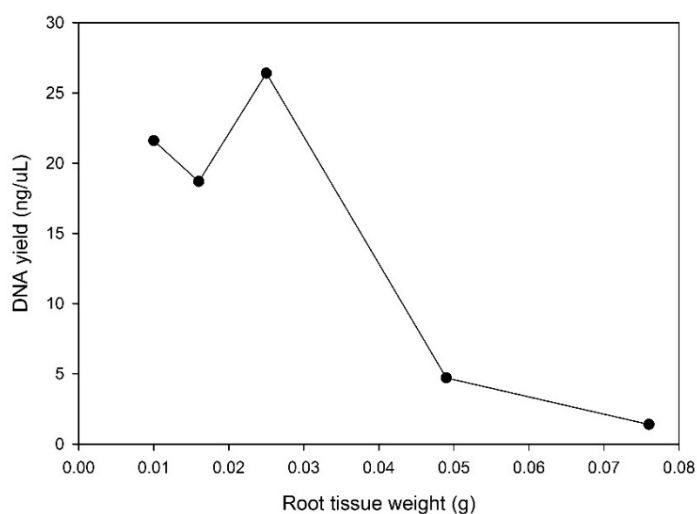


Figure 4.7. DNA concentration (ng/μL) yield. Yield was plotted over a range (experiment minimum and maximum) of *Zea mays* (maize) root tissue weights (g) using the MO BIO Power Plant Pro DNA isolation kit.

However, the plot of the mean *B. bassiana* PCR positive (*ef1α*) cycle threshold values over the maize root material weight (g), from all samples, demonstrated a weak positive regression (adjusted $R^2 = 0.34$), with CT values increasing only slightly on average with larger tissue samples weights (Figure 4.8).

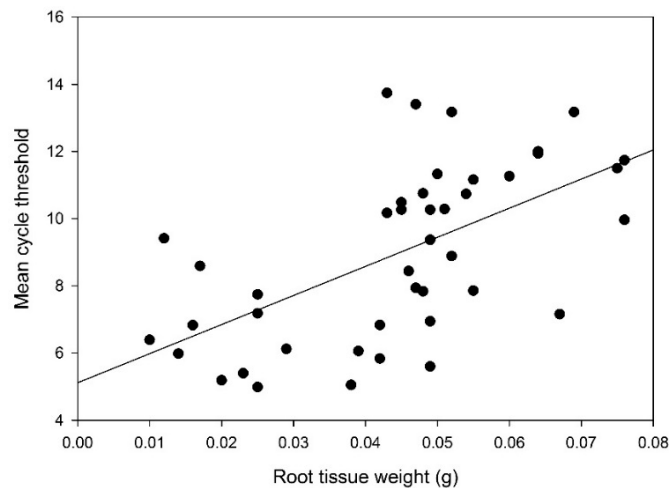


Figure 4.8. The relationship between DNA sample tissue weight and PCR amplification. Plot shows cycle threshold means for *ef1α* target (primers EF4F and EF4R) from all qPCR replicates (over three nested qPCR experiments and all sample times) of all samples treated with *Beauveria bassiana* (the no-inocula control samples are excluded here), plotted over root tissue weight in grams (g) and fitted with a linear regression line (adjusted $R^2 = 0.34$)

The qPCR experiments were found to be reproducible. The mean qPCR CT values obtained from standard curve data (linear equation average $12.32 + - 2.763x$; $R^2 = 0.99$), for each of the three qPCR experiments conducted and representing all root sample data, showed no statistically significant difference in PCR efficiencies or technical replication between experiments (5% LSD) (Figure 4.9).

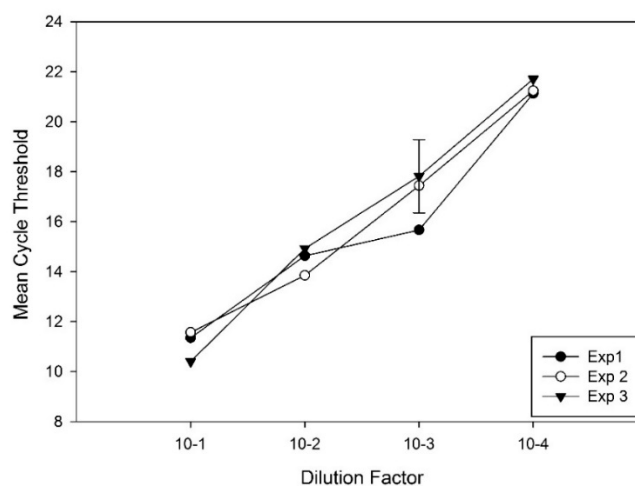


Figure 4.9. Amplification variation between thermal cycling experiments. Cycle threshold means (CT) compared over three real-time qPCR experiments for *ef1α* (primers EF4F and EF4R) amplifying the same DNA template (diluted 1/1000 $\mu\text{L H}_2\text{O}$); generated from primary PCR (amplicon from primers EF3F and EF5R) of pure *Beauveria bassiana* (0.32 ng/ μL), prepared prior in a 10-fold dilution series, to test consistency between PCR experiments

and replicates. A 5% least significant difference (LSD) bar representing all treatments is displayed.

Comparative analysis of cycle threshold values

No significant differences were observed in fungal DNA quantity in maize root DNA between the *B. bassiana* isolates (BG11, FRh2, J18), based on the comparison of the CT values in qPCR (Table 4.3). However, there was a statistically significant difference between all isolate treatments relative to the control ($P < 0.001$) (Table 4.3; Figure 4.10). Late-stage amplification of the control plant DNA was expected in the absence of the target template because the system was not sterile and the real-time PCR experiments were run for 40 cycles.

Table 4.3. Amplification of *Beauveria* isolates and non-target control. Tukey contrast pairwise comparisons with probability values show no differences between *Beauveria bassiana* isolate treatment mean cycle threshold (CT) values, except compared to the no-inoculum control (as expected). Based on amplifications on *Zea mays* (maize) root DNA, compared across three sample times: 6, 15, 30 days after inoculation (DAI).

CT mean Contrast	Probability ($> z $)	Significance level
BG11 - Control	1.00E-04	***
FRh2 - Control	1.00E-04	***
J18 - Control	1.00E-04	***
FRh2 - BG11	0.608	
J18 - BG11	0.995	
J18 - FRh2	0.793	

Furthermore, there was no significant difference observed between sampling times 6 and 15 DAI ($P = 0.89$), 6 and 30 DAI ($P = 0.11$) or for the +/- herbivory treatment ($P = 0.32$), when the CT values were compared in the generalised linear model (Figure 4.11).

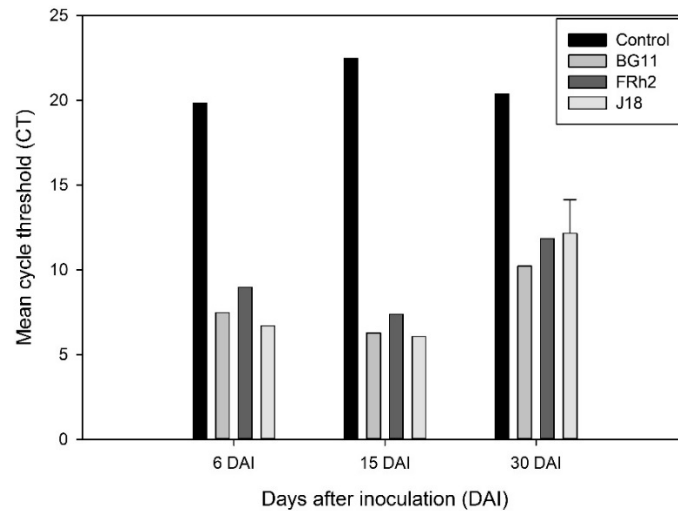


Figure 4.10. Amplification of *Beauveria* isolates and non-target control at different harvest times. Cycle threshold means (CT) from qPCR amplification of the *ef1α* *Beauveria* gene in or on the root tissue of *Zea mays* (maize) over three sampling events, 6, 15 and 30 days after inoculation (DAI). A 5% least significant difference (LSD) bar representing all treatments is displayed.

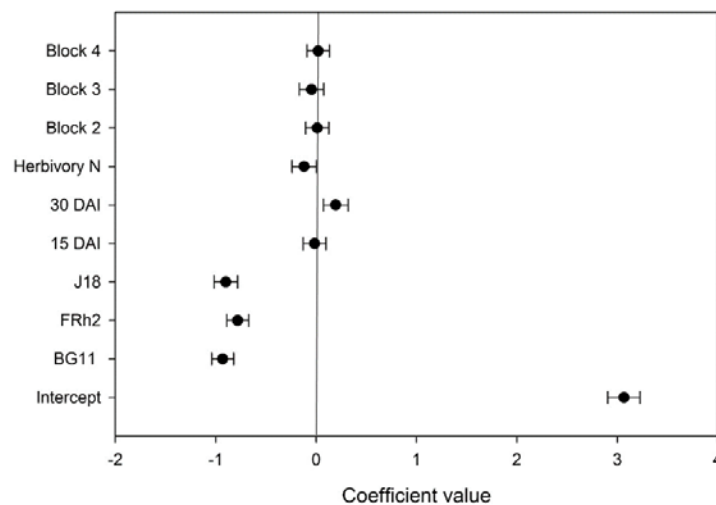


Figure 4.11. Depiction of the generalised linear model (GLM) to test isolate differences. Figure shows the coefficient plot of model estimates with standard error bars, based on cycle threshold (CT) values from qPCR amplification of the *ef1α* *Beauveria* gene in or on the root tissue of *Zea mays* (maize). The isolate treatment reference in the model is the control group, sample time reference is 6 days after inoculation (DAI), and the block reference is block 1.

A visual assessment of missing CT values from the entire data set indicated that by 30 DAI, *Beauveria* was not able to be detected in all of the samples (Table 4.4). However, for isolate BG11, *B. bassiana* was detected and confirmed in all samples tested. When the CT values were tested for differences

for the herbivory treatment factor, there was no significant difference between CT values in wounded and non-wounded plants.

Table 4.4. Number of missing data values representing absent cycle threshold values in qPCR experiments. Data represents *Beauveria* genus *ef1α* nested primer set (EF3-5; EF4-4) detected from root tissue of *Zea mays* (maize) at 6 and 30 days after inoculation (DAI).

DAI	Treatment group	# Missing values	Total values per group	% Missing
6	Control	1	4	25
30	Control	4	8	50
30	FRh2	2	8	25
30	J18	3	8	37.5

4.3.3 Assessment of the microbial community composition using DGGE

Visual assessment of denaturant gradient gel electrophoresis (DGGE) demonstrated variability between soil samples in the general microbial community composition for total fungi (Figure 4.12) and other groups (images not shown). The nMDS analyses of all groups (AMF, total fungi, alphaproteobacteria and betaproteobacteria) indicated marginal dissimilarities across both treatments (isolate and herbivory treatments) (Figure 4.13; 4.14), which was supported by significant R2 values and relatively low stress (Table 4.5).

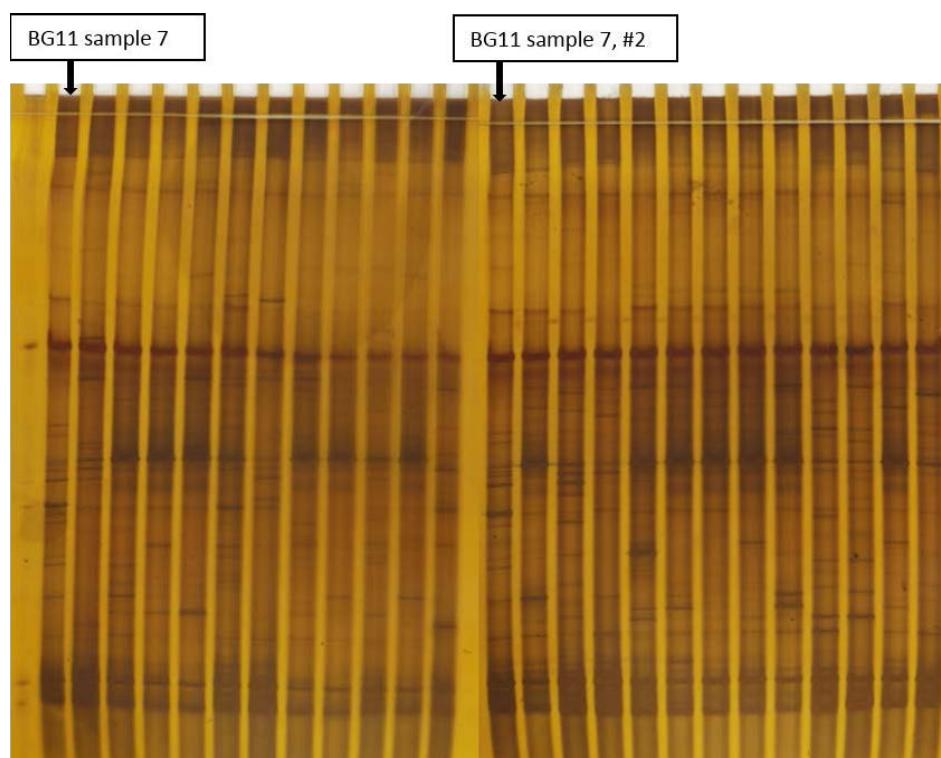


Figure 4.12. Denaturing gradient gel electrophoresis images. Gels show the general fungi set generated from PCR using the nested primer pairs AU2 & AU4 and FF-390 & FR1-GC, representing all fungi in the *Zea mays* (maize) rhizosphere soil DNA from 30 days after inoculation (DAI) samples (3 replicates per treatment). The first lane of each gel (2 gels

are shown with 12 lanes per gel) indicates the reference sample (BG11 sample 7) from which bands were calibrated in Phoretix™.

Table 4.5. Statistical support of all ordination models. Analysis table of non-metric multiple dimension scaling (nMDS) ordination stress tests on microbial community composition data from denaturing gradient gel electrophoresis (DGGE).

Target group	Linear R ²	Non-metric R ²	Stress
Arbuscular Mycorrhiza Fungi (AMF)	0.68	0.96	0.20
Fungi	0.80	0.94	0.24
Alphaproteobacteria	0.77	0.95	0.21
Betaproteobacteria	0.72	0.95	0.22

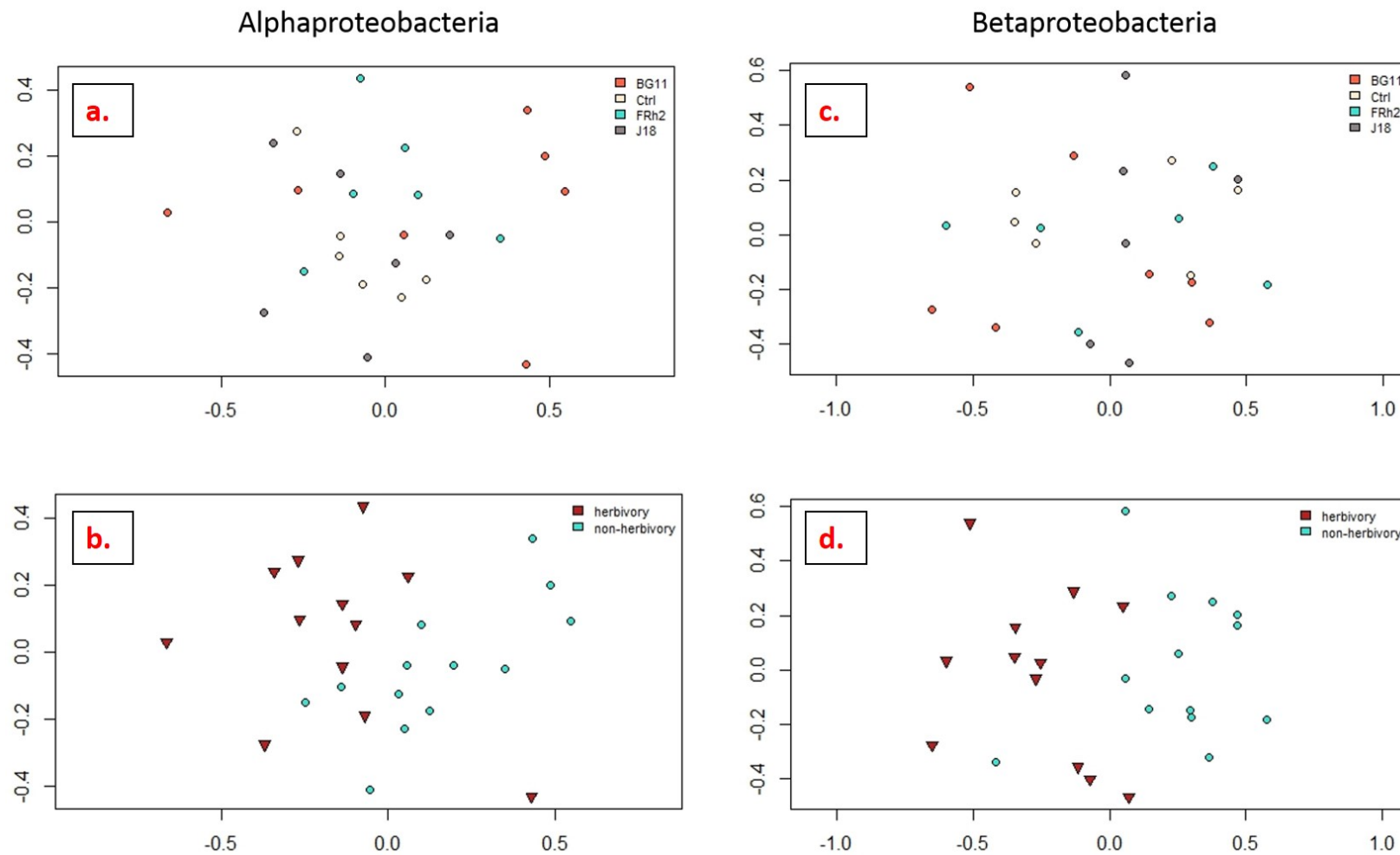


Figure 4.13. Grouping of community data visualised for *Beauveria* isolate versus for the herbivory treatment. Depicted by non-metric multiple dimension scaling (nMDS) plots representing dissimilarities between PCR amplicon profiles from denaturing gradient gel electrophoresis (DGGE) experiments on samples from 30 days after inoculation (DAI) of *Zea mays* (maize) rhizosphere soil DNA, with isolate and herbivory treatments indicated (plots legends), for alphaproteobacteria (a, b) and betaproteobacteria (c, d) groups.

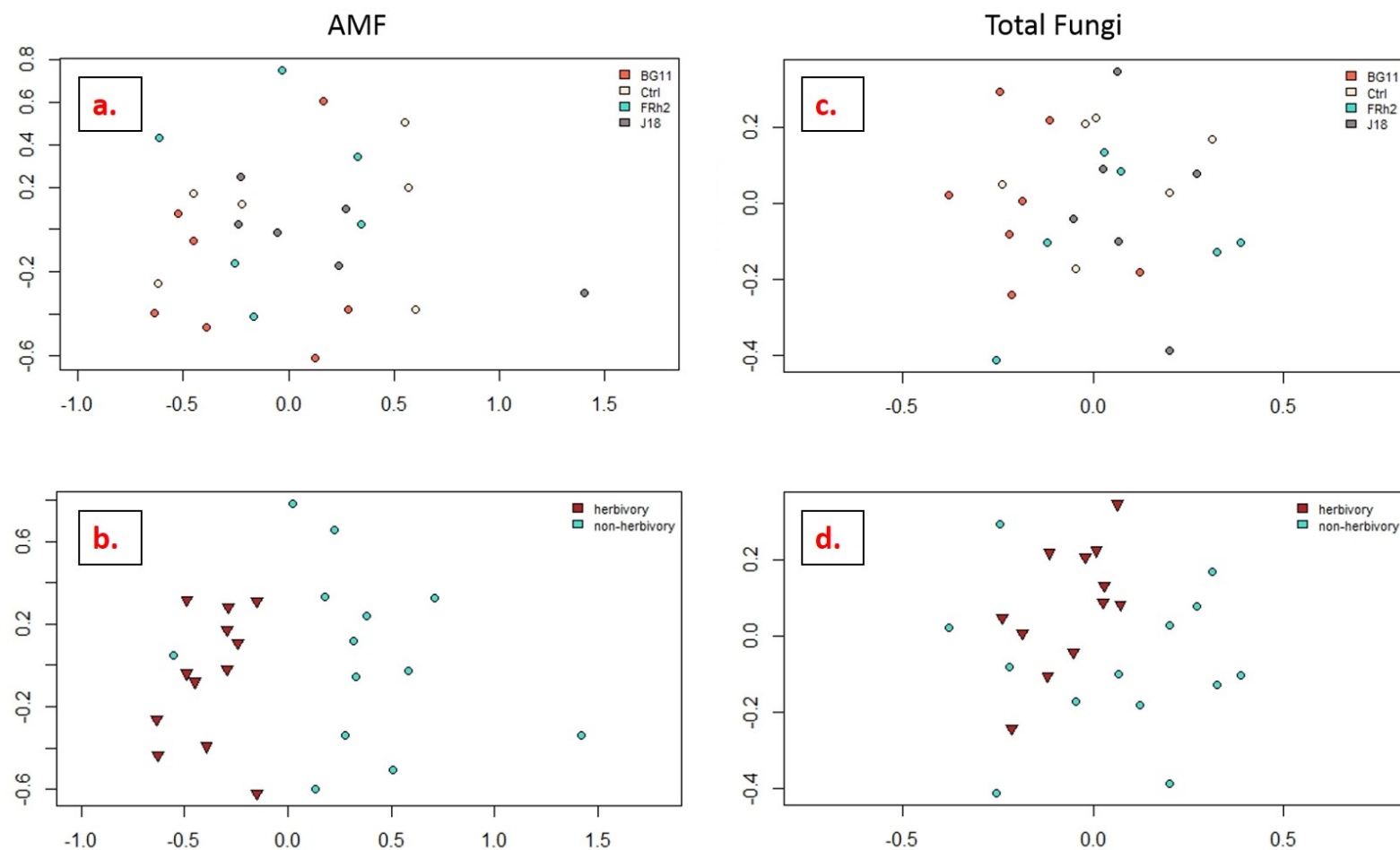


Figure 4.14. Grouping of community data visualised for *Beauveria* isolate versus for the herbivory treatment. Depicted by non-metric multiple dimension scaling (nMDS) plots representing dissimilarities between PCR amplicon profiles from denaturing gradient gel electrophoresis (DGGE) experiments on samples from 30 days after inoculation (DAI) of *Zea mays* (maize) rhizosphere soil DNA, with isolate and herbivory treatments indicated (plots legends), for arbuscular mycorrhizal fungi (a, b) and total fungi (c, d) groups.

4.3.4 Assessment of the microbial community function using MicroResp™

Carbon utilisation by the microbial communities in rhizosphere soils was not generally affected by the presence of the *B. bassiana* inocula, but was affected somewhat by the simulated herbivory treatment. This was demonstrated by the two-factor crossed analysis of similarities (ANOSIM) that was conducted in Primer-7 which showed statistical significance to the 5% level ($R = 0.079$, $P = 0.05$) to support no discernible grouping (dissimilarity) between the isolate treatments. However, pairwise comparisons produced subsequently from ANOSIM suggested that differences between BG11 and Ctrl (control) treatments solely contributed to any weak grouping observed ($R = 0.196$, $P = 0.01$) for the isolate treatment factor. This suggests that there may have been marginal differences in the microbial community function as a result of the presence of isolate BG11 on the roots of maize. All other pairwise comparisons between isolate treatments were not significant. The simulated herbivory (H) and non-herbivory treatments (N) across all isolates and control demonstrated marginal grouping ($R = 0.133$, $P < 0.001$). The nMDS analyses (R) supported also weak clustering with low stress (0.1647) in 2 dimensions with a non-metric R^2 of 0.973 and a linear adjusted R^2 of 0.866 for all data (from Euclidean distance) (Figure 4.15).

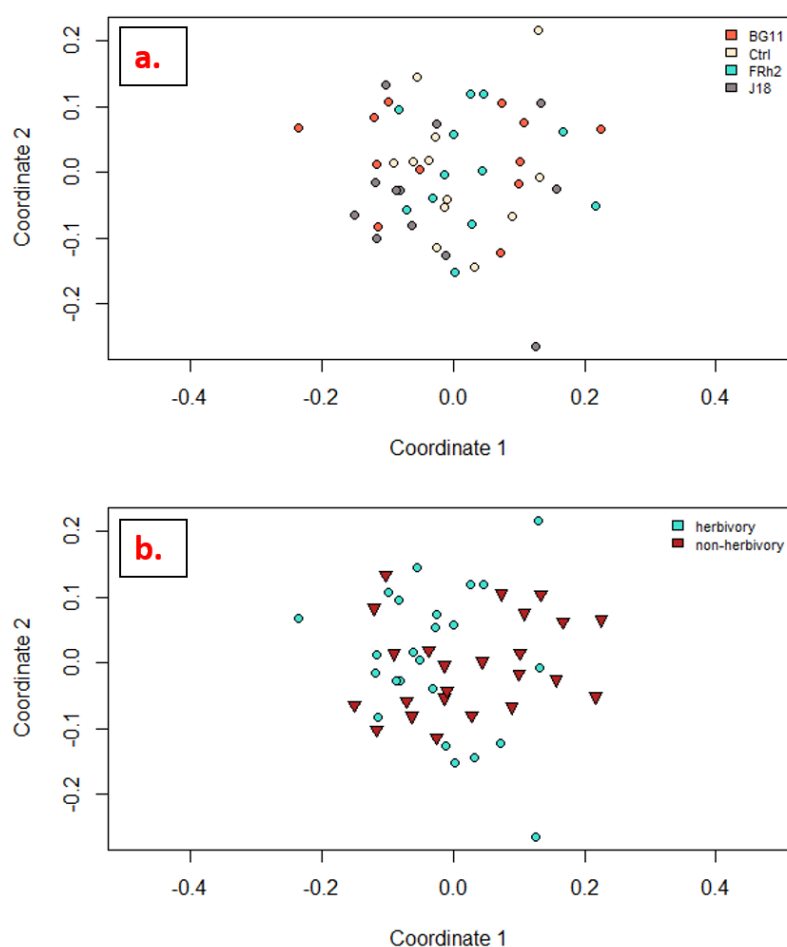


Figure 4.15. Grouping of functional community data visualised for *Beauveria* isolate versus for the herbivory treatment. Non-metric multiple dimension scaling (nMDS) plots representing

marginal dissimilarities in two dimensions, between respiration profiles of the microbial communities from 30 days after inoculation (DAI) of *Zea mays* (maize) rhizosphere soil, obtained from MicroResp™ colorimetric readings. Plots are distinguished by either isolate (a) or herbivory (b) treatments as grouping factors.

4.4 Discussion

In this chapter, effects of three different isolates of *B. bassiana* on the microbial community in the rhizosphere of maize roots were investigated. Specifically, the experiment had two aims: (1) to ascertain whether the applied isolates were retained in the rhizosphere soil and/or root material within 30 DAI, and (2) to investigate whether the three isolates influenced the soil microbial community structure and function differently as a result of their presence.

4.4.1 Quantification and detection of *Beauveria bassiana* in the rhizosphere

Using culture-dependent detection methodology, the number of colony forming units (CFU) in the rhizosphere soil for all three *B. bassiana* isolates was shown to decline from $\sim 10^5$ CFU to background levels by 30 DAI. *Beauveria* species' CFUs were either not detected or only detected at low levels in bulk soil samples. This suggests that the *Beauveria* isolates tested here cannot maintain rhizosphere colonisation in maize for more than 30 days. Although species of *Metarhizium* have been demonstrated to play a positive role in the rhizosphere (Liao et al. 2014), species of *Beauveria* have previously not often been tested to determine whether they may be functional in rhizosphere soil (Kepler et al. 2017, McKinnon 2011).

However, *Beauveria* species have been frequently isolated from soil (Bidochka et al. 1998; Bing and Lewis 1993; Jaronski 2008; Meyling et al. 2009; Zimmermann 1986), and only a few studies have previously investigated rhizosphere colonisation by *Beauveria*. Renwick et al. (1991) found no association of *Beauveria* in the rhizosphere of wheat following inoculation, although, the fungi was applied as a mycelial suspension to the base of the wheat plants and the potting medium used was sterilised sand. A survey by Bidochka et al. (1998) reported that *B. bassiana* was more abundant in forest soils, compared to *Metarhizium* spp. that was found more often in agricultural habitats. However, isolates of *Beauveria* were recovered from the rhizosphere of a number of plants (Fisher et al. 2011) such as grape and strawberry, and a recent study by Zitlalpopoca-Hernandez et al. (2017) recovered *B. bassiana* from soil of potted maize plants after seven weeks. In this instance, the soil (soil:sand) was inoculated with the *Beauveria* using a conidial suspension and mixed through prior to planting. When arbuscular mycorrhizal fungi (AMF) was dual-inoculated with the *B. bassiana* soil inoculum, the population density of *B. bassiana* in soil was shown to be lower than when *Beauveria* was used alone (Zitlalpopoca-Hernandez et al. 2017). This observed reduced population density may have been a result of competitive exclusion of the plant-derived nutrients by the AMF, suggesting that *Beauveria* soil populations may rely on plant roots to some extent for nutrients. Interestingly,

Gualandi et al. (2014) reported that the inoculation of AMF did not affect *B. bassiana* endophytic colonisation in the roots of *Echinacea*, which is consistent with the results of this present study since *Beauveria* was more frequently detected by PCR analysis in/on roots than in rhizosphere soil directly.

Furthermore, the decline observed in soil in this study may be attributed to a number of factors. Firstly, the carrying capacity of a single species population in the rhizosphere may be restricted to levels below that which was introduced, due to competition for host resources within the resident microbial community (Lugtenberg et al. 2002). However, a study by Hohmann et al. (2012), found that rhizosphere colonisation with the bio-inoculant *Trichoderma hamatum* was most successful when the inoculum was applied in a moderate concentration such as at 10^5 CFU per gram of soil, as compared to a conventional rate of above 10^7 , or lower concentrations of less than 10^3 CFU g⁻¹ soil. This colonisation efficacy was attributed to the Allee effect, which describes the dependency of population fitness on population density, particularly when establishing in a new environment (Kramer et al. 2009). It is possible therefore, that persistence in the rhizosphere of *B. bassiana* as a beneficial coloniser may be optimised by the inoculation method employed (Malusa et al. 2012), and that this Allee effect may explain the decline observed after inoculation for all isolates used in this study.

In the present study, the *B. bassiana* inocula were not applied to the soil directly but to the corn seedlings by dipping the roots in suspensions. Thus, the actual starting concentration for each isolate adhering to the root surface was not quantified. Any variation introduced at this stage, may have resulted in isolate variation in root surface colonisation ability (Liao et al. 2014). Upon introduction into non-sterile soil, competition for host exudates begins and this may hinder continued growth of the inocula (Malusa et al. 2012). Consequently, the growth rate of the plant may have exceeded that of the *Beauveria* in soil (Bonaldi et al. 2015). With rapid root growth including finer roots, the rhizosphere soil-volume potential also increases, and since the same quantity of rhizosphere soil was sampled at each harvest time, the surface area-volume ratio of roots and soil was likely disproportionate between sampling events (Judd et al. 2015). This change, combined together with the competition in the microbiome and the growth of the plant, may result over time in a reduction of the original inocula available for sampling, thus also contributing to the decline in frequency observed from 15 to 30 DAI from the rhizosphere.

However, *Beauveria* was more frequently detected in the rhizosphere when plants were subjected to herbivory, although this data set was not statistically analysed since replication was low and the success rate for the herbivory factor was too high for accurate model predictions (i.e. there was no variance). Under herbivory stress, plants can respond in a number of ways that may affect microbe-plant interactions (Howe and Jander 2008). Such responses include the activation of defences in distal parts, changes in root exudates, or through the modification of soil characteristics (Pangesti et

al. 2013). Plant systemic resistance may be induced in certain organs and tissues following pathogen or insect attack that activate signalling pathways to affect distant tissues, and can subsequently also affect below-ground microbes (Doornbos et al. 2011). For example, in pepper plants, herbivory by sap-sucking whiteflies or aphids has been shown to induce the up-regulation of transcription factors that govern both salicylic acid (SA)- and jasmonic acid (JA)-dependent pathways in leaves and in roots (Lee et al. 2012; Yang et al. 2012). Plants are also known to release a suite of volatiles that specifically attract natural enemies of the herbivores (Arimura et al. 2009; War et al. 2012).

Indeed, recruitment of beneficial rhizosphere-colonising microbes has been shown for bacterial and mycorrhizal species. For example, Lakshmanan et al. (2012) observed higher levels of beneficial rhizobacteria *Bacillus subtilis* in the rhizosphere of *Arabidopsis thaliana* when the plants were subjected to stress from foliar pathogen attack by *Pseudomonas syringae*. Specifically, foliar infection by the pathogen induced the expression of a malic acid transporter resulting in an increase of malic acid in the rhizosphere. Furthermore, the biofilm formation in *B. subtilis* on roots actually negated the suppression of microbe-associated molecular patterns (MAMPs), allowing continued defence against the disease. A study conducted on ragwort plants (*Jacobaea vulgaris*) showed that both above- and below-ground herbivory altered the composition of the soil fungal community, which was attributed to changes in root exudates (Kostenko et al. 2012). Evidence that insect herbivory can influence root-associated microbes via changes in root exudation has also been reported for maize plants. Root-feeding by western corn rootworm (WCR) larvae was shown to change the composition of the microbial community in the rhizosphere when analysed by denaturant gradient gel electrophoresis (DGGE). Interestingly, this effect was dependent on both the soil type and maize cultivar (Dematheis et al. 2012).

The present study also indicated that the maize cultivar 34H31 may actively recruit or support *B. bassiana* in the rhizosphere when under mechanical wound-stress. Considering that the simulated herbivory was shown to affect the microbial composition and function, it is possible that plant exudate changes contributed to the improved persistence of *B. bassiana* in the rhizosphere. Enhanced rhizosphere colonisation by *Beauveria* spp. of plants experiencing insect herbivory may be an adaptive strategy in these fungi to increase the likelihood of encountering susceptible insect hosts. Keyser et al. (2014) also hypothesised that root colonisation by *Metarhizium* spp. may be an adaptive strategy in these fungi to increase exposure to plant-associated insects, which would aid in dispersal. They tested the pathogenicity of the fungi to *Tenebrio molitor* larvae by exposing the insects to wheat roots that were inoculated prior with *Metarhizium* spp. as a seed treatment. Since the fungi were shown to disperse with roots and retain pathogenicity for up to 4 weeks from inoculation, they asserted that a plant-root association provides a benefit to the fungi by increasing the likelihood of encountering a susceptible insect host (Keyser et al. 2014).

Root detection studies

In the detection studies conducted on root DNA, *B. bassiana* was frequently confirmed present by amplification of the *ef1α* gene. However, the inocula may have occupied the plant as either an endophyte and/or within the rhizosphere (i.e. on the rhizoplane), since the root material was not surface sterilised prior to DNA extraction. The inclusion of surface inocula was deliberate, since reliable elimination of inocula DNA on plant root surfaces was not accomplished in prior experiments (see Chapter 2). Because viable propagules could not be distinguished from non-viable by PCR (Nocker et al. 2006), it is also possible that the presence of the fungal isolates in association with roots was overestimated using PCR, consequently, any differences in persistence within or between the isolate treatments was not demonstrated. Statistical analysis of the cycle threshold (CT) values obtained from qPCR on root DNA over the three time points also did not demonstrate any significant differences between the isolate treatments specifically, other than when individually contrasted with the control. However, the control treatment was expected to have some amplification with high cycle threshold values due to non-target amplification after many cycles (< 50 with nested PCR).

The *ef1α* gene primers and protocol developed for this present study once again demonstrated a relatively high level of sensitivity and were able to amplify multiple species of *Beauveria*, as inocula were not distinguished from background *Beauveria* by sequence analysis, but excluded maize DNA and most other non-target fungi present in the soil. Although some late cycle non-target amplification occurred, nucleotide analysis enabled the differentiation of *Beauveria* species (but not isolates), and the number of fungi from other genera that were amplified using the nested *ef1α* protocol was relatively restricted (3 genera, Appendix A). *Beauveria* species detected other than *B. bassiana* were considered non-target amplification. Although the *ef1α* nested PCR protocol was less sensitive in comparison to the nested PCR protocol developed by Landa et al. (2013) (see Chapter 2), *Beauveria* DNA was still detected in the present study by 30 DAI in/on roots and in soil, suggesting that the *ef1α* protocol was sufficiently sensitive to monitor even background levels of inocula within the plant environment.

4.4.2 The influence of inocula on the soil microbial community structure and function

The presence of the isolates had little to no influence on the microbial community composition and function in the rhizosphere by 30 DAI (DGGE and MicroRespTM analyses). This is not surprising given the decline observed over time to background levels by 30 DAI but may also indicate that initial inundative inoculation did not have any lasting effect. Multitrophic interactions are important to consider, in addition to any possible ecosystem impacts that may influence performance of a biocontrol agent applied to agroecosystems (Ownley et al. 2010). However, there is limited information on interactions between entomopathogenic fungi and other plant beneficial root

associated microorganisms (Gualandi et al. 2014; Zitlalpopoca-Hernandez et al. 2017). Recent studies have focused more on the biocontrol activity of entomopathogenic fungi against plant pathogens (Lozano-Tovar et al. 2017) and insect herbivores (Liao et al. 2017; Vidal and Jaber 2015). For instance, Lozano-Tovar et al. (2017) assessed *M. brunneum* and *B. bassiana* *in vitro* for activity against the soil-borne pathogens *Verticillium dahliae* and *Phytophthora megasperma* of olive and found that the entomopathogens produced antifungal secondary metabolites, which were able to inhibit growth.

In this present study, weak grouping for the effect of the isolate treatments on the soil microbial composition profiles may be either a consequence of the effect of previous inocula levels (e.g. at 15 DAI) or the result of chance, since there were only a small number of replicates that could be tested in the DGGE experiments. However, of all the groups, the total fungi group appeared to be affected to a limited extent by the presence of the isolate treatments and this may be the result of resource competition or allelopathy (i.e. by secondary metabolites) in the rhizosphere as a result of inoculation (Lozano-Tovar et al. 2017; Lugtenberg et al. 2017). A study by Cripps-Guazzone (2014) used DGGE to analyse microbial community composition changes and found that inoculation with *Trichoderma* spp. altered bacterial, fungal and AMF populations in the rhizosphere of maize. The presence of *T. harzianum* in the rhizosphere of soybean was also shown to significantly reduce *Glomus mosseae* mycorrhizal growth (Wyss et al. 1992). However, McLean et al. (2014) analysed the effect of a commercial *Trichoderma* biopesticide formulation on the native AMF populations in two ecosystems (podocarp forest and grassland) and found that the AMF populations were not affected in both instances. In this present study, significant changes in the rhizosphere microbiome were not observed in terms of composition and function, however, species diversity generally appeared high and neither of the methods used (DGGE, MicroResp™) determined taxa present or quantitative differences.

A greater influence on the rhizosphere microbial community was observed in the plants subjected to the simulated herbivory treatment. This result was supported by the MicroResp™ assay, which also demonstrated some grouping of the respiration profiles in the nMDS for the herbivory treatment. It is plausible therefore to conclude that in this experiment, the root exudate profile was altered by those plants under distress from the above-ground damage to foliage. It is well established that plants produce secondary metabolites and proteins that have toxic, repellent, and/or antinutritional effects on the herbivores (Usha Rani and Jyothsna 2010; War et al. 2012). Plants can therefore antagonise herbivores directly by affecting fecundity or host plant preference, as well as indirectly by recruiting natural enemies of the insect herbivores (Dudareva et al. 2006; Howe and Jander 2008). Mechanical wounding, such as that made by chewing insects, stimulates plant morphological changes that affect herbivores such as increased root hairs, trichomes, thorns, spines, and thicker leaves and may also induce the production of toxic chemicals such as terpenoids, alkaloids,

anthocyanins, phenols, and quinones, that may either kill or retard the development of the herbivores (Hanley et al. 2007). Since all three of *B. bassiana* isolates used in this study were retained in the rhizosphere of the wound-damaged plants in particular (refer to the discussion on the soil detection study), the presence of these isolates in these plants may be contributing significantly to the community functional shift observed. This is the first, albeit preliminary evidence, that *B. bassiana* can be directly supported by plants within the rhizosphere under certain conditions, such as during above-ground herbivory or stress (Lareen et al. 2016).

4.4.3 Conclusion

Root-associated microbial communities have been the focus of much research, especially for agriculturally important crops such as maize (Gomes et al. 2001; Lu et al. 2015; Santiago et al. 2017; Vargas et al. 2009). However, the factors and multipartite interactions that shape the root microbiome structure, and consequently affect plant health and development, are highly complex and not fully understood (Lareen et al. 2016). The questions remaining here for investigation are what species of the microbiome are included or excluded as a result of the presence of the inocula, and more particularly, are above-ground insect herbivores more at risk of infection by *Beauveria* as a result of this interaction in the rhizosphere? Furthermore, what mechanisms are involved within the plant in response to *B. bassiana* colonisation?

Chapter 5

Transcriptomic analysis of *Zea mays* in response to root colonisation by two *Beauveria bassiana* isolates

5.1 Introduction

The concept of the endophytic lifestyle of *Beauveria bassiana* has prompted recent research to discover the biocontrol potential of the fungi to control insect pests, while endophytically associated with host plants (Vidal and Jaber 2015). However, without properly understanding the interaction of the fungi with the plant-host or whether there are differences in the plant-host response to various fungal isolates, the potential may not be fully realised. Conventionally, entomopathogenic biocontrol agents have been selected on the basis of virulence to the insect targeted for control. In assessing whether endophytic entomopathogenic fungi (EPF) can be employed for biocontrol, both pathogenicity to the pest and endophytic performance should be assessed, as there may be differences in plant colonisation capability among isolates (Nieto-Jacobo et al. 2017). Variation in the endophytic ability of various fungal isolates within the species has received little consideration. A recent study, however, indicated that there may be variation in the endophytic persistence of six *B. bassiana* isolates tested in leaves and stems of maize (*Zea mays*) (Renuka et al. 2016).

Studies which attempt to eliminate surface inocula completely when confirming endophytic establishment may also miss potential variation in the fungal isolates' ability to penetrate the host tissues, which may be an important aspect of the plant-fungi/endophyte interaction to consider. An alternative approach to investigate fungal colonisation ability, or host interactions, is to study the molecular response of the plant to the inocula. Plants can adjust their phenotype to maximise interactions with beneficial organisms while minimising detrimental associations (Dicke 2016). To achieve this, plants need to be able to distinguish between beneficial and detrimental members of the microbial community and then adjust their phenotype accordingly. The mechanism to perceive herbivores and pathogens is based largely on chemical recognition. This involves damage-associated molecular patterns (DAMPs), pathogen-associated molecular patterns (PAMPs) and herbivore-associated molecular patterns (HAMPs) (Dicke 2016) (refer to Chapter 1).

In general, plants initially recognise endophytic fungi as invaders, triggering a primary immune response. Many genes associated with jasmonic acid (JA) and ethylene (ET) are induced that are involved in both hormone biosynthesis and signalling (Vos et al. 2015). In assessing plant gene differential expression, Brotman et al. (2013) found that beneficial fungi-plant interactions target various transcription factors (TFs) involved in the resistance against herbivores in particular.

Furthermore, the involvement of many reactive oxygen species (ROS) inducible genes, ROS scavengers (Shoresh and Harman 2008) and mitogen-activated protein kinase (MAPK) (Mathys 2012) encoding genes were reported. As discussed in Chapter 3, it is also possible that endophytic colonisation can enhance plant growth (Waller 2005). In a proteomic analysis, Gomez-Vidal et al. (2009) reported the production of proteins relating to plant defence or the stress response in *Phoenix dactylifera* leaves following colonisation by *B. bassiana*. The gene expression of the plant in response to the colonisation process may therefore provide insights into whether certain isolates of *B. bassiana* vary in their ability to colonise plant tissues. If isolates colonise plant tissues to varying degrees and at different rates, then these differences may be apparent in the transcriptomic response of the host.

In this chapter the endophytic performance of *B. bassiana* was investigated, indirectly, by means of analysing the plant response to early colonisation following localised inoculation. In particular, the objective was to ascertain the response of maize (*Z. mays*) to root colonisation by two isolates of *B. bassiana*; BG11 and J18, versus a no-inoculum control. This was accomplished in a microarray experiment to determine the genes that were differentially expressed in the plant. In prior experiments (Chapter 3 and 4), results indicated that isolates' BG11 and J18 may differ in their ability to colonise roots and the rhizosphere or rather, the plants respond differently to these isolates. It was plausible therefore, that these differences would be reflected in the gene expression of the plant in reaction to the inoculum. For the purpose of this experiment, rhizoplane as well as endophytic interactions with the host plant were included and thus the roots were not surface sterilised, in order that the isolates' ability to penetrate the host tissues was also considered.

5.2 Methods

5.2.1 Plant growth and inoculation

Seeds from maize cultivar 34H31 were surface sterilised (Chapter 2, section 2.2.3) and placed individually on solid 30 mL 1% agar in 500 mL volume sterile plastic jars with screw-top lids (Labserv). Growth room conditions for germination consisted of temperatures ranging from 20°C to 22°C with 60%-70% relative humidity, under a 12:12 h day/night cycle for 5 days. A total of 30 seedlings germinated and after 5 days were inoculated. Prior to inoculation, the seedlings were scored for size and thus arranged in size-blocks based on the primary root length. The size categories of root lengths consisted of: small (2.8-4 cm), medium (5-7 cm) and large (8-10 cm). Therefore, block 1 was small, block 2 medium and block 3 large.

Five day old maize seedlings were then inoculated by the root-dip method using freshly made conidial suspensions at a concentration of 10^7 conidia mL⁻¹ per isolate (BG11 and J18) (refer to Chapter 2, section 2.2.2 for suspension preparation), prepared in 25 mL sterile water containing

0.05% Tween 80. For the no-inoculum control group, plant seedlings were dipped in the same volume of sterile water with 0.05% Tween 80. The conidial suspensions were prepared from five week-old cultures of BG11 and J18 isolates grown on potato dextrose agar (PDA) plates (Difco, USA). Viability of the inocula was ascertained by determining conidia germination rate after 24 hours of incubation at room temperature (~19°C) on PDA, according to the method described by Jaber (2015). Briefly, 10 µL of each suspension was applied and spread with a hockey stick to a thin layer on 1% water agar, set on microscope slides. After 24 hours of incubation, the number of germinated spores (spores observed with tubes of at least half of their length) were counted under compound microscope (Laborlux K, Leitz Wetzlar, Germany) per 300 conidia, within three randomly selected fields of view at 20x optical zoom. Germination rates were found to exceed 90% for both isolates used in this experiment.

The plants were then placed back in their containers, sealed and allowed to grow for an additional three days after inoculation (DAI) before being destructively sampled for RNA extraction (section 5.2.3 below). At this time, ten of the seedlings (with representatives from each block) were then processed for RNA extraction according to the experimental design (see section 5.2.2). The time of harvest, three DAI, was selected on the basis of prior transcriptomic experiments with root colonising *Trichoderma virens* on *Z. mays* (Lawry 2016).

5.2.2 Experimental design

Plants were arranged in randomized complete block design (RCBD) in the growth room, in their respective blocks, with nine plants each for block one and two and ten plants for block three. Each treatment was represented in each block. The experimental layout for the ten plants processed for RNA extraction is as shown in Table 5.1. Each root-RNA sample represented one complementary RNA (cRNA) microarray. The entire experiment therefore consisted of ten microarrays with three replicates of BG11 and J18 inoculated roots, and four replicates of the no-inoculum control (Ctrl) roots.

Table 5.1. Experimental design layout for inoculated *Zea mays* (maize) plants used in the maize cRNA microarray experiment.

Sample Number	Treatment	Replicate	Array Label title
1	BG11	2	1941-001 (Maize) CEL
2	J18	1	1941-002 (Maize) CEL
3	Control	4*	1941-003 (Maize) CEL
4	BG11	1	1941-004 (Maize) CEL
5	Control	2	1941-005 (Maize) CEL
6	Control	3	1941-006 (Maize) CEL
7	BG11	3	1941-007 (Maize) CEL
8	J18	2	1941-008 (Maize) CEL
9	J18	3	1941-009 (Maize) CEL
10	Control	1	1941-010 (Maize) CEL

Note: treatments were randomised and arranged by replicate.

*The replicate number corresponds to the block position in growth room, except for control sample 4 which was in block 3.

5.2.3 RNA isolation from roots and quality assessment

Total RNA was extracted using the RNeasy Plant Mini Kit (Qiagen) as per the manufacturer's instructions. Four cm root samples were taken from the middle of the root, thus tips or woody sections were excluded, from the inoculated and control maize roots. Root samples were snap-frozen, ground to fine powder and maintained in liquid nitrogen to prevent thawing just prior to extraction. RNA quality was assessed by gel electrophoresis (2% agarose in TAE) and by electrophoretic analysis via the 2100 Bioanalyzer (Agilent Technologies) to obtain an RNA integrity number (RIN). DNA contamination and total RNA concentration were measured with the Qubit™ 3.0 Fluorometer high sensitivity double-stranded DNA and RNA assays, as per manufacturer's instructions. The RNA concentration and quality information can be viewed in Appendix D. The RNA concentration parameters required for microarray processing were as follows: total quantity of RNA required was ≥ 500 ng at a concentration of 100 ng/ μ l; quantified by Qubit. For quality, an OD260/280 ratio of ≥ 1.7 was expected, as was an RNA Integrity Number (RIN) ≥ 8 to assess RNA degradation; which was measured and provided by an RNA 6000 Nano Chip using the Agilent 2100 Bioanalyzer instrument.

5.2.4 Microarray processing and hybridisation

The microarray processing was conducted by New Zealand Genomics Limited (NZGL). The Affymetrix Maize Genome Array (Affymetrix) contained 17,555 probe sets to interrogate 14,850 maize transcripts, representing 13,339 genes. Total RNA was labelled using the GeneChip 3' IVT Plus Reagent Kit (Affymetrix), according to the manufacturers protocol. Briefly, 100 ng total RNA per array

was subjected to 1st and 2nd strand synthesis and subsequently underwent an *in vitro* transcription which incorporated a biotinylated ribonucleotide analogue into the complementary RNA (cRNA). The cRNA was then purified and fragmented according to kit instructions. The labelled samples were hybridised to the arrays while rotating at 60 rpm for 16 hours at 45°C. Following hybridisation, the microarrays were washed using the Affymetrix Fluidics Station according to the manufacturer's instructions. The arrays were then scanned in an Affymetrix 3000 7G scanner to produce the intensity data profiles.

5.2.5 Microarray data analysis

Data preparation

Microarray data preparation and statistical analyses were conducted initially by NZGL. The data was pre-processed and normalised using the robust multi-array average (RMA) method (Bolstad et al. 2003; Irizarry et al. 2003) from the R (version 3.2.2) Bioconductor (BiocLite) package 'affy' (Gautier et al. 2004). Briefly, normalisation by RMA involves calculating and correcting background spatial variation for the probe intensities, which distinguishes outliers within the probe set on a single array, while also recognising outliers across multiple arrays (Cheng and Li 2005).

Initially, a boxplot, correlation plot, and MvA plot were used to visualise the differences in intensities, if any, between the combined datasets of all arrays (data not provided). Affymetrix arrays are single colour, therefore the MvA plot used a pseudo-array for comparison, compiled from the median intensity values given for each probe over all the arrays in the experiment. The Affymetrix probe identities were annotated using the Affymetrix annotation file downloaded from the Affymetrix website (PrimeView Annotations, CSV format, Release 35 (33MB, 10/7/14).

Differential expression analysis

Pairwise comparisons for within treatments (contrasts of replicate arrays), and between the three treatments (i.e. BG11:J18, BG11: Ctrl, J18:Ctrl) were conducted to obtain and identify significant differentially expressed genes (DEGs). In order to accomplish this, a log₂ transformation was first applied to the normalised values. The empirical Bayes (eBayes) model was used to compare treatment groups (R package limma) (Smyth 2004). The eBayes model computes a moderated t-statistics test for each individual contrast that is equal to zero. For each probe (row), the moderated F-statistic tests whether all the contrasts are zero (and are therefore not different). The F-statistic is an overall test computed from the set of t-statistics for that probe. This is analogous to the relationship between t-tests and F-statistics in a conventional analysis of variance, except that the residual mean squares and residual degrees of freedom have been moderated between probes. Consequently, only data with a probability (P) value of < 0.05 and a log₂-fold change (FC) < -1 or > 1 were analysed further. All comparisons had the resulting p-values adjusted using the Benjamini-

Hochberg method. However, there were no significant pair-wise comparisons found for any genes, for differential expression, with a false discovery rate set to $P \leq 0.05$ using the adjustment. This was likely due to the small number of replicates available for each treatment (three for the isolates and four for control, respectively). Therefore, the investigation was continued using the nominal p-values.

Multi-dimensional scaling (MDS) plots were generated from Euclidean distance measures on the transformed-normalised probe densities in order to visualise grouping (similarities) between and within treatments. The purpose of the MDS plots produced in Limma, was to visualise and compare the grouping (or lack thereof) of the treatments (BG11, J18, Control), with the grouping of the replicate (or block) to determine if there were array batch effects.

Gene ontology analysis of differentially expressed genes

In order to analyse the biological function of the high confidence DEGs provided by NZGL, the data from the pairwise transcriptomic comparisons' (BG11: J18, BG11: Ctrl, Ctrl: J18) were first divided into multiple gene sets of either upregulated or downregulated DEGs. For this study, tables listing only known (annotated) transcripts and strictly for the BG11 versus J18 comparison, but relative to the no-control group were produced (Table 5.2; Table 5.3). These tables contain all significant DEGs (high and low confidence, to the 5% level) for downregulated and upregulated transcripts of BG11-treated plants relative to J18. To reiterate, the comparisons between the isolate treatment and control plants were not the focus of this study but rather the differences (if any) in gene expression, in the plant as a result of the isolate treatment. However, the high confidence DEG lists for the isolate versus no-inoculum control comparisons can be viewed in Appendix D.

Gene functional classification

The annotated DEG lists that were compiled from P values over 0.05 for the BG11 versus J18 comparison were submitted to the Database for Annotation, Visualization and Integrated Discovery (DAVID) v. 6.8 (Huang et al. 2009). This was performed in order to produce functional gene clusters with corresponding gene enrichment scores. Using DAVID, a gene functional classification analysis was accomplished with *Z. mays* as the species identifier, with the 'Affymetrix_3Prime_IVT_ID' annotation list as the background query. The focus of the analysis was to explore the most significant biological processes involved in the differences between the isolate treatments, by means of creating functional gene clusters from genes that are overrepresented in the differentially expressed gene list. Up- and downregulated DEG sets were assessed independently. A functional gene classification analysis in DAVID sorts related genes into functional groups or clusters using a heuristic fuzzy partition algorithm to identify gene families that are most likely to be important, based on standardised background expression profiles registered in the DAVID database, compiled from global high throughput microarray experiments. Gene clusters are subsequently ranked in importance by

enrichment scores. A higher enrichment score indicates that the genes in a group are biologically enriched and co-regulated. An enrichment score of 1.3 is equivalent to the non-log scale 0.05 (for significance). Although more attention should be given to scores above the 1.3 threshold, any clustering from a gene set may be important to consider irrespective of the enrichment score returned as small changes in gene families may result in differential biological effects.

5.3 Results

5.3.1 Assessment of the microarray samples for differential gene expression

Assessing the arrays by replicate

The ordination analysis using MDS indicated that there was no grouping of the sample replicates (i.e. the actual arrays) (Figure 5.1). Each point correspond to the sample number, e.g. 001 represents the data generated by array 1. Samples 1, 3 and 7 were considered potential outliers but also showed no consistency in their replicate number of the isolate treatment (section 5.3.2).

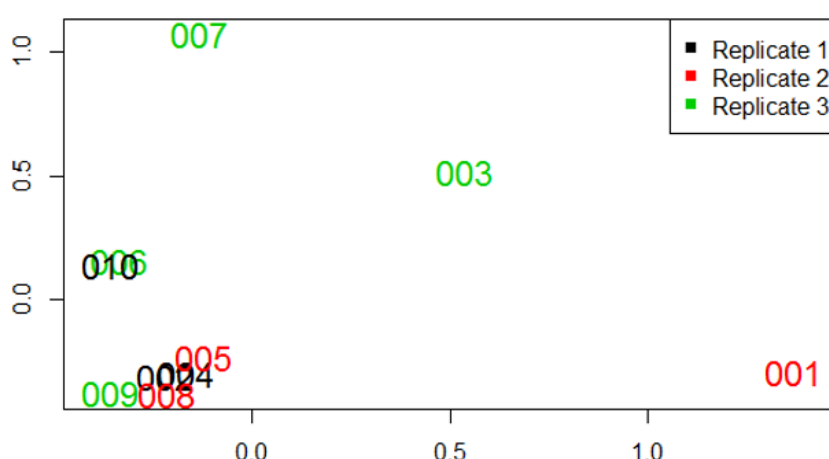


Figure 5.1. Multidimensional scaling (MDS) plot of maize microarrays replicates. MDS ordination plot based on Euclidean distance of the log₂ fold change (FC) values generated from microarray intensities to represent gene expression profiles from roots of *Z. mays* (maize) in response to colonisation/inoculation of two different *B. bassiana* isolates (BG11, J18) versus a no-inoculum control (green). Samples are coloured coded to microarray replicate.

Assessing the arrays by inocula treatment

The MDS analysis by isolate group showed overall weak grouping of the isolate transformed-normalised probe densities (Figure 5.2). There was some improvement in the grouping, particularly for isolate J18 and the control treatment arrays, when sample outlier 001 (BG11) was omitted (data not shown). However, the MDS illustrates that J18 and the control were grouping independently (even considering the control outlier sample 003) but BG11 samples did not due to within-group variation.

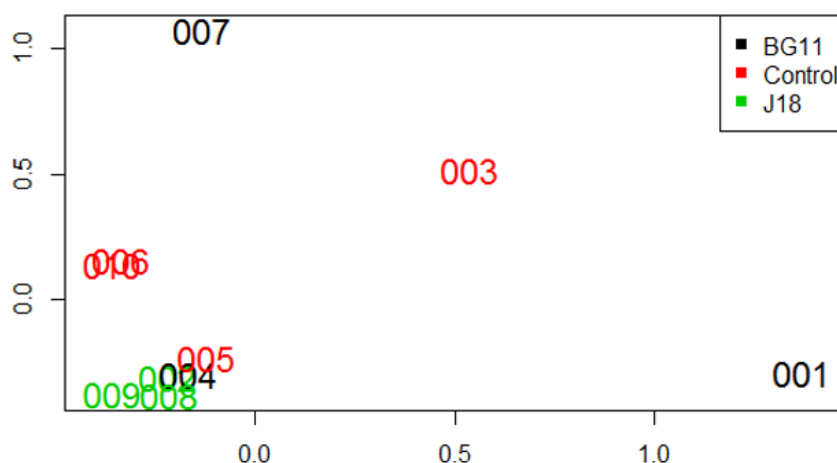


Figure 5.2. Multidimensional scaling (MDS) plot of maize microarrays by treatment. MDS ordination plot based on Euclidean distance of the log₂ fold change (FC) values generated from microarray intensities, to represent gene expression profiles from the roots of *Z. mays* (maize) in response to colonisation/inoculation of two different *B. bassiana* isolates (BG11, J18) versus a no-inoculum control (green). Samples are coloured by inoculum treatment or control.

5.3.2 Differential gene expression and gene ontology

Comparative transcriptome analysis

From the pairwise comparisons of the normalised-transformed data, the list of significant ($P \leq 0.05$; minimum log₂ fold change) DEGs obtained for the BG11 versus J18 treatment comparison in maize consisted of 474 total transcripts. Of these, 212 transcripts (44.7 %) were lower in BG11 compared to J18-treated roots and 262 transcripts (55.3 %) were higher in BG11-treated roots. From the putatively 'downregulated' set produced from the BG11 (vs. J18) treatment, 172 transcripts were uncharacterised/hypothetical proteins and 40 transcripts were known (annotated) proteins. From the putatively 'upregulated' set (BG11 vs J18), 200 transcripts were uncharacterised proteins and 62 transcripts were known (annotated) proteins. Table 5.2 lists known and downregulated gene transcripts and Table 5.3 lists known and upregulated gene transcripts. Descriptions of suggested associated biological functions are included (column 3 of each Table) for the BG11 versus J18 comparison, for genes that are in common and significantly differentially expressed ($P \leq 0.05$) in maize roots, in response to the presence of these isolate inocula treatments.

Table 5.2. Comparison of the response of *Zea mays* (maize) roots to fungal colonisation at 3 days after inoculation (DAI). Comparisons made using microarray probe intensity value isolate-treatment means (reported in real space), to represent differential gene expression ($P \leq 0.05$). Plants were treated with either *Beauveria bassiana* isolate BG11 or J18. The gene list comprises annotated transcripts of maize only (uncharacterised genes omitted). Data is presented for genes downregulated in BG11-treated plants relative to J18 and ordered by indicated gene function. Group means for the control plants (non-inoculated group) are highlighted in grey. In the BG11 and J18 treatment mean columns (4 and 5), either orange or green is used to indicate direction of gene expression relative to the control group: orange infers downregulation and green infers upregulation.

Probe Set ID ¹	Gene Title ²	Indicated Function ³	Control	BG11	J18	Log2 Fold Change (BG11 vs. J18)	P value
Zm.298.1.S1_a_at	Dxr protein	Plant defence - terpenoid biosynthesis	754	510	658	-1.11	0.0424
ZmAfx.12.1.S1_at	Kaurene synthase 2	Plant defence - terpene biosynthesis	619	268	593	-3.44	0.00078
Zm.8714.1.A1_at	Acc oxidase (ethylene-forming enzyme)	Plant defence - signalling	305	212	369	-2.39	0.00388
Zm.10830.1.S1_at	BRASSINOSTEROID INSENSITIVE 1-associated receptor kinase 1	Plant defence - signalling	56	37	57	-1.79	0.01181
Zm.948.1.A1_at	Receptor-like protein kinase	Plant defence - signalling	176	148	203	-1.36	0.01443
Zm.7462.1.A1_at	NAC domain-containing protein 21/22	Plant defence - signalling	96	72	108	-1.75	0.0186
Zm.18148.1.A1_at	Protein kinase	Plant defence - signalling	43	43	54	-0.96	0.04193
Zm.5036.1.A1_at	Serine/threonine-protein kinase NAK	Plant defence - signalling	289	234	291	-0.95	0.04358
Zm.6659.1.A1_at	Pathogenesis related protein-5	Plant defence - SAR salicylic pathway	736	515	1461	-4.51	0.00206
Zm.15280.1.A1_s_at	Pathogenesis related protein4	Plant defence - SAR salicylic pathway	1588	594	1160	-2.9	0.01716
Zm.411.1.A1_at	Nucleoredoxin1	Plant defence - regulation response to oxidative stress	704	598	827	-1.4	0.01361
Zm.18344.1.A1_at	Major facilitator superfamily defense1	Plant defence - metabolite transport	111	77	233	-4.79	0.00138
Zm.499.1.S1_at	Hypersensitive induced reaction3	Plant defence - cell death/lesion response	728	672	937	-1.44	0.01866
Zm.11896.1.A1_at	SNF1-related protein kinase regulatory subunit beta-1	Plant defence - ATP-binding	17	15	20	-1.2	0.02051
Zm.1663.1.A1_at	VQ motif family protein	Plant defence - regulation response to oxidative stress	180	144	214	-1.71	0.00703
Zm.16973.1.S1_at	VQ motif family protein	Plant defence - regulation response to oxidative stress	118	92	124	-1.3	0.01636
Zm.5565.1.S1_at	Cysteine protease1	Plant defence - protein degradation	4795	5019	6377	-1.04	0.03032
Zm.2376.2.S1_at	Physical impedance induced protein	Plant growth - regulator	667	752	1465	-2.89	0.00137
Zm.2376.2.S1_x_at	Physical impedance induced protein	Plant growth - regulator	1239	1380	2232	-2.08	0.00391
Zm.11758.1.A1_at	Gibberellin 20 oxidase 2	Electron transport catalyst	1491	773	1436	-2.68	0.01491
Zm.17313.1.A1_at	Glycerol-3-phosphate acyltransferase 8	Plant growth - lipid biosynthesis	600	535	718	-1.27	0.01914
ZmAfx.896.1.S1_at	Transmembrane protein20	Plant growth - integral membrane	73	58	81	-1.43	0.02981

Zm.9689.1.A1_at	Plant integral membrane protein TIGR01569 containing protein	Plant growth - cell wall organisation	53	46	66	-1.57	0.01794
Zm.125.1.S1_at	Nitrate reductase (NAD(P)H)	Mitochondrial iron-sulphur protein	241	149	272	-2.61	0.03389
Zm.18542.1.A1_at	TAK14	Glycolysis - ATP-binding and signalling	171	128	199	-1.93	0.00974
Zm.7422.1.A1_at	Anthocyanidin 3-O-glucosyltransferase	Plant defence - flavanoid biosynthesis	58	84	114	-1.34	0.0191
Zm.17735.1.A1_at	Lipid binding protein	Fatty acid uptake/transport	272	262	334	-1.05	0.02991
Zm.9366.1.A1_at	Aldo-keto reductase/ oxidoreductase	Electron transport catalyst	41	39	51	-1.12	0.03488
Zm.16805.3.S1_x_at	Basic endochitinase C	Plant defence - chitinase activity	851	423	727	-2.35	0.04727
Zm.627.1.A1_at	Glutathione transferase 24	Cell detox/kinase signalling inhibition	193	102	194	-2.79	0.00159
Zm.13591.1.S1_at	Glutathione transferase 42	Cell detox/kinase signalling inhibition	274	232	381	-2.16	0.00667
Zm.10134.1.A1_at	Glutathione S-transferase	Cell detox/kinase signalling inhibition	164	149	296	-2.97	0.01978
Zm.813.1.S1_at	Glutathione S-transferase GST 18	Cell detox/kinase signalling inhibition	1334	1172	1460	-0.95	0.03883
Zm.9873.1.A1_at	Lichenase-2	Carbohydrate metabolism	723	466	1024	-3.41	0.01063
Zm.1684.1.S1_at	Profilin homolog1	Actin-binding	63	83	106	-1.07	0.0483
Zm.617.1.A1_at	Tonoplast intrinsic protein4	Transporter activity	28	20	28	-1.43	0.01291
Zm.16929.1.S1_at	Ribosomal protein S15	Translation activity	55	78	211	-4.29	0.00718
Zm.6977.5.S1_a_at	Sucrose synthase	Sucrose metabolism	562	512	752	-1.66	0.03563
Zm.3504.1.A1_at	Ribonuclease III domain protein1	RNA processing	121	98	125	-1.02	0.04217
Zm.3307.1.A1_a_at	ADP-ribosylation factor	Regulatory element	222	200	246	-0.9	0.04848

¹ Affymetrix microarrays

² Affymetrix PrimeView Annotations, CSV format, Release 35 (33MB, 10/7/14).

³ UniProtKB.

Table 5.3. Comparison of the response of *Zea mays* (maize) roots to fungal colonisation at 3 days after inoculation (DAI). Comparisons made using microarray probe intensity value isolate treatment means (reported in real space), to represent significantly different gene expression (where $P \leq 0.05$). Plants were treated with either *Beauveria bassiana* isolate BG11 or J18. The gene list comprises annotated transcripts of maize only (uncharacterised genes omitted). Data is presented for genes upregulated in BG11-treated plants relative to J18 and ordered by indicated gene function. Group means for the control plants (non-inoculated group) are highlighted in grey. In the BG11 and J18 treatment mean columns (4 and 5), either orange or green is used to indicate direction of gene expression relative to the control group: orange infers downregulation and green infers upregulation.

Probe Set ID ¹	Gene Title ²	Indicated Function ³	Control	BG11	J18	Log2 Fold Change (BG11 vs. J18)	P value
Zm.15061.1.S1_at	calmodulin	Plant defence - calcium binding kinase stimulator	85	118	76	1.87	0.02576
Zm.12139.1.A1_at	EF-hand Ca ²⁺ -binding protein CCD1	Plant defence - calcium binding kinase stimulator	436	806	441	2.62	0.04997
Zm.8261.1.A1_at	BCL-2 binding anthanogene-1	Plant defence - cell death regulation	58	127	49	4.12	0.00098
Zm.10528.1.A1_at	transparent testa 12 protein	Plant defence - cell detox/drug transporter	823	945	755	0.97	0.03754
Zm.13865.1.S1_at	R2R3 Myb transcription factor MYB-IF35	Plant defence - DNA binding	30	45	33	1.33	0.02107
Zm.15818.1.S1_at	ferredoxin5	Plant defence - electron transport	19	22	15	1.59	0.02267
Zm.7960.1.A1_at	oxidoreductase	Plant defence - electron transport catalyst	67	78	62	0.97	0.04423
Zm.2569.1.A1_at	agmatine coumaroyltransferase	Plant defence - hydroxycinnamic acid amides biosynthesis	538	558	371	1.76	0.04735
Zm.19134.1.A1_at	peptide transporter PTR2	Plant defence - protein transporter	192	240	185	1.13	0.02677
Zm.4802.1.A1_at	F-box family member	Plant defence - signal transduction	860	1054	855	0.91	0.04829
Zm.11745.1.A1_at	NPK1-related protein kinase-like protein	Plant defence - signalling	22	43	21	3.15	0.00815
Zm.222.1.S1_at	cytokinin response regulator2	Plant defence - signalling, ethylene	356	359	292	0.9	0.0451
Zm.9621.1.A1_at	ethylene-responsive transcription factor 3	Plant defence - signalling, ethylene transcription regulator	423	529	410	1.1	0.03109
Zm.12317.1.S1_at	ethylene-responsive transcription factor 4	Plant defence - signalling, ethylene transcription regulator	510	771	523	1.68	0.01446
Zm.10676.1.S1_at	12-oxo-phytodienoic acid reductase1	Plant defence - signalling, jasmonic acid and ISR	297	356	277	1.08	0.04136
Zm.14971.1.S1_at	AMP binding protein	Plant defence - signalling/transcription regulation	87	168	85	2.96	0.00373
Zm.7611.2.A1_at	IAA24 - auxin-responsive Aux/IAA family member	Plant defence - signalling/transcription regulation	45	108	41	4.21	0.0062
Zm.7611.1.A1_a_at	IAA24 - auxin-responsive Aux/IAA family member	Plant defence - signalling/transcription regulation	78	177	64	4.4	0.02759

Zm.10423.1.S1_at	fatty acid desaturase8	Plant defence - stress response to cold. Lipid metabolism	130	197	130	1.8	0.0065
Zm.151.1.A1_at	fatty acid desaturase7	Plant defence - stress response to cold. Lipid metabolism	427	623	346	2.55	0.0031
Zm.1524.1.A1_at	dehydration-responsive element-binding protein 1D	Plant defence - stress response/signalling/transcription regulation	16	58	15	5.71	0.00068
Zm.436.1.S1_at	liguleless3	Plant defence - transcription regulator	428	408	318	1.08	0.02956
Zm.94.1.S1_at	DNA binding with one finger2	Plant defence - transcription regulator	102	140	105	1.23	0.02162
Zm.13245.1.S1_at	DRE-binding protein3	Plant defence - transcription regulator	14	20	15	1.35	0.01495
Zm.10147.1.A1_at	NAC1 transcription factor	Plant defence - transcription regulator	126	183	127	1.58	0.04711
Zm.12114.1.S1_at	DNA-binding protein RAV1	Plant defence - transcription regulator	224	334	224	1.73	0.0157
Zm.17519.1.A1_at	FIP1	Plant defence - transcription regulator	247	426	236	2.55	0.02548
Zm.10181.1.A1_at	ERF-like protein	Plant defence - transcription regulator	19	40	19	3.23	0.00223
Zm.51.1.A1_at	RR6 - Corn type-A response regulator	Plant defence - transcription regulator	105	159	74	3.32	0.02241
Zm.11891.1.A1_at	helix-loop-helix DNA-binding domain containing protein	Plant defence - transcription regulator	44	112	48	3.67	0.00232
Zm.9463.1.A1_at	DRE-binding protein 4	Plant defence - transcription regulator	12	35	10	5.35	0.01592
Zm.16376.1.S1_at	AP2 domain containing protein	Plant defence - transcription regulator	7	27	7	5.5	0.00037
Zm.10120.1.A1_at	DNA binding like	Plant defence - transcription regulator	7	25	6	5.91	0.00016
Zm.11811.1.S1_at	glycosyltransferase 5	Plant defence - transferase activity	376	479	373	1.09	0.04677
Zm.5504.1.A1_at	inositol polyphosphate 2-kinase	Plant defence and growth, intracellular signalling/ATP binding	344	405	328	0.91	0.04739
Zm.15283.1.A1_at	calcium-dependent protein kinase, isoform AK1	Plant defence and growth, intracellular signalling/ATP binding	484	619	480	1.1	0.03025
Zm.13514.2.S1_a_at	phytoene synthase2	Plant growth - carotenoid biosynthesis	43	55	42	1.18	0.0211
ZmAfx.720.1.A1_at	roothair defective 3	Plant growth - cell development, nucleotide-binding	148	237	153	1.89	0.01469
ZmAfx.1005.1.S1_at	tassel seed1	Plant growth - cell development, oxidoreductase	73	112	70	2.03	0.0237
Zm.1527.2.A1_a_at	xyloglucan endotransglucosylase/hydrolase protein 23	Plant growth - cell wall biogenesis and degradation	105	291	90	5.09	0.00402
Zm.402.1.S1_a_at	endo-1,3-1,4-beta-D-glucanase	Plant growth - cell wall biogenesis and degradation, auxin response	1804	2379	1606	1.7	0.04723
Zm.10011.1.A1_at	glycine-rich protein GRP5	Plant growth - cell wall synthesis	23	28	21	1.25	0.02306
Zm.14951.1.S1_a_at	cell wall protein (put.); putative	Plant growth - cell wall synthesis	430	496	371	1.26	0.03306
Zm.605.1.S1_a_at	plasma membrane intrinsic protein2	Plant growth - integral membrane	780	900	736	0.87	0.04845

Zm.8647.1.A1_at	cytochrome P450 10	Plant growth - integral membrane	104	138	111	0.91	0.04567
Zm.604.1.A1_at	plasma membrane intrinsic protein1	Plant growth - integral membrane	307	457	319	1.55	0.01019
Zm.12410.1.A1_at	CP5	Plant growth - lipid binding, integral membrane	169	260	150	2.37	0.03138
Zm.7091.1.A1_x_at	light harvesting chlorophyll a/b binding protein6	Plant growth - photosynthesis	174	175	133	1.18	0.0395
Zm.14566.2.A1_at	photosystem II 11 kD protein	Plant growth - photosynthesis	33	33	22	1.73	0.01058
Zm.7091.1.A1_at	Chlorophyll a/b-binding apoprotein CP24 precursor	Plant growth - photosynthesis	180	178	112	2.01	0.03468
Zm.1076.1.S1_at	photosystem II subunit29	Plant growth - photosynthesis	147	127	65	2.9	0.04603
Zm.9396.1.A1_x_at	early light-inducible protein ELIP	Plant growth - photosynthesis, light-stress response	30	50	23	3.39	0.0412
Zm.669.1.S1_at	alpha-expansin 5	Plant growth - root hair emergence	71	84	60	1.44	0.02792
Zm.312.1.A1_at	ADP glucose pyrophosphorylase small subunit leaf1	Plant growth - starch biosynthesis	97	102	78	1.16	0.03792
Zm.17964.1.A1_at	Endoglucanase 1	Carbohydrate metabolism	94	121	97	0.95	0.03879
Zm.9194.1.A1_at	Ribose-5-phosphate isomerase	Cellular function - carbohydrate metabolism	160	191	127	1.77	0.01459
Zm.6398.2.S1_at	transposon protein Mutator sub-class	Gene tagging system	112	120	96	1	0.03396
Zm.6398.1.A1_at	transposon protein Mutator sub-class	Gene tagging system	257	272	205	1.22	0.03838
Zm.11922.1.A1_at	transposon protein	Gene tagging system	1393	1480	975	1.81	0.04521
Zm.8365.1.A1_at	hexokinase-1	Glycolysis - ATP-binding and signalling	321	419	299	1.45	0.01774
Zm.11586.1.A1_at	PVR3-like protein	Lipid transporter	49	62	49	1.05	0.03028
Zm.10036.2.S1_a_at	Anthocyanidin 5, 3-O-glucosyltransferase	Pigment biosynthesis	903	1218	891	1.35	0.03372

5.3.3 Gene functional classification

Functional classification using DAVID from the annotated DEGs produced four gene cluster tables out of the BG11 versus J18 comparison, two tables for the downregulated DEG set (Table 5.4) and two for the upregulated set (Table 5.5). From the downregulated set, 36 genes were identified with eight represented in the cluster tables (5.4) and 28 not included in the output. For the upregulated set, there were 49 genes submitted with 17 featuring in the two cluster groups (Table 5.5) and 32 not included in the output.

Table 5.4. Differential gene expression in gene families. Table shows functional gene clusters with corresponding enrichment scores produced from Gene Set Enrichment Analysis (GSEA) in the database for annotation, visualisation and identification (DAVID) based on the putatively downregulated (coded in orange) differentially expressed gene list compiled from annotated transcripts produced from *Zea mays* (maize) in response to two different *Beauveria bassiana* isolate inocula (BG11 versus J18).

Gene Group 1	Enrichment Score: 2.8
AFFYMETRIX_3PRIME_IVT_ID	Gene Name
Zm.627.1.A1_at	glutathione transferase 24 (gst24)
Zm.813.1.S1_at	glutathione S-transferase GST 18 (LOC541833)
Zm.10134.1.A1_at	glutathione S-transferase (LOC100281369)
Zm.13591.1.S1_at	glutathione transferase 42 (LOC541850)
Gene Group 2	Enrichment Score: 0.1
AFFYMETRIX_3PRIME_IVT_ID	Gene Name
ZmAfx.896.1.S1_at	transmembrane protein 20 (tm20)
Zm.617.1.A1_at	tonoplast intrinsic protein 4 (tip4a)
Zm.9689.1.A1_at	plant integral membrane protein TIGR01569 containing protein (LOC100285307)
Zm.18344.1.A1_at	major facilitator superfamily defense 1(mfsd1)

Based on the enrichment scores, the comparison of differentially expressed genes (DEGs) between *B. bassiana* isolate BG11 versus J18, in the gene set enrichment analysis (GSEA), indicated possible and significant downregulation of a set of glutathione S-transferase (GST) encoding genes in BG11 compared to J18 (refer to Table 5.2 for the control expression levels of GST genes). Although not as significantly enriched as the GST family, the GSEA also indicated possible downregulation of a set of

intrinsic transmembrane protein encoding genes in BG11 compared to J18, and also compared to expression levels in controls (Table 5.2).

Table 5.5. Differential gene expression in gene families. Table shows functional gene clusters with corresponding enrichment scores produced from the gene set enrichment analysis (GSEA) in the database for annotation, visualisation and identification (DAVID) based on the upregulated (coded in green) differentially expressed gene list compiled from annotated transcripts produced from *Zea mays* (maize) in response to two different *Beauveria bassiana* isolate inocula (BG11 versus J18).

Gene Group 1	Enrichment Score: 4.7
AFFYMETRIX_3PRIME_IVT_ID	Gene Name
Zm.16376.1.S1_at	AP2 domain containing protein (LOC100283357)
Zm.13245.1.S1_at	DRE-binding protein 3 (dbf3)
Zm.1524.1.A1_at	dehydration-responsive element-binding protein 1D (LOC100281239)
Zm.9463.1.A1_at	DRE-binding protein 4 (DBP4)
Zm.10147.1.A1_at	NAC1 transcription factor (NAC1)
Zm.12317.1.S1_at	ethylene-responsive transcription factor 4 (EREB92)
Zm.9621.1.A1_at	ethylene-responsive transcription factor 3 (EREB98)
Zm.10181.1.A1_at	ERF-like protein (LOC100286307)
Zm.7611.1.A1_a_at	IAA24 - auxin-responsive Aux/IAA family member (LOC100280600)
Zm.12114.1.S1_at	DNA-binding protein RAV1 (LOC100284738)
Gene Group 2	Enrichment Score: 0.2
AFFYMETRIX_3PRIME_IVT_ID	Gene Name
Zm.12410.1.A1_at	CP5 (LOC100281983)
ZmAffx.720.1.A1_at	roothair defective 3 (rth3)
Zm.19134.1.A1_at	peptide transporter PTR2 (LOC100281619)
Zm.605.1.S1_a_at	plasma membrane intrinsic protein 2 (pip2b)
Zm.13514.2.S1_a_at	phytoene synthase 2 (psy2)
Zm.7960.1.A1_at	transparent testa 12 protein (LOC100281401)
Zm.151.1.A1_at	omega-3 fatty acid desaturase (LOC101027135)

5.4 Discussion

The initial analysis of the microarray data indicated substantial variation within the *B. bassiana* isolate BG11 replicate arrays, which resulted in a lack of grouping for this treatment. In contrast, the control and J18 treatment arrays were reasonably consistent in gene expression and grouped accordingly. The within group variation for BG11 may be the result of a number of explanatory factors. However, as already discussed in previous chapters, plant colonisation by endophytic *B. bassiana* is inconsistent and therefore such variability in the plant response is not unexpected. Even with a high inoculum load, penetration beyond epidermal tissues has rarely been observed. Wagner and Lewis (2000) originally demonstrated the mode of penetration of *B. bassiana* conidia into the leaves of maize using light and electron microscopy techniques. According to their results, approximately 3% of the conidia germinated, and then with less than 1% of that succeeding to penetrate through stomata across the leaf surface. Similar observations were demonstrated on the leaves of opium poppy, *Papaver somniferum* (Quesada-Moraga et al. 2006). Again, endophytic colonisation was rarely observed on leaf material of poppy following inoculation and the endophytic growth that was detected appeared to be opportunistic irrespective of the inoculum concentration used.

Despite the variability in gene expression observed in the BG11 arrays, differential gene expression between the two isolate treatments, relative to the controls expression levels, were observed.

5.4.1 Biological functions of enriched differentially expressed genes

Determining possible phenotypic differences in microarray data

The purpose of DNA microarrays was to measure and compare the amount of gene expression in different samples. However, this method of comparison is not always sensitive enough to detect subtle differences between the expression of individual genes. Furthermore phenotypic differences, between genetically similar organisms or cells, often can involve entire clusters of genes. Multiple genes may be linked to a single biological pathway and there may be an accumulated effect resulting from small changes in expression within gene sets, leading to differences in phenotypic expression. Gene Set Enrichment Analysis (GSEA) focuses on the changes of expression in gene clusters. Consequently this method resolves the problem of the detection of subtle but important changes in the expression of single genes, to enable biological interpretation of microarray data, which may otherwise seem insignificant (Mootha et al. 2003). In the following section, the gene clusters returned by GSEA that are most likely to result in phenotypic differences between maize plants treated with either of the *B. bassiana* isolates are discussed.

Glutathione S-transferases (GSTs)

The enrichment analysis for the comparison of differentially expressed genes (DEGs), between *B. bassiana* isolate BG11 versus J18, indicated putative downregulation of a small set of glutathione S-transferase encoding genes in BG11 compared to J18, and also relative to the control treatment plants.

Glutathione S-transferases (GSTs) represent an ancient and ubiquitous gene family that encode 25 to 29 kDa proteins (Alfenito et al. 1998). Plant GSTs are produced at every stage of plant development, from early embryogenesis through to senescence (Sharma et al. 2012). First recognised in animals in the 1960s for their role in the metabolism and detoxification of drugs (Wilce and Parker 1994), the presence of GSTs in plants was identified when the protection of maize from damage by the herbicide chloro-S-triazine atrazine was demonstrated (Frear and Swanson 1970). The GST protein family is thought to function to protect against oxidative damage in cells by quenching reactive molecules via conjugation with glutathione (GSH) (Licciardello et al. 2014). Conjugated molecules are rendered water-soluble and inactive and are subsequently transported into vacuoles via ATP-binding cassette transporters (McGonigle et al. 2000). The importance of GSTs in plant cell protection from xenobiotics was further demonstrated when the expression of the maize GST isoform IV in tobacco plants provided protection against the herbicide metolachlor (Jepson et al. 1997). GSTs are thus considered to be significant antioxidant enzymes, important for oxidative defence against ROS. Rapid ROS accumulation is a key indicator of the plant defence response to pathogen attack as ROS production corresponds with a nitrosative burst (Ferreira et al. 2013) and is eventually accompanied also by host cell death. ROS can also function as signalling molecules to induce the mitogen-activated protein kinase (MAPK) cascade, thus triggering a defensive immune response (Frederickson Matika and Loake 2014) (see Chapter 1). Therefore, higher concentrations of antioxidant GSTs can presumably inhibit kinase signalling by targeting more ROS molecules, while also reducing potential damage to host cells. Whether ROS molecules act as signal molecules, however, or as free radicals causing cellular damage, is dependent upon their concentration. For example, at lower concentrations, ROS molecules can act as second messengers in a variety of important hormone signalling cascades aside from MAPK, with subsequent plant immune responses such as stomatal closure, programmed cell death, gravitropism, and acquisition of tolerances to various biotic and abiotic stresses (Sharma et al. 2012).

The lower degree of expression of certain GSTs in isolate BG11 treated plants compared to J18 may therefore indicate a number of potential outcomes: (1) the modulation of certain phytohormones resulting in a more pronounced plant immune response, since an increase in GST expression (as in J18) corresponds to an increase in antioxidant activity, leading to the cessation of active ROS as signalling molecules and thus a reduction in plant defence responses. (2) Alternatively, an increase in

antioxidant production in J18, may result in an optimum (low) concentration of ROS and therefore a greater diversity of signalling cascades being elicited for plant immunity (Sharma et al. 2012). As a result BG11 treated plants may be more susceptible to continued colonisation compared to J18 treated plants or (3) lower GST levels produced *in planta* may simply imply a difference in the rate of colonisation of plant roots between the two isolates and thus the response to oxidative burst may be being observed at different stages at 3 DAI. In any case, the higher concentrations of GSTs are indicative of oxidative stress and are transcriptional response to higher levels of ROS. This implies potential harm inflicted by the fungal colonisation, but perhaps also improved cellular resistance to pathogenicity. Indeed, a different set of GSTs were also possibly more highly expressed in the J18 treatment relative to the control treated plants (refer to the DEG list in Table 5.2). Experiments with the root endophytic fungus *Piriformospora indica*, in barley, demonstrated enhanced foliar antioxidant capacity when the glutathione pool (GSH and oxidized glutathione) was analysed (Waller 2005). Also in barley, enhanced GSH concentrations have been associated with resistance to powdery mildew disease (Vanacker et al. 2000) suggesting a benefit to increased concentrations of oxidative GSTs. Furthermore, both the accumulation of ROS and the production of antioxidants have also been shown to co-occur in legume plants in response to beneficial nitrogen-fixing rhizobia (Anderson et al. 2010; Cardenas et al. 2008). It is plausible therefore, that the levels of antioxidant production observed in this present study are also indicative of endophytic colonisation by *B. bassiana*.

Major intrinsic protein (MIP) family and the major facilitator super family (MFS)

The gene set enrichment analysis for the *B. bassiana* isolate DEGs in maize indicated enrichment and the putative downregulation of a set of integral membrane protein encoding genes, in BG11 compared to J18 treated plants.

Generally, the plasma membrane regulates the movement of water and solutes, and maintains an optimal solute composition in cells. Various ions, nutrients and water are transported through certain integral membrane proteins (Chrispeels et al. 1999), aquaporins, which are classified into several families and found in all living species (Chaumont et al. 2000). A well characterised family from among these transport protein families is the major intrinsic protein (MIP) family (Gorin et al. 1984). In plants, four MIP subfamilies are distinguished based on their sequence similarity and are usually associated with their subcellular location: (1) the plasma membrane intrinsic proteins (PIPs), (2) the tonoplast intrinsic proteins (TIPs), (3) the nodulin26-like intrinsic proteins (NIPs) and (4) the small basic intrinsic proteins (SIPs). PIPs are located in the plasma membrane and TIPs in the tonoplast, whereas the subcellular location of NIPs and SIPs remains uncertain (Gomes et al. 2009). Irrespective of their subcellular location, most plant MIPs investigated have been demonstrated to enhance membrane permeability for water transportation (Maurel 2007). However, some MIPs are

able to transport some small neutral molecules, such as glycerol and urea (Ishikawa et al. 2005). Gases such as CO₂ ammonia, hydrogen peroxide (H₂O₂) may also be carried by MIPs. Transport of the metalloids silicon, boron, arsenite, and antimony has also been described (Bienert et al. 2008; Gomes et al. 2009).

Plasma membrane intrinsic proteins are primarily found in organs and tissues that require large fluxes of water such as vascular tissues. For example, the *Arabidopsis* PIP AtPIP2;2 is highly expressed in roots, cortex, endodermis, and stele (Javot et al. 2003). TIPs or aquaporins are the most abundant proteins in the tonoplast, and consequently, the water permeability of the tonoplast is actually higher than that of the plasma membrane (Maeshima 2001). A particular aquaporin of maize, ZmTIP1 (Chaumont et al. 1998), has been found to be highly expressed in cells involved in water uptake, particularly in tissues undergoing cell elongation and enlargement such as in the root epidermis and endodermis (Barrieu et al. 1998). Enhanced expression of these proteins suggests rapid growth of these tissues and/or the need for efficient intracellular osmotic equilibration, to permit rapid water flow through the vacuoles in those tissues experiencing large transcellular water flow volumes (Barrieu et al. 1998; Chaumont et al. 2000). Notably, recent studies have demonstrated that PIPs and TIPs also have the ability to transport hydrogen peroxide (H₂O₂), a ROS messenger involved in plant responses to wounding or pathogen attack (Dynowski et al. 2008). More particularly, hydrogen peroxide can either directly trigger chemical reactions and influence receptive targets, such as metabolites or proteins, or act within signalling pathways including those involving MAPK kinases (Bienert and Chaumont 2014). Thus certain aquaporins may play a crucial role in cell-cell communication and plant defensive processes (Dynowski et al. 2008).

Along with certain aquaporins (tm20, TIP4- α , MIP), another crucial transmembrane protein, Zm-Mfs1, was enriched in the present study in plants treated with both *B. bassiana* isolates but significantly higher in plants treated with J18. Zm-Mfs1 is a member of the major facilitator super family (MFS), which are a large group of transmembrane proteins involved in the transportation of antibiotics, sugars, amino acids, metal ions and various other molecules (Simmons et al. 2003). Zm-Mfs1 is thought to be a prototype of a class of plant defence-related proteins that may be involved in (1) the exportation of antimicrobial compounds produced by plant pathogens; (2) the exportation of plant-produced antimicrobial compounds; or (3) potassium import or export, which is known to contribute to plant defensive reactions. (Simmons et al. 2003).

The increase in expression of all transmembrane proteins implies a more pronounced pathogen effector or metabolite defence response in J18 treated maize plants, compared to BG11 treated plants (and relative to control treated plants). The higher level of expression of the Zm-Mfs1 gene in J18 compared to both BG11 and the control (Table 5.2), suggests that antimicrobial metabolites may

be challenging the plant host. The increase of these proteins generally indicates that these plants may be responding to a perceived pathogenic attack with the colonisation of J18, especially in contrast with BG11. Furthermore, these plants may be responding to certain toxic metabolites or ROS, by increasing the growth of those tissues responsible for antibiotic and water efflux (Barrieu et al. 1998; Bienert and Chaumont 2014).

Plant defence and stress tolerance

The enrichment analysis for the comparison of differentially expressed genes (DEGs) between *B. bassiana* isolate BG11 versus J18, indicated putative upregulation of multiple transcription factors involved in the response to stress, in the BG11 compared to J18 treated plants.

Ethylene responsive factor (AP2/ERF) family

Transcription factors of the APETALA2/Ethylene Responsive Factor (AP2/ERF) family are widespread in higher plants. They play a pivotal role in functions related to signal transduction that activate or suppress defence gene expression, as well as in the regulation of interactions between different signalling pathways (Xu et al. 2011). Transcription factors are thus regulatory proteins that govern primary and secondary metabolism, growth and development, and are involved in processes enabling various responses to environmental stimuli. Originally, ERF proteins were isolated as transcription factors that bind to promoter regions of stress-responsive genes. These transcription factors can be induced by a range of biotic and abiotic stresses, including: pathogen attack, salt and osmotic stress, wounding, dehydration, hypoxia, temperature stress, in addition to the stress-related hormones ethylene, jasmonic acid and abscisic acid (Licausi et al. 2013).

In addition to ERFs, dehydration responsive element binding proteins (DREBs) are another major subfamily of the AP2/ERF family which regulate abiotic- and biotic-stress responses. DREB transcription factors activate various dehydration/cold-regulated (RD/COR) genes by interacting with dehydration-responsive element (DRE)/C-repeat element (CRT) cis-acting elements, found at the promoters of RD/COR genes, (Stockinger et al. 1997; Xu et al. 2011). ERF transcription factors directly regulate pathogenesis-related (PR) gene expression by the mechanism of DNA-binding with the GCC-box (GCCGCC), a sequence found upstream within the promoter regions of genes such as *prb-1b* (PR1), β -1, 3-glucanase (PR2), chitinase (PR3), and osmotin (PR5) (Ohme-Takagi and Shinshi 1995; Xu et al. 2011; Zarei et al. 2011).

Ethylene responsive transcription factors have been shown to exhibit multiple, complex and dynamic expression patterns (Xu et al. 2011). To better understand the mediation of plant defence responses by ERF, it is necessary to elucidate the signalling pathways that they regulate. However, several important signalling pathways may be induced by the hormone signal molecules ethylene (ET), JA, salicylic acid (SA), and abscisic acid (ABA) (McGrath et al. 2005) and there is thought to be a complex

cross-talk among these signal molecules. The apparent coordination of these hormone pathways is thought to finely modulate the defence response during a specific pathogen attack (Xu et al. 2011). For example, ET and JA pathways can potentially both be induced by ERF transcription factors (Gutterson and Reuber 2004). In transgenic plants, overexpression of certain ERFs involved in the ET and JA pathways, resulted in an increased resistance to multiple fungal and bacterial pathogens (McGrath et al. 2005; Xu et al. 2011). There is a fitness cost associated with the activation of hormone-regulated defence pathways (Vos et al. 2015). For example, exogenous application of SA and JA has been shown to inhibit plant growth and seed production (Ellis and Turner 2001; Heidel et al. 2004). However, it has recently been established that other hormones like brassinosteroids, gibberellins, and auxin act as crucial regulators of the defence-growth trade-off induced by perceived pathogen attack (Vos et al. 2015).

In the present study, a suite of genes associated with plant growth and development were putatively upregulated in BG11 compared to both J18 and to the control treatment plants (refer to Table 5.3; DEG list). This suggests that by three days following the introduction of *B. bassiana* isolate BG11, the maize plant is actively challenging a perceived pathogen attack by coordinating the activation of specific hormone-regulated defence pathways via ERF transcription factors, while simultaneously regulating those elements required to compensate for potential growth and development inhibition. In particular, the expression of an auxin-responsive gene of the indole-3 acetic acid (IAA) gene family was observed in the gene set enrichment analysis to be significantly higher in BG11 compared to J18 and control plants. Although the persistence of these two isolates in the plant tissues were not assessed further in this study, the plant's initial response to BG11 in particular indicates that beneficial effects to the plant may have been eventually observed.

Aux/IAA gene family

The phytohormone auxin plays a highly important role in plant growth and development. Auxin regulates various aspects of plant physiology such as apical dominance, tropisms, the differentiation of vascular tissues, in addition to the division, elongation, and differentiation of cells. On the molecular level, auxin modulates gene expression and membrane functions (Ludwig et al. 2013). In barley and Chinese cabbage, auxin-regulated genes were differentially expressed in response to the presence of the root endophyte, *P. indica*, which caused a significant growth-promotion effect (Franken 2012). A recent study by (Liao et al. 2017) showed that *Metarhizium robertsii* produced IAA and promoted lateral root growth and root hair development of *Arabidopsis* seedlings, which was attributed in part through an auxin-dependent mechanism in the plant, thus it is also plausible that *B. bassiana* may produce IAA during root colonisation.

5.4.2 Conclusions

Endophytic entomopathogenic fungi (EPF) can be employed for biocontrol purposes, however, when considering isolate selection for a given plant and pest, both pathogenicity to the pest and the endophytic performance should be assessed. This study, albeit limited in scope, suggests that there may be significant variation in the endophytic ability of various fungal isolates and/or in the host response to colonisation. This may be one reason why a population decline is often observed following inoculation to plant tissues. Although this study requires further validation by means of reverse-transcription quantitative PCR (RT-qPCR) experimentation to confirm differential gene expression, putatively, many genes involved in pathogen and/or endophyte response in maize were observed, particularly for the isolate BG11-treated plants relative to the J18 and control group plants.

Chapter 6

General discussion

This study aimed to investigate differences in the plant colonisation ability of selected *Beauveria* isolates. Consequently, plant-fungal interactions of three *B. bassiana* isolates with maize were investigated for differences at the physiological, ecological and molecular level. Previous studies have focused primarily on the potential for activity against insects and plant pathogens *in planta* by these endophytic entomopathogenic fungi. However, the functional role of the fungi in relation to plant tissues and/or the plant response to colonisation by different *B. bassiana* isolates is generally not well understood. Understanding the function and phenotypic variation that may occur between isolates relative to their plant colonisation capability will generate knowledge to improve the selection, application and establishment of *B. bassiana* as an endophytic biocontrol agent in agricultural systems.

This study was the first to compare the impact of different (putative) endophytic *B. bassiana* isolates on maize plants in order to investigate the ecological role of different isolates *in planta*. This was accomplished using a number of approaches. By (1) introducing the fungi into the plant directly as a presumed endophyte for comparison with a known plant-beneficial isolate of *Trichoderma atroviride*, and then measuring the plant growth response; by (2) investigating how inundative inoculation of roots influenced the rhizosphere microbiome and how, in turn, plants may support root colonisation of isolates in the rhizosphere when subjected to simulated herbivory stress; and by (3) directly quantifying gene expression levels in maize plants in response to fungal colonisation of roots by two different *B. bassiana* isolates.

For the purposes of this study, a sensitive and selective PCR-based detection method was developed for direct detection of multiple *Beauveria* species from maize, onion (Chapter 2) and soil DNA (Chapter 4). The nested PCR protocol was optimised to minimise non-target amplification while still remaining sensitive enough to amplify less than 0.32 pg/ μ L, or between 1-17 *ef1 α* gene copies. However, the elimination of inoculum and DNA on plant surfaces proved problematic for reliable PCR detection of *Beauveria* endophytes. This was exemplified by experiments that used the nested PCR protocol with a PMA dye treatment on inoculated and surface sterilised onion epidermis to deal with and assess residual DNA remaining from inocula. This was further validated by a histological study of the isolates applied to maize roots using confocal microscopy (Moran-Diez, unpublished), which showed only superficial colonisation of internal tissues. Surface sterilisation of plant tissues was thus deemed not sufficiently reliable to exclude surface inoculum for endophyte detection using PCR for subsequent experiments. Based on these results, current and previous methods reported in

literature pertaining to plant tissue preparation for PCR-based detection of *Beauveria* may have been inadequate to effectively remove epiphytic DNA of inocula, particularly in studies that used a topical application of the inoculum.

However, the adherence of *B. bassiana* on plant surfaces (i.e. as an epiphyte) may be as important in eliciting a plant-host response as internal (endophytic) colonisation. Indeed, the results of the microarray transcriptome analysis indicated that the plant host both perceives and reacts to external colonisation of *B. bassiana*, for instance, by the upregulation of various genes involved in plant defence signalling pathways such as ethylene responsive transcription factors and auxin responsive genes (IAA) (Chapter 5; Table 5.3). Therefore, surface inocula may be more important than previously realised in contributing to effects frequently observed in plants such as growth promotion or morphological changes (e.g. in root architecture), indirect effects to insect herbivores and the induction of systemic resistance to disease.

Future studies that aim to verify endophytic establishment of *Beauveria* spp. in plants may require an alternative and more comprehensive approach that does not rely on surface sterilisation of plant surfaces. For example, DNA can be first isolated from plant surfaces independently, then DNA can be obtained subsequently from whole (remaining) tissues and PCR-based detection performed to assess the microbial diversity differences using sequencing analysis. This could be accomplished with next generation sequencing (NGS) technology and complemented by the use of the *ef1α* nested qPCR protocol developed in this study to quantify *Beauveria* genome copy number separately from outer and inner surfaces. Indeed, non-disruptive DNA isolation methods already exist to obtain epiphytic DNA from leaves without causing mechanical damage (Suda et al. 2008), as do methods for obtaining DNA from insect cuticle of museum samples which may be adapted for use with plant material (Phillips and Simon 1995). Furthermore, this epiphytic DNA-subtractive approach may not only help to resolve the issues associated with surface sterilisation efficacy, but also enable investigation of possible effects to the natural internal and external plant microbiome following inoculation with these entomopathogens.

In this study, the growth of maize was measured following artificial inoculation with isolates of *B. bassiana* versus the *Trichoderma atroviride* isolate LU132, an isolate known to promote growth. The isolates were inoculated using the invasive 'micro-slit' technique commonly used for artificial inoculation of *Epichloë* grass endophytes (Latch and Christensen 1985), as described in Chapter 3. The rationale for adopting this particular method of inoculation was to increase the likelihood of systemic colonisation, as previously inferred from a study by El-Deeb et al. (2012), and therefore to increase the likelihood of identifying positive effects to plants based on the assumption that the selected *B. bassiana* isolates were functional beneficial endophytes. Previous literature frequently

reports positive growth in plants as a result of inoculation with *B. bassiana*, however, in most cases the fungi are introduced via plant surfaces (leaves, roots) in liquid conidial suspensions. The results of the present study showed a predominantly neutral or negative plant growth response in maize, based on plant dry biomass and shoot lengths. However, the plants exhibited root architecture changes as a result of one *B. bassiana* isolate, FRh2, and a higher indicated chlorophyll content for another isolate, J18, providing initial evidence for phenotypic differences between the study isolates.

Though possible that introduction of *B. bassiana* by the invasive inoculation method used was occasionally detrimental to plant growth, the comparison with *Trichoderma* suggests that *B. bassiana* may sometimes be marginally more commensalistic *in planta* rather than directly beneficial as has previously been reported for other endophytic *B. bassiana* isolates. However, general endophyte studies indicate that genotype-specific interactions may occur between plants and endophytes, and/or that the type of effects observed to the host plants are subject to environmental conditions, therefore, the same endophyte species can either enhance, reduce, or have no effect on plant fitness (Nieto-Jacobo et al. 2017; Rodriguez et al. 2009; Saikkonen et al. 2010a). Ultimately, it may be inferred from the results of this study that it is important to screen potential endophytic biocontrol isolates of *B. bassiana* under variable conditions in order to determine differential effects to the intended host plant.

Phenotypic variation between the selected *B. bassiana* isolates was less evident in the ecological study of the rhizosphere of maize. Previous literature pertaining to *Beauveria* indicated that the species may not be active in rhizosphere soil in comparison with species of *Metarhizium* (Bruck 2010; Kepler et al. 2017). However, in Chapter 4, *Beauveria* was more frequently detected in the rhizosphere when plants were subjected to simulated herbivory, or wound stress specifically. Elliot et al. (2000) first raised the hypothesis that plants may use entomopathogenic fungi as 'bodyguards'. Indeed, the results presented in Chapter 4 support the theory that recruitment of entomopathogenic fungi by plants may occur as an indirect defensive strategy against herbivory stress. Furthermore, these results also supports the findings of Keyser et al. (2014), whom tested whether root colonisation by *Metarhizium* may be an adaptive strategy in these fungi to increase exposure to plant-associated insects and thus aid their dispersal. These hypotheses were further supported by the results of the MicroRespTM assay, in which the root exudate profile was altered by those plants under distress from the above-ground damage to foliage, as demonstrated by observed differences in the functional microbial community composition. Plants are known to antagonise herbivores directly by affecting insect fecundity via volatile emission, as well as indirectly by recruiting natural enemies of the insect herbivores in the rhizosphere (Dudareva et al. 2006; Howe and Jander 2008), thus it is plausible that *B. bassiana* can be supported by plants within the rhizosphere as a natural

enemy of insect herbivores. Consequently, this research project suggests that the relationship between *Beauveria* and the plant host may be predominantly modulated by the plant host.

Future studies are warranted to further test these hypotheses and address the specific mechanisms that may be involved. For example, studies to determine the precise root exudate(s) components that enhance rhizosphere retention during herbivory, would not only be interesting from an evolutionary ecology perspective, but may also support the formulation of these exudates for practical application to artificially enhance rhizosphere colonisation by these fungi. It may also be necessary to assess the relationship between insect mortality and/or fecundity differences in association with plants subjected to extensive herbivory damage, compared to healthy plants, in order to elucidate or quantify the biocontrol potential of rhizosphere colonisation.

In Chapter 5, putative differences were observed in the plant response to colonisation by the two *B. bassiana* isolates' BG11 and J18. The gene families that contributed to observed differences in gene expression levels suggested that these plants may have been responding to reactive oxygen species (ROS) or to secondary metabolites associated with fungal colonisation, and were differentially exhibiting induced resistance to early fungal invasion. Given that the inocula of both isolates were applied to the plant roots in high quantity, differences in plant gene expression between the two treatments relative to the no-inoculum control plants indicated possible differences in colonisation ability between these two isolates. Furthermore, a suite of genes associated with plant growth and development were putatively upregulated in BG11 compared to both J18 and to the control treatment plants. This suggested that by three days following the introduction of *B. bassiana* isolate BG11, the maize plant was actively compensating for potential growth inhibition within the roots. In the growth study (Chapter 3), root colonisation was not observed as a result of the inoculation method employed for BG11-treated plants, yet certain effects to root architecture were observed for the other *B. bassiana* isolate (FRh2) which was unfortunately not tested further in the transcriptome analysis (due to cost restrictions). Further experiments could thus be conducted to measure the growth or physiological response in the roots as a result of all these isolates (BG11, FRh2, J18), by using the root-dip inoculation method.

As previously stated in Chapter 5, the transcriptome study requires further validation by means of RT-qPCR experimentation to confirm differential gene expression levels, for selected genes involved in the endophyte colonisation response in maize. Possible genes of interest for further investigation of expression levels may be inferred from the gene set enrichment analysis, such as the maize auxin-responsive gene, the ethylene responsive transcription factors, major facilitator superfamily defence gene and/or the glutathione S-transferase genes. However, there are other differentially expressed genes (DEGs) that may be of interest listed in Chapter 5, from Table 5.2 and Table 5.3. For example,

pathogenesis related protein 5 involved in signalling for plant systemic acquired resistance (SAR) (Jones and Dangl 2006) was significantly upregulated in J18 compared to both the control and BG11-treated plants, and significantly downregulated in BG11 compared to both other treatments. In contrast with what was previously observed in Chapter 3, J18-treated plants showed a reduction in the expression levels for various photosynthesis and chlorophyll related genes in the microarray DEG list (Table 5.3); whereas BG11 treated plants were not different to the control plant expression levels. However, this contrast between the chlorophyll content observed in growth experiments and gene expression levels for J18-treated plants may be attributed to a number of factors such as light source differences, the inoculation method used and the nutrient availability for 35 day-old plants versus germinating seedlings. Further studies using next generation sequencing technology (RNA-seq) could also be conducted to provide more detailed data on gene expression in both maize and *Beauveria* during colonisation. However, this requires more and improved annotation of the *B. bassiana* genome, which currently is still quite limited (Xiao et al. 2012).

Traditionally, entomopathogenic fungi applied inundatively have often performed inconsistently in the field, which may be due in part to a lack of understanding of their ecology and biology, in addition to the expectation that they should perform similarly to synthetic pesticides (Roy et al. 2010). Historically, biocontrol isolates of *B. bassiana* have been selected for release in the field based solely on their efficacy in laboratory bioassays, irrespective of their microhabitat preferences and ecological constraints (Bidochka et al. 2001). More recently, evidence has accumulated for the potential to use endophytic entomopathogenic fungi for biocontrol purposes (Vidal and Jaber 2015), and thus there is increasing importance to understand the ecology and life history of these fungi in association with plants. To conclude, this study demonstrated the fundamental importance of considering isolate variation within the species, specifically, for the ability to affect plant health.

Appendix A

Phylogenetic identification of genera and/or species

For all amplicon-based phylogenetic identification of fungal species (ITS5_F and ITS4_R; EF4F and EF4R), evolutionary history was inferred by using the Maximum-Likelihood method based on the model by Tamura and Nei (1993). For the ITS gene tree, the highest log likelihood estimated by the model is shown (-2510.4865) in Figure A.1. For *ef1 α* gene tree, the highest log likelihood (-266.9200) is shown in Figure A.2. These inferential evolutionary analyses were conducted in MEGA5 (Tamura et al. 2011). In the Maximum Likelihood method, when the number of common sites < 100 or less than one fourth of the total number of sites, the maximum parsimony method is used; otherwise the BIONJ method with MCL distance matrix is used. Species were identified based on both the confidence of their alignment with sequences obtained from Genbank (National Center for Biotechnology Information; NCBI database), where the significance value is $P \leq 0.05$ (obtained from the phylogenetic analysis), and from the BLASTn search results from the sequence queries (Altschul et al. 1990). Based on these results, taxa were identified and listed as in Chapter 2; Table 2.1.

In addition to the phylogenetic gene tree produced from the *ef1 α* sequences, the electrophoresis gel images (representing PCR technical replicate 1) produced from the nested PCR conducted on the maize root DNA for the detection of *B. bassiana*, as described in Chapter 4 (see section 4.2.6) is depicted in Figure A.3.

Non-target amplification in root DNA are indicated on the gel image by numbers. These numbers correspond with the experimental sample/pot number which in turn correspond with the *ef1 α* gene tree (Figure A.2; Figure A.3). Interestingly, non-target amplification bands on the gel appeared in lower quantity relative to the *Beauveria* bands that were produced, suggesting that further PCR optimisation may be possible in order to avoid sequencing, when sequencing is not feasible (Figure A.3).

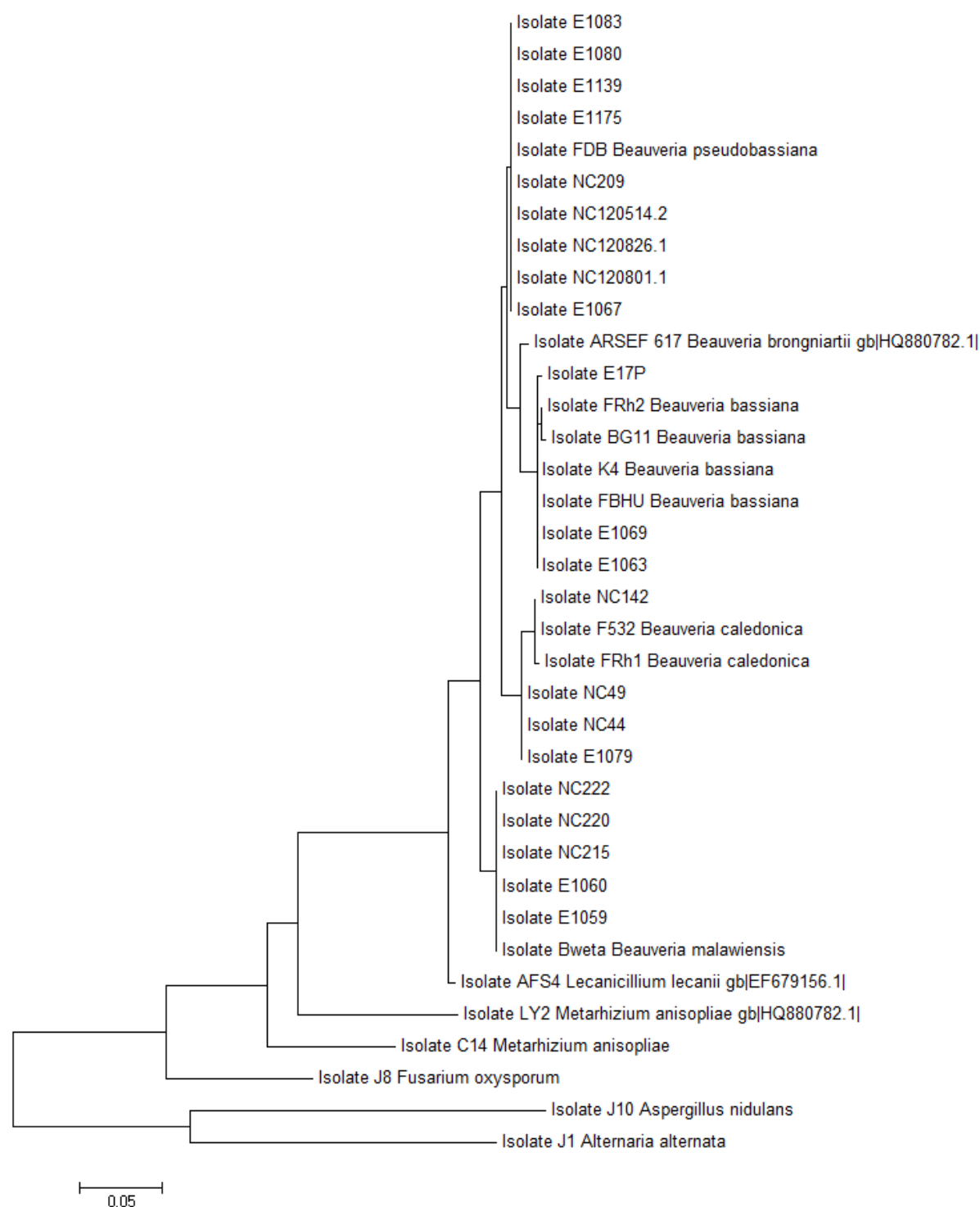


Figure A.1. Taxonomic identification using fungal internal transcribed spacer region (ITS) DNA amplicon from ITS5F and ITS4R. Tree constructed by the Maximum-Likelihood Method based on 384 base-pair fragments in the sequence alignment.

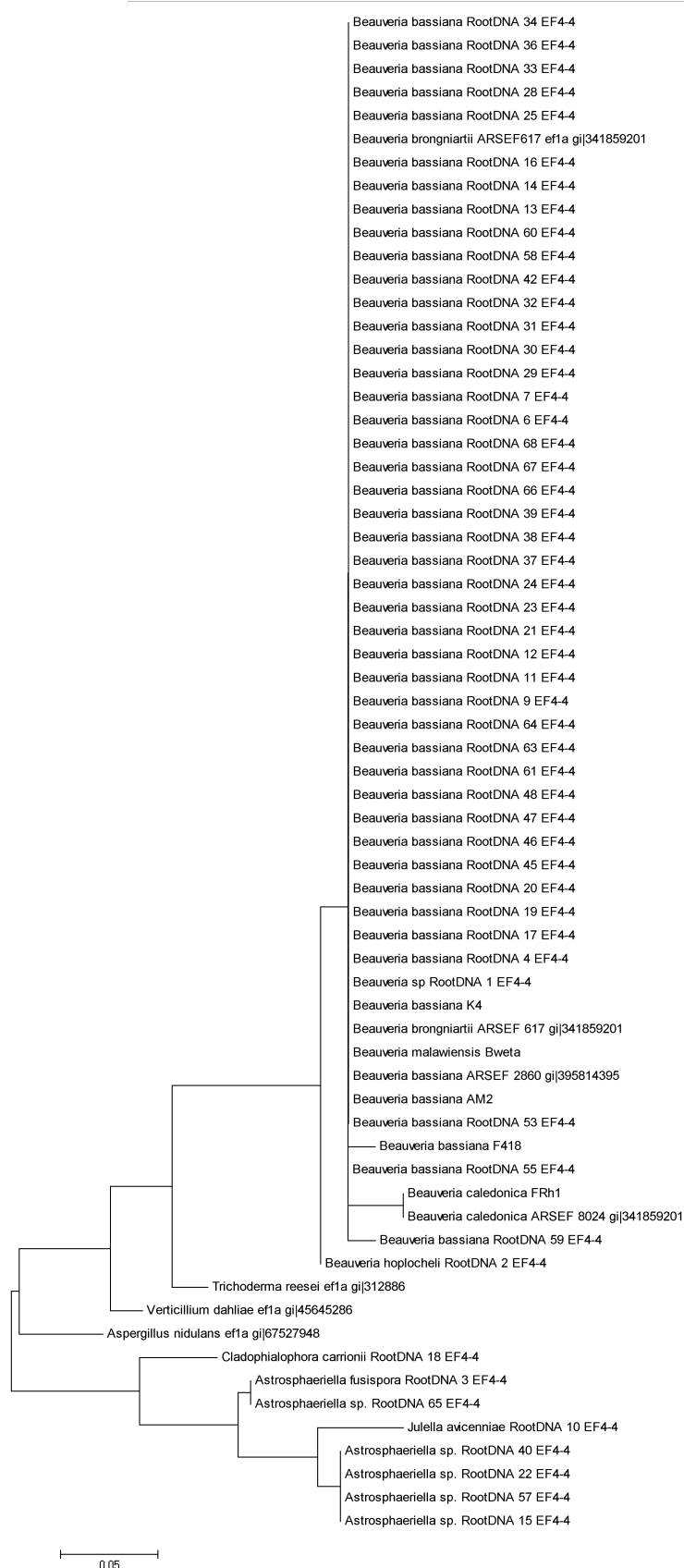


Figure A.2. Taxonomic identification using fungal translation elongation factor (*ef1α*) DNA amplicon from EF4F and EF4R (from nested PCR). Tree constructed by the Maximum-Likelihood Method based on 115 base-pair fragments in the sequence alignment.

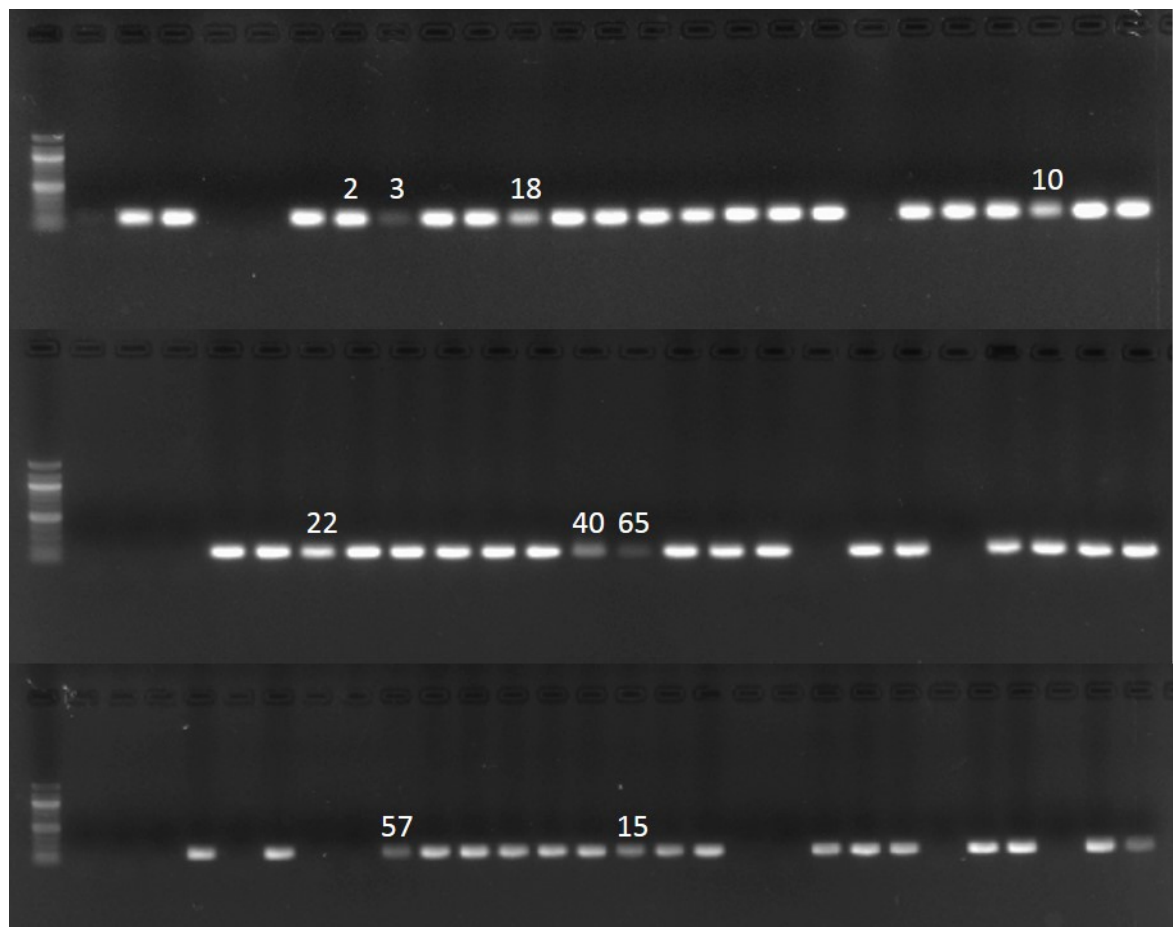


Figure A.3 Electrophoresis gel image of *ef1α* product. Bands (176 bp) amplified using EF4F and EF4R primers in the second step of a nested PCR from the rhizosphere of *Zea mays* (maize) plants at 6, 15 and 30 days after inoculation (DAI) with *Beauveria bassiana* isolates BG11, FRh2 and J18. In wells' 1-3 are the no-template controls (NTC) (from the 1st and 2nd PCRs), followed by a *B. bassiana* positive control (pure gDNA) and positive template control (EF3F and EF5R); then the experimental samples in random order. Numbered bands indicate non-target amplification, which correspond with *ef1α* amplicons and taxa in the tree in Figure A.2. All other bands are *Beauveria* spp.

Appendix B

Pioneer maize hybrid cultivars

Hybrid	Maturity			Yield		Plant and agronomic traits										Grain quality traits					Food grade characteristics							Disease resistance ratings ²⁶										Recommended established plant populations (plants/ha)			Hybrid
	CRM to grain harvest moisture (24%)	CRM to silking ²	CRM to black layer	Grain yield for maturity ⁴	Adoption to high population ⁵	Adoption to low population (ear leaf) ⁶	Drought tolerance	Stalk strength	Root strength	Early growth ⁷	Plant height ⁸	Ear height ⁹	Staygreen ¹⁰	Husk cover ¹¹	Grain drydown ¹²	Grain appearance ¹³	Grain crude protein ¹⁴	Grain oil content ¹⁵	Starch total ¹⁶	Test weight	Processing use ¹⁷	Kernel density ¹⁸	Kernel crown ¹⁹	Pericarp removal ²⁰	Kernel red streak ²¹	Kernel size ²²	Hardy endosperm ²³	Kernel colour ²⁴	Northern Leaf Blight ²⁵	Common Rust	Eyepot ²⁶	Head Smut	Fusarium Ear Rot	Diplodia Ear Rot	Gibberella Ear Rot	Anthraxnose Stalk Rot	Challenging yield environments	Medium yield environments	High yield environments		
39G12	77	78	77	9	7	7	7	6	5	8	8	7	5	5	8	9	5	9	6	6	n/a	n/a	n/a	n/a	n/a	n/a	n/a	n/a	4	6	-	8	-	-	5	-	104	108	115	39G12	
38V12	91	91	91	9	9	9	8	6	8	7	5	6	7	6	7	6	-	-	-	5	n/a	n/a	n/a	n/a	n/a	n/a	n/a	n/a	6	6	-	-	-	-	5	-	95	104	110	38V12	
38P05	93	94	94	9	9	8	7	5	5	5	5	5	6	6	6	7	9	7	7	6	n/a	n/a	n/a	n/a	n/a	n/a	n/a	n/a	6	5	5	7	5	-	5	4	88	94	100	38P05	
P9400	94	94	94	9	8	9	7	7	7	7	8	7	6	5	6	7	-	-	-	7	n/a	n/a	n/a	n/a	n/a	n/a	n/a	n/a	7	6	-	7	5	-	6	-	85	95	105	P9400	
37Y12	97	100	96	9	8	6	8	5	6	6	6	5	5	7	8	7	9	6	7	6	n/a	5	4	5	7	6	4	4	6	5	6	6	5	5	5	4	88	96	102	37Y12	
P0021	100	100	100	9	8	9	6	6	7	7	6	5	7	6	6	6	-	-	-	5	n/a	n/a	n/a	n/a	n/a	n/a	n/a	n/a	7	6	-	7	6	-	5	-	85	95	100	P0021	
36Y84	103	102	101	9	9	7	7	5	7	7	4	4	6	6	6	7	8	8	7	7	n/a	6	5	6	5	5	5	3	5	6	-	7	6	5	4	4	88	94	100	36Y84	
36B08	103	100	102	8	9	7	8	6	6	7	4	3	6	7	5	6	9	6	7	7	n/a	6	7	4	8	7	-	7	7	5	6	8	5	4	5	5	88	94	100	36B08	
P0537	105	105	105	9	9	7	7	6	5	6	6	5	6	6	6	6	7	6	9	8	n/a	n/a	n/a	n/a	n/a	n/a	n/a	n/a	6	6	-	8	6	6	6	-	88	96	102	P0537	
35Y33	107	106	108	9	9	5	8	6	5	6	6	5	7	6	6	7	9	7	8	8	HT/AC	9	6	5	7	7	7	6	7	5	-	5	4	5	3	5	88	94	100	35Y33	
34D71	107	108	108	9	8	8	7	7	5	6	7	6	7	7	5	6	7	7	8	6	n/a	n/a	n/a	n/a	n/a	n/a	n/a	n/a	7	5	-	6	5	5	5	5	NR	94	100	34D71	
34K77	107	108	110	7	7	8	7	4	5	6	6	5	6	8	7	7	8	8	8	6	HT/AC	7	7	5	8	5	7	7	5	6	6	7	6	3	5	4	88	94	94	34K77	
P0891	107	107	107	9	9	6	7	8	6	6	7	4	7	5	6	9	-	-	-	8	n/a	7	6	5	5	6	7	5	6	5	-	5	4	5	5	5	88	94	105	P0891	
34B97	108	109	109	9	7	7	7	5	4	6	6	5	7	7	6	8	8	7	8	7	AC	7	7	5	7	8	5	6	6	4	-	3	6	4	4	4	NR	94	94	34B97	
34H31	109	108	107	9	8	4	8	7	6	5	5	5	7	6	6	9	8	7	9	8	HT/AC	8	6	5	7	7	8	6	6	4	-	5	5	5	4	5	88	94	100	34H31	
34F95	109	108	108	9	8	8	7	7	5	7	7	5	8	5	6	6	7	7	8	5	n/a	n/a	n/a	n/a	n/a	n/a	n/a	n/a	6	6	-	7	6	4	5	5	88	94	100	34F95	
34P88	109	109	110	9	8	9	7	6	5	7	7	5	6	6	6	6	7	7	9	5	n/a	n/a	n/a	n/a	n/a	n/a	n/a	n/a	5	5	-	6	5	5	6	4	88	94	100	34P88	
P1253	109	109	109	9	9	6	6	8	5	6	6	5	8	6	5	7	-	-	-	7	n/a	n/a	n/a	n/a	n/a	n/a	n/a	n/a	6	5	-	5	5	5	3	6	88	94	100	P1253	
NEW = New hybrid		= Elite Performer			= Proven Performer		CRM = Comparative Relative Maturity					RATINGS: 9 = Outstanding					1 = Poor		- = Insufficient data available			n/a = Not applicable			NR = Not recommended			HT/AC = Refer to page 28, point 17													

= New hybrid

= Elite Performer

= Proven Performer

CRM = Comparative Relative Maturity

RATINGS: 9 = Outstanding

1 = Poor

- = Insufficient data available

n/a = Not applicable

NR = Not recommended

HT/AC = Refer to page 28, point 17

Figure B.1. Maize cultivar characteristics of Pioneer hybrid lines. Sourced from: http://www.pioneer.co.nz/assets/maizegrain/hybrids/hybridtrait_full_table.pdf

Appendix C

Soil nutrient analysis

R. J. Hill Laboratories Limited (NZ) conducted the soil nutrient analysis on the pasture silt and Waimakariri river sand mix (silt and sand mixed approximates 'loam' for the purpose of sampling). Soil was collected from Iverson 13 at Lincoln University (Lincoln, New Zealand) prior to the initiation of all experiments (January 2015) and stored at ambient temperature. The soil sample analysed was taken from ~15 cm depth, as advised for nutrient analysis of soil intended for growing crops by Hill Laboratories. This depth is advised as soil nutrients are usually more concentrated at the surface (i.e. < 7.5 cm depth). The soil used in these experiments was extracted from below growing pasture (predominantly rye grass and tall fescue turf grasses), thus the soil nutrient availability was generally expected to be poor. The nutrient analysis report (Figure B.1) below was conducted in February of 2015, during the period of the experimental trials.

Table C.1. Soil Nutrient Analysis Table, provided by Hill Laboratories Limited (NZ).

Sample Name: G.E. 2 Loam				Lab Number: 1471161.1		
Sample Type: SOIL Arable (S56)						
Analysis		Level Found	Medium Range	Low	Medium	High
pH	pH Units	6.0	5.7 - 6.2	<div><div></div></div>		
Olsen Phosphorus	mg/L	10	20 - 30	<div><div></div></div>		
Potassium	me/100g	0.19	0.30 - 0.60	<div><div></div></div>		
Calcium	me/100g	7.6	5.0 - 12.0	<div><div></div></div>		
Magnesium	me/100g	0.94	0.60 - 1.20	<div><div></div></div>		
Sodium	me/100g	0.20	0.00 - 0.30	<div><div></div></div>		
CEC	me/100g	13	12 - 25	<div><div></div></div>		
Total Base Saturation	%	70	50 - 85	<div><div></div></div>		
Volume Weight	g/mL	1.15	0.60 - 1.00	<div><div></div></div>		
Sulphate Sulphur	mg/kg	7	10 - 20	<div><div></div></div>		
Available Nitrogen (15cm Depth)*	kg/ha	65	100 - 150	<div><div></div></div>		
Anaerobically Mineralisable N*	µg/g	38		<div><div></div></div>		
Soil Sample Depth*	mm	0-150		<div><div></div></div>		
Base Saturation %		K 1.5	Ca 59	Mg 7.3	Na 1.6	
MAF Units		K 4	Ca 11	Mg 24	Na 11	

The above nutrient graph compares the levels found with reference interpretation levels. NOTE: It is important that the correct sample type be assigned, and that the recommended sampling procedure has been followed. R J Hill Laboratories Limited does not accept any responsibility for the resulting use of this information. IANZ Accreditation does not apply to comments and interpretations, i.e. the 'Range Levels' and subsequent graphs.

Appendix D

RNA quality control assessment

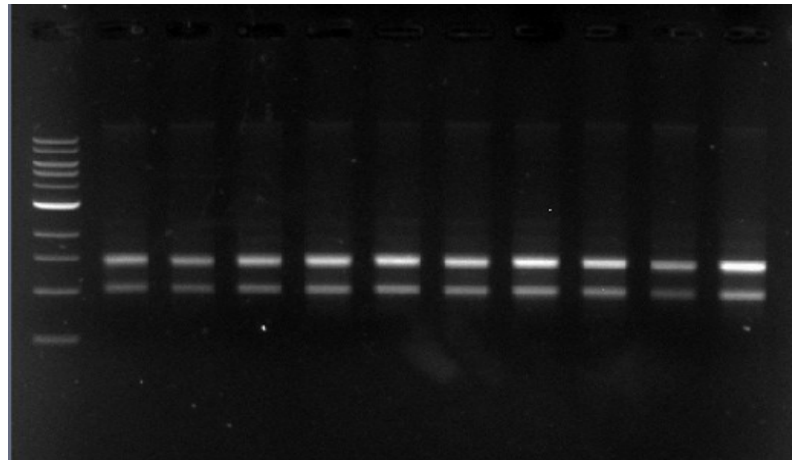


Figure D.1. Electrophoresis gel image of total RNA. RNA obtained from *Zea mays* (maize) roots at 3 days after inoculation (DAI) with *Beauveria bassiana* isolates BG11 and J18, or a no-inoculum control representing samples 1-10 used in the RNA microarray of Chapter 5. Samples are run against a 1 kb DNA ladder (Hyperladder II, Bioline, USA).

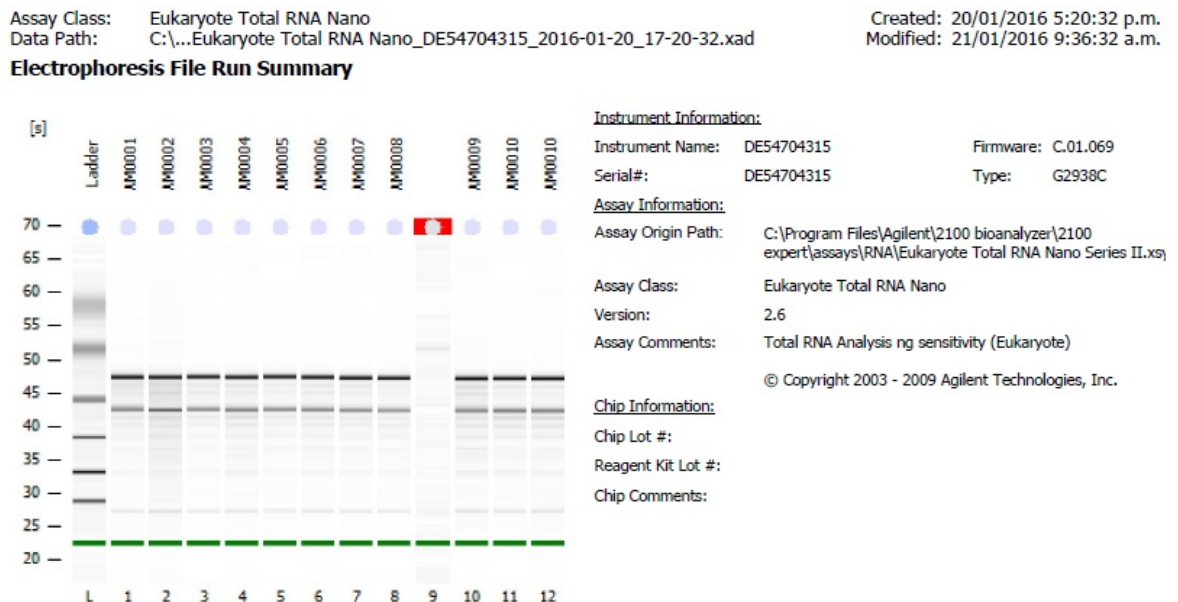


Figure D.2. RNA quality analysis report of total RNA. RNA obtained from *Zea mays* (maize) roots at 3 days after inoculation (DAI) with *Beauveria bassiana* isolates BG11 and J18, or a no-inoculum control representing samples 1-10 used in the RNA microarray of Chapter 5. Sample quality was assessed using the RNA 6000 Nano Chip using the Agilent 2100 Bioanalyzer instrument (Agilent Technologies). Report supplied by New Zealand Genomics Limited (NZGL).

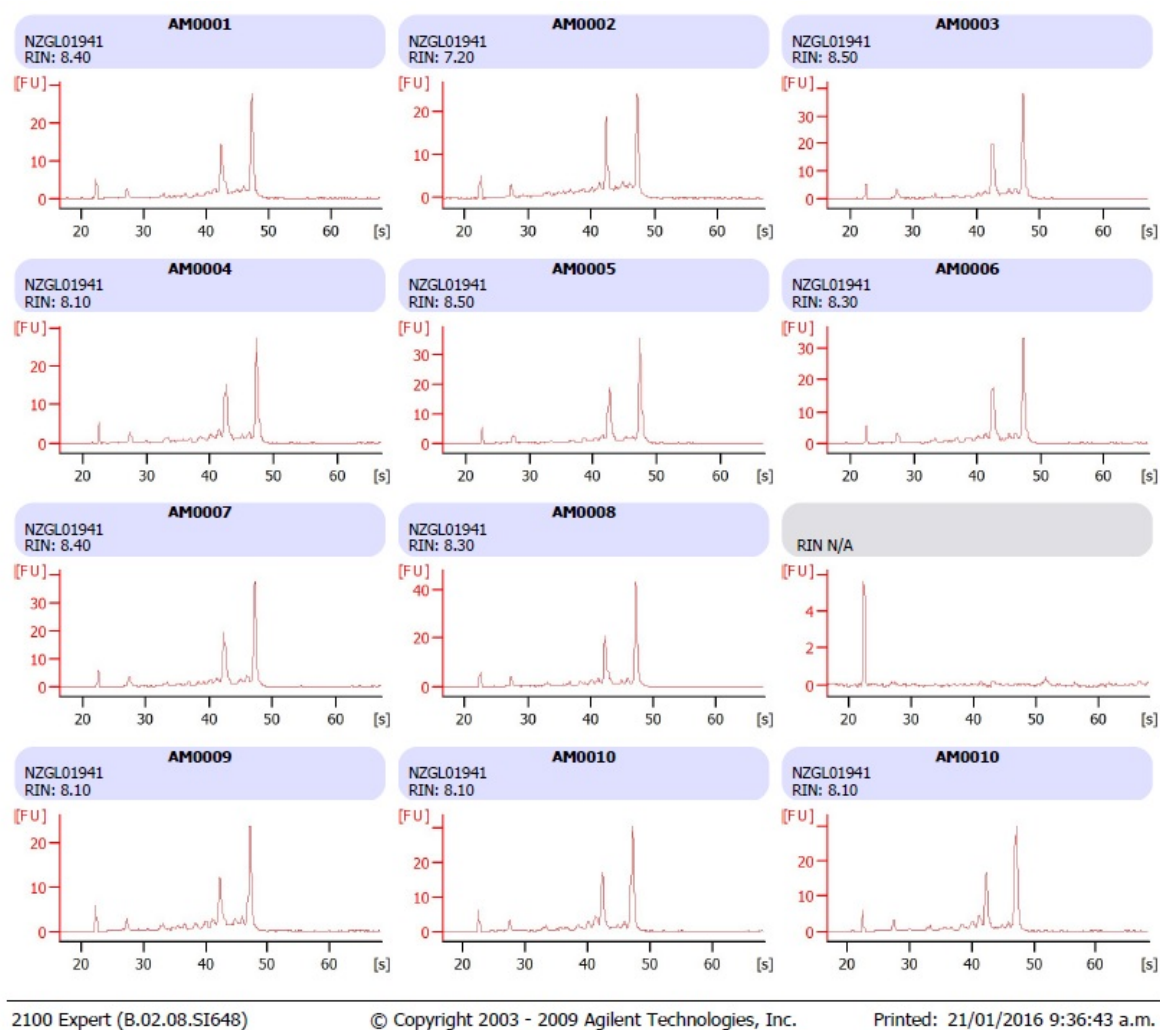


Figure D.2. RNA degradation analysis for quality of total RNA. RNA obtained from *Zea mays* (maize) roots at 3 days after inoculation (DAI) with *Beauveria bassiana* isolates BG11 and J18, or a no-inoculum control representing samples 1-10 used in the RNA microarray of Chapter 5. Sample quality was assessed using the 2100 Bioanalyzer (Agilent Technologies). RNA Integrity Number (RIN) for microarray processing was required to be ≥ 8 . Array samples are labelled 1-10 for each sample, as described in Chapter 5; but with AM (Aimee McKinnon) as the code. Report supplied by New Zealand Genomics Limited (NZGL).

Appendix E

Differentially expressed gene (DEG) lists

for *Beauveria bassiana* isolate BG11- and J18- versus control comparisons

Table E.1. Differential gene expression table for the *Beauveria bassiana* BG11-treated *Zea mays* (maize) versus no-inoculum control comparison. Table lists putatively downregulated known (annotated) genes.

Probe ID	Gene title	BG11	Control	Fold Change	P. Value
Zm.6659.1.A1_at	pathogenesis related protein-5	515.1067	1754.323	-5.3001891	0.00107503
Zm.15280.1.A1_s_at	pathogenesis related protein4	593.9229	1587.843	-4.2447146	0.00477308
Zm.18344.1.A1_at	major facilitator superfamily defense1	77.08453	197.6965	-3.9604099	0.00219906
ZmAfx.12.1.S1_at	kaurene synthase2	267.543	619.2207	-3.6157528	0.00057746
Zm.11758.1.A1_at	gibberellin 20 oxidase 2	772.8702	1491.422	-2.9540788	0.00982987
Zm.627.1.A1_at	glutathione transferase24	102.0921	192.6568	-2.7582447	0.00143033
Zm.67.1.S1_at	Actin-depolymerizing factor	9.514198	15.31269	-2.5054857	0.00871093
Zm.4471.2.S1_a_at	pyruvate, orthophosphate dikinase1	8.497757	11.71614	-1.9391583	0.00551439
Zm.11985.1.A1_at	hemoglobin 2	44.208	62.9249	-1.9326111	0.00537139
Zm.617.1.A1_at	tonoplast intrinsic protein4	19.9267	27.6928	-1.5622779	0.00877557
Zm.14496.1.A1_at	terpene synthase11	130.057	794.5596	-7.5671265	0.01552072
Zm.16805.3.S1_x_at	basic endochitinase C	422.7748	851.2152	-3.0216804	0.02109153
Zm.16805.3.S1_at	basic endochitinase C	185.2506	365.9078	-2.9505782	0.03687842
Zm.125.1.S1_at	nitrate reductase (NAD(P)H)	148.6615	241.4119	-2.5312708	0.03268371
Zm.15280.2.A1_at	Pathogenesis related protein4	37.59839	59.90421	-2.0187071	0.0117277
Zm.1085.1.A1_a_at	Chitinase chem5	4050.437	6444.391	-1.9141287	0.02801339
Zm.298.1.S1_a_at	dxr protein	509.5338	754.3884	-1.7021461	0.01114127
Zm.10207.2.A1_a_at	carboxylic ester hydrolase	93.95656	128.0867	-1.5963191	0.01198025
Zm.10830.1.S1_at	BRASSINOSTEROID INSENSITIVE 1-associated receptor kinase 1	37.49375	55.8879	-1.5739319	0.0152189
Zm.8714.1.A1_at	acc oxidase	212.2727	305.2669	-1.5687053	0.01224981
Zm.559.1.A1_at	glutathione S-transferase GST 34	99.57055	133.7257	-1.4463456	0.02161924
Zm.13583.1.S1_at	Secretory protein	755.0928	1093.319	-1.3525657	0.01304062
Zm.649.1.S1_at	ADP-glucose pyrophosphorylase small subunit	48.28293	60.53776	-1.3308613	0.03319005
Zm.1663.1.A1_at	VQ motif family protein	144.4696	197.2558	-1.206573	0.01745118
Zm.1738.2.A1_at	soluble inorganic pyrophosphatase	1176.922	1527.399	-1.191479	0.01858051
Zm.505.1.S1_at	Glucose translocator1	45.10623	58.18645	-1.1735002	0.02324337
Zm.9646.1.A1_at	negatively light-regulated protein	37.21542	48.71537	-1.1731848	0.04350421
Zm.4471.4.A1_at	erg28 like protein	115.3429	144.9985	-1.1430122	0.02251952
Zm.4471.5.A1_at	protein kinase APK1B	11.03674	13.1815	-1.1288158	0.02621964
Zm.18542.1.A1_at	TAK14	127.5557	171.1154	-1.1250388	0.03998828
Zm.52.1.A1_at	root cap protein 1	497.8954	587.518	-1.1179117	0.02194611
Zm.10300.1.S1_at	D-3-phosphoglycerate dehydrogenase /// hypothetical protein LOC100501398	188.049	226.9606	-1.0517171	0.04117078
Zm.12626.1.A1_at	craniofacial development protein 1	57.35439	70.11886	-1.0458761	0.0262162
Zm.13938.2.S1_at	60S ribosomal protein L31	671.4345	800.5616	-1.0428327	0.04418312
Zm.5930.1.S1_at	60S ribosomal protein L37a /// 60S ribosomal protein L37a	564.0082	684.7113	-1.0404404	0.02839101
Zm.2672.1.A1_at	SET domain containing protein	84.99632	104.3522	-1.0321028	0.02975796
Zm.5048.6.A1_a_at	endoplasmic reticulum chaperone /// shepherd-like1	1445.341	1789.943	-1.0131398	0.04965072
Zm.13884.2.S1_x_at	R2R3MYB-domain protein /// R2R3MYB-domain protein /// hypothetical protein LOC100384270	58.0481	74.47346	-1.0107322	0.03171008

Zm.16490.1.S1_at	3-methyl-2-oxobutanoate hydroxymethyltransferase	92.10129	111.7633	-1.0050878	0.03051956
ZmAffx.189.1.A1_at	Testis intracellular mediator protein	27.84378	33.77489	-0.9886889	0.0307551
Zm.5390.1.A1_at	single-stranded DNA-binding protein	371.9265	442.0363	-0.9761711	0.03176427
Zm.8134.1.S1_at	snRK1-interacting protein 1	55.03349	65.3794	-0.9651514	0.03269356
Zm.3504.1.A1_at	ribonuclease III domain protein1	98.49458	121.2454	-0.9614383	0.04374212
Zm.6625.2.S1_at	60S ribosomal protein L9	526.4852	630.797	-0.9585815	0.0384587
Zm.15925.1.S1_at	50S ribosomal protein L29	27.33114	31.8985	-0.9554176	0.03424643
Zm.3349.1.S1_at	barley mlo defense gene homolog4	98.56498	118.343	-0.9516145	0.04734856
Zm.465.1.A1_at	acidic ribosomal protein P2a-3	718.6976	841.6201	-0.9444792	0.03583133
Zm.10502.1.S1_at	actin-depolymerizing factor	97.80419	110.6088	-0.9265505	0.04398406
Zm.10528.1.A1_at	oxidoreductase	77.82662	87.73384	-0.9235542	0.04491636
Zm.15424.1.S1_s_at	Metallothionein-like protein type 2	452.642	522.5335	-0.9225276	0.0374847
Zm.7032.1.A1_at	60S ribosomal protein L7-1	611.1511	710.8306	-0.9214672	0.03850387
Zm.329.2.S1_a_at	shrunken2	15.67401	18.51819	-0.9084225	0.04430423
Zm.5048.6.A1_at	endoplasmic	3021.432	3685.819	-0.9074471	0.04977677
Zm.2895.2.A1_a_at	60S ribosomal protein L44 /// 60S ribosomal protein L44 /// hypothetical protein LOC100384095	1418.387	1696.837	-0.906645	0.04939165
Zm.12331.1.S1_at	Coiled-coil-helix-coiled-coil-helix domain-containing protein 4	189.7471	229.6455	-0.9050024	0.03889537
Zm.14073.2.S1_a_at	60S ribosomal protein L28	1117.961	1306.285	-0.9031081	0.04147143
Zm.12429.1.A1_at	conserved protein	148.2091	174.4817	-0.8970347	0.04142772
Zm.16973.1.S1_at	VQ motif family protein	92.17549	118.3024	-0.8951746	0.04054816
Zm.16177.1.S1_at	40S ribosomal protein S10	1074.384	1248.711	-0.8743969	0.04669364
Zm.13944.4.A1_a_at	60S ribosomal protein L29 /// glycine-rich RNA-binding protein 8	722.2667	865.2841	-0.8732965	0.04661381
Zm.318.2.S1_a_at	plastid phosphate/phosphoenolpyruvate translocator2	1298.31	1511.605	-0.8708422	0.04536784
Zm.15815.1.S1_at	NADH:nitrate reductase	6.017473	6.970326	-0.8639637	0.04411499
Zm.18422.1.S1_at	nuclear transcription factor Y subunit C-2	129.7178	154.3133	-0.8517178	0.04987868
Zm.10128.1.S1_a_at	mitochondrial import receptor subunit TOM20	550.7351	645.1991	-0.8500659	0.04772182
Zm.6991.1.A1_at	ribosomal protein L35 containing protein	501.3807	577.6487	-0.8396052	0.04737799

Table E.2. Differential gene expression table for the *Beauveria bassiana* BG11-treated *Zea mays* (maize) versus no-inoculum control comparison. Table lists putatively upregulated known (annotated) genes.

Probe ID	Gene title	BG11	Control	Fold Change	P. Value
Zm.140.1.A1_at	root preferential4	1245.402	981.7574	1.599923	0.008706
Zm.7422.1.A1_at	anthocyanidin 3-O-glucosyltransferase	83.55425	57.81319	1.787656	0.0071
Zm.8365.1.A1_at	hexokinase-1	418.9359	284.9317	1.812117	0.008109
Zm.151.1.A1_at	fatty acid desaturase7	622.9337	410.7561	2.005244	0.005698
Zm.12114.1.S1_at	DNA-binding protein RAV1	334.3349	208.2256	2.163508	0.007073
Zm.10423.1.S1_at	fatty acid desaturase8	196.9785	123.0139	2.178274	0.003137
Zm.12317.1.S1_at	ethylene-responsive transcription factor 4	770.5357	474.1278	2.277879	0.005038
Zm.604.1.A1_at	plasma membrane intrinsic protein1	456.6385	261.6309	2.373658	0.002387
Zm.11809.1.A1_at	phi-1-like phosphate-induced protein	645.4753	372.9202	2.756931	0.00542
Zm.11745.1.A1_at	NPK1-related protein kinase-like protein	43.14714	21.91614	3.027554	0.008069
Zm.8261.1.A1_at	BCL-2 binding anthanogene-1	127.1961	60.89645	3.119097	0.002066
Zm.14971.1.S1_at	AMP binding protein	168.3993	80.69752	3.420572	0.002077
Zm.7611.2.A1_at	IAA24 - auxin-responsive Aux/IAA family member	108.1493	45.97157	3.821626	0.007279
Zm.10181.1.A1_at	ERF-like protein	40.44385	17.14725	3.87489	0.001095
Zm.11891.1.A1_at	helix-loop-helix DNA-binding domain containing protein	111.6284	43.32124	4.174835	0.001344
Zm.13366.1.A1_a_at	RNA binding protein	122.6875	72.0302	4.686377	0.000263

Zm.1527.2.A1_a_at	xyloglucan endotransglucosylase/hydrolase protein 23	291.3643	97.37086	4.860857	0.004047
Zm.16376.1.S1_at	AP2 domain containing protein	26.60444	6.764052	5.880083	0.000259
Zm.10120.1.A1_at	DNA binding like	24.93722	6.464356	5.934236	0.000138
Zm.1524.1.A1_at	dehydration-responsive element-binding protein 1D	57.98109	13.42483	6.640411	0.000363
Zm.12010.1.A1_at	deoxyhypusine synthase 2	10.34289	8.587919	0.838437	0.04831
Zm.19214.1.S1_at	ankyrin repeat domain-containing protein 2	283.459	238.1546	0.847878	0.046402
Zm.4068.2.A1_at	Ferredoxin-NADP reductase precursor	21.49789	17.63188	0.859971	0.046762
Zm.13919.1.A1_at	hypoxically induced transcript 3	11.60063	9.762003	0.86533	0.047262
Zm.9082.1.A1_at	Protein phosphatase 2C isoform gamma	50.69481	41.89221	0.872365	0.045381
Zm.741.1.A1_at	kelch motif family protein	765.366	642.4365	0.876157	0.042537
Zm.3757.1.A1_at	ferredoxin-3	31.50823	25.84431	0.88471	0.045677
Zm.4161.2.S1_at	Rhodopsin	51.18901	42.63094	0.896929	0.04702
Zm.17762.1.S1_at	hydrophobic protein LTI6B	1486.076	1252.658	0.904044	0.040014
Zm.14518.1.A1_at	pyruvate decarboxylase	12.02709	9.833447	0.913586	0.046088
Zm.11768.1.S1_at	RING-H2 finger protein ATL2B	161.2344	135.5003	0.929021	0.036216
Zm.430.1.S1_at	sigma-like factor2B	14.65511	12.29492	0.938093	0.035885
Zm.10336.1.S1_at	cytosolic aldehyde dehydrogenase RF2C	3309.524	2852.317	0.938181	0.042072
ZmAfx.1461.1.S1_at	ATP synthase epsilon chain	213.3671	168.0723	0.94472	0.034839
Zm.19134.1.A1_at	peptide transporter PTR2	240.0878	194.8168	0.949402	0.037952
Zm.10088.1.A1_at	remorin	55.99761	46.17261	0.952715	0.040981
Zm.11932.1.A1_at	Ocs element-binding factor 1	35.56072	29.08522	0.958752	0.037282
Zm.20.1.S1_at	calcium dependent protein kinase	1033.544	848.5691	0.96831	0.032516
Zm.10832.1.A1_at	ZIM motif family protein	498.3431	415.0884	0.976976	0.036043
Zm.12309.1.S1_at	ABA-induced protein	77.58667	63.78196	0.978741	0.036485
Zm.864.1.S1_at	glutathione transferase30	911.847	763.9099	0.986011	0.032596
Zm.94.1.S1_at	DNA binding with one finger2	555.4866	429.3382	1.003737	0.031203
Zm.9001.1.A1_a_at	heavy metal-associated domain containing protein	139.9516	109.4751	1.008252	0.033199
Zm.9982.1.A1_at	spotted leaf protein 11	486.7704	400.767	1.032415	0.027944
Zm.11586.1.A1_at	PVR3-like protein	191.0439	152.2809	1.041615	0.034672
Zm.14909.1.A1_at	Tonoplast intrinsic protein1	61.90436	47.2597	1.044011	0.027396
Zm.1087.1.S1_at	iron-sulfur protein2	92.70544	74.69754	1.049748	0.041024
Zm.2637.1.A1_at	oleosin Bn-V	181.6024	142.2247	1.082652	0.030306
Zm.3165.1.A1_at	terpene synthase 7	28.96835	24.09359	1.105658	0.044729
Zm.14566.1.S1_a_at	photosystem II 11 kD protein /// photosystem II 11 kD protein	90.29711	76.811	1.110718	0.031085
Zm.6788.1.A1_at	Zea floricaula/leafy1	32.59376	24.86212	1.113641	0.038916
Zm.681.1.A1_at	barley mlo defense gene homolog2	37.19256	28.6129	1.114046	0.043039
Zm.11874.1.A1_at	CIPK-like protein 1	134.0161	102.5136	1.119255	0.037404
Zm.19091.1.S1_at	fiber protein Fb2	612.6574	486.3003	1.139538	0.03487
Zm.14566.2.A1_at	photosystem II 11 kD protein	267.2375	208.8632	1.180529	0.029456
Zm.8647.1.A1_at	F-box family member	32.94257	24.96836	1.182332	0.027918
Zm.7568.1.A1_at	blue copper protein	1054.006	814.2562	1.183377	0.020844
Zm.1684.1.S1_at	profilin homolog1	993.3061	742.2106	1.188778	0.044179
Zm.7342.1.A1_at	legumin1	82.69618	63.02676	1.193567	0.032025
Zm.18990.1.A1_at	BRASSINOSTEROID INSENSITIVE 1-associated receptor kinase 1	18.16655	13.83155	1.207818	0.019068
Zm.12037.1.S1_at	bHLH transcription factor PTF1	502.6335	401.627	1.218239	0.036373
Zm.11848.1.A1_at	calmodulin	565.198	434.221	1.219257	0.018794
Zm.9563.1.A1_at	cytochrome P450 12	223.6109	172.166	1.23064	0.02854
Zm.9667.1.A1_at	transcription factor MYB42	1266.922	1065.033	1.240867	0.048208
Zm.240.1.S1_at	SBP-domain protein 6	220.1175	166.7064	1.250776	0.017843
Zm.456.1.S1_at	maize insect resistance1	26.11828	19.25307	1.261305	0.042144
Zm.15885.1.S1_at	flavanone 3-hydroxylase1	58.44313	46.40119	1.261674	0.021225
Zm.608.1.S1_at	plasma membrane intrinsic protein2	2875.454	2268.257	1.274669	0.022761
Zm.17181.1.S1_at	O-succinylhomoserine sulfhydrylase	53.55975	40.72969	1.275019	0.01522
Zm.17964.1.A1_at	Endoglucanase 1	130.2878	100.6201	1.285865	0.031789
Zm.7143.1.S1_at	myc transcription factor7	121.0941	92.52363	1.290048	0.014569
Zm.5504.1.A1_at	cytochrome P450 10	270.0212	205.7631	1.291072	0.040155

Zm.15818.1.S1_at	ferredoxin5	137.5691	101.8842	1.345492	0.013609
Zm.82.1.S1_at	colored plant1	21.50298	14.95757	1.366478	0.030399
Zm.13245.1.S1_at	DRE-binding protein3	36.57809	28.14523	1.443894	0.0369
Zm.9621.1.A1_at	ethylene-responsive transcription factor 3	20.14214	14.47706	1.452114	0.010545
Zm.15283.1.A1_at	calcium-dependent protein kinase, isoform AK1	528.6183	392.4237	1.455673	0.012375
Zm.9194.1.A1_at	Ribose-5-phosphate isomerase	618.6478	457.5454	1.461399	0.0118
Zm.13865.1.S1_at	R2R3 Myb transcription factor MYB-IF35	191.447	138.6528	1.46164	0.022448
Zm.13728.1.S1_at	alpha-expansin 4	713.0032	550.5838	1.469181	0.038506
Zm.10660.1.A1_at	Plasma membrane-bound peroxidase 2b	44.71653	32.86686	1.472778	0.013812
Zm.332.1.A1_at	androgenic embryo3	164.2264	121.2994	1.477825	0.033814
Zm.1425.1.S1_at	senescence-associated protein DH	1942.728	1297.408	1.52712	0.028154
Zm.12391.1.S1_at	endochitinase PR4	59.33253	42.4276	1.547404	0.017039
Zm.8866.1.A1_at	expansin-like 3	880.9783	661.2306	1.562226	0.03113
Zm.10147.1.A1_at	NAC1 transcription factor	122.2175	86.68971	1.58396	0.018162
ZmAfx.720.1.A1_at	roothair defective3	143.5667	103.6674	1.590206	0.022651
Zm.12410.1.A1_at	CP5	182.8996	131.2834	1.605986	0.04061
ZmAfx.1005.1.S1_at	tassel seed1	237.0709	155.3582	1.809713	0.014651
Zm.17690.2.A1_a_at	dirigent-like protein	259.9264	166.3996	2.112215	0.037948
Zm.17519.1.A1_at	FIP1	111.7763	72.24284	2.156806	0.017482
Zm.18004.1.A1_at	dihydroflavonol-4-reductase	842.7272	457.6459	2.64704	0.010014
Zm.7611.1.A1_a_at	IAA24 - auxin-responsive Aux/IAA family member	425.7759	228.582	2.842572	0.016464
Zm.10850.1.S1_at	ZIM motif family protein	149.2168	69.48932	3.255649	0.046007
Zm.9463.1.A1_at	DRE-binding protein 4	176.9981	81.84146	3.520011	0.044695

Table E.3. Differential gene expression table for the *Beauveria bassiana* J18-treated *Zea mays* (maize) versus no-inoculum control comparison. Table lists putatively downregulated known (annotated) genes.

Probe ID	Gene title	J18	Control	Fold Change	P. Value
Zm.6398.2.S1_at	transposon protein Mutator sub-class	95.71094	131.0402	-1.50671	0.009109
Zm.10528.1.A1_at	oxidoreductase	62.19588	87.73384	-1.89389	0.005666
Zm.6398.1.A1_at	transposon protein Mutator sub-class	204.873	308.4533	-1.94525	0.008965
Zm.4471.2.S1_a_at	pyruvate, orthophosphate dikinase1	7.804075	11.71614	-2.30772	0.003211
Zm.6569.7.A1_x_at	40S ribosomal protein S15	3521.199	4111.662	-0.83627	0.048171
Zm.17096.1.S1_at	pale aleurone color1	472.7498	550.0545	-0.8382	0.047859
Zm.12634.5.S1_x_at	60S ribosomal protein L23	2001.869	2345.466	-0.84853	0.046029
Zm.14451.2.S1_at	60S ribosomal protein L29	2157.723	2515.501	-0.85242	0.045499
Zm.7097.2.A1_x_at	40S ribosomal protein S18	2948.043	3465.387	-0.85392	0.045816
Zm.6748.1.A1_x_at	ribosomal protein L26	2578.568	3010.72	-0.87014	0.043942
Zm.10128.1.S1_a_at	mitochondrial import receptor subunit TOM20	547.4862	645.1991	-0.87567	0.044178
Zm.6465.1.A1_at	60S ribosomal protein L23a	1843.845	2175.075	-0.87649	0.042279
Zm.16532.1.A1_x_at	60S ribosomal protein L18a	1152.125	1363.946	-0.8778	0.042116
Zm.8134.1.S1_at	snRK1-interacting protein 1	56.11329	65.3794	-0.88105	0.04174
Zm.16508.3.A1_x_at	ribosomal protein L39	1041.219	1219.408	-0.88283	0.049376
Zm.4665.1.A1_at	heat shock 70 kDa protein	265.6019	313.1762	-0.8836	0.048123
Zm.11805.1.A1_at	gibberellin-regulated protein 1	49.96933	58.50487	-0.88451	0.04282
Zm.878.2.S1_at	60S ribosomal protein L35	1670.042	1982.17	-0.88451	0.041863
Zm.14412.1.S1_a_at	LOC100194289 /// 60S ribosomal protein L32	2971.082	3507.619	-0.88931	0.040856
Zm.206.4.A1_x_at	40S ribosomal subunit protein S21	1198.622	1425.536	-0.89273	0.046007
Zm.12604.1.A1_at	DAG protein	95.96072	115.5579	-0.90411	0.03913
Zm.15855.3.A1_a_at	40S ribosomal protein S25-1	2227.208	2632.966	-0.90446	0.042973

ZmAffx.474.1.A1_at	U3 small nucleolar RNA-associated protein 11	202.0754	241.0197	-0.90555	0.039301
Zm.16963.2.S1_at	Voltage-gated potassium channel beta subunit	181.6239	214.198	-0.90569	0.039258
Zm.52.1.A1_at	root cap protein 1	521.5574	587.518	-0.91696	0.037902
Zm.878.1.S1_x_at	60S ribosomal protein L35	1830.954	2159.134	-0.91732	0.042796
Zm.497.1.A1_at	stomatin1	195.6856	229.5123	-0.91826	0.038022
Zm.3213.1.A1_at	40S ribosomal protein S25-1	1907.02	2252.263	-0.92085	0.041059
Zm.17271.8.A1_at	40S ribosomal protein S10	1192.202	1411.297	-0.92333	0.044726
Zm.6207.2.A1_at	60S ribosomal protein L15	2010.093	2378.561	-0.92405	0.03866
Zm.15936.1.A1_a_at	acidic ribosomal protein P1a	2625.003	3133.857	-0.92465	0.040361
Zm.878.1.S1_at	60S ribosomal protein L35	1415.126	1670.199	-0.93421	0.04241
Zm.16508.3.A1_at	ribosomal protein L39	718.5072	854.8417	-0.93533	0.041952
Zm.13514.2.S1_a_at	phytoene synthase2	41.75675	49.77021	-0.94574	0.034612
Zm.12148.1.S1_at	small nuclear ribonucleoprotein Sm D1	211.5115	252.4625	-0.94735	0.042831
Zm.9403.1.A1_at	ras-related protein Rab11B /// hypothetical protein LOC100382957	226.7253	270.4569	-0.94757	0.034351
Zm.14073.1.S1_s_at	60S ribosomal protein L28	1731.175	2046.609	-0.9487	0.041133
Zm.208.1.S1_at	TATA-binding protein2	220.0163	271.5787	-0.95753	0.033703
Zm.2489.1.A1_at	mitochondrial chaperonin-60	1202.949	1428.141	-0.97584	0.03196
Zm.9595.1.A1_at	seven transmembrane domain protein	103.4669	123.6452	-0.9816	0.031875
Zm.16304.1.A1_at	60S ribosomal protein L12	1918.352	2263.498	-0.98436	0.034895
Zm.317.1.S1_at	farnesyl pyrophosphate synthase1	390.2646	459.5221	-0.99566	0.030159
Zm.4471.4.A1_at	erg28 like protein	119.3069	144.9985	-0.99677	0.032933
Zm.12735.1.A1_at	mitochondrial 2-oxoglutarate/malate carrier protein /// LOC100274318	1514.308	1818.55	-0.99996	0.030428
Zm.6206.1.A1_at	60S ribosomal protein L35	226.5221	272.5152	-1.00522	0.039055
Zm.12089.1.S1_at	GPI-anchored protein	302.3392	365.5699	-1.00857	0.042456
Zm.3169.3.S1_at	60S ribosomal protein L33-B	1709.366	2069.702	-1.0098	0.028856
Zm.6991.1.A1_at	ribosomal protein L35 containing protein	481.8043	577.6487	-1.01198	0.028736
Zm.6207.5.S1_at	60S ribosomal protein L15	1700.418	2063.695	-1.01658	0.0296
Zm.7300.1.S1_at	acidic ribosomal protein P2a-2	2606.513	3175.395	-1.01795	0.029572
Zm.7165.1.A1_at	60S ribosomal protein L19-3	1005.12	1214.364	-1.01921	0.039872
Zm.6684.1.S1_a_at	60S ribosomal protein L29	1390.558	1660.549	-1.01983	0.0346
Zm.6625.2.S1_at	60S ribosomal protein L9	518.7944	630.797	-1.02227	0.032336
Zm.16533.1.S1_at	60S ribosomal protein L37	1643.892	1979.707	-1.02584	0.046857
Zm.15837.1.S1_at	60S ribosomal protein L37	1193.471	1450.249	-1.02864	0.043328
Zm.16532.4.S1_x_at	60S ribosomal protein L18a	409.7072	493.6776	-1.03112	0.044878
Zm.15424.1.S1_at	Metallothionein-like protein type 2	1034.035	1238.508	-1.0325	0.035532
Zm.13583.1.S1_at	Secretory protein	812.9129	1093.319	-1.03323	0.028215
Zm.6569.4.A1_a_at	40S ribosomal protein S15	947.5795	1145.795	-1.03558	0.034392
Zm.89.1.A1_at	mitochondrial chaperonin 60	732.637	879.3326	-1.03655	0.028855
Zm.999.1.A1_at	60S ribosomal protein L34	1438.367	1754.096	-1.03759	0.027941
Zm.14471.2.A1_at	60S ribosomal protein L7-2	2680.753	3249.796	-1.04579	0.0296
Zm.6532.2.S1_at	DNA binding protein	87.88976	111.0073	-1.05377	0.028433
Zm.2895.9.A1_x_at	60S ribosomal protein L44	1823.433	2212.847	-1.05516	0.029166
Zm.12819.1.S1_at	3-isopropylmalate dehydratase small subunit 2	702.917	882.2768	-1.06137	0.033659
Zm.3169.3.S1_x_at	60S ribosomal protein L33-B	2052.996	2514.253	-1.06845	0.024704
Zm.13938.2.S1_at	60S ribosomal protein L31	666.7583	800.5616	-1.07308	0.040984
Zm.15837.2.S1_s_at	60S ribosomal protein L37	1914.635	2354.277	-1.0857	0.023578
Zm.2076.1.A1_a_at	40S ribosomal protein S16	2773.016	3400.528	-1.09457	0.023469
Zm.14497.8.A1_x_at	60S ribosomal protein L27 /// 60S ribosomal protein L27	729.7298	894.2809	-1.10254	0.022807
Zm.12876.1.S1_at	24-methylenesterol C-methyltransferase 2	391.2522	487.4527	-1.10342	0.038786
Zm.2895.2.A1_a_at	60S ribosomal protein L44 /// 60S ribosomal protein L44 /// hypothetical protein LOC100384095	1352.989	1696.837	-1.11095	0.028709
Zm.7012.8.S1_a_at	Ribosomal protein S8	25.36471	31.51367	-1.11785	0.031266
Zm.436.1.S1_at	liguleless3	317.7297	424.8556	-1.12313	0.023679
Zm.16177.1.S1_at	40S ribosomal protein S10	1012.498	1248.711	-1.13117	0.023218

Zm.7081.2.S1_a_at	60S ribosomal protein L24 /// 60S ribosomal protein L24	2290.359	2849.84	-1.14082	0.034435
Zm.19006.1.S1_at	metal tolerance protein C3	29.09771	38.94516	-1.14801	0.033602
Zm.15424.1.S1_s_at	Metallothionein-like protein type 2	428.3762	522.5335	-1.161	0.019811
Zm.8277.1.S1_at	Granule bound starch synthase IIa precursor	33.10363	40.92177	-1.17731	0.019981
Zm.7081.3.S1_x_at	60S ribosomal protein L24	2224.631	2790.355	-1.17904	0.018914
Zm.16482.3.A1_x_at	60S ribosomal protein L4	1389.543	1738.391	-1.19051	0.01996
Zm.4781.1.S1_at	AGP16	195.2345	245.9201	-1.19593	0.01799
Zm.4471.5.A1_at	protein kinase APK1B	10.86284	13.1815	-1.19755	0.022205
Zm.13812.2.S1_x_at	60S ribosomal protein L11-1	1007.789	1261.135	-1.19971	0.021392
Zm.11259.1.A1_at	MADS19	72.07939	90.97287	-1.20361	0.025091
Zm.12097.1.A1_at	permease I	39.31204	48.18151	-1.2059	0.043881
Zm.7032.1.A1_at	60S ribosomal protein L7-1	571.8184	710.8306	-1.20938	0.018074
Zm.1056.1.S1_a_at	ribosomal protein S10p/S20e /// ribosomal protein S22 homolog	964.0031	1209.277	-1.21895	0.019969
Zm.12429.1.A1_at	conserved protein	137.4281	174.4817	-1.22391	0.017498
Zm.16482.3.A1_at	60S ribosomal protein L4	984.7169	1249.199	-1.23546	0.016459
Zm.5930.1.S1_at	60S ribosomal protein L37a /// 60S ribosomal protein L37a	538.5545	684.7113	-1.24031	0.017259
Zm.5139.1.S1_at	40S ribosomal protein SA	1207.417	1525.775	-1.26461	0.024198
Zm.295.1.A1_at	fatty acid elongase1	379.0839	468.3859	-1.29662	0.025334
Zm.14073.2.S1_a_at	60S ribosomal protein L28	1017.083	1306.285	-1.31241	0.01458
Zm.551.1.A1_at	glutathione S-transferase GST 25	76.95777	103.2624	-1.31468	0.026896
Zm.188.1.S1_s_at	ypt homolog1	106.1487	138.0537	-1.31907	0.029273
Zm.3349.1.S1_at	barley mlo defense gene homolog4	90.18582	118.343	-1.33614	0.018669
Zm.14497.16.S1_s_at	60S ribosomal protein L27	16.52461	21.7517	-1.36978	0.020211
Zm.1738.2.A1_at	soluble inorganic pyrophosphatase	1122.065	1527.399	-1.39807	0.011635
Zm.649.1.S1_at	ADP-glucose pyrophosphorylase small subunit	47.50378	60.53776	-1.40127	0.028819
Zm.6602.1.A1_at	homeobox-leucine zipper protein HAT7	77.41966	101.0687	-1.4205	0.038136
Zm.188.1.S1_at	ypt homolog1	27.57415	35.91009	-1.42161	0.011144
Zm.7960.1.A1_at	transparent testa 12 protein	755.0081	1004.849	-1.44999	0.010647
Zm.465.1.A1_at	acidic ribosomal protein P2a-3	636.3377	841.6201	-1.47126	0.010085
Zm.11985.1.A1_at	hemoglobin 2	48.80366	62.9249	-1.50457	0.01148
Zm.6146.1.A1_at	brassinosteroid biosynthesis-like protein	815.7466	1095.108	-1.5146	0.014268
Zm.5476.2.S1_at	IQ calmodulin-binding motif family protein	225.8117	301.318	-1.52682	0.015486
Zm.13691.1.S1_at	inositolphosphorylceramide-B C-26 hydroxylase	210.294	275.9144	-1.52817	0.011098
Zm.10011.1.A1_at	glycine-rich protein GRP5	20.8768	28.13418	-1.54918	0.011005
Zm.312.1.A1_at	ADP glucose pyrophosphorylase small subunit leaf1	78.40881	106.7028	-1.56066	0.014457
Zm.10207.2.A1_a_at	carboxylic ester hydrolase	91.97947	128.0867	-1.68837	0.010135
ZmAfx.126.1.A1_at	SSXT protein	101.2894	138.7573	-1.76031	0.026375
Zm.12726.1.S1_at	ADP-glucose pyrophosphorylase	88.63129	134.7703	-1.93274	0.033989
Zm.669.1.S1_at	alpha-expansin 5	60.13345	89.10541	-1.93282	0.010456
Zm.67.1.S1_at	Actin-depolymerizing factor	10.62973	15.31269	-2.02563	0.016368

Table E.4. Differential gene expression table for the *Beauveria bassiana* J18-treated *Zea mays* (maize) versus no-inoculum control comparison. Table lists putatively upregulated known (annotated) genes.

Probe ID	Gene title	J18	Control	Fold Change	P. Value
Zm.16929.1.S1_at	ribosomal proteinS15	210.7286	54.67376	5.998544	0.002215
Zm.13366.1.A1_a_at	RNA binding protein	132.3082	72.0302	5.01312	0.000212
Zm.2376.2.S1_at	Physical impedance induced protein	1464.771	666.9861	3.553539	0.000615
Zm.7422.1.A1_at	anthocyanidin 3-O-glucosyltransferase	113.8146	57.81319	3.125359	0.001233
Zm.2376.2.S1_x_at	Physical impedance induced protein	2231.656	1239.014	2.621297	0.001646
Zm.1684.1.S1_at	profilin homolog1	105.8402	63.02676	2.261551	0.004891
Zm.140.1.A1_at	root preferential4	1442.489	981.7574	2.23577	0.003102
Zm.10088.1.A1_at	remorin	67.60429	46.17261	1.767963	0.006915
Zm.3049.1.A1_s_at	DNA binding protein /// hypothetical protein LOC100381478	1026.616	763.9099	1.499109	0.009767
Zm.9001.1.A1_a_at	heavy metal-associated domain containing protein	539.0298	400.767	1.473786	0.009973
Zm.17690.2.A1_a_at	dirigent-like protein	754.0954	457.6459	2.166084	0.018073
Zm.11809.1.A1_at	phi-1-like phosphate-induced protein	535.5355	372.9202	1.948792	0.015393
Zm.7568.1.A1_at	blue copper protein	1169.207	742.2106	1.894438	0.011925
Zm.332.1.A1_at	androgenic embryo3	63.58521	42.4276	1.847008	0.010109
Zm.2032.1.S1_at	F-box protein interaction domain containing protein	426.4885	297.779	1.785767	0.024579
Zm.10827.1.S1_at	yellow stripe-like transporter 12	358.3965	253.2761	1.701472	0.040057
Zm.9001.2.A1_at	Heavy metal-associated domain containing protein	1343.16	955.5527	1.693845	0.011405
Zm.10660.1.A1_at	Plasma membrane-bound peroxidase 2b	1973.073	1297.408	1.594202	0.024977
Zm.2637.1.A1_at	oleosin Bn-V	32.22589	24.09359	1.566885	0.017062
Zm.3165.1.A1_at	terpene synthase 7	99.69891	76.811	1.539412	0.012223
Zm.17525.1.S1_at	sucrose transporter4	1217.394	881.2176	1.527496	0.013786
Zm.6977.5.S1_a_at	sucrose synthase	752.1472	562.2631	1.523608	0.040036
Zm.2376.1.A1_x_at	physical impedance induced protein1	6555.252	4675.833	1.470683	0.016794
Zm.7023.2.S1_a_at	surfactant protein B containing protein	1418.21	1085.525	1.46052	0.017651
Zm.7677.1.A1_at	metal ion binding protein	1473.51	1099.594	1.428414	0.048581
Zm.456.1.S1_at	maize insect resistance1	60.71415	46.40119	1.426673	0.014885
Zm.5565.1.S1_at	cysteine protease1	6376.971	4794.843	1.401438	0.011239
Zm.11848.1.A1_at	calmodulin	231.4582	172.166	1.379924	0.020691
Zm.11367.1.A1_at	nucleoside transporter	1555.076	1181.951	1.352667	0.018688
Zm.9001.1.A1_x_at	heavy metal-associated domain containing protein	416.7643	319.3615	1.345677	0.013915
Zm.94.1.A1_at	DNA binding with one finger2	54.14289	40.71605	1.342503	0.026753
Zm.7023.2.S1_x_at	surfactant protein B containing protein	1298.518	1016.699	1.306516	0.017259
Zm.255.1.A1_at	Legumain-like protease	412.6172	312.4058	1.271876	0.022808
Zm.3785.1.S1_at	nuclear protein /// hypothetical protein LOC100303799	1381.459	1147.296	1.270793	0.04656
Zm.13591.1.S1_at	glutathione transferase42	381.4134	274.4136	1.248753	0.028996
Zm.1585.1.S1_at	profilin homolog2	48.79334	37.23922	1.240041	0.039801
Zm.608.1.S1_at	plasma membrane intrinsic protein2	52.48614	40.72969	1.187381	0.018711
Zm.8215.1.A1_at	anther-specific proline-rich protein APG	18.8275	14.67534	1.1832	0.025111
Zm.9689.1.A1_at	plant integral membrane protein TIGR01569 containing protein	66.37838	52.61582	1.162559	0.036542
Zm.6788.1.A1_at	<i>Zea floricaula</i> /leafy1	37.4907	28.6129	1.148603	0.039704
Zm.17762.1.S1_at	hydrophobic protein LTI6B	1572.437	1252.658	1.148527	0.020684
Zm.499.1.S1_at	hypersensitive induced reaction3	937.1212	727.7788	1.136611	0.032102
Zm.10032.1.S1_at	heat shock factor protein 4	253.5183	204.1579	1.131412	0.033883
Zm.12309.1.S1_at	ABA-induced protein	80.36052	63.78196	1.130775	0.024536
Zm.6905.3.S1_at	Histone H1-like protein	31.78439	24.56064	1.102227	0.04617
Zm.305.1.A1_at	crinkly4	42.90509	33.17172	1.096401	0.027577
Zm.7342.1.A1_at	legumin1	17.66686	13.83155	1.087103	0.025698
Zm.13870.2.A1_at	R2R3MYB-domain protein	75.21666	60.21594	1.083612	0.046627
Zm.17315.1.A1_at	L-ascorbate oxidase	1875.757	1526.104	1.081156	0.042603

Zm.17735.1.A1_at	Lipid binding protein	334.3975	271.5642	1.077737	0.024904
Zm.2376.1.A1_a_at	cortical cell-delineating protein /// physical impedance induced protein1	6069.936	4697.065	1.075194	0.026603
Zm.662.1.S1_at	FDR3	26.21688	20.99364	1.058778	0.03746
Zm.13257.1.S1_at	scarecrow-like1	32.09078	27.12417	1.051686	0.03195
Zm.737.1.A1_at	cysteine protease2	4466.622	3551.917	1.049344	0.042495
Zm.14909.1.A1_at	Tonoplast intrinsic protein1	92.3779	74.69754	1.034429	0.042645
Zm.548.1.S1_at	glutathione transferase19	1038.293	881.4248	1.029746	0.033546
Zm.14528.1.S1_at	embryo-sac basal-endosperm-layer embryo-surrounding-region2	17.67167	14.06051	1.029431	0.030809
Zm.584.1.S1_a_at	pericarp color1	57.68725	47.38813	1.012034	0.036925
Zm.5319.1.S1_a_at	lipoxygenase	269.8549	219.1112	1.011022	0.029483
ZmAffx.880.1.S1_at	protein kinase-like	74.95136	60.17009	0.997338	0.037904
Zm.737.1.A1_a_at	cysteine protease2	6883.162	5531.259	0.996822	0.036119
Zm.8711.1.S1_a_at	autophagy-related 8d	1814.093	1500.518	0.996172	0.035689
Zm.864.1.S1_at	glutathione transferase30	553.9576	429.3382	0.991807	0.032239
Zm.368.1.A1_a_at	glucose-6-phosphate/phosphate- translocator precursor /// hypothetical protein LOC100193334	1221.349	999.6353	0.952975	0.034419
Zm.4803.1.S1_at	actin2	3117.471	2484.172	0.948025	0.037681
Zm.8711.2.S1_x_at	autophagy-related 8d	1802.338	1493.589	0.947013	0.044695
Zm.18955.1.A1_at	tRNA-splicing endonuclease subunit Sen2	309.5232	259.2515	0.938467	0.037285
Zm.11932.1.A1_at	Ocs element-binding factor 1	35.27637	29.08522	0.924004	0.041129
Zm.8611.2.A1_at	rapid alkalization factor 1	204.078	166.0661	0.91702	0.047738
Zm.11768.1.S1_at	RING-H2 finger protein ATL2B	160.0908	135.5003	0.898212	0.039631
Zm.3830.1.S1_at	aspartic proteinase oryzasin-1	3023.556	2608.847	0.896056	0.043473
Zm.13935.1.S1_at	teosinte branched1	14.75692	11.89888	0.893952	0.043387
Zm.15817.1.S1_x_at	protein kinase catalytic domain	139.1578	113.2614	0.893849	0.047178
Zm.14916.4.S1_a_at	ubiquitin-conjugating enzyme E2-21 kDa 1 /// LOC100193596	1953.307	1653.928	0.89232	0.048026
Zm.822.1.A1_x_at	Meiosis 5	28.43097	23.66332	0.869095	0.043505
Zm.4068.2.A1_at	Ferredoxin-NADP reductase precursor	21.4652	17.63188	0.853384	0.047702
Zm.237.1.S1_at	SBP-domain protein3	30.75763	25.92706	0.832296	0.049245

References

- Alexandrov NN, Brover VV, Freidin S, Troukhan ME, Tatarinova TV, Zhang H, Swaller TJ, Lu YP, Bouck J, Flavell RB, Feldmann KA (2009) Insights into corn genes derived from large-scale cDNA sequencing. *Plant Mol Biol* 69:179–94.
- Alfano G, Ivey MLL, Cakir C, Bos JIB, Miller SA, Madden LV, Kamoun S, Hoitink HAJ (2007) Systemic modulation of gene expression in tomato by *Trichoderma hamatum* 382. *Phytopath* 97: 429–437
- Alfenito MR, Souer E, Goodman CD, Buell R, Mol J, Koes R, Walbot V (1998) Functional complementation of anthocyanin sequestration in the vacuole by widely divergent glutathione S-transferases. *Plant Cell* 10:1135–1149
- Altschul SF, Gish W, Miller W, Myers EW, Lipman DJ (1990) Basic local alignment search tool. *J Mol Biol* 215:403–410
- Altschul SF, Madden TL, Schäffer AA, Zhang J, Zhang Z, Miller W, Lipman DJ (1997) Gapped BLAST and PSI-BLAST: a new generation of protein database search programs. *Nucleic Acids Res* 25:3389–3402
- Anderson JP, Gleason CA, Foley RC, Thrall PH, Burdon JB, Singh KB (2010) Plants versus pathogens: an evolutionary arms race. *Func Plant Biol: FPB* 37:499–512
- Anderson MJ (2001) A new method for non-parametric multivariate analysis of variance. *Austral Ecol* 26:32–46 doi:10.1111/j.1442-9993.2001.01070.pp.x
- Andreote FD, de Araujo WL, de Azevedo JL, van Elsas JD, da Rocha UN, van Overbeek LS (2009) Endophytic colonization of potato (*Solanum tuberosum* L.) by a novel competent bacterial endophyte, *Pseudomonas putida* strain P9, and its effect on associated bacterial communities. *App Environ Microbiol* 75:3396–3406
- Applied Biosystems (2003). http://www6.appliedbiosystems.com/support/tutorials/pdf/quant_pcr.pdf
- Argenta G, Silva PRFd, Sangoi L (2004) Leaf relative chlorophyll content as an indicator parameter to predict nitrogen fertilization in maize. *Ciência Rural* 34:1379–1387
- Arimura G, Matsui K, Takabayashi J (2009) Chemical and molecular ecology of herbivore-induced plant volatiles: proximate factors and their ultimate functions. *Plant Cell Phys* 50:911–923
- Arnold AE, Lutzoni F (2007) Diversity and host range of foliar fungal endophytes: Are tropical leaves biodiversity hotspots? *Ecol* 88:541–549
- Bacon CW, White JF (2016) Functions, mechanisms and regulation of endophytic and epiphytic microbial communities of plants. *Symbiosis* 68:87–98
- Badri DV, Vivanco JM (2009) Regulation and function of root exudates. *Plant Cell Environ* 32:666–681 doi:10.1111/j.1365-3040.2009.01926.x
- Bae H, Roberts DP, Lim HS, Strem MD, Park SC, Ryu CM, Melnick RL, Bailey BA (2011) Endophytic *Trichoderma* isolates from tropical environments delay disease onset and induce resistance against *Phytophthora capsici* in hot pepper using multiple mechanisms. *Mol Plant-Microbe Interact* 24:336–351
- Bae H, Sicher RC, Kim MS, Kim SH, Strem MD, Melnick RL, Bailey BA (2009) The beneficial endophyte *Trichoderma hamatum* isolate DIS 219b promotes growth and delays the onset of the drought response in *Theobroma cacao*. *J Exp Bot* 60:3279–3295
- Bailey BA, Bae H, Strem MD, Roberts DP, Thomas SE, Crozier J, Samuels GJ, Choi IY, Holmes KA (2006) Fungal and plant gene expression during the colonization of cacao seedlings by endophytic isolates of four *Trichoderma* species. *Planta* 224, 1449–1464.
- Baker R (1991) Diversity in biological-control. *Crop Protect* 10:85–94
- Baltruschat H, Fodor J, Harrach BD, Niemczyk E, Barna B, Gullner G, Janeczko A, Kogel KH, Schäfer P, Schwarczinger I, Zuccaro A, Skoczowski A. (2008) Salt tolerance of barley induced by the root endophyte *Piriformospora indica* is associated with a strong increase in antioxidants. *New Phytol* 180: 501–510

- Banhara A, Ding Y, Kuhner R, Zuccaro A, Parniske M (2015) Colonization of root cells and plant growth promotion by *Piriformospora indica* occurs independently of plant common symbiosis genes. *Front Plant Sci* 6:667 doi:10.3389/fpls.2015.00667
- Barea JM, Azcon R, Azcon-Aguilar C (2002) Mycorrhizosphere interactions to improve plant fitness and soil quality. *Antonie van Leeuwenhoek* 81:343-351
- Barelli L, Moonjely S, Behie SW, Bidochka MJ (2016) Fungi with multifunctional lifestyles: endophytic insect pathogenic fungi. *Plant Mol Biol* 90:657-664
- Barrieu F, Chaumont F, Chrispeels MJ (1998) High expression of the tonoplast aquaporin ZmTIP1 in epidermal and conducting tissues of maize. *Plant Phys* 117:1153-1163
- Behie SW, Bidochka MJ (2014) Ubiquity of insect-derived nitrogen transfer to plants by endophytic insect-pathogenic fungi: an additional branch of the soil nitrogen cycle. *App Environ Microbiol* 80:1553-1560
- Behie SW, Jones SJ, Bidochka MJ (2015) Plant tissue localization of the endophytic insect pathogenic fungi *Metarhizium* and *Beauveria*. *Fungal Ecol* 13:112-119
- Behie SW, Zelisko PM, Bidochka MJ (2012) Endophytic insect-parasitic fungi translocate nitrogen directly from insects to plants. *Science* 336:1576-1577
- Beneloujaephajri E, Costa A, L'Haridon F, Metraux JP, Binda M (2013) Production of reactive oxygen species and wound-induced resistance in *Arabidopsis thaliana* against *Botrytis cinerea* are preceded and depend on a burst of calcium. *BMC Plant Biol* 13:160
- Bidochka MJ, Kamp AM, Lavender TM, Dekoning J, De Croos JNA (2001) Habitat association in two genetic groups of the insect-pathogenic fungus *Metarhizium anisopliae*: Uncovering cryptic species? *App Environ Microbiol* 67:1335-1342
- Bidochka MJ, Kasperski JE, Wild GAM (1998) Occurrence of the entomopathogenic fungi *Metarhizium anisopliae* and *Beauveria bassiana* in soils from temperate and near-northern habitats. *Can J Bot* 76:1198-1204
- Bienert GP, Chaumont F (2014) Aquaporin-facilitated transmembrane diffusion of hydrogen peroxide. *Biochimica Et Biophysica Acta* 1840:1596-1604
- Bienert GP, Schussler MD, Jahn TP (2008) Metalloids: essential, beneficial or toxic? Major intrinsic proteins sort it out. *Trends Biochem Sci* 33:20-26
- Bing LA, Lewis LC (1991) Suppression of *Ostrinia nubilalis* (Hubner) (Lepidoptera, Pyralidae) by endophytic *Beauveria bassiana* (Balsamo) Vuillemin. *Environ Ento* 20:1207-1211
- Bing LA, Lewis LC (1992a) Endophytic *Beauveria bassiana* (Balsamo) Vuillemin in corn: the influence of the plant growth stage and *Ostrinia nubilalis* (Hubner). *Biocon Sci Tech* 2:39-47
- Bing LA, Lewis LC (1992b) Temporal relationships between *Zea mays*, *Ostrinia nubilalis* (Lep, Pyralidae) and endophytic *Beauveria bassiana*. *Entomophaga* 37:525-536
- Bing LA, Lewis LC (1993) Occurrence of the entomopathogen *Beauveria bassiana* (Balsamo) Vuillemin in different tillage regimes and in *Zea mays* L and virulence towards *Ostrinia nubilalis* (Hubner). *Agric Ecosyst Environ* 45:147-156
- Bissett J, Widden P (1988) A new species of *Beauveria* isolated from scottish moorland soil. *Can J Bot-Rev Can Bot* 66:361-362
- Biswas C, Dey P, Satpathy S, Satya P (2012) Establishment of the fungal entomopathogen *Beauveria bassiana* as a season long endophyte in jute (*Corchorus olitorius*) and its rapid detection using SCAR marker. *Biocon* 57:565-571
- Bjorkman T, Blanchard LM, Harman GE (1998) Growth enhancement of shrunken-2 (sh2) sweet corn by *Trichoderma harzianum* 1295-22: Effect of environmental stress. *J Am Soc Hort Sci* 123:35-40
- Bolstad BM, Irizarry RA, Astrand M, Speed TP (2003) A comparison of normalization methods for high density oligonucleotide array data based on variance and bias. *Bioinformatics (Oxford, England)* 19:185-193
- Bonaldi M, Chen XYL, Kunova A, Pizzatti C, Saracchi M, Cortesi P (2015) Colonization of lettuce rhizosphere and roots by tagged *Streptomyces*. *Front Microbiol* 6
- Bonfante P, Genre A (2010) Mechanisms underlying beneficial plant-fungus interactions in mycorrhizal symbiosis. *Nature Comm* 1:48

- Bonkowski M (2004) Protozoa and plant growth: the microbial loop in soil revisited *New Phytol* 162:617-631
- Bordiec, S, Paquis, S, Lacroix, H, Dhondt, S, Ait Barka, E, Kauffmann, S, Jeandet, P, Mazeyrat-Gourbeyre, F, Clement, C, Baillieul, F, Dorey, S, (2011) Comparative analysis of defence responses induced by the endophytic plant growth-promoting rhizobacterium *Burkholderia phytofirmans* strain PsJN and the non-host bacterium *Pseudomonas syringae* pv. pisi in grapevine cell suspensions. *J Exp Bot* 62:595-603
- Brimner TA, Boland GJ (2003) A review of the non-target effects of fungi used to biologically control plant diseases *Agric Ecosys Environ* 100:3-16
- Brotman Y, Landau, U, Cuadros-Inostroza, A, Takayuki, T, Fernie, AR, Chet, I, Viterbo, A, Willmitzer, L. (2013) *Trichoderma*-plant root colonization: Escaping early plant defense responses and activation of the antioxidant machinery for saline stress tolerance. *PLoS Path* 9 doi:10.1371/journal.ppat.1003221
- Brown SDJ, Collins RA, Boyer S, Lefort M-C, Malumbres-Olarte J, Vink CJ, Cruickshank RH (2012) Spider: An R package for the analysis of species identity and evolution, with particular reference to DNA barcoding. *Mol Ecol Resources* 12:562-565 doi:10.1111/j.1755-0998.2011.03108.x
- Brownbridge M, Reay SD, Nelson TL, Glare TR (2012) Persistence of *Beauveria bassiana* (Ascomycota: Hypocreales) as an endophyte following inoculation of radiata pine seed and seedlings. *Biol Control* doi:http://dx.doi.org/10.1016/j.biocontrol.2012.01.002
- Bruck DJ (2005) Ecology of *Metarhizium anisopliae* in soilless potting media and the rhizosphere: implications for pest management. *Biol Control* 32:155-163 doi:10.1016/j.biocontrol.2004.09.003
- Bruck DJ (2010) Fungal entomopathogens in the rhizosphere. *Biocon* 55:103-112 doi:10.1007/s10526-009-9236-7
- Burgdorf RJ, Laing MD, Morris CD, Jamal-Ally SF (2014) A procedure to evaluate the efficiency of surface sterilization methods in culture-independent fungal endophyte studies. *Brazilian J Microbiol* 45:977-983
- Burgmann H, Meier S, Bunge M, Widmer F, Zeyer J (2005) Effects of model root exudates on structure and activity of a soil diazotroph community. *Environ Microbiol* 7:1711-1724 doi:10.1111/j.1462-2920.2005.00818.x
- Campbell CD, Chapman SJ, Cameron CM, Davidson MS, Potts JM (2003) A rapid microtiter plate method to measure carbon dioxide evolved from carbon substrate amendments so as to determine the physiological profiles of soil microbial communities by using whole soil. *App Environ Microbiol* 69:3593-3599 doi:10.1128/aem.69.6.3593-3599.2003
- Campos RA, Boldo JT, Pimentel IC, Dalfovo V, W.L. Araújo WL, Azeved JL, Vainstein MH, Barros NM (2010) Endophytic and entomopathogenic strains of *Beauveria* sp to control the bovine tick *Rhipicephalus (Boophilus) microplus*. *Gen Mol Res* 9:1421-1430 doi:10.4238/vol9-3gmr884
- Cardenas L, Martinez A, Sanchez F, Quinto C (2008) Fast, transient and specific intracellular ROS changes in living root hair cells responding to Nod factors (NFs). *Plant J* 56:802-813 doi:10.1111/j.1365-313X.2008.03644.x
- Carroll G (1988) Fungal endophytes in stems and leaves – from latent pathogen to mutualistic symbiont. *Ecol* 69:2-9 doi:10.2307/1943154
- Carroll GC (1986) The biology of endophytism in plants with particular reference to woody perennials In: Fokkema N.J. vdHJ (ed) *Microbiology in the Phyllosphere*. Cambridge University Press, Cambridge, pp 205-222
- Castillo-Lopez D, Sword GA (2015) The endophytic fungal entomopathogens *Beauveria bassiana* and *Purpureocillium lilacinum* enhance the growth of cultivated cotton (*Gossypium hirsutum*) and negatively affect survival of the cotton bollworm (*Helicoverpa zea*). *Biol Control* 89:53-60 doi:10.1016/j.biocontrol.2015.03.010
- Castillo-Lopez D, Zhu-Salzman K, Ek-Ramos MJ, Sword GA (2014) The entomopathogenic fungal endophytes *Purpureocillium lilacinum* (formerly *Paecilomyces lilacinus*) and *Beauveria bassiana* negatively affect cotton aphid reproduction under both greenhouse and field conditions. *PLoS One* 9:e103891-e103891 doi:10.1371/journal.pone.0103891

- Castrillo LA, Vandenberg JD, Wraight SP (2003) Strain-specific detection of introduced *Beauveria bassiana* in agricultural fields by use of sequence-characterized amplified region markers. *J Invertebr Pathol* 82:75-83
- Castro FA, Campostrini E, Torres Netto A, Viana LH (2011) Relationship between photochemical efficiency (JIP-Test Parameters) and portable chlorophyll meter readings in papaya plants. *Brazilian J Plant Phys* 23:295-304
- Chandler D, Bailey AS, Tatchell GM, Davidson G, Greaves J, Grant WP (2011) The development, regulation and use of biopesticides for integrated pest management. *Philosophical Transactions of the Royal Society B: Biol Sci* 366:1987-1998 doi:10.1098/rstb.2010.0390
- Chassot C, Buchala A, Schoonbeek HJ, Metraux JP, Lamotte O (2008) Wounding of *Arabidopsis* leaves causes a powerful but transient protection against *Botrytis* infection. *Plant J* 55:555-567 doi:10.1111/j.1365-313X.2008.03540.x
- Chaumont F, Barrieu F, Herman EM, Chrispeels MJ (1998) Characterization of a maize tonoplast aquaporin expressed in zones of cell division and elongation. *Plant Physiol* 117:1143-1152
- Chaumont F, Barrieu F, Jung R, Chrispeels MJ (2000) Plasma membrane intrinsic proteins from maize cluster in two sequence subgroups with differential aquaporin activity. *Plant Physiol* 122:1025-1034 doi:10.1104/pp.122.4.1025
- Chen W-H, Han Y-F, Liang Z-Q, Jin D-C (2017) A new araneogenous fungus in the genus *Beauveria* from Guizhou, China. *Phytotaxa* 302:8 doi:10.11646/phytotaxa.302.1.5
- Cheng C, Li LM (2005) Sub-array normalization subject to differentiation. *Nucleic Acids Res* 33:5565-5573 doi:10.1093/nar/gki844
- Cheplick GP, Clay K (1988) Acquired chemical defenses in grasses – the role of fungal endophytes. *Oikos* 52:309-318 doi:10.2307/3565204
- Cherry AJ, Lomer CJ, Djegui D, Schulthess F (1999) Pathogen incidence and their potential as microbial control agents in IPM of maize stem borers in West Africa. *Biocon* 44:301-327 doi:10.1023/a:1009991724251
- Chisholm ST, Coaker G, Day B, Staskawicz BJ (2006) Host-microbe interactions: shaping the evolution of the plant immune response. *Cell* 124:803-814 doi:10.1016/j.cell.2006.02.008
- Choudhary DK, Prakash A, Johri BN (2007) Induced systemic resistance (ISR) in plants: mechanism of action. *Indian J of Microbiol* 47:289-297 doi:10.1007/s12088-007-0054-2
- Chrispeels MJ, Crawford NM, Schroeder JI (1999) Proteins for transport of water and mineral nutrients across the membranes of plant cells. *Plant Cell* 11:661-675
- Christensen MJ, Bennett RJ, Ansari HA, Koga H, Johnson RD, Bryan GT, Simpson WR, Koolaard JP, Nickless EM, Voisey CR (2008) *Epichloë* endophytes grow by intercalary hyphal extension in elongating grass leaves. *Fungal Genetics Biol* 45:84-93 doi:10.1016/j.fgb.2007.07.013
- Clarke JD, Zhu T (2006) Microarray analysis of the transcriptome as a stepping stone towards understanding biological systems: practical considerations and perspectives. *Plant J* 45:630-650 doi:10.1111/j.1365-313X.2006.02668.x
- Clarke KR, Gorley RN, Somerfield PJ, Warwick RM (2014) Change in marine communities: an approach to statistical analysis and interpretation. 3 edn. PRIMER-E, Plymouth, UK.
- Clarke KR, Green RH (1988) Statistical design and analysis for a biological effects study. *Marine Ecology Progress Series* 46:213-226 doi:10.3354/meps046213
- Clay K (1989) Clavicipitaceous endophytes of grasses - their potential as biocontrol agents. *Mycol Res* 92:1-12
- Clay K, Jones JP (1984) Transmission of *Atkinsonella hypoxylon* (Clavicipitaceae) by cleistogamous seed of *Danthonia spicata* (Gramineae). *Can J Bot-Rev Can Bot* 62:2893-2895
- Coleman DC (2008) From peds to paradoxes: linkages between soil biota and their influences on ecological processes. *Soil Biol Biochem* 40:271-289
- Conrath U, Pieterse CM, Mauch-Mani B (2002) Priming in plant-pathogen interactions. *Trends Plant Sci* 7:210-216
- Cook RJ (1993) Making greater use of introduced microorganisms for biological-control of plant-pathogens. *Ann Rev Phytopath* 31:53-80 doi:10.1146/annurev.py.31.090193.000413
- Cripps-Guazzone N (2014) Rhizosphere competence of selected *Trichoderma* species. PhD thesis. Lincoln University

- da Silva KRA, Salles JF, Seldin L, van Elsas JD (2003) Application of a novel *Paenibacillus*-specific PCR-DGGE method and sequence analysis to assess the diversity of *Paenibacillus* spp. in the maize rhizosphere. J Microbiol Methods 54:213-231 doi:10.1016/s0167-7012(03)00039-3
- Dangl JL, Jones JD (2001) Plant pathogens and integrated defence responses to infection. Nature 411:826-833 doi:10.1038/35081161
- De Bary A (1866) Morphologie und physiologie der pilze, flechten und myxomyceten. W. Engelmann.
- Deacon JW, Berry LA (1993) Biocontrol of soil-borne plant-pathogens - concepts and their application. Pest Sci 37:417-426 doi:10.1002/ps.2780370417
- Dematheis F, Zimmerling U, Flocco C, Kurtz B, Vidal S, Kropf S, Smalla K (2012) Multitrophic interaction in the rhizosphere of maize: Root feeding of Western Corn Rootworm larvae alters the microbial community composition. PLoS One 7:e37288 doi:10.1371/journal.pone.0037288
- Dempsey DA, Klessig DF (2012) SOS - too many signals for systemic acquired resistance? Trends Plant Sci 17:538-545 doi:10.1016/j.tplants.2012.05.011
- Dicke M (2016) Plant phenotypic plasticity in the phytobiome: a volatile issue. Curr Opin Plant Biol 32:17-23 doi:10.1016/j.pbi.2016.05.004
- Doornbos RF, Geraats BP, Kuramae EE, Van Loon LC, Bakker PA (2011) Effects of jasmonic acid, ethylene, and salicylic acid signaling on the rhizosphere bacterial community of *Arabidopsis thaliana*. Mol Plant-microbe Inter 24:395-407 doi:10.1094/mpmi-05-10-0115
- Dudareva N, Negre F, Nagegowda DA, Orlova I (2006) Plant volatiles: Recent advances and future perspectives. Critical Reviews in Plant Sciences 25:417-440 doi:10.1080/07352680600899973
- Dwyer LM, Tollenaar M, Houwing L (1991) A nondestructive method to monitor leaf greenness in corn. Can J Plant Sci 71:505-509 doi:10.4141/cjps91-070
- Dynowski M, Schaaf G, Loque D, Moran O, Ludewig U (2008) Plant plasma membrane water channels conduct the signalling molecule H₂O₂. Biochem J 414:53-61 doi:10.1042/bj20080287
- Eaton CJ, Cox MP, Ambrose B, Becker M, Hesse U, Schardl CL, Scott B (2010) Disruption of signaling in a fungal-grass symbiosis leads to pathogenesis. Plant Physiol 153:1780-1794 doi:10.1104/pp.110.158451
- Eilenberg J, Hajek A, Lomer C (2001) Suggestions for unifying the terminology in biological control. Biocont 46:387-400 doi:10.1023/a:1014193329979
- El-Deeb HM, Lashin SM, Arab YA (2012) Reaction of some tomato cultivars to tomato leaf curl virus and evaluation of the endophytic colonisation with *Beauveria bassiana* on the disease incidence and its vector, *Bemisia tabaci*. Arch Phytopath Plant Prot 45:1538-1545 doi:10.1080/03235408.2012.681246
- Elasri M et al. (2001) Acyl-homoserine lactone production is more common among plant-associated *Pseudomonas* spp. than among soilborne *Pseudomonas* spp. App Environ Microbiol 67:1198-1209 doi:10.1128/aem.67.3.1198-1209.2001
- Elliot SL, Sabelis MW, Janssen A, van der Geest LPS, Beerling EAM, Fransen J (2000) Can plants use entomopathogens as bodyguards? Ecol Letters 3:228-235
- Ellis C, Turner JG (2001) The *Arabidopsis* mutant cev1 has constitutively active jasmonate and ethylene signal pathways and enhanced resistance to pathogens. Plant Cell 13:1025-1033
- Erb M, Flors V, Karlen D, De Lange E, Planchamp C, D'Alessandro M, Turlings TCJ, Ton J (2009) Signal signature of aboveground-induced resistance upon belowground herbivory in maize. Plant J 59:292-302 doi:10.1111/j.1365-3113X.2009.03868.x
- Ernst M, Mendgen KW, Wirsig SG (2003) Endophytic fungal mutualists: seed-borne *Stagonospora* spp. enhance reed biomass production in axenic microcosms. Mol Plant-Microbe Inter 16:580-587 doi:10.1094/mpmi.2003.16.7.580
- Fakruddin MM (2013) Methods for analyzing diversity of microbial communities in natural environments. Ceylon J Sci:19-33
- Fang WG, St Leger RJ (2010) Mrt, a gene unique to fungi, encodes an oligosaccharide transporter and facilitates rhizosphere competency in *Metarhizium robertsii*. Plant Physiol 154:1549-1557 doi:10.1104/pp.110.163014

- Faria MRD, Wraight SP (2007) Mycoinsecticides and *Mycoacaricides*: A comprehensive list with worldwide coverage and international classification of formulation types. *Biol Control* 43:237-256 doi.org/10.1016/j.biocontrol.2007.08.001
- Felitti S, Shields K, Ramsperger M, Tian P, Sawbridge T, Webster T, Logan E, Erwin T, Forster J, Edwards D, Spangenberg G (2006) Transcriptome analysis of *Neotyphodium* and *Epichloe* grass endophytes. *Fungal Gen Biology* 43:465-475 doi:10.1016/j.fgb.2006.01.013
- Felten J, Kohler A, Morin E, Bhalerao RP, Palme K, Martin F, Ditengou FA, Legué V. (2009) The ectomycorrhizal fungus *Laccaria bicolor* stimulates lateral root formation in poplar and *Arabidopsis* through auxin transport and signaling. *Plant Physiol* 151:1991-2005 doi:10.1104/pp.109.14723
- Ferreira GF, Baltazar Lde M, Santos JR, Monteiro AS, Fraga LA, Resende-Stoianoff MA, Santos DA (2013) The role of oxidative and nitrosative bursts caused by azoles and amphotericin B against the fungal pathogen *Cryptococcus gattii*. *The Journal of antimicrobial chemotherapy* 68:1801-1811 doi:10.1093/jac/dkt114
- Fisher JJ, Rehner SA, Bruck DJ (2011) Diversity of rhizosphere associated entomopathogenic fungi of perennial herbs, shrubs and coniferous trees. *J of Invert Path* 106:289-295 doi:10.1016/j.jip.2010.11.001
- Fitter AH, Gilligan CA, Hollingworth K, Kleczkowski A, Twyman RM, Pitchford JW (2005) Biodiversity and ecosystem function in soil. *Functional Ecology* 19:369-377 doi:10.1111/j.0269-8463.2005.00969.x
- Francis R, Read DJ (1995) Mutualism and anamorphism in the mycorrhizal symbiosis, with special reference to impacts on plant community structure. *Can J Bot-Rev Can Bot* 73:S1301-S1309
- Franken P (2012) The plant strengthening root endophyte *Piriformospora indica*: potential application and the biology behind. *Appl Microbiol Biotechnol* 96:1455-1464 doi:10.1007/s00253-012-4506-1
- Frear DS, Swanson HR (1970) Biosynthesis of S-(4-ethylamino-6-isopropylamino-2-s-triazino) glutathione: Partial purification and properties of a glutathione S-transferase from corn. *Phytochemistry* 9:2123-2132 doi:http://dx.doi.org/10.1016/S0031-9422(00)85377-7
- Frederickson Matika DE, Loake GJ (2014) Redox regulation in plant immune function. *Antioxidants Redox Signaling* 21:1373-1388 doi:10.1089/ars.2013.5679
- Freeman WM, Walker SJ, Vrana KE (1999) Quantitative RT-PCR: pitfalls and potential. *BioTechniques* 26:112-122, 124-115
- Frey-Klett P, Burlinson P, Deveau A, Barret M, Tarkka M, Sarniguet A (2011) Bacterial-Fungal Interactions: Hyphens between Agricultural, Clinical, Environmental, and Food Microbiologists. *Microbiol Mol Biol Rev* 75:583-+ doi:10.1128/mmb.00020-11
- Fu ZQ, Dong X (2013) Systemic acquired resistance: turning local infection into global defense. *Annual review of plant biology* 64:839-863 doi:10.1146/annurev-arplant-042811-105606
- Ganley RJ, Newcombe G (2006) Fungal endophytes in seeds and needles of *Pinus monticola*. *Mycol Res* 110:318-327 doi:10.1016/j.mycres.2005.10.005
- Gao KX, Mendgen K (2006) Seed-transmitted beneficial endophytic *Stagonospora* sp. can penetrate the walls of the root epidermis, but does not proliferate in the cortex, of *Phragmites australis*. *Can J Bot-Rev Can Bot* 84:981-988 doi:10.1139/b06-056
- Gautier L, Cope L, Bolstad BM, Irizarry RA (2004) affy--analysis of Affymetrix GeneChip data at the probe level *Bioinformatics (Oxford, England)* 20:307-315 doi:10.1093/bioinformatics/btg405
- Glare TR, Inwood AJ (1998) Morphological and genetic characterisation of *Beauveria* spp. from New Zealand. *Mycol Res* 102:250-256
- Glare TR, Reay SD, Nelson TL, Moore R (2008) *Beauveria caledonica* is a naturally occurring pathogen of forest beetles. *Mycol Res* 112:352-360 doi:10.1016/j.mycres.2007.10.015
- Glazebrook J (2005) Contrasting mechanisms of defense against biotrophic and necrotrophic pathogens. *Annu Rev Phytopathol* 43:205-227 doi:10.1146/annurev.phyto.43.040204.135923
- Glick BR, Penrose DM, Li J (1998) A model for the lowering of plant ethylene concentrations by plant growth-promoting bacteria. *J Theor Biol* 190:63-68 doi:10.1006/jtbi.1997.0532

- Goettel MS, Eilenberg J, Glare TR (2010) Entomopathogenic fungi and their role in regulation of insect populations. Academic Press, London
- Gomes D, Agasse A, Thiebaud P, Delrot S, Geros H, Chaumont F (2009) Aquaporins are multifunctional water and solute transporters highly divergent in living organisms. *Biochimica Et Biophysica Acta-Biomembranes* 1788:1213-1228 doi:10.1016/j.bbamem.2009.03.009
- Gomes NCM, Heuer H, Schonfeld J, Costa R, Mendonca-Hagler L, Smalla K (2001) Bacterial diversity of the rhizosphere of maize (*Zea mays*) grown in tropical soil studied by temperature gradient gel electrophoresis. *Plant Soil* 232:167-180 doi:10.1023/a:1010350406708
- Gomez-Gomez L, Boller T (2002) Flagellin perception: a paradigm for innate immunity. *Trends Plant Sci* 7:251-256
- Gomez-Vidal S, Lopez-Llorca LV, Jansson HB, Salinas J (2006) Endophytic colonization of date palm (*Phoenix dactylifera* L.) leaves by entomopathogenic fungi. *Micron* 37:624-632 doi:10.1016/j.micron.2006.02.003
- Gomez-Vidal S, Salinas J, Tena M, Lopez-Llorca LV (2009) Proteomic analysis of date palm (*Phoenix dactylifera* L.) responses to endophytic colonization by entomopathogenic fungi. *Electrophoresis* 30:2996-3005 doi:10.1002/elps.200900192
- Gonzalez F, Tkaczuk C, Dinu MM, Fiedler Z, Vidal S, Zchori-Fein E, Messelink GJ (2016) New opportunities for the integration of microorganisms into biological pest control systems in greenhouse crops. *J Pest Sci* 89:295-311 doi:10.1007/s10340-016-0751-x
- Gonzalez V, Tello ML (2011) The endophytic mycota associated with *Vitis vinifera* in central Spain. *Fungal Divers* 47:29-42 doi:10.1007/s13225-010-0073-x
- Gorin MB, Yancey SB, Cline J, Revel JP, Horwitz J (1984) The major intrinsic protein (MiP) of the bovine lens fiber membrane – characterization and structure based on cDNA cloning. *Cell* 39:49-59 doi:10.1016/0092-8674(84)90190-9
- Grant JJ, Loake GJ (2000) Role of reactive oxygen intermediates and cognate redox signaling in disease resistance. *Plant Physiol* 124:21-29
- Green H, Larsen J, Olsson PA, Jensen DF, Jakobsen II (1999) Suppression of the biocontrol agent *Trichoderma harzianum* by mycelium of the arbuscular mycorrhizal fungus *Glomus intraradices* in root-free soil. *Appl Environ Microbiol* 65:1428-1434
- Greenfield M, Gómez-Jiménez MI, Ortiz V, Vega FE, Kramer M, Parsa S (2016) *Beauveria bassiana* and *Metarhizium anisopliae* endophytically colonize cassava roots following soil drench inoculation. *Biol Control* 95:40-48 doi:10.1016/j.biocontrol.2016.01.002
- Griffin M, Ownley B, Klingeman W, Pereira R (2005) Biocontrol of *Rhizoctonia* damping-off of cotton with endophytic *Beauveria bassiana*. *Phytopath* 95:S36-S36
- Gualandi RJ et al. (2014) Fungal mutualists enhance growth and phytochemical content in *Echinacea purpurea*. *Symbiosis* 63:111-121 doi:10.1007/s13199-014-0293-z
- Gunatilaka AA (2006) Natural products from plant-associated microorganisms: distribution, structural diversity, bioactivity, and implications of their occurrence. *J Nat Prod* 69:509-526 doi:10.1021/np058128n
- Guo L-D (2010) Molecular diversity and identification of endophytic fungi. In: Gherbawy Y, Voigt K (eds) *Molecular Identification of Fungi*. Springer Berlin Heidelberg, Berlin, Heidelberg, pp 277-296. doi:10.1007/978-3-642-05042-8_13
- Gurulingappa P, McGee PA, Sword G (2011) Endophytic *Lecanicillium lecanii* and *Beauveria bassiana* reduce the survival and fecundity of *Aphis gossypii* following contact with conidia and secondary metabolites. *Crop Protect* 30:349-353 doi:10.1016/j.cropro.2010.11.017
- Gurulingappa P, Sword GA, Murdoch G, McGee PA (2010) Colonization of crop plants by fungal entomopathogens and their effects on two insect pests when *in planta*. *Biol Control* 55:34-41 doi:10.1016/j.biocontrol.2010.06.011
- Gutterson N, Reuber TL (2004) Regulation of disease resistance pathways by AP2/ERF transcription factors. *Curr Opin Plant Biol* 7:465-471 doi:10.1016/j.pbi.2004.04.007
- Hallmann J, QuadtHallmann A, Mahaffee WF, Kloepper JW (1997) Bacterial endophytes in agricultural crops. *Canad J Microbiol* 43:895-914

- Hanley ME, Lamont BB, Fairbanks MM, Rafferty CM (2007) Plant structural traits and their role in anti-herbivore defence. *Persp Plant Ecol Evol System* 8:157-178
doi:<http://dx.doi.org/10.1016/j.ppees.2007.01.001>
- Hardoim PR van Overbeek LS, Berg G, Pirttilä AM, Compant S, Campisano A, Döring M, Sessitsch A (2015) The hidden world within plants: ecological and evolutionary considerations for defining functioning of microbial endophytes. *Microbiol Mol Biol Rev* 79:293-320
doi:10.1128/MMBR.00050-14
- Hardoim PR, van Overbeek LS, Elsas JD (2008) Properties of bacterial endophytes and their proposed role in plant growth. *Trends Microbiol* 16:463-471 doi:10.1016/j.tim.2008.07.008
- Harman GE (2006) Overview of Mechanisms and Uses of *Trichoderma* spp. *Phytopath* 96:190-194
doi:10.1094/phyto-96-0190
- Harman GE, Howell CR, Viterbo A, Chet I, Lorito M (2004a) *Trichoderma* species - opportunistic, avirulent plant symbionts. *Nat Rev Micro* 2:43-56
- Harman GE, Petzoldt R, Comis A, Chen J (2004b) Interactions between *Trichoderma harzianum* strain T22 and maize inbred line Mo17 and effects of these interactions on diseases caused by *Pythium ultimum* and *Colletotrichum graminicola*. *Phytopath* 94:147-153
doi:10.1094/phyto.2004.94.2.147
- Harrison MJ (2005) Signaling in the arbuscular mycorrhizal symbiosis. *Annual review of microbiology* 59:19-42 doi:10.1146/annurev.micro.58.030603.123749
- Harvey-Samuel T, Morrison NI, Walker AS, Marubbi T, Yao J, Collins HL, Gorman K, Davies TG, Alphey N, Warner S, Shelton AM, Alphey L (2015) Pest control and resistance management through release of insects carrying a male-selecting transgene. *BMC Biol* 13:49 doi:10.1186/s12915-015-0161-1
- Hegedus DD, Khachatourians GG (1993) Construction of Cloned DNA Probes for the Specific Detection of the Entomopathogenic fungus *Beauveria bassiana* in grasshoppers. *J Invertebr Pathol* 62:233-240 doi:<http://dx.doi.org/10.1006/jipa.1993.1105>
- Hegedus DD, Khachatourians GG (1996a) Detection of the Entomopathogenic fungus *Beauveria bassiana* within infected migratory grasshoppers (*Melanoplus sanguinipes*) using polymerase chain reaction and DNA probe. *J Invertebr Pathol* 67:21-27
doi:<http://dx.doi.org/10.1006/jipa.1996.0004>
- Hegedus DD, Khachatourians GG (1996b) Identification and differentiation of the entomopathogenic fungus *Beauveria bassiana* using polymerase chain reaction and single-strand conformation polymorphism analysis *J Invertebr Pathol* 67:289-299 doi:10.1006/jipa.1996.0044
- Heidel AJ, Clarke JD, Antonovics J, Dong X (2004) Fitness costs of mutations affecting the systemic acquired resistance pathway in *Arabidopsis thaliana*. *Genetics* 168:2197-2206
doi:10.1534/genetics.104.032193
- Henry E, Yadeta KA, Coaker G (2013) Recognition of bacterial plant pathogens: local, systemic and transgenerational immunity. *New Phytol* 199:908-915 doi:10.1111/nph.12214
- Higgins DG, Sharp PM (1988) CLUSTAL: a package for performing multiple sequence alignment on a microcomputer. *Gene* 73:237-244
- Higuchi R, Fockler C, Dollinger G, Watson R (1993) Kinetic PCR analysis: real-time monitoring of DNA amplification reactions. *Bio/technology* 11:1026-1030
- Hiltner (1904) Arbeit vol 98. Deutsche Landwirts, Berlin
- Hiruma K, Gerlach N, Sacristán S, et al. (2016) Root endophyte *Colletotrichum tofieldiae* confers plant fitness benefits that are phosphate status dependent. *Cell* 165:464-474
doi.org/10.1016/j.cell.2016.02.028
- Hofte H, Whiteley HR (1989) Insecticidal crystal proteins of *Bacillus thuringiensis*. *Microbiol Rev* 53:242-255
- Hohmann P, Jones EE, Hill RA, Stewart A (2012) Ecological studies of the bio-inoculant *Trichoderma hamatum* LU592 in the root system of *Pinus radiata*. *FEMS Microbiol Ecol* 80:709-721
doi:10.1111/j.1574-6941.2012.01340.x
- Howe GA, Jander G (2008) Plant immunity to insect herbivores. *Ann Rev Plant Biol* 59:41-66.
doi:10.1146/annurev.arplant.59.032607.092825

- Hu G, St Leger J (2002) Field studies using a recombinant mycoinsecticide (*Metarhizium anisopliae*) reveal that it is rhizosphere competent. *Appl Environ Microbiol* 68:6383-6387 doi:10.1128/aem.68.12.6383-6387.2002
- Huang DW, Sherman BT, Lempicki RA (2009) Systematic and integrative analysis of large gene lists using DAVID bioinformatics resources. *Nature Protocols* 4:44-57 doi:10.1038/nprot.2008.211
- Humber RA (2008) Evolution of entomopathogenicity in fungi. *J Invertebr Pathol* 98:262-266 doi:10.1016/j.jip.2008.02.017
- Hyde KD, Soyong K (2008) The fungal endophyte dilemma. *Fungal Diversity* 33:163-173
- Irizarry RA, Hobbs B, Collin F, Beazer-Barclay YD, Antonellis KJ, Scherf U, Speed TP (2003) Exploration, normalization, and summaries of high density oligonucleotide array probe level data *Biostatistics* (Oxford, England) 4:249-264 doi:10.1093/biostatistics/4.2.249
- Ishikawa F, Suga S, Uemura T, Sato MH, Maeshima M (2005) Novel type aquaporin SIPs are mainly localized to the ER membrane and show cell-specific expression in *Arabidopsis thaliana*. *FEBS Letters* 579:5814-5820 doi:10.1016/j.febslet.2005.09.076
- Jaber LR (2015) Grapevine leaf tissue colonization by the fungal entomopathogen *Beauveria bassiana* s.l. and its effect against downy mildew. *Biocont* 60:103-112 doi:10.1007/s10526-014-9618-3
- Jaber LR, Enkerli J (2017) Fungal entomopathogens as endophytes: can they promote plant growth? *Biocon Sci Technol* 27:28-41 doi:10.1080/09583157.2016.1243227
- Jacobs S, Zechmann B, Molitor A, Trujillo M, Petutschnig E, Lipka V, Kogel K-H, Schäfer P (2011) Broad-spectrum suppression of innate immunity is required for colonization of *Arabidopsis* roots by the fungus *Piriformospora indica*. *Plant Physiol* 156:726-740 doi:10.1104/pp.111.176446
- Jaronski ST (2008) Soil ecology of the entomopathogenic Ascomycetes: a critical examination of what we (think) we know. In: Ekesi S, K. MN (eds) *Use of entomopathogenic fungi in biological pest management*. Research Signpost, pp 91-144
- Javot H et al. (2003) Role of a single aquaporin isoform in root water uptake. *Plant Cell* 15:509-522 doi:10.1105/tpc.008888
- Jepson I, Holt D, Roussel V, Wright S, Greenland A (1997) Transgenic plant analysis as a tool for the study of maize glutathione S-transferases. In: *Regulation of enzymatic systems detoxifying xenobiotics in Plants* (KK Hatzios, ed). Kluwer Academic Publishers, Boston pp 313-323
- Jia Y, Zhou J-Y, He J-X, Du W, Bu Y-Q, Liu C-H, Dai C-C (2013) Distribution of the Entomopathogenic Fungus *Beauveria bassiana* in Rice Ecosystems and Its Effect on Soil Enzymes. *Current Microbiol* 67:631-636 doi:10.1007/s00284-013-0414-6
- Jones DL, Nguyen C, Finlay RD (2009) Carbon flow in the rhizosphere: carbon trading at the soil–root interface. *Plant Soil* 321:5-33 doi:10.1007/s11104-009-9925-0
- Jones JD, Dangl JL (2006) The plant immune system. *Nature* 444:323-329 doi:10.1038/nature05286
- Judd L, Jackson B, Fonteno W (2015) Advancements in root growth measurement technologies and observation capabilities for container-grown plants. *Plants* 4:369
- Kabaluk JT, Ericsson JD (2007) *Metarhizium anisopliae* Seed Treatment Increases Yield of Field Corn When Applied for Wireworm Control. *Agronomy J* 99:1377-1381 doi:10.2134/agronj2007.0017N
- Kale SD, Tyler BM (2011) Entry of oomycete and fungal effectors into plant and animal host cells *Cellular Microbiol* 13:1839-1848 doi:10.1111/j.1462-5822.2011.01659.x
- Kaul S, Sharma T, K. Dhar M (2016) “Omics” Tools for better understanding the plant–endophyte interactions. *Frontiers Plant Sci* 7 doi:10.3389/fpls.2016.00955
- Kauppinen M, Saikkonen K, Helander M, Pirttilä AM, Wali PR (2016) *Epichloe* grass endophytes in sustainable agriculture. *Nature Plants* 2 doi:10.1038/nplants.2015.224
- Kepler RM, Maul JE, Rehner SA (2017) Managing the plant microbiome for biocontrol fungi: examples from Hypocreales. *Curr Opin Microbiol* 37:48-53 doi:https://doi.org/10.1016/j.mib.2017.03.006
- Keyser CA, Thorup-Kristensen K, Meyling NV (2014) *Metarhizium* seed treatment mediates fungal dispersal via roots and induces infections in insects. *Fungal Ecol* 11:122-131 doi:10.1016/j.funeco.2014.05.005

- Khan A, Bassett S, Voisey C, Gaborit J, Johnson L, Christensen M, McCulloch A, Bryan G, Johnson R (2010) Gene expression profiling of the endophytic fungus *Neotyphodium lolii* in association with its host plant perennial ryegrass. *Aust Plant Pathol* 39:467-476 doi:10.1071/ap09084
- Khan AL, Hamayun M, Kang SM, Kim YH, Jung HY, Lee JH, Lee IJ (2012a) Endophytic fungal association via gibberellins and indole acetic acid can improve plant growth under abiotic stress: an example of *Paecilomyces formosus* LHL10. *BMC Microbiol* 12:3 doi:10.1186/1471-2180-12-3
- Khan AL, Hamayun M, Kang SM, Kim YH, Jung HY, Lee JH, Lee IJ (2012b) Pure culture of *Metarhizium anisopliae* LHL07 reprograms soybean to higher growth and mitigates salt stress. *World J Microbiol Biotechnol* 28:1483-1494 doi:10.1007/s11274-011-0950-9
- Kia SH, Glynou K, Nau T, Thines M, Piepenbring M, Macia-Vicente JG (2017) Influence of phylogenetic conservatism and trait convergence on the interactions between fungal root endophytes and plants. *Isme J* 11:777-790 doi:10.1038/ismej.2016.140
- Kirkland BH, Keyhani NO (2011) Expression and purification of a functionally active class I fungal hydrophobin from the entomopathogenic fungus *Beauveria bassiana* in *E. coli*. *J Industrial Microbiol Biotechnol* 38:327-335 doi:10.1007/s10295-010-0777-7
- Klimek B, Chodak M, Jazwa M, Solak A, Tarasek A, Niklinska M (2016) The relationship between soil bacteria substrate utilisation patterns and the vegetation structure in temperate forests. *Europ J For Res* 135:179-189 doi:10.1007/s10342-015-0929-4
- Kloepper JW, Ryu C-M (2006) Bacterial endophytes as elicitors of induced systemic resistance. In: Schulz BJE, Boyle CJC, Sieber TN (eds) *Microbial Root Endophytes*. Springer Berlin Heidelberg, Berlin, Heidelberg, pp 33-52. doi:10.1007/3-540-33526-9_3
- Kloepper JW, Ryu CM, Zhang S (2004) Induced systemic resistance and promotion of plant growth by *Bacillus* spp. *Phytopath* 94:1259-1266 doi:10.1094/phyto.2004.94.11.1259
- Koo AJK, Howe GA (2009) The wound hormone jasmonate. *Phytochem* 70:1571-1580 doi:10.1016/j.phytochem.2009.07.018
- Kostenko O, van de Voorde TF, Mulder PP, van der Putten WH, Martijn Bezemer T (2012) Legacy effects of aboveground-belowground interactions. *Ecol Lett* 15:813-821 doi:10.1111/j.1461-0248.2012.01801.x
- Kosuta S, Chabaud M, Loughon G, Gough C, Denarie J, Barker DG, Becard G (2003) A diffusible factor from arbuscular mycorrhizal fungi induces symbiosis-specific MtENOD11 expression in roots of *Medicago truncatula*. *Plant Physiol* 131:952-962 doi:10.1104/pp.011882
- Kramer AM, Dennis B, Liebhold AM, Drake JM (2009) The evidence for Allee effects. *Population Ecol* 51:341-354 doi:10.1007/s10144-009-0152-6
- L'Haridon F, Besson-Bard A, Binda M, Serrano M, Abou-Mansour E, Balet F, Schoonbeek H-J, Hess S, Mir R, Léon J, Lamotte O, Métraux J-P (2011) A permeable cuticle is associated with the release of reactive oxygen species and induction of innate immunity. *PLoS Path* 7:e1002148 doi:10.1371/journal.ppat.1002148
- Lahrmann U, Ding Y, Banhara A, Rath M, Hajirezaei MR, Döhlemann S, von Wirén N, Parniske M, Zuccaro A (2013) Host-related metabolic cues affect colonization strategies of a root endophyte. *Proc Natl Acad Sci USA* 110:13965-13970 doi:10.1073/pnas.1301653110
- Lahrmann U, Zuccaro A (2012) Opprimo ergo sum--evasion and suppression in the root endophytic fungus *Piriformospora indica*. *Mol Plant-Microbe Inter* 25:727-737 doi:10.1094/mpmi-11-11-0291
- Lakshmanan V, Kitto SL, Caplan JL, Hsueh YH, Kearns DB, Wu YS, Bais HP (2012) Microbe-associated molecular patterns-triggered root responses mediate beneficial rhizobacterial recruitment in *Arabidopsis*. *Plant Physiol* 160:1642-1661 doi:10.1104/pp.112.200386
- Landa BB, Lopez-Diaz C, Jimenez-Fernandez D, Montes-Borrego M, Munoz-Ledesma FJ, Ortiz-Urquiza A, Quesada-Moraga E (2013) In-plant detection and monitorization of endophytic colonization by a *Beauveria bassiana* strain using a new-developed nested and quantitative PCR-based assay and confocal laser scanning microscopy. *J Invertebr Pathol* 114:128-138 doi:10.1016/j.jip.2013.06.007
- Lareen A, Burton F, Schafer P (2016) Plant root-microbe communication in shaping root microbiomes. *Plant Mol Biol* 90:575-587 doi:10.1007/s11103-015-0417-8

- Larsen J, Jaramillo-Lopez P, Najera-Rincon M, Gonzalez-Esquivel CE (2015) Biotic interactions in the rhizosphere in relation to plant and soil nutrient dynamics. *Journal of Soil Sci Plant Nutrition* 15:449-463
- Latch GCM, Christensen MJ (1985) Artificial infection of grasses with endophytes. *Ann Appl Biol* 107:17-24 doi:10.1111/j.1744-7348.1985.tb01543.x
- Lawry R (2016) Cross-communication between *Trichoderma* and plants during root colonisation. PhD Thesis. Lincoln University
- Lee B, Lee S, Ryu CM (2012) Foliar aphid feeding recruits rhizosphere bacteria and primes plant immunity against pathogenic and non-pathogenic bacteria in pepper. *Annals Bot* 110:281-290 doi:10.1093/aob/mcs055
- Lee J, Lee S, Young JPW (2008) Improved PCR primers for the detection and identification of arbuscular mycorrhizal fungi. *FEMS Microbiol Ecol* 65:339-349 doi:10.1111/j.1574-6941.2008.00531.x
- Lee S, Yap M, Behringer G, Hung R, Bennett JW (2016) Volatile organic compounds emitted by *Trichoderma* species mediate plant growth. *Fungal Biol Biotech* 3:7 doi:10.1186/s40694-016-0025-7
- Leuchtmann A, Bacon CW, Schardl CL, White JF, Tadych M (2014) Nomenclatural realignment of *Neotyphodium* species with genus *Epichloë*. *Mycologia* 106:202-215 doi:10.3852/13-251
- Li HY, Wang TY, Shi YS, Fu JJ, Song YC, Wang GY, Li Y (2007) Isolation and characterization of induced genes under drought stress at the flowering stage in maize (*Zea mays*). *DNA Sequence* 18:443-458 doi:10.1080/10425170701292051
- Liao X, Lovett B, Fang W, St Leger RJ (2017) *Metarhizium robertsii* produces indole-3-acetic acid, which promotes root growth in *Arabidopsis* and enhances virulence to insects. *Microbiol* doi:10.1099/mic.0.000494
- Liao X, O'Brien TR, Fang W, St Leger RJ (2014) The plant beneficial effects of *Metarhizium* species correlate with their association with roots. *Appl Microbiol Biotechnol* 98:7089-7096 doi:10.1007/s00253-014-5788-2
- Licausi F, Ohme-Takagi M, Perata P (2013) APETALA/Ethylene Responsive Factor (AP2/ERF) transcription factors: mediators of stress responses and developmental programs. *New Phytol* 199:639-649 doi:10.1111/nph.12291
- Licciardello C, D'Agostino N, Traini A, Recupero GR, Frusciante L, Chiusano ML (2014) Characterization of the glutathione S-transferase gene family through ESTs and expression analyses within common and pigmented cultivars of *Citrus sinensis* (L.). *Osbeck. BMC Plant Biology* 14:39 doi:10.1186/1471-2229-14-39
- Lozano-Tovar MD, Garrido-Jurado I, Quesada-Moraga E, Raya-Ortega MC, Trapero-Casas A (2017) *Metarhizium brunneum* and *Beauveria bassiana* release secondary metabolites with antagonistic activity against *Verticillium dahliae* and *Phytophthora megasperma* olive pathogens. *Crop Protect* 100:186-195 doi:https://doi.org/10.1016/j.cropro.2017.06.026
- Lu P, Lin YH, Yang ZQ, Xu XP, Tan F, Jia XD, Wang M, Xu DR, Wang XZ (2015) Effects of application of corn straw on soil microbial community structure during the maize growing season. *J Basic Microbiol* 55:22-32 doi:10.1002/jobm.201300744
- Ludwig Y, Zhang YX, Hochholdinger F (2013) The Maize (*Zea mays* L.) AUXIN/INDOLE-3-ACETIC ACID Gene Family: Phylogeny, Synteny, and Unique Root-Type and Tissue-Specific Expression Patterns during Development. *PLoS One* 8 doi:10.1371/journal.pone.0078859
- Lugtenberg B, Rozen DE, Kamilova F (2017) Wars between microbes on roots and fruits. *F1000 Research* 6:343 doi:10.12688/f1000research.10696.1
- Lugtenberg BJJ, Chin-A-Woeng TFC, Bloembergen GV (2002) Microbe-plant interactions: principles and mechanisms Antonie Van Leeuwenhoek Intern J Gen Mol Microbiol 81:373-383 doi:10.1023/a:1020596903142
- Macia-Vicente JG, Jansson HB, Talbot NJ, Lopez-Llorca LV (2009) Real-time PCR quantification and live-cell imaging of endophytic colonization of barley (*Hordeum vulgare*) roots by *Fusarium equiseti* and *Pochonia chlamydosporia*. *New Phytol* 182:213-228 doi:10.1111/j.1469-8137.2008.02743.x

- Madelin M (2012) Diseases caused by hyphomycetous fungi Insect pathology: an advanced treatise 2:233-271
- Maeshima M (2001) Tonoplast transporters: Organization and function. Ann Review Plant Physiol Plant Mol Biol 52:469-+ doi:10.1146/annurev.arplant.52.1.469
- Maillet F, Poinso V, André O, et al. (2011) Fungal lipochitooligosaccharide symbiotic signals in arbuscular mycorrhiza. Nature 469:58-63 doi:10.1038/nature09622
- Malinowski DP, Brauer DK, Belesky DP (1999) The endophyte *Neotyphodium coenophialum* affects root morphology of tall fescue grown under phosphorus deficiency. J Agron Crop Sci 183:53-60 doi:10.1046/j.1439-037x.1999.00321.x
- Malusa E, Sas-Pasz L, Ciesielska J (2012) Technologies for beneficial microorganisms inocula used as biofertilizers. Sci World J doi:10.1100/2012/491206
- Manter DK, Delgado JA, Holm DG, Stong RA (2010) Pyrosequencing reveals a highly diverse and cultivar-specific bacterial endophyte community in potato roots. Microbiol Ecol 60:157-166 doi:10.1007/s00248-010-9658-x
- Marone D, Russo MA, Laidò G, De Leonardis AM, Mastrangelo AM (2013) Plant Nucleotide Binding Site–Leucine-Rich Repeat (NBS-LRR) genes: Active guardians in host defense responses. Inter J Mol Sci 14:7302-7326 doi:10.3390/ijms14047302
- Maroni M, Fanetti AC, Metruccio F (2006) Risk assessment and management of occupational exposure to pesticides in agriculture. La Medicina del lavoro 97:430-437
- Martínez-Medina A, Fernández I, Sánchez-Guzmán MJ, Jung SC, Pascual JA, Pozo MJ (2013) Deciphering the hormonal signalling network behind the systemic resistance induced by *Trichoderma harzianum* in tomato. Frontiers Plant Sci 4:206 doi:10.3389/fpls.2013.00206
- Martinez-Medina A, Pascual JA, Perez-Alfocea F, Albacete A, Roldan A (2010) *Trichoderma harzianum* and *Glomus intraradices* modify the hormone disruption induced by *Fusarium oxysporum* infection in melon plants. Phytopathol 100:682-688 doi:10.1094/phyto-100-7-0682
- Mathys JDC, K. Timmermans, P. Van Kerckhove, S. Lievens, B. Vanhaecke, M. Cammue, B. P. A. De Coninck, B. (2012) Genome-wide characterization of ISR induced in *Arabidopsis thaliana* by *Trichoderma hamatum* T382 against *Botrytis cinerea* infection. Frontiers Plant Sci 3 doi:10.3389/fpls.2012.00108
- Matzinger P (2002) The danger model: a renewed sense of self. Science 296:301-305 doi:10.1126/science.1071059
- Maurel C (2007) Plant aquaporins: Novel functions and regulation properties. FEBS Letters 581:2227-2236 doi:10.1016/j.febslet.2007.03.021
- McGonigle B, Keeler SJ, Lan SMC, Koeppe MK, O'Keefe DP (2000) A genomics approach to the comprehensive analysis of the glutathione S-transferase gene family in soybean and maize. Plant Physiol 124:1105-1120 doi:10.1104/pp.124.3.1105
- McGrath KC, Dombrecht D, Manners JM et A,. (2005) Repressor- and activator-type ethylene response factors functioning in jasmonate signaling and disease resistance identified via a genome-wide screen of *Arabidopsis* transcription factor gene expression. Plant Physiol 139:949-959 doi:10.1104/pp.105.068544
- McKinnon AC (2011) Rhizosphere colonisation of *Beauveria* Vuillemin species (Ascomycota: Hypocreales) (*B. bassiana* and *B. caledonica*). Lincoln University
- McKinnon AC, Saari S, Moran-Diez ME, Meyling NV, Raad M, Glare TR (2017) *Beauveria bassiana* as an endophyte: a critical review on associated methodology and biocontrol potential. BioControl 62:1-17 doi:10.1007/s10526-016-9769-5
- McLean KL, Dodd SL, Minchin RF, Ohkura M, Bienkowski D, Stewart A (2014) Non-target impacts of the biocontrol agent *Trichoderma atroviride* on plant health and soil microbial communities in two native ecosystems in New Zealand. Aust Plant Pathol 43:33-45 doi:10.1007/s13313-013-0229-8
- McNear Jr, DH (2013) The Rhizosphere - Roots, Soil and Everything In Between. Nature Education Knowledge 4:1
- Meyling NV, Lubeck M, Buckley EP, Eilenberg J, Rehner SA (2009) Community composition, host range and genetic structure of the fungal entomopathogen *Beauveria* in adjoining

- agricultural and seminatural habitats. *Mol Ecol* 18:1282-1293 doi:10.1111/j.1365-294X.2009.04095.x
- Miller JC, Tanksley SD (1990) RFLP analysis of phylogenetic relationships and genetic variation in the genus *Lycopersicon*. *Theor Appl Gen* 80:437-448 doi:10.1007/bf00226743
- Mitchell C, Brennan RM, Graham J, Karley AJ (2016) plant defense against herbivorous pests: exploiting resistance and tolerance traits for sustainable crop protection. *Frontiers Plant Sci* 7:1132 doi:10.3389/fpls.2016.01132
- Mootha VK, Lindgren cm, Eriksson K-F, et al. (2003) PGC-1alpha-responsive genes involved in oxidative phosphorylation are coordinately downregulated in human diabetes. *Nature Genetics* 34:267-273 doi:10.1038/ng1180
- Moran-Diez E, Rubio B, Dominguez S, Hermosa R, Monte E, Nicolas C (2012) Transcriptomic response of *Arabidopsis thaliana* after 24 h incubation with the biocontrol fungus *Trichoderma harzianum*. *J Plant Physiol* 169:614-620 doi:10.1016/j.jplph.2011.12.016
- Morgan JA, Bending GD, White PJ (2005) Biological costs and benefits to plant-microbe interactions in the rhizosphere *J Exp Bot* 56:1729-1739 doi:10.1093/jxb/eri205
- Morrison TB, Weis JJ, Wittwer CT (1998) Quantification of low-copy transcripts by continuous SYBR Green I monitoring during amplification. *BioTechniques* 24:954-958, 960, 962
- Muhling M, Woolven-Allen J, Murrell JC, Joint I (2008) Improved group-specific PCR primers for denaturing gradient gel electrophoresis analysis of the genetic diversity of complex microbial communities. *Isme J* 2:379-392 doi:10.1038/ismej.2007.97
- Muyzer G, Dewaal EC, Uitterlinden AG (1993) Profiling of complex microbial-populations by denaturing gradient gel-electrophoresis analysis of polymerase chain reaction genes-coding for 16s ribosomal RNA. *Appl Environ Microbiol* 59:695-700
- Naveed M, Hussain MB, Zahir ZA, Mitter B, Sessitsch A (2014a) Drought stress amelioration in wheat through inoculation with *Burkholderia phytofirmans* strain PsJN. *Plant Growth Regulation* 73:121-131 doi:10.1007/s10725-013-9874-8
- Naveed M, Mitter B, Reichenauer TG, Wiecezorek K, Sessitsch A (2014b) Increased drought stress resilience of maize through endophytic colonization by *Burkholderia phytofirmans* PsJN and *Enterobacter* sp. FD17. *Environ Exp Bot* 97:30-39 doi:http://dx.doi.org/10.1016/j.envexpbot.2013.09.014
- Nieto-Jacobo MF, Steyaert JM, Salazar-Badillo FB, et al. (2017) Environmental Growth Conditions of *Trichoderma* spp. Affects Indole Acetic Acid Derivatives, Volatile Organic Compounds, and Plant Growth Promotion. *Front Plant Sci* 8:102 doi:10.3389/fpls.2017.00102
- Nocker A, Cheung C-Y, Camper AK (2006) Comparison of propidium monoazide with ethidium monoazide for differentiation of live vs. dead bacteria by selective removal of DNA from dead cells. *J Microbiol Methods* 67:310-320 doi:10.1016/j.mimet.2006.04.015
- Nocker A, Sossa KE, Camper AK (2007) Molecular monitoring of disinfection efficacy using propidium monoazide in combination with quantitative PCR. *J Microbiol Methods* 70:252-260 doi:10.1016/j.mimet.2007.04.014
- Oerke EC (2006) Crop losses to pests. *J Agricul Sci* 144:31-43 doi:10.1017/s0021859605005708
- Ohme-Takagi M, Shinshi H (1995) Ethylene-inducible DNA binding proteins that interact with an ethylene-responsive element. *Plant Cell* 7:173-182 doi:10.1105/tpc.7.2.173
- Oldroyd GE, Harrison MJ, Paszkowski U (2009) Reprogramming plant cells for endosymbiosis. *Science* 324:753-754 doi:10.1126/science.1171644
- Ownley BH, Dee MM, Gwinn KD (2008a) Effect of conidial seed treatment rate of entomopathogenic *Beauveria bassiana* 11-98 on endophytic colonization of tomato seedlings and control of *Rhizoctonia* disease. *Phytopathol* 98:S118-S118
- Ownley BH, Griffin MR, Klingeman WE, Gwinn KD, Moulton JK, Pereira RM (2008b) *Beauveria bassiana*: Endophytic colonization and plant disease control. *J Invertebr Pathol* 98:267-270 doi:10.1016/j.jip.2008.01.010
- Ownley BH, Gwinn KD, Vega FE (2010) Endophytic fungal entomopathogens with activity against plant pathogens: ecology and evolution. *Biocont* 55:113-128 doi:10.1007/s10526-009-9241-x

- Ownley BH, Pereira RM, Mingeman WE, Quigley NB, Leckie BM (2004) *Beauveria bassiana*, a dual purpose biocontrol organism, with activity against insect pests and plant pathogens. *Emerg Concepts Plant Health Manag*:255-269
- Pangesti N, Pineda A, Pieterse CMJ, Dicke M, van Loon JJA (2013) Two-way plant-mediated interactions between root-associated microbes and insects: from ecology to mechanisms. *Frontiers Plant Sci* 4 doi:10.3389/fpls.2013.00414
- Parry C, Blonquist JM, Bugbee B (2014) *In situ* measurement of leaf chlorophyll concentration: analysis of the optical/absolute relationship. *Plant, Cell Environ* 37:2508-2520 doi:10.1111/pce.12324
- Pava-Ripoll M, Angelini C, Fang W, Wang S, Posada FJ, St Leger R (2011) The rhizosphere-competent entomopathogen *Metarhizium anisopliae* expresses a specific subset of genes in plant root exudate. *Microbiol-(UK)* 157:47-55 doi:10.1099/mic.0.042200-0
- Pavlo A, Leonid O, Iryna Z, Natalia K, Maria PA (2011) Endophytic bacteria enhancing growth and disease resistance of potato (*Solanum tuberosum* L.). *Biol Control* 56:43-49 doi:http://dx.doi.org/10.1016/j.biocontrol.2010.09.014
- Petrini O (1986) Taxonomy of endophytic fungi of aerial plant tissues. In: Fokkema NJ vdHJ (ed) *Microbiology of the phyllosphere*. Cambridge University Press, Cambridge, UK, pp 175–187
- Philippot L, Raaijmakers JM, Lemanceau P, van der Putten WH (2013) Going back to the roots: the microbial ecology of the rhizosphere. *Nat Rev Micro* 11:789-799 doi:10.1038/nrmicro3109
- Phillips AJ, Simon C (1995) Simple, efficient, and non-destructive DNA extraction protocol for arthropods. *Ann Ento Soc Am* 88:281-283 doi:10.1093/aesa/88.3.281
- Piekielek WP, Fox RH, Toth JD, Macneal KE (1995) Use of a chlorophyll meter at the early dent stage of corn to evaluate nitrogen sufficiency. *Agronomy J* 87:403-408 doi:10.2134/agronj1995.00021962008700030003x
- Pieterse CM, Dicke M (2007) Plant interactions with microbes and insects: from molecular mechanisms to ecology. *Trends Plant Sci* 12:564-569 doi:10.1016/j.tplants.2007.09.004
- Porras-Alfaro A, Bayman P (2011) Hidden fungi, emergent properties: endophytes and microbiomes. *Ann Rev Phytopathol* 49:291-315. doi:10.1146/annurev-phyto-080508-081831
- Powell WA, Klingeman WE, Ownley BH, Gwinn KD (2009) Evidence of endophytic *Beauveria bassiana* in seed-treated tomato plants acting as a systemic entomopathogen to larval *Helicoverpa zea* (Lepidoptera: Noctuidae) *J Ento Sci* 44:391-396
- Prabhavathi MK, Thyagaraj NE, Ghosh SK, Pradeepa SD (2013) Studies on the endophytic properties of entomopathogenic fungi, *Beauveria bassiana* (Balsamo) against banana pseudostem weevil, *Odoiporous longicollis* Olivier Uttar Pradesh. *J Zool* 33:159-168
- Qawasmeh A, Raman A, Wheatley W (2015) Volatiles in perennial ryegrass infected with strains of endophytic fungus: impact on African black beetle host selection. *J App Ent* 139:94-104 doi:10.1111/jen.12140
- Quesada-Moraga E, Landa BB, Munoz-Ledesma J, Jimenez-Diaz RM, Santiago-Alvarez C (2006) Endophytic colonisation of opium poppy, *Papaver somniferum*, by an entomopathogenic *Beauveria bassiana* strain. *Mycopathologia* 161:323-329 doi:10.1007/s11046-006-0014-0
- Quesada-Moraga E, Lopez-Diaz C, Beatriz Landa B (2014) The hidden habit of the entomopathogenic fungus *Beauveria bassiana*: First demonstration of vertical plant transmission. *PLoS One* 9 doi:10.1371/journal.pone.0089278
- Quesada-Moraga E, Munoz-Ledesma FJ, Santiago-Alvarez C (2009) Systemic Protection of *Papaver somniferum* L. Against *Iraella luteipes* (Hymenoptera: Cynipidae) by an endophytic strain of *Beauveria bassiana* (Ascomycota: Hypocreales). *Environ Ento* 38:723-730
- Raad M (2016) Plant-mediated interactions between the entomopathogenic fungus *Beauveria bassiana*, insect herbivores and a plant pathogen. PhD thesis. Lincoln University
- Raaijmakers JM, Paulitz TC, Steinberg C, Alabouvette C, Moënne-Loccoz Y (2009) The rhizosphere: a playground and battlefield for soilborne pathogens and beneficial microorganisms. *Plant Soil* 321:341-361 doi:10.1007/s11104-008-9568-6
- Ramirez CA, Kloepper JW (2010) Plant growth promotion by *Bacillus amyloliquefaciens* FZB45 depends on inoculum rate and P-related soil properties. *Biol Fertility Soils* 46:835-844 doi:10.1007/s00374-010-0488-2

- Ramonell K, Berrocal-Lobo M, Koh S, Wan J, Edwards H, Stacey G, Somerville S (2005) Loss-of-function mutations in chitin responsive genes show increased susceptibility to the powdery mildew pathogen *Erysiphe cichoracearum*. *Plant Phys* 138(2):1027–1036. <http://doi.org/10.1104/pp.105.060947>
- Ravnskov S, Jensen B, Knudsen IMB, Bødker L, Funck Jensen D, Karliński L, Larsen J (2006) Soil inoculation with the biocontrol agent *Clonostachys rosea* and the mycorrhizal fungus *Glomus intraradices* results in mutual inhibition, plant growth promotion and alteration of soil microbial communities. *Soil Biol Biochem* 38:3453–3462 [doi:http://dx.doi.org/10.1016/j.soilbio.2006.06.003](http://dx.doi.org/10.1016/j.soilbio.2006.06.003)
- Reay SD, Brownbridge M, Gicquel B, Cummings NJ, Nelson TL (2010) Isolation and characterization of endophytic *Beauveria* spp. (Ascomycota: Hypocreales) from *Pinus radiata* in New Zealand forests. *Biol Control* 54:52–60 [doi:10.1016/j.biocontrol.2010.03.002](http://dx.doi.org/10.1016/j.biocontrol.2010.03.002)
- Reddy NP, Khan APA, Devi UK, Sharma HC, Reineke A (2009) Treatment of millet crop plant (*Sorghum bicolor*) with the entomopathogenic fungus (*Beauveria bassiana*) to combat infestation by the stem borer, *Chilo partellus* Swinhoe (Lepidoptera: Pyralidae). *J Asia-Pacific Ent* 12:221–226
- Reddy PV, Lam CK, Belanger FC (1996) Mutualistic fungal endophytes express a proteinase that is homologous to proteases suspected to be important in fungal pathogenicity. *Plant Physiol* 111:1209–1218
- Redman RS, Dunigan DD, Rodriguez RJ (2001) Fungal symbiosis from mutualism to parasitism: who controls the outcome, host or invader? *New Phytol* 151:705–716 [doi:10.1046/j.0028-646x.2001.00210.x](http://dx.doi.org/10.1046/j.0028-646x.2001.00210.x)
- Rehner SA, Buckley E (2005) A *Beauveria* phylogeny inferred from nuclear ITS and EF1- α sequences: evidence for cryptic diversification and links to *Cordyceps* teleomorphs. *Mycologia* 97:84–98
- Rehner SA, Minnis AM, Sung G, Luangsa-ard JJ, Devotto L, Humber RA (2011) Phylogeny and systematics of the anamorphic, entomopathogenic genus *Beauveria*. *Mycologia* 103:1055–73. [doi: 10.3852/10-302](http://dx.doi.org/10.3852/10-302)
- Rehner SA, Posada F, Buckley EP, Infante F, Castillo A, Vega FE (2006) Phylogenetic origins of African and Neotropical *Beauveria bassiana* s.l. pathogens of the coffee berry borer, *Hypothenemus hampei*. *J Invertebr Pathol* 93:11–21 [doi:10.1016/j.jip.2006.04.005](http://dx.doi.org/10.1016/j.jip.2006.04.005)
- Renuka S, Ramanujam B, Poornesha B (2016) Endophytic ability of different isolates of entomopathogenic fungi *Beauveria bassiana* (Balsamo) Vuillemin in stem and leaf tissues of Maize (*Zea mays* L.). *Indian J Microbiol* 56:126–133 [doi:10.1007/s12088-016-0574-8](http://dx.doi.org/10.1007/s12088-016-0574-8)
- Renwick A, Campbell R, Coe S (1991) Assessment of in vivo screening systems for potential biocontrol agents of *Gaeumannomyces graminis*. *Plant Path* 40:524–532 [doi:10.1111/j.1365-3059.1991.tb02415.x](http://dx.doi.org/10.1111/j.1365-3059.1991.tb02415.x)
- Roald S, Rheim X, Vigdis F, Lid T, Goks, J (1989) Phenotypical divergences between populations of soil bacteria isolated on different media. *Microb Ecol* 17:181–192
- Robert-Seilanianantz A, Grant M, Jones JD (2011) Hormone crosstalk in plant disease and defense: more than just jasmonate-salicylate antagonism. *Annu Rev Phytopathol* 49:317–343 [doi:10.1146/annurev-phyto-073009-114447](http://dx.doi.org/10.1146/annurev-phyto-073009-114447)
- Rodriguez R, Redman R (2008) More than 400 million years of evolution and some plants still can't make it on their own: plant stress tolerance via fungal symbiosis. *J Exp Bot* 59:1109–1114 [doi:10.1093/jxb/erm342](http://dx.doi.org/10.1093/jxb/erm342)
- Rodriguez RJ et al. (2008) Stress tolerance in plants via habitat-adapted symbiosis. *The ISME J* 2:404–416 [doi:10.1038/ismej.2007.106](http://dx.doi.org/10.1038/ismej.2007.106)
- Rodriguez RJ, White JF, Jr., Arnold AE, Redman RS (2009) Fungal endophytes: diversity and functional roles. *New Phytol* 182:314–330 [doi:10.1111/j.1469-8137.2009.02773.x](http://dx.doi.org/10.1111/j.1469-8137.2009.02773.x)
- Roy HE, Brodie EL, Chandler D, Goettel MS, Pell JK, Wajnberg E, Vega FE (2010) Deep space and hidden depths: understanding the evolution and ecology of fungal entomopathogens. *Biocontrol* 55:1–6 [doi:10.1007/s10526-009-9244-7](http://dx.doi.org/10.1007/s10526-009-9244-7)
- Rudrappa T, Czymmek KJ, Pare PW, Bais HP (2008) Root-secreted malic acid recruits beneficial soil bacteria. *Plant Physiol* 148:1547–1556 [doi:10.1104/pp.108.127613](http://dx.doi.org/10.1104/pp.108.127613)

- Rutledge RG, Cote C (2003) Mathematics of quantitative kinetic PCR and the application of standard curves. *Nucleic Acids Res* 31:e93
- Saikkonen K, Saari S, Helander M (2010a) Defensive mutualism between plants and endophytic fungi? *Fungal Diversity* 41:101-113 doi:10.1007/s13225-010-0023-7
- Saikkonen K, Wäli PR, Helander M (2010b) Genetic Compatibility Determines Endophyte-Grass Combinations. *PLoS One* 5:e11395 doi:10.1371/journal.pone.0011395
- Sang T, Crawford D, Stuessy T (1997) Chloroplast DNA phylogeny, reticulate evolution, and biogeography of *Paeonia* (Paeoniaceae). *Am J Bot* 84:1120
- Santiago R, Cao A, Butron A, Lopez-Malvar A, Rodriguez VM, Sandoya GV, Malvar RA (2017) Defensive changes in maize leaves induced by feeding of Mediterranean corn borer larvae. *Bmc Plant Biology* 17 doi:10.1186/s12870-017-0991-9
- Sasan RK, Bidochka MJ (2012) The insect-pathogenic fungus *Metarhizium robertsii* (Clavicipitaceae) is also an endophyte that stimulates plant root development. *Am J Bot* 99:101-107 doi:10.3732/ajb.1100136
- Saville DJ (1990) Multiple comparison procedures - the practical solution. *Am Statistician* 44:174-180 doi:10.2307/2684163
- Scheepmaker JWA, Butt TM (2010) Natural and released inoculum levels of entomopathogenic fungal biocontrol agents in soil in relation to risk assessment and in accordance with EU regulations *Biocont Sci Tech* 20:503-552 doi:10.1080/09583150903545035
- Schenk PM, Kazan K, Wilson I, Anderson JP, Richmond T, Somerville SC, Manners JM (2000) Coordinated plant defense responses in *Arabidopsis* revealed by microarray analysis. *Proc Natl Acad Sci* 97:11655-11660 doi:10.1073/pnas.97.21.11655
- Schmittgen TD (2001) Real-time quantitative PCR. *Methods* 25:383-385 doi:10.1006/meth.2001.1260
- Schulz B, Boyle C (2005) The endophytic continuum. *Mycol Res* 109:661-686 doi:10.1017/s095375620500273x
- Schulz B, Guske S, Dammann U, Boyle C (1998) Endophyte-host interactions. II. Defining symbiosis of the endophyte-host interaction. *Symbiosis* 25:213-227
- Schulz B, Rommert AK, Dammann U, Aust HJ, Strack D (1999) The endophyte-host interaction: a balanced antagonism? *Mycol Res* 103:1275-1283 doi:10.1017/s0953756299008540
- Schulz B, Wanke U, Draeger S, Aust HJ (1993) Endophytes from herbaceous plants and shrubs - effectiveness of surface sterilization methods. *Mycol Res* 97:1447-1450
- Seki M, Kamei A, Yamaguchi-Shinozaki K, Shinozaki K (2003) Molecular responses to drought, salinity and frost: common and different paths for plant protection. *Curr Opin Biotech* 14:194-199
- Senthilraja G, Anand T, Kennedy JS, Raguchander T, Samiyappan R (2013) Plant growth promoting rhizobacteria (PGPR) and entomopathogenic fungus bioformulation enhance the expression of defense enzymes and pathogenesis-related proteins in groundnut plants against leafminer insect and collar rot pathogen. *Phys Mol Plant Path* 82:10-19 doi:10.1016/j.pmp.2012.12.002
- Sessitsch A, Reiter B, Pfeifer U, Wilhelm E (2002) Cultivation-independent population analysis of bacterial endophytes in three potato varieties based on eubacterial and Actinomycetes-specific PCR of 16S rRNA genes. *FEMS Microbiol Ecol* 39:23-32 doi:10.1111/j.1574-6941.2002.tb00903.x
- Sharma P, Jha AB, Dubey RS, Pessarakli M (2012) Reactive oxygen species, oxidative damage, and antioxidative defense mechanism in plants under stressful conditions. *J Bot* 2012:26 doi:10.1155/2012/217037
- Shoresh M, Harman GE (2008) The relationship between increased growth and resistance induced in plants by root colonizing microbes. *Plant Signal Behav* 3:737-739
- Shoresh M, Harman GE, Mastouri F (2010) Induced systemic resistance and plant responses to fungal biocontrol agents. *Annu Rev Phytopathol* 48:21-43 doi:10.1146/annurev-phyto-073009-114450
- Siegel MR et al. (1990) Fungal endophyte-infected grasses: Alkaloid accumulation and aphid response *J Chem Ecol* 16:3301-3315 doi:10.1007/bf00982100
- Sikes, BA (2010) When do arbuscular mycorrhizal fungi protect plant roots from pathogens? *Plant Signal Behav* 5:763-765.

- Simmons CR, Fridlender M, Navarro PA, Yalpani N (2003) A maize defense-inducible gene is a major facilitator superfamily member related to bacterial multidrug resistance efflux antiporters. *Plant Mol Biol* 52:433-446 doi:10.1023/a:1023982704901
- Simon L, Lalonde M, Bruns TD (1992) Specific amplification of 18S fungal ribosomal genes from vesicular-arbuscular endomycorrhizal fungi colonizing roots. *App Environ Microbiol* 58:291-295
- Singh LP, Singh Gill S, Tuteja N (2011) Unraveling the role of fungal symbionts in plant abiotic stress tolerance. *Plant Signal Behav* 6:175-191 doi:10.4161/psb.6.2.14146
- Smyth GK (2004) Linear models and empirical bayes methods for assessing differential expression in microarray experiments. *Stat App Genetics Mol Biol* 3:Article3 doi:10.2202/1544-6115.1027
- St. Leger RJ (2008) Studies on adaptations of *Metarhizium anisopliae* to life in the soil. *J Invertebr Pathol* 98:271-276 doi:10.1016/j.jip.2008.01.007
- Steyaert JM (2007) Studies on the regulation of conidiation in species of *Trichoderma*. PhD thesis. Lincoln University
- Stockinger EJ, Gilmour SJ, Thomashow MF (1997) *Arabidopsis thaliana* CBF1 encodes an AP2 domain-containing transcriptional activator that binds to the C-repeat/DRE, a cis-acting DNA regulatory element that stimulates transcription in response to low temperature and water deficit. *Proc Natl Acad Sci USA* 94:1035-1040
- Straub D, Yang H, Liu Y, Tsap T, Ludewig U (2013) Root ethylene signalling is involved in *Miscanthus sinensis* growth promotion by the bacterial endophyte *Herbaspirillum frisingense* GSF30(T) *J Exp Bot* 64:4603-4615 doi:10.1093/jxb/ert276
- Suda W, Oto M, Amachi S, Shinoyama H, Shishido M (2008) A Direct method to isolate DNA from phyllosphere microbial communities without disrupting leaf tissues. *Microbes Environ* 23:248-252 doi:10.1264/jsme2.23.248
- Sun C, Johnson JM, Cai D, Sherameti I, Oelmüller R, Lou B (2010) *Piriformospora indica* confers drought tolerance in Chinese cabbage leaves by stimulating antioxidant enzymes, the expression of drought-related genes and the plastid-localized CAS protein. *J Plant Physiol* 167:1009-1017 doi:10.1016/j.jplph.2010.02.013
- Sung G-H, Hywel-Jones NL, Sung J-M, Luangsa-ard JJ, Shrestha B, Spatafora JW (2007) Phylogenetic classification of *Cordyceps* and the clavicipitaceous fungi. *Stud Mycol* 57:5-59 doi:10.3114/sim.2007.57.01
- Tamura K, Nei M (1993) Estimation of the number of nucleotide substitutions in the control region of mitochondrial DNA in humans and chimpanzees. *Mol Biol Evol* 10:512-526
- Tamura K, Peterson D, Peterson N, Stecher G, Nei M, Kumar S (2011) MEGA5: molecular evolutionary genetics analysis using maximum likelihood, evolutionary distance, and maximum parsimony methods. *Mol Biol Evol* 28:2731-2739 doi:10.1093/molbev/msr121
- Vakili, NG (1990) Biocontrol of stalk rot in corn. In: Proc of the Forty-fourth Ann Corn and Sorghum Industry Research Conference, December 6-7, 1989, Chicago, IL. American Seed Trade Association, Washington DC. p, 87-105.
- Vega, FE, Tanada Y, Kaya, HK (2012) *Insect Pathology* 2nd Ed. Academic Press, San Diego, USA.
- Tanaka A, Tapper BA, Popay A, Parker EJ, Scott B (2005) A symbiosis expressed non-ribosomal peptide synthetase from a mutualistic fungal endophyte of perennial ryegrass confers protection to the symbiotum from insect herbivory. *Mol Microbiol* 57:1036-1050 doi:10.1111/j.1365-2958.2005.04747.x
- Tanksley SD (2004) The genetic, developmental, and molecular bases of fruit size and shape variation in tomato. *Plant Cell* 16 Suppl:S181-189 doi:10.1105/tpc.018119
- Tate JA, Simpson BB (2003) Paraphyly of *Tarasa* (Malvaceae) and Diverse Origins of the Polyploid Species. *System Bot* 28:723-737 doi:10.1043/02-64.1
- Tellenbach C, Grunig CR, Sieber TN (2010) Suitability of Quantitative Real-Time PCR To Estimate the Biomass of Fungal Root Endophytes. *App Environ Microbiol* 76:5764-5772 doi:10.1128/aem.00907-10
- Thomas P, Sekhar AC (2014) Live cell imaging reveals extensive intracellular cytoplasmic colonization of banana by normally non-cultivable endophytic bacteria. *AoB PLANTS* 6 doi:10.1093/aobpla/plu002

- Torres Netto A, Campostrini E, Oliveira JGd, Yamanishi OK (2002) Portable chlorophyll meter for the quantification of photosynthetic pigments, nitrogen and the possible use for assessment of the photochemical process in *Carica papaya* L. Brazilian J Plant Physi 14:203-210
- Tyler HL, Triplett EW (2008) Plants as a habitat for beneficial and/or human pathogenic bacteria. Annu Rev Phytopathol 46:53-73 doi:10.1146/annurev.phyto.011708.103102
- Uddling J, Gelang-Alfredsson J, Piikki K, Pleijel H (2007) Evaluating the relationship between leaf chlorophyll concentration and SPAD-502 chlorophyll meter readings. Photosynth Res 91:37-46 doi:10.1007/s11120-006-9077-5
- Usha Rani P, Jyothsna Y (2010) Biochemical and enzymatic changes in rice plants as a mechanism of defense. Acta Physiologiae Plantarum 32:695-701 doi:10.1007/s11738-009-0449-2
- Vainio EJ, Hantula J (2000) Direct analysis of wood-inhabiting fungi using denaturing gradient gel electrophoresis of amplified ribosomal DNA. Mycol Res 104:927-936 doi:10.1017/s0953756200002471
- Van der Biezen EA, Jones JD (1998) Plant disease-resistance proteins and the gene-for-gene concept. Trends Biochem Sci 23:454-456
- Vanacker H, Carver TLW, Foyer CH (2000) Early H₂O₂ accumulation in mesophyll cells leads to induction of glutathione during the hyper-sensitive response in the barley-powdery mildew interaction. Plant Phys 123:1289-1300 doi:10.1104/pp.123.4.1289
- Vargas WA, Mandawe JC, Kenerley CM (2009) Plant-Derived Sucrose Is a Key Element in the Symbiotic Association between *Trichoderma virens* and Maize Plants. Plant Phys 151:792-808 doi:10.1104/pp.109.141291
- Varma A, Savita V, Sudha, Sahay N, Bütehorn B, Franken P (1999) *Piriformospora indica*, a Cultivable Plant-Growth-Promoting Root Endophyte. App Environ Microbiol 65:2741-2744
- Vega FE et al. (2009) Fungal entomopathogens: new insights on their ecology. Fungal Ecol 2:149-159 doi:10.1016/j.funeco.2009.05.001
- Vega FE, Posada F, Aime MC, Pava-Ripoll M, Infante F, Rehner SA (2008) Entomopathogenic fungal endophytes. Biol Control 46:72-82 doi:10.1016/j.biocontrol.2008.01.008
- Vidal S, Jaber LR (2015) Entomopathogenic fungi as endophytes: plant-endophyte-herbivore interactions and prospects for use in biological control. Curr Sci 109:46-54
- Vos IA, Moritz L, Pieterse CMJ, Van Wees SCM (2015) Impact of hormonal crosstalk on plant resistance and fitness under multi-attacker conditions. Front Plant Sci 6:639 doi:10.3389/fpls.2015.00639
- Waage JK (1997) Biopesticides at the crossroads: IPM products or chemical clones? In: Microbial Insecticides: Novelty or Necessity? British Crop Protection Council Symposium Proceedings, vol 68. pp 11-19
- Wagner BL, Lewis LC (2000) Colonization of corn, *Zea mays*, by the entomopathogenic fungus *Beauveria bassiana*. Appl Environ Microbiol 66:3468-3473
- Wakelin S, Lombi E, Donner E, MacDonald L, Black A, O'Callaghan M (2013) Application of MicroResp™ for soil ecotoxicology. Environ Pollution 179:177-184 doi:http://dx.doi.org/10.1016/j.envpol.2013.04.010
- Waller FA, B. Baltruschat, H. Fodor, J. Becker, K. Fischer, M. Heier, T. Huckelhoven, R. Neumann, C. von Wettstein, D. Franken, P. Kogel, K. H. (2005) The endophytic fungus *Piriformospora indica* reprograms barley to salt-stress tolerance, disease resistance, and higher yield. Proc Nat Acad Sci USA 102:13386-13391 doi:10.1073/pnas.0504423102
- Wang CS, St Leger RJ (2007) The MAD1 adhesin of *Metarhizium anisopliae* links adhesion with blastospore production and virulence to insects, and the MAD2 adhesin enables attachment to plants. Eukaryotic Cell 6:808-816 doi:10.1128/ec.00409-06
- War AR, Paulraj MG, Ahmad T, Buhroo AA, Hussain B, Ignacimuthu S, Sharma HC (2012) Mechanisms of plant defense against insect herbivores. Plant Signal Behav 7:1306-1320 doi:10.4161/psb.21663
- Wellburn AR (1994) The spectral determination of chlorophylls a and b, as well as total carotenoids, using various solvents with spectrophotometers of different resolution. J Plant Physiol 144:307-313 doi:http://dx.doi.org/10.1016/S0176-1617(11)81192-2

- Whipps JM (1997) Developments in the biological control of soil-borne plant pathogens. *Adv Plant Pathol* 26 26:1-134
- Whipps JM (2001) Microbial interactions and biocontrol in the rhizosphere. *J Exp Bot* 52:487-511
- White Jr JF, Torres MS, Johnson H, Irizarry I, Tadych M (2014) A functional view of plant microbiomes: endosymbiotic systems that enhance plant growth and survival. In: *Advances in endophytic research*. Springer, pp 425-439
- White TJ, Bruns T, Lee S, Taylor J (1990) Amplification and direct sequencing of fungal ribosomal RNA genes for phylogenetics PCR protocols: a guide to methods and applications 18:315-322
- Wicaksono WA, Jones EE, Monk J, Ridgway HJ (2016) The bacterial signature of *Leptospermum scoparium* (Manuka) reveals core and accessory communities with bioactive properties. *PLoS One* 11 doi:10.1371/journal.pone.0163717
- Wilce MCJ, Parker MW (1994) Structure and function of glutathione S-transferases. *Biochimica Et Biophysica Acta-Protein Structure and Molecular Enzymology* 1205:1-18 doi:10.1016/0167-4838(94)90086-8
- Wilson D (1995) Endophyte – the evolution of a term, and clarification of its use and definition. *Oikos* 73:274-276 doi:10.2307/3545919
- Wyrebek M, Huber C, Sasan RK, Bidochka MJ (2011) Three sympatrically occurring species of *Metarhizium* show plant rhizosphere specificity. *Microbiol* 157:2904-2911 doi:10.1099/mic.0.051102-0
- Wyss P, Boller T, Wiemken A (1992) Testing the effect of biological control agents on the formation of vesicular arbuscular mycorrhiza. *Plant Soil* 147:159-162 doi:10.1007/bf00009382
- Xiao G, Wieckowski MR, Chinopoulos C, Kepp O, Kroemer G, Galluzzi L, Pinton P (2012) Genomic perspectives on the evolution of fungal entomopathogenicity in *Beauveria bassiana* *Sci Rep* 2 doi:10.1038/srep00483
- Xiong D, Chen J, Yu T, Gao W, Ling X, Li Y, Peng S, Huang J (2015) SPAD-based leaf nitrogen estimation is impacted by environmental factors and crop leaf characteristics *Sci Rep* 5:13389 doi:10.1038/srep13389
- Xu ZS, Chen M, Li LC, Ma YZ (2011) Functions and Application of the AP2/ERF Transcription Factor Family in Crop Improvement. *J Integ Plant Biol* 53:570-585 doi:10.1111/j.1744-7909.2011.01062.x
- Yang D-L, Yao J, Mei CS, Tong XH, Zeng LJ, Li Q, Xiao LT, Sun TP, Li J, Deng XW, Lee CM, Thomashow MF, Yang Y, He Z, He SY. (2012) Plant hormone jasmonate prioritizes defense over growth by interfering with gibberellin signaling cascade. *Proc Nat Acad Sci* 109:E1192–E1200 doi:10.1073/pnas.1201616109
- Young CA, Felitti S, Shields K, Spangenberg G, Johnson RD, Bryan GT, Saikia S, Scott B (2006) A complex gene cluster for indole-diterpene biosynthesis in the grass endophyte *Neotyphodium lolii*. *Fungal Gen Biol* 43:679-693 doi:10.1016/fgb.2006.04.004
- Yun BW, Feechan A, Yin M. et al. (2011) S-nitrosylation of NADPH oxidase regulates cell death in plant immunity. *Nature* 478:264-268 doi:10.1038/nature10427
- Zambell CB, White JF (2015) In the forest vine *Smilax rotundifolia*, fungal epiphytes show site-wide spatial correlation, while endophytes show evidence of niche partitioning. *Fungal Divers* 75:279-297 doi:10.1007/s13225-014-0316-3
- Zamioudis C, Pieterse CM (2012) Modulation of host immunity by beneficial microbes. *Mol Plant-Microbe Interactions* 25:139-150 doi:10.1094/mpmi-06-11-0179
- Zarei A, Korbes AP, Younessi P, Montiel G, Champion A, Memelink J (2011) Two GCC boxes and AP2/ERF-domain transcription factor ORA59 in jasmonate/ethylene-mediated activation of the PDF1.2 promoter in *Arabidopsis*. *Plant Mol Biol* 75:321-331 doi:10.1007/s11103-010-9728-y
- Zhang FG, Yuan J, Yang XM, Cui YQ, Chen LH, Ran W, Shen QR (2013) Putative *Trichoderma harzianum* mutant promotes cucumber growth by enhanced production of indole acetic acid and plant colonization. *Plant Soil* 368:433-444 doi:10.1007/s11104-012-1519-6
- Zhang L, Vidal S (2012) The effects of *Beauveria bassiana* and *Trichoderma harzianum* as endophytes on herbivores. *Julius-Kuhn-Archiv*:385-385

- Zhang SZ, Xia YX, Kim B, Keyhani NO (2011) Two hydrophobins are involved in fungal spore coat rodlet layer assembly and each play distinct roles in surface interactions, development and pathogenesis in the entomopathogenic fungus, *Beauveria bassiana*. *Mol Microbiol* 80:811-826 doi:10.1111/j.1365-2958.2011.07613.x
- Zhang Z, Schwartz S, Wagner L, Miller W (2000) A greedy algorithm for aligning DNA sequences. *J of Computational Biol* 7:203-214 doi:10.1089/10665270050081478
- Zimmermann G (1986) The galleria bait method for detection of entomopathogenic fungi in soil. *J of App Ento-Zeitschrift Fur Angewandte Entomologie* 102:213-215
- Zimmermann G (2007) Review on safety of the entomopathogenic fungi *Beauveria bassiana* and *Beauveria brongniartii*. *Biocontrol Sci and Tech* 17:553-596 doi:10.1080/09583150701309006
- Zipfel C, Felix G (2005) Plants and animals: a different taste for microbes? *Curr Opin Plant Biol* 8:353-360 doi:10.1016/j.pbi.2005.05.004
- Zitlalpopoca-Hernandez G, Najera-Rincon MB, del-Val E, Alarcon A, Jackson T, Larsen J (2017) Multitrophic interactions between maize mycorrhizas, the root feeding insect *Phyllophaga vetula* and the entomopathogenic fungus *Beauveria bassiana*. *App Soil Ecol* 115:38-43 doi:https://doi.org/10.1016/j.apsoil.2017.03.014
- Zuccaro A, Lahrmann U, Gueldener U, Langen G, Pfiffi S, Biedenkopf D, Wong P, Samans B, Grimm C, Basiewicz M, Murat C, Martin F, Kogel KH (2011) endophytic life strategies decoded by genome and transcriptome analyses of the mutualistic root Symbiont *Piriformospora indica*. *PLoS Pathogens* 7 doi:10.1371/journal.ppat.1002290